Interaction of Metal Salts with Polyethers

Farahman Hakiempoor B.Sc.

A thesis presented for the degree of

Doctor of Philosophy

to

The University of Aston in Birmingham

October 1985

Interaction of Metal Salts with Polyethers

A thesis presented for the degree of
Doctor of Philosophy
to
The University of Aston in Birmingham
by
Farahman Hakiempoor B.Sc.
1985

Summary

The dielectric properties of pure low to medium molecular weight poly(ethylene glycol) and poly(propylene glycol) and a variety of their salt complexes have been studied through the measurement of the dielectric permittivity and dielectric loss over a range of frequency and temperature. The major proportion of this study has been concerned with the examination of the nature of the interaction between mercuric chloride and poly(propylene glycol)(PPG). Other salt-polyether combinations have also been considered such as cobalt chloride-PPG, cadmium chloride-PPG, zinc chloride-PPG and ferric chloride-PEG (polyethylene glycol). Some of this work was also supported by chemical shift and spin-lattice Nuclear Magnetic Resonance (N.M.R.) spectroscopy. The dielectric permittivity data were analysed using the Onsager relation to calculate the mean dipole moment per dipolar unit. This approach was employed in the discussion of various models proposed for the structure of salt-polyether complexes. The effect of mercuric chloride on the statistical conformations of poly(propylene-glycol) was studied in a quantitative manner using the relationships of Marchal-Benoit. The dielectric relaxation activation energy and mean energy difference between gauche and trans conformations of poly(propylene glycol) in the presence of mercuric chloride, both showed a distinct minimum when the concentration of mercuric chloride was close to 5 mole %. Opposite behaviour was observed for the Cole-Cole parameter. It was concluded that the majority of the dielectric data could be rationalised in terms of a 5-membered cyclic complex formed between mercuric chloride and PPG in which the complexed segment of the polyether-($OMeCH_2CH_2O$)- adopted either gauche or cis conformations.

Key Words

POLYETHERS
METAL SALTS
DIELECTRIC PERMITTIVITY AND LOSS
DIPOLE MOMENTS
NUCLEAR MAGNETIC RESONANCE

ACKNOWLEDGEMENTS

I am grateful to my supervisor Dr M. S. Beevers for his encouragement, patience and helpful discussion throughout this work and for his help in the writing of some of the computer programs. My sincere thanks are extended to my family for their financial support during the period 1982-1985. I am indebted to my dear friend Faroukh-Zeghiebi who gave me moral support during this period. My thanks are also extended to Dr A. J. Amass for his assistance in the analysis of polymer samples using gel permeation Chromatography. Dr J. Homer, my joint supervisor and Mr M. C. Perry are gratefully acknowledged for their advice and assistance in the N.M.R. analysis of samples. Mr H. S. Hindle and Mr J. E. Evans are also thanked for their help and patience. Miss C. A. Jakeman is thanked for her assistance in the infra-red analysis of polymer samples. Workshop facilities are gratefully acknowledged and particular thanks are extended to Mr R. W. Wheeler and Mr P. McGuire. I would also like to offer my thanks to Mr S. Ludlow who gave me much assistance during the first year of my period of research. Finally, but by no means least, I would like to thank my friends and colleagues at the University of Aston.

LIST OF CONTENTS

LIST OF TABLES

LIST OF FIGURES

INTRODUCTION

For several decades the role and importance of polymer materials, relative to metals, has steadily increased. The spectrum of applications for polymers, both synthetic and naturally occurring, is now very wide and continues to increase. Many articles and components, long produced or fabricated from metals, are now being manufactured using polymers. The ease with which certain synthetic polymers form fibres led to a dramatic increase in their usage in the textile industry and almost completely replaced the long established cotton-based technology. The ability to easily melt and mould thermoplastic polymers (as distinct from thermosetting polymers)[1] at the low cost and high throughput is now largely taken for granted. Many interesting innovations have also taken place, some closely related to advances in processing technology, others as a result of the synthesis of novel polymer structures. The latter aspect, in which the constitution and structure of a polymer is deliberately chosen to suit a particular application, has given rise to the phrase 'tailor-made polymer'. The potential number of polymer based materials is immense and although many have been prepared and examined using a variety of physical and chemical techniques the subtleties of the relationship between composition and properties are still being actively pursued. Although the variety of applications for polymers appears to be endless it must be borne in mind

that their relationship and interplay with other materials, especially metals, is very important. For example, in some areas it is necessary to consider and allow for the often marked difference in the temperature coefficient of volume expansion of polymers and metals, especially in instances where the two materials are structurally integral. The tensile and flexural moduli of metals and plastics are often substantially different, sometimes by several orders of magnitude. Impact strength and hardness are well known examples of attributes that can vary widely for metals and plastics. If these differences are regarded as deficiencies in polymer materials then the advancements in composite plastics materials have resulted in significant improvements in these properties.

Until recently the traditional role of polymers in the electronics industries has been that of an electrical insulator or a dielectric material. The majority of the well known thermoplastics are good electrical insulators, whereas many, naturally occurring polymers, because of their ability to absorb water, give rise to significant electrical conductivity. For some applications, the possession of a small electrical conductivity can be useful, since it permits the steady discharge of static electricity. Good electrical insulators such as polyethylene polypropylene, polytetra fluorethylene PTFE, polystyrene and polymethylmethacrylate (Perspex) absorb only very small quantities of water, but some polymers for example polystyrene, are easily attacked by common organic solvents.

With the notable exception of PTFE the majority of polymers are prone to 'tracking', the production of an electrically conductive carbon track, and corona arcing , in the presence of high electric field strengths.

It has long been known that insulating polymers can be rendered moderately electrically conductive by the physical blending of the polymer together with a suitable conductive (or semi-conductive) material such as carbon black or a metal. Usually the resulting composites are only able to support relatively small current densities which restricts their range of applications; low level heating, for example. A more serious problem, concerning electrically conductive composites, concerns the steady decline in mechanical properties with increase in filler content. Nevertheless, composites have played and still do play an important role in the development of electrically conductive plastics materials.

From spectroscopic studies of unsaturated organic molecules, especially molecules that possess extended conjugated structures, it has been concluded that certain electrons, the π - electrons, enjoy an extensive degree of mobility within the molecular framework. This behaviour of electrons in conjugated molecules together with the discovery of polyacetylene provided the basis for the development of conductive polymers that has taken place over the last ten to fifteen years. Although the general aim of research workers has been to synthesise and produce

an electrically conductive polymer that could be readily processed it has to be admitted that such a goal has proved more difficult to achieve than anticipated. There appears to be three major problems associated with this exercise. Firstly, although pure polymers have been made that exhibit modest electrical conductivity (ie. semiconductors) nearly all require doping with a second molecule such as I_2 or AsF_5 before high electrical conductivities are achieved. The doped materials tend to be air and water sensitive as indeed are the doped polyacetylenes. Secondly, as a fairly general rule, the more conductive the polymer the more brittle and intractable it becomes. Despite these severe problems there have been notable successes. Many potentially useful materials have been produced although, with the exception of thermoplastic composites, there is still not available a highly conductive polymer (undoped) that may be repetitively processed using processing technology developed for thermoplastic materials. It is noted that carefully controlled pyrolysis of certain unsaturated polymers, especially those in fibre form, can lead to highly conductive materials that have potentially important commercial applications. However, such materials tend to involve 'one-shot' processes and usually require in-situ fabrication since once produced the final molecular structure cannot be readily broken down and reformed as required in a re-processing operation.

In the quest for a highly electrically conductive polymer much important information has been acquired concerning polymer synthesis and polymer structure. The research has provided much impetus to the development of new synthetic routes. Furthermore, the study of the resultant polymers, in both doped and undoped forms, has revealed many interesting and potentially very useful chemical and physical properties. A notable success involves poly(N-vinylcarbazole) (PVK) which possesses photo conductive properties. PVK when suitably doped is now used extensively as a replacement for selenium in the xerography photocopying process.

In the quest for an easily processed, highly electrically conductive polymer, much effort has been expended in the synthesis of polymers that possess extended conjugation based on either an entirely carbon skeleton or heteratom system incorporating sulphur atoms, for example. However, the successful synthesis of a polymer for which electrons are intramoleculary mobile is not necessarily a guarantee that the bulk material will conduct. Bulk conduction requires the electrons to jump or migrate from one polymer molecule to another. It is this intermolecular motion of electrons, or lack of it, that constitutes the third major problem in the search for a pure electrically conductive polymer. It is interesting to note that some polymers, thought to be possible promising electrical conductors before synthesis, but proved not to be did however exhibit very large dielectric constants indicative of high polaris-

ability. In other words the electrons were free to move along the molecular framework in the presence of an electric field but were unable to progress from one molecule to another.

The commercial applications arising from the synthesis of the right type of electrically conductive polymer are varied. The use of conductive polymers in batteries is one area that has already enjoyed some success and is also currently receiving much attention. A great deal of emphasis has also been placed on the development of polymers that exhibit truly electronic conduction rather than ionic conduction. There are a number of reasons for preferring electronic mechanisms. (ie. electron or positive hole flow). Conduction is usually more efficient for electrons and holes than it is for ions, which find it difficult to diffuse through a polymer matrix. Ions tend to be electrically neutralised when reaching the electrodes giving rise to various electrochemical problems. Thus, for materials required simply for the role of conductors the major carriers are either electrons or positive holes. This is not to state that ions are completely unwanted. In the area concerned with lightweight, efficient, low power sources the correct choice of polymer and ions may form an essential chemical component (ie. a half cell reaction) of the battery. Some additional applications, not previously mentioned, are electrical shielding, heat conduction, conversion of mechanical deformation into electrical signals, electrets,

electrochemical sensors and electrolytes.

The effect of ions on the physical properties of polymers is often dramatic. Inorganic polymers have been studied for many years and have been reviewed periodically. The incorporation of salts or ions in basically organic polymers is relatively new, although Nature has provided us with many naturally occurring examples of polyelectrolyte systems. However, this review will confine itself mainly to materials broadly classed as synthetic or laboratory made. There is now a great deal of experimental evidence to show that poly(ethylene oxide) can form well defined, highly crystalline complexes with a wide range of inorganic compounds. One of the earliest reports of complex formation between poly(ethylene oxide) (PEO) and an inorganic salt was that published by Doscher, Myers and Atkins in 1951[2]. These workers examined interactions between PEO and calcium chloride. A systematic study of interactions between metal salts and poly alkylethers can be traced back to the early 1960's. Blumberg et al in 1964 reported infra-red and X-ray studies of complexes formed by exposing fibres of high molecular weight poly (ethylene oxide) to saturated ether solutions of mercuric chloride at room temperature[3]. The resultant complexes were rigid and brittle and insoluble in water. Blumberg made the important observation that complex formation did not result in any measurable chain scission, as judged from comparative solution viscosity measurements. The chemical formula of the complex was given as (CH_2 CH_2

$O)_4$ Hg $C\ell_2$ and unit cell was believed to be orthorhombic. The same workers also prepared complexes of PEO and cadmium chloride and noted that these were isomorphous to those of PEO - mercuric chloride. In 1966, Blumberg and Wyatt[4] published further studies on the PEO - mercury halide complexes in which they examined the conductivities of complexes formed in aqueous solution containing PEO and the mercury halides Hg $C\ell_2$, Hg Br_2 and Hg I_4^{2-}. In accordance with their earlier paper they observed discontinuities in conductance at a monomer unit-to-halide ratio of 3.86 for the chloride and 4.00 for the bromide. No break was observed for the iodide. Careful mass measurements also showed that fibres exposed to the three mercuric halides gave mass increments corresponding to monomer unit-to-mercuric halide ratios of 4:1 for the chloride and bromide and 5:1 for the iodide. It is interesting to note that Laurent and Arsenio[5] in 1958 and Hendra and Powell[6] in 1960 had reported on dioxanate-metal compounds especially those formed from 1, 4 - dioxane and mercuric chloride.

A more detailed structural determination of complexes formed between poly(ethylene oxide) and mercuric chloride was undertaken by Tadokoro and Co-workers[7] in the late 1960's. They reported on two different types of complex, Type I and Type II. For the former type, which has the composition $(CH_2\ CH_2\ O)_4$ Hg $C\ell_2$ they found that the unit cell was orthorhombic with each unit cell containing four Hg $C\ell_2$ molecules and sixteen - $CH_2\ CH_2\ O$ - units. They concluded

that the conformation of the polyethylene oxide was

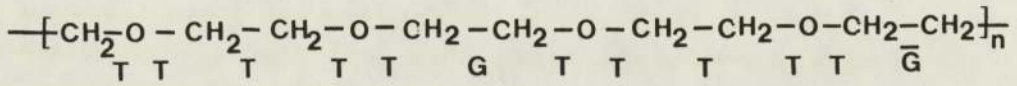

where T, G and $\bar{G}$ donate trans and right- and left-handed gauche forms, respectively. Tadokoro and co-workers also deduced the structure of a second type of complex, Type II. This was orthorhombic, like type I, but the unit cell contains four molecules of $HgCl_2$ and four $\{ CH_2\ CH_2\ O \}$ units. The conformation of the poly(ethylene oxide chain) was represented by

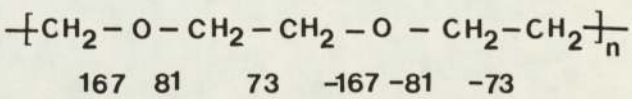

One of the earliest studies to report on interactions between poly(ethylene oxide) and salts of alkali metals was that published by Landberg, Bailey and Callara[8] in 1966. This was primarily a viscometric study of interaction between various alkali salts and poly(ethylene oxide) in solution in methanol. Reduced viscosity data was presented for the fluoride, chloride, bromide and iodide salts of potassium and for the fluoride, chloride and iodide salts of rubidium. A progressive increase in reduced viscosity was observed for the series KI<KBr<KCl<KF and similar behaviour was found for the rubidium halides.

The authors noted that PEO was normally insoluble in methanol but that the addition of as little as 0.5% of potassium iodide converts methanol into an excellent solvent. The results of equilibrium dialysis techniques applied to solutions of PEO and KI suggested that one molecule of KI is complexed or associated with about nine ethylene oxide units and that the nature of the association is due to ion-dipole interactions.

An important study, concerning the potential use of polyalkylether - salt complexes as electrical conductors etc, was that published by Fenton, Parker and Wright[9] in 1973. These workers reported the preparation of crystalline complexes of poly(ethylene oxide) and sodium iodide from solution in methanol following removal of the solvent. They found that the complex consisted of 1 mol of sodium iodide to 4 mol of ethylene oxide. Sodium and potassium thiocyanate were also observed to form similar highly crystalline complexes with PEO. It was noted that similarities in the infra-red spectra of cyclic ether - salt complexes and poly(ethylene oxide) - salt complexes indicate that the cations are associated with the ether oxygen atoms. The effect of inorganic salts on the glass transition temperatures of polyethers has been studied in some detail by Wetton and co-workers.[10] They found that low molecular weight poly(propylene glycol) (M_n~2000) forms complexes with $ZnCl_2$. The complexes are colorless, viscous liquids above their glass transition temperature T_g and brittle glasses below T_g. Complexes

formed between $ZnC\ell_2$ and high molecular weight ($\sim 10^5$) poly(propylene glycol) were transparent, leathery materials, and only slightly water sensitive. X-ray analysis indicated a single-phase amorphous system. At room temperature, poly(propylene glycol) ($\bar{M}_n \sim 2000$) and Co $C\ell_2$ formed complexes that were deep blue liquids at low cobalt (II) chloride concentrations, and deep blue transparent brittle glasses at higher concentrations. The complexes formed between high molecular weight poly(propylene glycol) and Co $C\ell_2$ were blue, opaque, exhibited stress - whitening effects and readily absorbed water and became pink colored. Wetton et al, suggested that this particular system existed as two phases with the Co $C\ell_2$ acting as a filler. The glass temperature behaviour of poly(propylene glycol) - $ZnC\ell_2$ complexes, as a function of mole fraction of coordinated monomer, was similar to that expected for a random copolymer, with the observation of a linear dependence of Tg on the mole fraction of $ZnC\ell_2$, over the range 0-0.85. Similar behaviour was claimed for poly(ethylene glycol). The marked elevation of Tg in poly(propylene glycol) by $ZnC\ell_2$ was believed to be a consequence of the formation of a five-membered chelating ring involving two adjacent other oxygen atoms and one molecule of $ZnC\ell_2$. The Tg of a fully coordinated polymer was predicted to be $44^{o}C$. A more extensive study of the elevation of the glass transition temperature of polyethers by metal salts was published by James, Wetton and Brown in 1979.[11] The Tg

increases depended upon both the amount and type of salt with Tg following a sigmoidal dependence on the amount of salt. The Tg data were, once again, interpreted in terms of a chelate ring model involving two adjacent ether oxygen atoms and one molecule of the salt. The overall behaviour of the polymer-salt complex was then considered to be that of a random copolymer comprised of complexed and 'free' repeat units. Mechanical relaxation data for the poly(propylene glycol) - Zn $C\ell_2$ system demonstrated an increase in the rubbery modulus that was interpreted in terms of Zn $C\ell_2$ forming a few, weak intermolecular cross-links.

The glass-transition temperature, kinetics of the glass-transition temperature and melt viscosity behaviour of mixtures of a phenoxy polymer and calcium thiocynate have been studied by Harmon and Wissbrum[12]. Marked increases in Tg were observed for increasing concentrations of salt. The flow behaviour and glass transition of nylon-6 containing Li $C\ell$, Li Br or K $C\ell$ have been investigated by Acierno and co-workers[13]. For the composition range 0 - 7% W/W, the glass transition temperature Tg was not affected by the type and concentrations of salt. However, the Newtonian melt viscosity of the mixtures was consistently greater than that observed for pure nylon-6. The apparent activation energy for viscous flow of nylon-6 is not affected by Li Br and Li Cl, but it is decreased by K $C\ell$. These results were interpreted in terms of interactions between polymer segments carrying bound Li^+ and Br^- ions,

and of insoluble K Cℓ inclusions in the polymer matrix. The general effect of lithium salts is to depress the crystallization temperature of polyamides and to increase the melt viscosity. This effect enables the melt viscosity of nylon-6 to be adjusted to an value that yields optimal processing conditions. Killis, Nest, Gandini and Cheradame[14] have studied the dynamic mechanical behaviour of polyether-based polyurethane networks containing sodium tetraphenylborate.[15] They undertook a quantitative analysis of the storage modulus dependence on temperature, frequency and salt concentration. Their data could be described by just three superposition correlations; frequency-temperature, frequency-concentration and concentration-temperature. They found that the frequency-temperature superposition followed William-Landel-Ferry (WLF)[16] behaviour, with the remaining two correlations being approximately linear expressions. In another publication, the same authors[17] reported on the ionic conductivity of polyether-polyurethane networks containing alkali metal salts such as sodium tetraphenylborate or lithium perchlorate. The variation of the conductivity with salt concentration, at constant free volume fraction (constant reduced temperature (T-Tg) was examined for two types of materials: urethane - cross linked poly(ethylene glycol) (M = 400) containing Na B Ph_4 and urethane - cross linked poly(ethylene glycol) (M = 1000) containing Li $C\ell O_4$. For the system PEG 400 - Na B Ph_4 it was claimed that the salt was totally dissociated up to the highest concentration (0.6 mol Kg^{-1}) studied. For the

PEG 1000 - Li $C\ell O_4$ networks the degree of dissociation of Li $C\ell O_4$ was observed to be close to unity up to about 1 mol Kg^{-1}. For a reduced temperature of T-Tg = 75°C the ionic mobility of sodium and lithium ions were calculated to be about 2×10^{-12} m^2 V^{-1} S^{-1} and 10^{-11} m^2 $V^{-1}S^{-1}$, respectively. Both of these values are typical of ion mobilities in bulk polymers. The authors concluded that complete dissociation of the lithium salt is achieved as long as there are available sites along the chains of poly(ethylene glycol). ^{7}Li broadline NMR, used as a means of investigating the salt dissociation in PEG 1000 - Li $C\ell O_4$ networks, also indicated the appearance of a new phase at salt concentrations higher than about 5% Li/-O- due to co-ordination of polyether segments to several salt molecules or ions.

The exact nature of the molecular interaction between the polyether backbone and the ions of salts has been the subject of many studies. A central question was whether the polymer-ion interaction was cationic, anionic or both. The proton resonance and electrophoresis studies of Liu on PEG-KI indicated that the positively charged potassium ion interacted with the etherate oxygen of PEG.[18] Proton spin - lattice relaxation time measurements of the same system, performed by Liu and Anderson[19] demonstrated the polymer - salt interaction produced a significant reduction in the segmental mobility of the polymer chain. A more recent paper by Ricard,[20] employing ^{23}Na-NMR spectroscopy, found evidence of interaction of Na^+

ions with PEG. Measurements of ^{13}C-NMR Spectra and spin-lattice relaxation times (T_1) have been undertaken by Ibemesi and Kinsinger on poly(ethylene oxides) (M = 6000, 10,000 and 20,000) containing sodium tetraphenylborate.[21] In all three samples the ^{13}C chemical shift of PEO moves towards a lower magnetic field with increase in salt concentration. These observations were interpreted as a result of PEO association with positively charged sodium ions, since the interaction of the etherate oxygen atoms with the Na^+ ions will reduce electron density around the methylene carbons and lead to resonance absorption at a lower magnetic field. ^{13}C-NMR T_1 measurements of PEO-6000 (0.17 M in acetonitrile) containing various amounts of Na TPB, indicate a decrease of T_1 from 2.17 sec with no salt to 0.34 sec in the presence of 0.3 M Na TPB. These results, together with the shift findings were taken to provide reasonable evidence for the cooperative binding of the sodium cation with etherate oxygen atoms of the polymer.

An extensive study of multinuclear magnetic relaxation of aqueous poly(ethylene oxide) solutions of alkali halides has been published by Florin.[22] In this study the nuclear magnetic relaxation rates of ^{7}Li, ^{23}Na, ^{133}Cs, $^{35}C\ell$ and ^{81}Br were measured for various alkali halide - poly(ethylene oxide) - water mixtures. The addition of PEO to aqueous salt solutions markedly increases the relaxation rates for all of the nuclei

studied, with the largest effect being observed for ^{133}Cs (ca x 65 for 1.0 **M** Cs Br containing 45% PEO). The increases in T_1 were attributed to asymmetric hydration of the ions caused by the presence of PEO and to direct cation - ether oxygen interactions.

Wright and co-workers have continued to examine a variety of aspects concerned with the structure and physical properties of poly(ethylene oxide) - salt complexes. Using differential thermal analysis, Lee and Wright[23] have observed order-disorder transformations, of the 'lambda' type, in some samples of sodium iodide and ammonium complexes of PEO 60,000. For NaI/PEO complexes T_λ occurs at 373K while for NH_4SCN/PEO T_λ was observed at 342K, below the melting point of 249.5K. In a later paper, Lee and Wright, using morphological and differential thermal analysis techniques, showed that the melting temperature (~463K) of the principal crystalline lamellar phase of PEO/NaI and PEO/Na SCN complexes is independent of the nature of the anion.[24] Their studies included electron micrographs of the complexes showing lamellar-like structures. Further information concerning the nature of the disorder-order processes was obtained from broad N.M.R spectra of the complexes. As the disordered, Phase II, is approached the migration of ionic components commences. This gives rise to enhanced molecular motion of the PEO chains in Phase I (the highly crystalline domain) with narrowing of the N.M.R

broadline commencing at ~330K for NaSCN-PEO and 360K for NaI-PEO λ-type isotherms.[25] For samples of NaI-PEO possessing excess NaI (ie. saturated with respect to NaI) the Arrhenius plot of conductivity (log σ vs 1/T) shows increasing activation energy with increasing temperature. Similar studies, involving complexes of poly(ethylene oxide) and lithium salts have been published by Payne and Wright.[26]

Although the electrical conductivity and dynamic mechanical properties of PEO and PPO polymers and their salt complexes has received a fair amount of attention the dielectric behaviour of these materials (especially those of the salt complexes of PPO) has not been extensively studied. Classical studies involving the measurement of the dipole moments of PEO and PPO in solution are well documented. Theoretical studies of the conformations of polyethers in general have also been extensively reported. Many of these studies have compared experimentally derived dipole moments of polyethers with values calculated using rotational isomeric state models to represent the conformational behaviour of the polymer chains. Studies of the static dielectric permittivity and dielectric loss in pure (bulk) polyethers has also been actively pursued. Difficulties arising as a result of the presence of water and crystallinity have been encountered, especially in samples of poly(methylene oxide) and poly(ethylene oxide).

CHAPTER 2

THEORY

The purpose of this chapter is to provide a theoretical basis for the interpretation of the dielectric data acquired for the solutions of inorganic salts and small organic molecules in poly(propylene glycol).

Aspects of this theory will be used to describe the relaxation effects observed in these chemical systems . Through the determination of the effective dipole moment of the polymer-salt complexes an attempt will be made to deduce information concerning the degree of complex formation and the structure of such complexes .

It is well known that nuclear magnetic resonance studies can provide valuable information concerning the extent and type of complex formation . The measurement of N.M.R spin-lattice relaxation times , T_1 , enables the rotational freedom of molecules and groups to be examined. The majority of modern N.M.R Spectrometers are now capable of performing T_1 measurments on a wide range of nuclei, thus rendering it possible to study the relative motion of different parts of a heteronuclear system . For these reasons it was believed that the measurement of N.M.R relaxation times would complement the dielectric relaxation data and would also enable a more discriminating appraisal of possible models chosen to describe the various relaxation processess occurring in the poly(propylene glycol)-salt systems .

2.1 Determination of the dielectric constant of a material

The relative static dielectric permittivity , which is often simply referred to as the dielectric constant , of a material may be determined by measuring the change in electrical capacitance that occurs when the material is placed between the plates (electrodes) of a capacitor. Using C_o and C to denote respectively the capacitance of the capacitor

(cell) when empty and when filled with a dielectric then the ratio, measured at zero frequency[27],

$$\epsilon = \frac{C}{C_o} \qquad (2.1)$$

is called the relative static dielectric permittivity or the dielectric constant of the material . The dielectric constant varies from one material to another and for a large number of substances its value lies in the range 2.0 - 30.0 .

However , there are many examples of materials that possess dielectric constants that lie well outside this range . One of the best known examples is water which has a dielectric constant of 78.3 at 298K. One even larger value (158) is exhibited by hydrocyanic acid . However , these values are far exceeded by some poly(acene quinone radical) polymers which possess dielectric constants in the range 20,000 to 50,000. The wide range of dielectric constant is a reflection of differences in the electronic and dipolar polarisation of materials .

The measurement of the dielectric constant provides a useful means of revealing certain aspects of molecular structure and is particular useful in determining the disposition of polar groups in flexible or rigid molecules .

The theoretical relationship between the experimentally determined dielectric permittivity and the dipole moment of a molecule was considered by Debye in 1929[28] . Debye described the behaviour of a small polar molecule in an electric field and derived the relationship between the dipole moment, μ_o, and the static dielectric constant , ϵ_o, which is

$$\frac{\epsilon_o - 1}{\epsilon_o + 1} = \frac{4}{3}\pi N \left[\alpha_e + \frac{\mu_o^2}{3kT}\right] \qquad (2.2)$$

Where N is the number of molecules per cm^3, α_e is the electronic

distortion polarisation of the molecules and k and T are the Boltzmann constant and absolute temperature , respectively . The Debye equation has been used successfully to describe the dielectric properties of dilute solutions of polar molecules in non-polar solvents . However , the Debye equation fails to accurately describe the dielectric behaviour of condensed , polar liquids . In order to solve this problem , Onsager, in 1936[29] , developed a new theory in which the polar molecule was placed at the centre of a spherical cavity of radius a . The molecular dipole was treated as a point dipole at the centre of the cavity . The Onsager theory introduced an important factor known as the Reaction Field , R , which is a component of the local field , E_L, that acts on the point dipole along with another component , G , the cavity field.

$$E_L = G + R \qquad (2.3)$$

The magnitude of the cavity field , present at the centre of the cavity in a dielectric of static permittivity , ϵ , in the presence of an applied electric field , E , is given by,

$$G = \frac{3\epsilon}{2\epsilon + 1} E \qquad (2.4)$$

The Reaction Field , which arises from the polarisation of the medium by the molecule in the cavity , is related to the molecular dipole by ,

$$R = \frac{2(\epsilon - 1)}{\epsilon_0(2\epsilon + 1)a^3} \mu \qquad (2.5)$$

It is important to realise that the Onsager theory relates to rigid polar molecules and neglects the effects arising from orientational correlations between molecules and their neighbouring molecules . The Onsager equation is normally written ,

as

$$\mu_o^2 = \frac{3\,R\,T}{4\pi N}\,\frac{2\epsilon_o + \epsilon_\infty}{3\,\epsilon_o}\left(\frac{3}{\epsilon_\infty + 2}\right)^2 (\epsilon_o - \epsilon_\infty) \qquad (2.6)$$

Where μ_o is the effective vacuum dipole moment and ϵ_∞ is the dielectric permittivity at high frequency .

In the theories considered thus far, several important factors have been avoided . These are(i) the orientational correlation between molecules and (ii)the deformation polarisation of the molecules .

In 1949 , Fröhlich[30] developed a very general dielectric theory that included the orientational correlation and distortion polarisation effects . We will now consider the simple model used in the Fröhlich dielectric theory for the static permittivity of polar molecules in the condensed phase . Fröhlich begins by considering a spherical region , of macroscopic volume , V , within an infinitely large specimen . This spherical region contains elementary dipole units . The major advantage of this approach , over previous theories , is that the distortion polarisation of a molecule can be taken into account ; the dielectric permittivity , ϵ_∞, is larger , by approximately 5 to 10% than the corresponding square of the refractive index n^2.

The spherical region contains N_o elementary dipole units, so that the number of elementary dipole units per unit volume of material is given simply by

$$N = N_o / V \qquad (2.7)$$

When an electric field is applied , the average polarisation is found by the appropriate summation of the elementary dipole units from which is obtained the general Fröhlich equation , (2.8)

$$(\epsilon_o - \epsilon_\infty) = \frac{3\,\epsilon_o}{(2\epsilon_o - \epsilon_\infty)}\,4\pi N\,\frac{\overline{m.m^*}}{3\,K\,T} \qquad (2.8)$$

Where m is the moment of reference dipole unit and m^* is the moment associated with the spherical region .

Fröhlich's theory can be extended to non-rigid molecules such as polymer molecules . The molecule is then regarded as a spherical region with a dielectric constant ϵ , that corresponds to a molecule in the vacuum state with a dipole moment μ^* and a dipole moment of μ for the reference molecule . The required product $\mu_i \mu^*_j$ is given by

$$m_i m^*_j = \mu_i \mu^*_j = \mu^2 \left[1 + \sum_{\substack{j \\ j \neq i}}^{N_o} \overline{\cos \delta_{ij}} \right] \qquad (2.9)$$

Where δ_{ij} is the angle between moments j and i . Since all values of δ_{ij} are equally probable in the liquid phase then $\overline{\cos \delta_{ij}} = 0$ and

$$(\epsilon_o - \epsilon_\infty) = \frac{3 \epsilon_o}{(2 \epsilon_o + \epsilon_\infty)} \frac{4 \pi N}{3 R T} g \mu^2 \qquad (2.10)$$

The Fröhlich and Onsager theories lead to different values for the vacuum dipole moment μ_o . This difference may be summarised by the expressions

$$\mu_o = \frac{3}{\epsilon_o + 2} \mu \qquad (\text{Fröhlich}) \quad 2.11)$$

$$\mu_o = \frac{3(2 \epsilon_o + \epsilon_\infty)}{(\epsilon_\infty + 2)(2 \epsilon_o + 1)} \mu \qquad (\text{Onsager}) (2.12)$$

Which indicate that μ_o derived using the Fröhlich expression will be smaller then μ_o obtained using the theory of Onsager .

The quantity , g , is a measure of the angular correlations between an arbitrarily chosen reference molecule and its nearest neighbours . For a pure liquid comprised of one type of molecule in which each molecule is surrounded by Z molecules , then

$$g = 1 + Z\,\overline{\cos\delta}$$

Employing the cavity model of Fröhlich , defined previously .

$$g = 1 + \sum_{\substack{j \\ j\neq i}}^{N_o} \cos\delta_{ij}$$

For a system of molecules in which there are no angular correlations between molecules then g=1 and the Fröhlich equation reduces to the form specified by Onsager .

For the particular example of polypropylene glycol the ether linkages endow a permanent degree of electrical polarity on to each repeat unit $-[(CH_3)CH\text{-}CH_2\text{-}O]-$. Individual molecules possess a cumulative dipole moment that has a magnitude proportional to the end-to-end distance of the molecule[31] . Fig.(2.1)

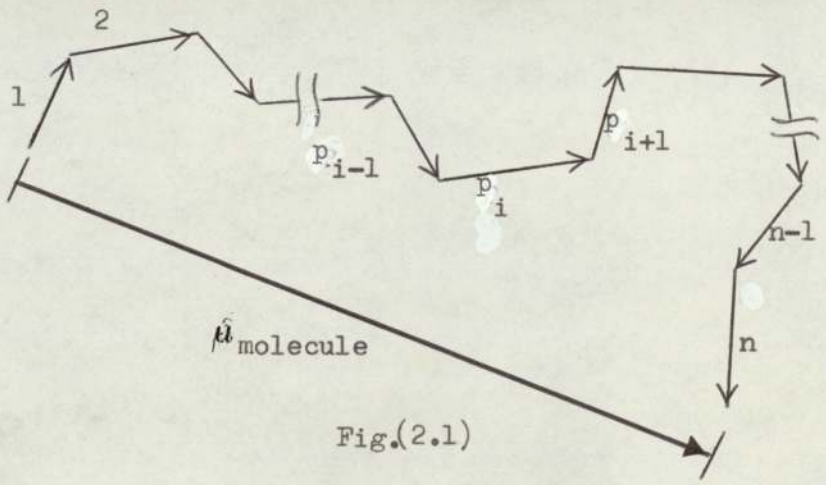

Fig.(2.1)

Although , in principle , the whole molecule may rotate in an end-over-end fashion it is generally accepted that in pure liquid polymers the rotation and changes in the magnitude of $\mu_{molecule}$ occur most easily by changes in the conformation of the molecule , induced by Brownian-motion . It is interesting to note that for changes in conformation involving simultaneous rotations about a pair of bonds separated by three skeleted bonds , the molecular dipole moment remains unchanged .

Assigning a fixed dipole moment of P to a repeat unit then the molecular dipole moment $\mu_{molecule}$ will be the vector sum of the n dipole moment vectors for a chain containing n repeat units , i.e.

$$\mu = \sum_{k=1}^{n} p_k$$

In practise it is the mean-square dipole moment that is obtained experimentally and from calculations based on the vectorial addition of link dipole moments . A suitable expression for the latter purpose is

$$\overline{\mu^2} = \sum_{i=1}^{n} p_i \sum_{j=1}^{n} p_j \qquad (2.13)$$

which may be expanded to give

$$\overline{\mu^2} = p^2\left[n + \sum_{i}^{n} \sum_{j}^{n} \overline{\cos\delta_{ij}} \right] = g_m p^2 \qquad i \neq j$$

The quantity $\overline{\cos\delta}_{ij}$ is the average of the cosine of the angle between the dipole moment vectors of repeat units i and j of the polymer chain . A suitable equation , based on the Fröhlich theory , for the evaluation of dielectric data of polymeric systems is given by

$$(\epsilon_o - \epsilon_\infty) = \frac{3\ \epsilon_o}{(2\ \epsilon_o + \epsilon_\infty)} \quad \frac{4\pi N}{3\ k\ T} \quad \left(\frac{\epsilon_\infty + 2}{3}\right)^2 \left(\frac{g_m}{n}\right) p_o^2 \qquad (2.14)$$

in which g_m/n is the effective orientational correlation factor g per unit of the chain and p_o is the dipole moment of the repeat unit in vacuum .

The next section of this chapter will be devoted to the development of theories that relate molecular dipole moments to the conformational behaviour of polymer chains , and in particular , the polyether chain . The problem may be treated as two separate parts . The first part is concerned with the interpretation of experimental

dielectric permittivities in order to obtain molecular dipole moments. This aspect has already been discussed . The second part concerns the relationship between molecular dipole moments and conformation .

Marchal and Benoit[32-37] and other workers developed a theory that related the conformations of a polyether and the molecular dipole moment . This approach demands a detailed analysis of the structure and conformation of the molecule . Assignment of dipole moments to skeletal bonds then permits the calculation of a theoretical molecular dipole moment which may then be compared to the value derived from measurements of dielectric permittivity .

The polyether molecule possesses a zig-zag type of chain in which there are two types of backbone skeletal bonds , C-O and C-C[31].

Fig. (2.2) shows a short section of poly(propylene glycol)

(R= CH_3)

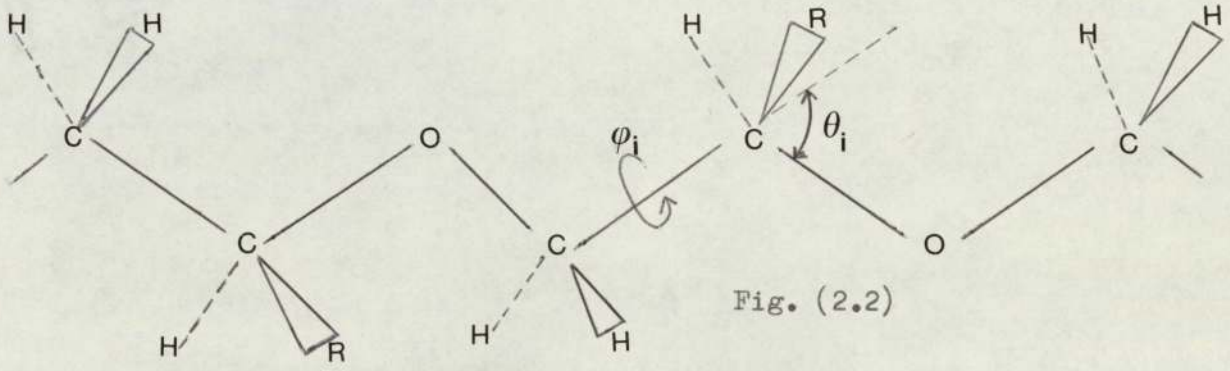

Fig. (2.2)

Strictly speaking the polyether $-(\ RCHCH_2O\ )_x-$ possesses three types of bond angle supplement , θ , and three types of rotational bond angles, φ .For poly(propylene glycol) the bond angles $\angle$OCO and $\angle$COC are nearly equal to one another and of fixed values( ) . The various rotational bond angles , φ, may adopt a large number of values and an accurate description of the conformation of the polymer chain would be an extremely complicated task . The

conformational analysis of a polymer chain can be substantially simplified , without an unacceptable loss of rigour , by recognizing that the continuous form of the rotational energy potential function of the skeletal bonds can be replaced by a number of discrete rotational states . These states normally arise fairly naturally from the six-fold symmetry properties associated with bonds attached to tetrahedrally substituted carbon atoms .

The simplest molecule related to the polyethers is ethane . The profile of the energy barrier restricting rotation of the methyl groups about the carbon-carbon bond is known in some detail.[38,39] The energy barrier restricting rotational movement between the staggered and eclipsed conformers is close to 12.6 kJ/mol.

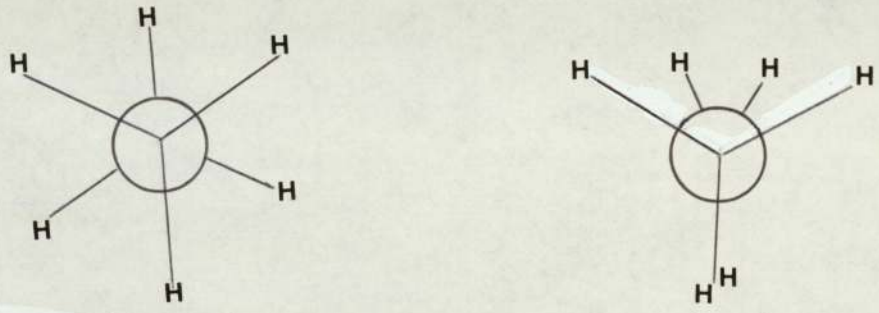

staggered eclipsed

conformation of ethane

Replacement of two hydrogens of ethane by methyl groups to give n-butane substantially modifies the rotational potential energy function. The conformational properties of the molecule n-butane may now be discussed in terms of four different types of conformers . These are the trans(a) , gauche(b), eclipsed(c) and fully eclipsed(d)forms

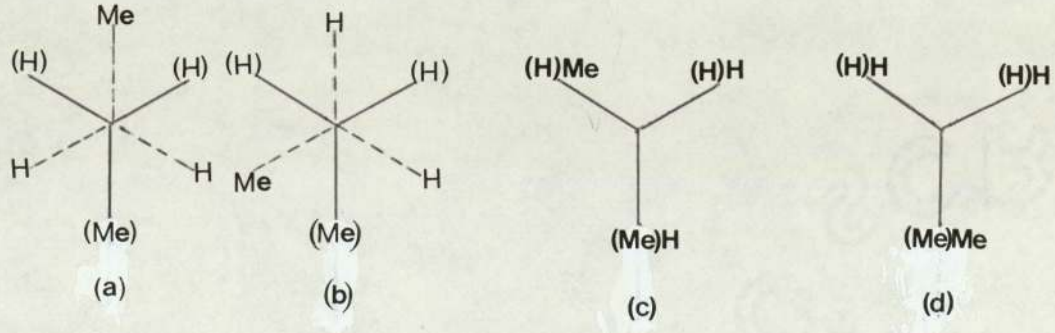

The extent of rotation about the central C-C bond of n-butane is defined relative to the trans conformation . Thus , $\varphi = 0^{o}$ for the trans conformer and $\varphi = \pm 120^{o}$ (or $+120^{o}, +240^{o}$) for the two possible gauche conformers . From a complete knowledge of the values of the angles φ and θ along with appropriate bond dipole moments a theoretical dipole moment may be calculated for a polymer molecule . Values of μ^2/n may then be compared with those determined experimentally .

The calculation of molecular dipole moments of the polyalkylethers has been attempted previously using fairly simplistic descriptions of the chain conformations . In these calculations a number of important assumptions were made . The principal assumptions were as follows . $\angle$ COC and $\angle$ OCO are equal and chosen to be tetrahedral . The rotational energy barriers are symmetrical functions of φ relative to $\varphi = 0^{o}$. The rotational energy barrier of C-O and C-C bonds are the same and independent of one another .

The mean dipole moment ratio of various polyethers $-(CH_2)_p O-$ for p=1-4 may be calculated using the following expressions . (2.15to18)

Poly(oxymethylene) p=1

$$\frac{\langle \mu^2 \rangle}{n} = \mu_o^2 \frac{1}{1+\cos\alpha} \quad \frac{1+\eta}{1-\eta} \qquad (2.15)$$

Poly(ethylene oxide) p=2

$$\frac{\langle \mu^2 \rangle}{n} = \mu_o^2 \frac{(1-\eta^2)(1+\cos\alpha)}{3\eta + (1-\eta)^2(1+\cos\alpha+\cos^2\alpha)} \qquad (2.16)$$

This expression is identical to that published by Marchal and Benoit

Poly(trimethylene oxide) p=3

$$\frac{\langle \mu^2 \rangle}{n} = \mu_o^2 \frac{(1+\eta)(1+\eta^2+2\eta\cos\alpha+(1-\eta)^2\cos^3\alpha)}{(1-\eta)(1+\eta)^2-4\eta\cos^2\alpha-(1-\eta)^2\cos^4\alpha} \qquad (2.17)$$

Poly(tetramethylene oxide) p=4

$$\frac{\mu^2}{n} = \mu_o^2(1-\eta^2)(1-\eta)\times \frac{1+\eta+\eta^2-3\eta\cos^2\alpha-(1-\eta)^2\cos^4\alpha}{1-\eta^5-5\eta^2(1-\eta)\cos\alpha-5\eta(1-\eta)^3\cos^3\alpha+(1-\eta)^5\cos^5\alpha} \qquad (2.18)$$

In each of these expressions μ_o denotes the dipole moment associated with the ether group COC . The direction of μ_o lies along the bisector of the angle $\angle$COC . The angles α and η are the supplements of the bond angle θ and rotational bond angle φ , respectively , and n is the total number of sketelal bonds in the chain .

2.2 Dielectric Relaxation

2.21 Single Relaxation Behaviour

The application of a low frequency sinusoidal(a.c.) electric field to a mixture of polar molecules causes them to partly reorient before the field reverses its polarity . The reorientation of the polar molecules in this way is equivalent to a displacement of electric charges along the direction of the applied electric field . This movement of electric charge is known as the displacement current in the dielectric . When the frequency of the applied electric voltage is gradually increased the molecules , because of their inertia , begin to lag behind the charges occurring in the polarity of the field. In the liquid state the majority of molecules are unable to follow charges in the electric field at frequencies of 100 GHz or greater .

Two consequences arise as a result of this lag in the rotational response of polar molecules . The current acquires a component that has the same phase as the applied voltage . This leads

to a dissipation of energy in the form of heat , a phenomenon known as "dielectric loss" . The out of phase component of the current contributes to the dielectric constant of the material . The relationship between the real part (dielectric constant) and imaginary part (dielectric loss) may be expressed in the complex plane

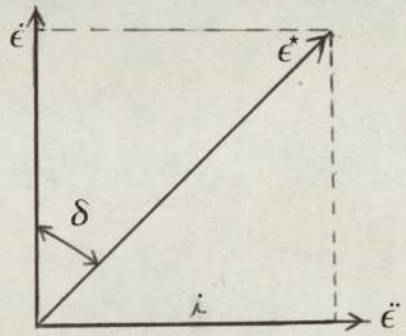

in which ϵ^* is the complex permittivity defined by

$$\epsilon^* = \epsilon' - i\epsilon''$$

The factor $i(=\sqrt{-1})$ is effectively an operator representing a rotation through 90^o in the complex plane[27].

For a single relaxation process Debye deduced relationships for the frequency dependence of ϵ' and ϵ'' an angular frequency ω (radian 1/s) These are shown by equations[28]

$$\epsilon' = \epsilon'_{\infty} + \frac{(\epsilon'_o - \epsilon'_{\infty})}{1 + (\omega\tau)^2} \qquad (2.19)$$

and

$$\epsilon'' = \frac{(\epsilon'_o - \epsilon'_{\infty})\omega\tau}{1 + (\omega\tau)^2} \qquad (2.20)$$

Where ϵ'_o is the static dielectric permittivity , i.e. the dielectric-constant measured at frequencies approaching zero Hertz , ϵ'_{∞} is the high frequency dielectric permittivity , τ is the natural rotational relaxation time of the rigid molecules .

From an examination of the frequency dependence of equation(2.20) it can

be seen that ϵ'' reaches a maximum when $\omega=1/\tau$. At this point

$$\epsilon''_{max} = \frac{(\epsilon'_o - \epsilon'_\infty)}{2} \qquad (1)$$

The corresponding value of the dielectric permittivity under conditions of maximum loss is given

$$\epsilon' = \frac{(\epsilon'_o + \epsilon'_\infty)}{2} \qquad (2)$$

The dependence of ϵ' and ϵ'' on frequency ω may be summarised, for a single relaxation process , in diagrammatic form ,as shown in Fig.2.3

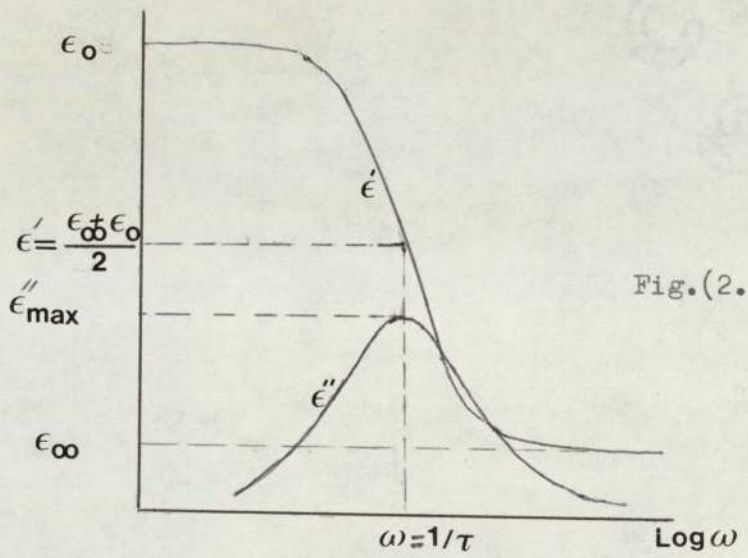

Fig.(2.3)

The strength of the relaxation process is defined as the difference between the values obtained for the low and high frequency dielectric permittivity .

Elimination of the product $\omega\tau$ from equations 1 and 2 yields the expression

$$\left(\epsilon' - \frac{\epsilon_o + \epsilon_\infty}{2}\right)^2 + \epsilon''^2 = \left(\frac{\epsilon_o - \epsilon_\infty}{2}\right)^2 \qquad (2.21)$$

This represents the equation of a semi-circle with a centre located at $\left[(\epsilon_o + \epsilon_\infty)/2 \, , \, 0\right]$ for plots of ϵ'' against ϵ' ,as shown in Fig2.4

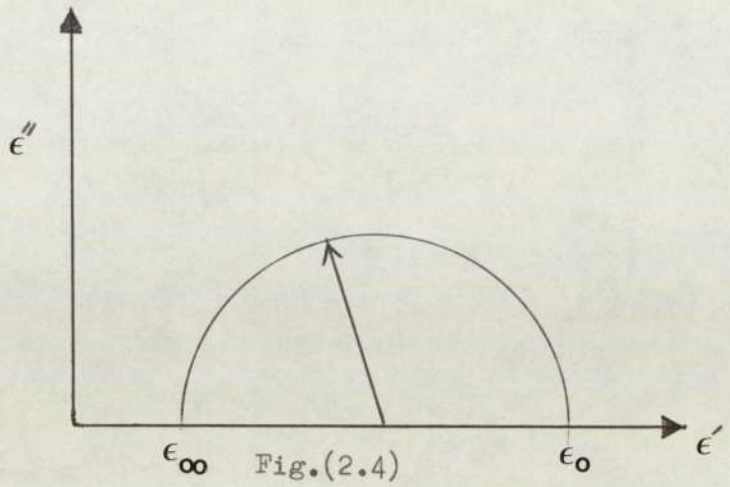

Fig.(2.4)

This relationship of ϵ'' to ϵ' is independent of the relaxation time τ . For many relaxing systems there is a variety of mechanisms available for the reorientation of molecules , each associated with a different relaxation time . Thus there is a distribution of relaxation times about a mean relaxation time . In 1941 Cole and Cole (**40**) modified the Debye equation ,to take into account the distribution of relaxation process , by replacing the term $1+i\omega\tau$ (that appears in equation for the complex permittivity) by $1+(i\omega\tau)^{\overline{\beta}}$ where $\overline{\beta}$ is an empirical parameter possessing values in the range 0 to 1

Hence

$$\frac{\epsilon^*(\omega) - \epsilon_\infty}{\epsilon_c - \epsilon_\infty} = \frac{1}{1 + (i\omega\tau)^{\overline{\beta}}} \qquad (2.22)$$

Equ. (2.22) represents a circle with a centre , C , located at

$$\frac{(\epsilon_o + \epsilon_\infty)}{2} , \quad - \frac{(\epsilon_\alpha - \epsilon_o)}{2} \cot an \frac{\overline{\beta}\pi}{2}$$

and a radius of $\left(\frac{\epsilon_o - \epsilon_\infty}{2}\right) \operatorname{cosec}\frac{\overline{\beta}\pi}{2}$

Although the Cole-Cole treatment of dielectric relaxation data has been widely used to discribe relaxation in polymer systems it is known to fail when the distribution of relaxation process is not symmetrical about the mean relaxation time . This problem was partly solved by Davidson and Cole[41], who proposed the relationship

$$\frac{\epsilon^*(\omega) - \epsilon_o}{(\epsilon_\infty - \epsilon_o)} = \frac{1}{(1 + i\omega\tau)^{\gamma}}$$

to describe the dielectric relaxation of polymers with γ lying in the range 0 to 1 . The maximum dielectric loss is achieved for the condition

$$\omega_{max}\tau = \tan\left\{\frac{\pi}{2(\gamma+1)}\right\}$$

A comparison of plots of ϵ'' Vs ϵ' for various relationships is shown in Fig (2.5)

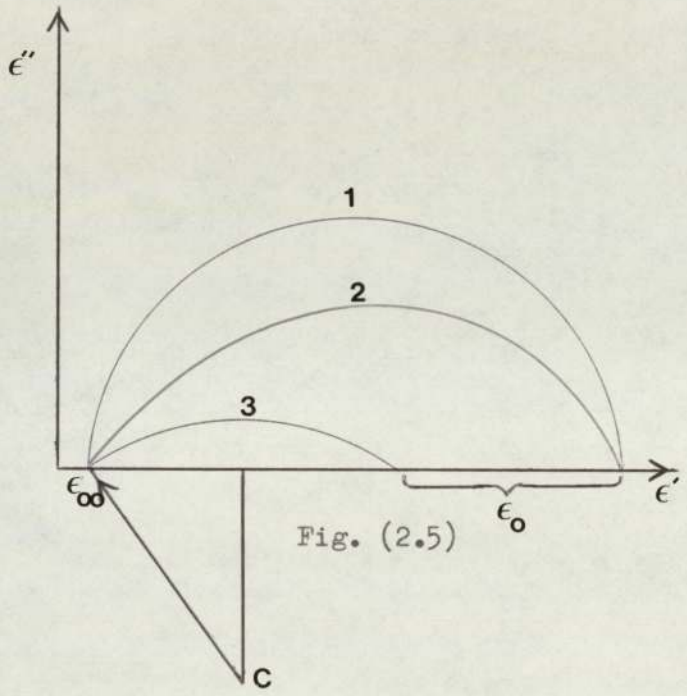

Fig. (2.5)

Where curve (1) represents ideal Debye behaviour , curve (2) Davidson-Cole behaviour and curve (3)represents Cole-Cole behaviour.

2.22 Temperature and Dielectric Relaxation

The conformation and dynamic behaviour of flexible polymer chains are affected by changes in temperature. A rise in temperature leads to an increase in the population of the higher energy conformation and also promotes the rate of interchange between conformations. For a single relaxation process associated with an activation enthalpy ΔH^* the corresponding average relaxation time , τ , is given by the

Boltzmann equation[42]

$$\tau = A \exp (\Delta H^{*} / RT) \qquad (2.23)$$

in which A represents a pre-exponential constant involving entropy changes undergone during the relaxation process .

Substitution of equ. (2.23)into equations (2.19)and(2.20) permits the temperature dependence of the dielectric permittivity , ϵ' , and dielectric loss , ϵ'' ,

$$\epsilon' = \epsilon_{o} + \frac{(\epsilon_{o} - \epsilon_{\infty}) \omega^{2} A^{2} \exp (2 \Delta H^{*} / RT)}{1 + \omega^{2} A^{2} \exp (2 \Delta H^{*} / RT)} \qquad (2.24)$$

$$\epsilon'' = \frac{(\epsilon_{o} - \epsilon_{\infty}) \omega A \exp (\Delta H^{*} / R T)}{1 + \omega^{2} A^{2} \exp (2 \Delta H^{*} / RT)} \qquad (2.25)$$

respectively . The effect of varying the temperature at constant frequency is similar to the effect of varying the frequency at constant temperature (see Fig.2.3)

2.23 Molecular Relaxation in Polymers

In this section a description is presented of the orientational relaxation process that can occur in a polymer molecule . A summary of various models , developed by previous workers, for relaxation in polymers will also be given.

The relaxation behaviour of the majority of flexible polymer molecules departs quite noticeably from ideal behaviour, i.e. single relaxation process . This divergence from ideal behaviour has been noted previously in the section dealing with the measurement and evaluation of the experimentally determined quantities ϵ' and ϵ'' . The problem now to be addressed is that concerning the development of molecular-based theories of relaxation in polymers.

2.24 Primary and Secondary Relaxation

Before proceeding further a brief definition of primary and secondary relaxation will be given in the context of dielectric relaxation . A primary relaxation (α) process is attributed to the orientational motion of the backbone of the polymer , or more strictly, the orientational motion of dipole moments rigidly attached to the atoms of the polymer backbone , Secondary relaxation (β) is normally used to describe the orientational motion of sidegroups that can rotate almost independently of the polymer backbone .

In this section a progression will be made from the rather simplistic models of polymer relaxation through to the more complicated models , such as these developed by Rouse and other workers (43-51)

One approach used to obtain relationships for describing the α-dielectric relaxation process incorporates the following assumptions :

(i) The distribution of the end-to-end distances of the polymer chains is Gaussion ,

(ii) The chain may be represented by a large number of identical independent segments ,

(iii) The volume occupied by the polymer remains unchanged during changes in conformation ,

(a) Neglect of hydrodynamic interactions

Employing the above assumptions it may be deduced that for a particular relaxation mode (process) p the relaxation time is given by equation (2.26)

$$\tau_p = A\,\eta \exp\left(\rho^2_T\right)^{-1} \qquad (2.26)$$

Where η is the viscosity of the liquid , T , the absolute temperature and A is a constant with a value that depends on several factors .

These include, bond type , the length of the polymer chains and a friction coefficient . Equ.(2.26) states that the relaxation times decrease with increasing temperature and that they vary in direct proportion with changes in the viscosity of the liquid . It may also been shown that the contribution of a relaxation mode to the configurational entropy is given by

$$S_o = k \ln \rho_v \qquad (2.27)$$

where ρ_v is the number of submolecules
and k is the Boltzmann constant . This simple relationship may be used as a starting point for the development of equations that describe the dielectric permittivity and dielectric loss of a flexible molecule in which there are ν different relaxation modes . These relationships are

$$\epsilon' = N k T \sum_{p=1}^{\nu} e^{-t/\tau_p}$$

and

$$\epsilon'' = N k T \sum_{p=1}^{\nu} \frac{\omega^2 \tau_p^2}{1+\omega^2 \tau_p^2}$$

(b) Inclusion of Hydrodynamic Interactions

In this approach the effects of hydrodynamic interactions accompanying conformational changes are included in a set of rate equations . The solution of the rate equation yields a unique set of eigenvalues λ_p. These eigenvalues correspond to the allowed relaxation times of the various orientational processes . For relaxation occurring in viscous media , described by viscosity η

$$\tau_p = \frac{M \eta [\eta]}{0.586 \lambda_p RT}$$

In the theories presented , thus far, the resulting equations have been rather empirical and lacking in molecular detail. More realistic types of theory have been presented by Kirkwood and others (see proceeding sections), at this juncture, some conclusions and

a few general comments may be useful .

Curves have already been presented that show how the dielectric permittivity, ϵ' , and loss, ϵ'' , depend on frequency for a simple model with a single relaxation time. It is recognised that rearrangements of polymer chains involve distributions of relaxation times and that this results in the experimentally determined curves of, ϵ'', and, ϵ' against $\log\omega$ being significantly different from the curves constructed using equations(2.19 and 2.20). The experimental dielectric permittivity curve is usually flatter and extends over a wider frequency range while the experimental dielectric loss curve normally exhibits a smaller maximum absorption than that predicted by equation(2.27). However, the curves are still symmetrical for such a distribution of relaxation times. The equations, initially presented to describe single relaxation processes, may be extended to systems possessing a continuous distribution of relaxation processes

Thus
$$\epsilon' = \epsilon_\infty + (\epsilon_o - \epsilon_\infty) \int \frac{F(\tau)\, d\tau}{1+\omega^2\tau^2} \qquad (2.27a)$$

and
$$\epsilon'' = (\epsilon_o - \epsilon_\infty) \int \frac{\omega\tau F(\tau) d\tau}{1+\omega^2\tau^2} \qquad (2.27b)$$

Where the quantity $F(\tau)d\tau$ represents the fraction of molecules possessing relaxation times between τ and $\tau+d\tau$ at any given instant in time .

The Kirkwood theory predicts a broad symmetrical curve for ϵ'' but the high frequency side differs from that observed experimentally for glass-rubber relaxation processes. This non-symmetry is a typical feature of α-relaxation peaks of amorphous polymers.
A molecular theory that accounts for the skewness of the ϵ'' curves of amorphous polymers has been proposed to explain these observations

by Yamafuji[52]. This theory provides a reasonably accurate representation of experimental behaviour for many types of polymer in that the theoretically predicted loss curves are non-symmetrical on the high-frequency side. However, the half-width predicted by this theory, is significantly less than that observed experimentally. Fig. (2.6) shows several master curves of $\epsilon''(\omega)/\epsilon''_{max}$ and ϵ' plotted against $\log(\omega/\omega_{max})$ for several different polymers.

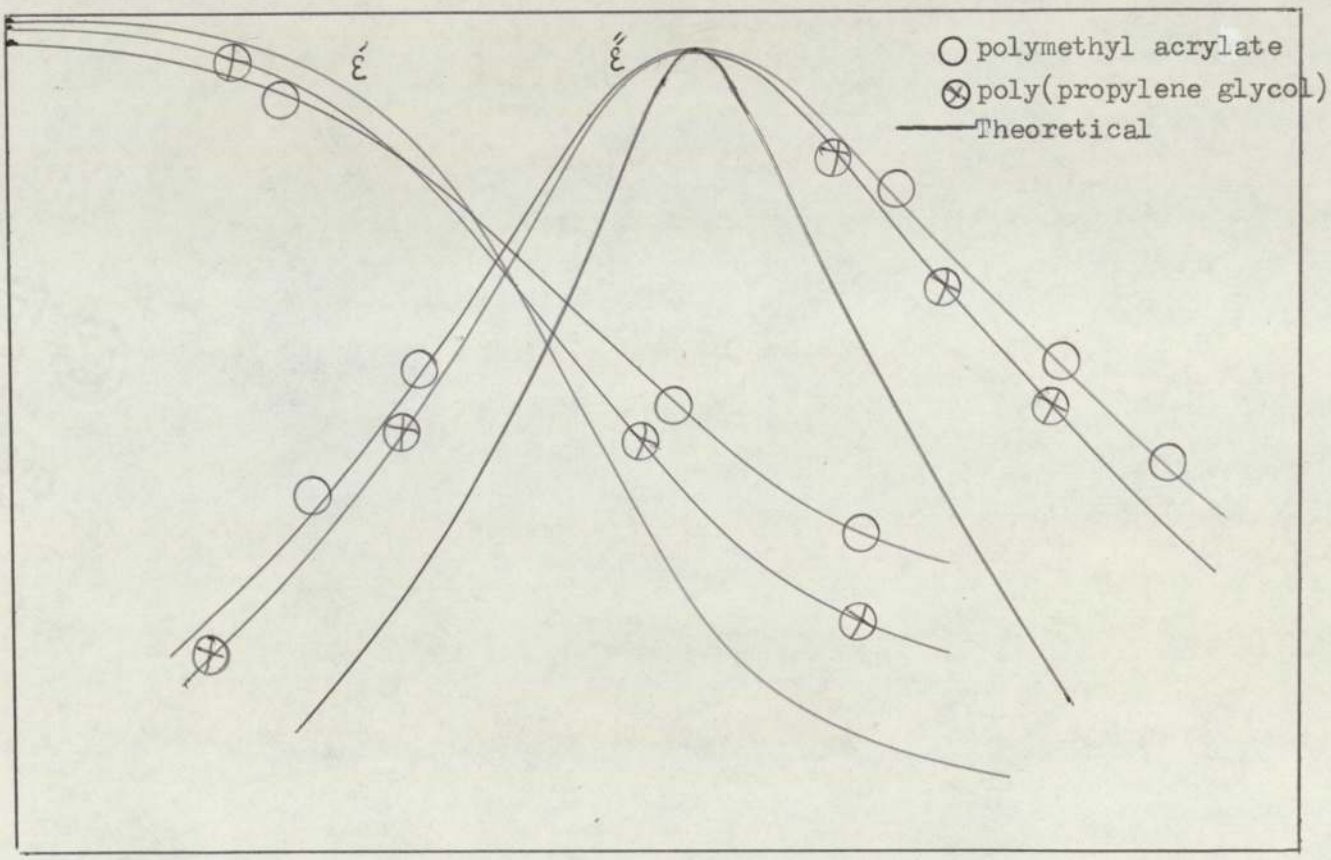

Fig. (2.6)

CHAPTER 3

3.1.1 Experimental Methods

The experimental techniques employed in this thesis are mainly concerned with the measurement of dielectric permittivity and dielectric loss over a range of frequencies and at various temperatures . The measurement of the static dielectric permittivity and the calculation of the permanent dipole moment therefrom is a long established method for the detailed investigation of molecular structure .

Considerable information concerning the motion and flexibility of polymer molecules can be deduced from the frequency dependence of the dielectric permittivity and dielectric loss .

Two main types of equipment were employed to measure the dielectric properties of pure poly(propylene glycols) and solutions of poly(propylene glycols) containing salts .
One apparatus was comprised of a Wayne Kerr Universal Bridge Type B221 , an Advance Type J Model 2 Audio Frequency Generator and a General Radio Tuned Amplifier and Null Detector Type 1232-A . The sample cell Fig-3.1 was connected to the input terminals of the Bridge by two screened cables . The second apparatus was a single unit based on a General Radio Model 1689 Bridge.

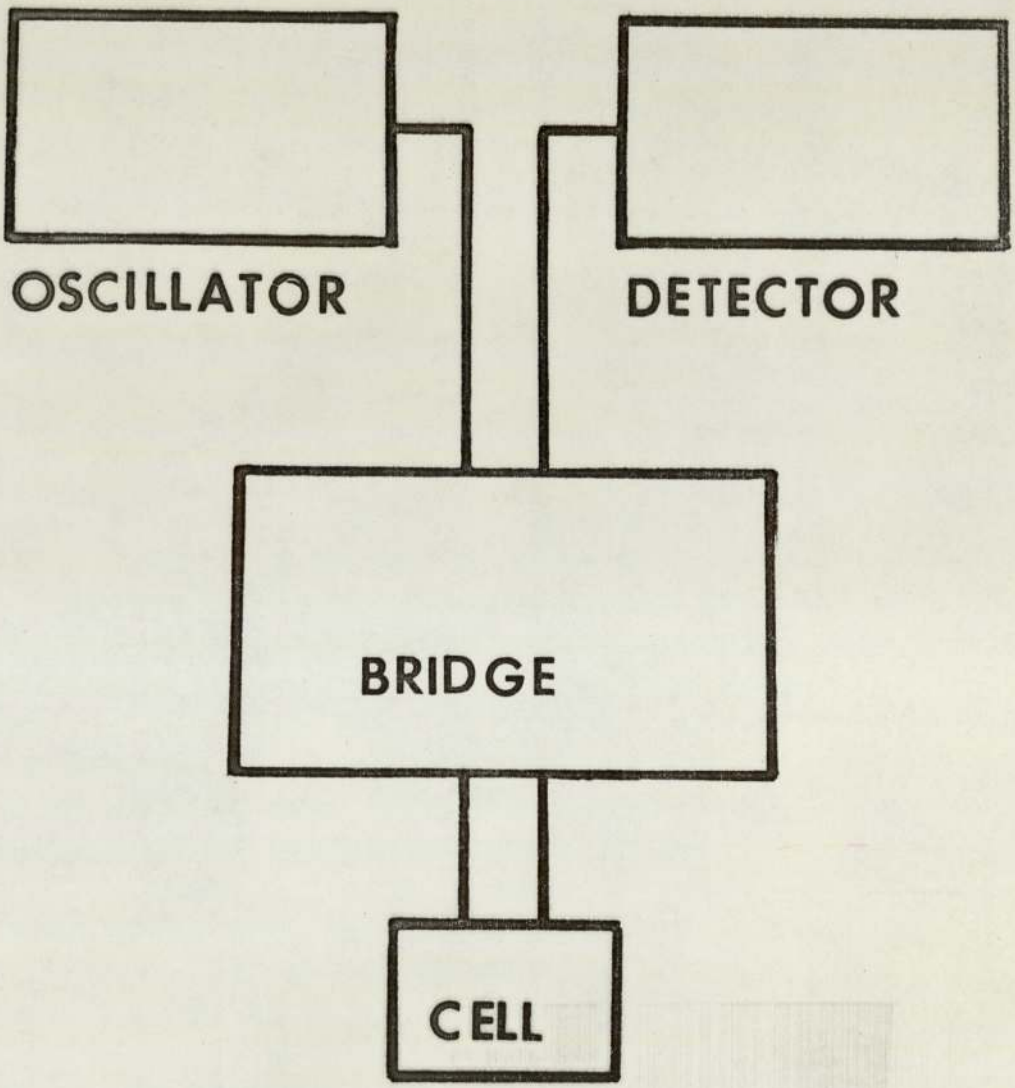

Fig-3·1

DIELECTRIC APPARATUS

3.1.2 Dielectric Cell

In order to facilitate dielectric measurements on small volumes of sample over a wide range of temperatures two terminal cell was designed in this labaratory and constructed by the Glass Blowing Workshop and the Mechanical Workshop . The essential components of the cell are shown in Fig-3.2 . Rectangular shaped electrodes were cut from 1mm thick stainless-steel and measured approximately 33mm by 11mm . Small squares of polytetrafluoroethylene (P.T.F.E.) positioned between the electrodes ensured that the gap between the electrodes was approximately 1mm . Connection to the electrodes were made by welding a stout tungsten wire to each electrode . These wires passed through and were fixed into a B19 Quickfit male adaptor . This electrode assembly fitted into an air-tight Pyrex glass tube . The volume of the tube was approximately 30 cm^3 . The sample volume was somewhat less then this .

3.1.3 Calibration of the dielectric cell

If the dimensions of a dielectric cell are accurately known then from the measurement of electrical capacitance , C , and a.c. conductance , G , the dielectric permittivity , ϵ' , and dielectric loss , ϵ'' , may in principle , be calculated using the relationships

$$\epsilon' = \frac{3.6\,\pi\,dC}{A} \qquad (3.1)$$

$$\epsilon'' = \frac{3.6\,\pi\,dG}{A} \qquad (3.2)$$

where d is the separation between electrodes of equal area A . However , this approach , though essential for the absolute determination of dielectric properties, is difficult to accomplish because of a several experimental difficulties related to the accuracy of cell construction , stray capacitance in connecting

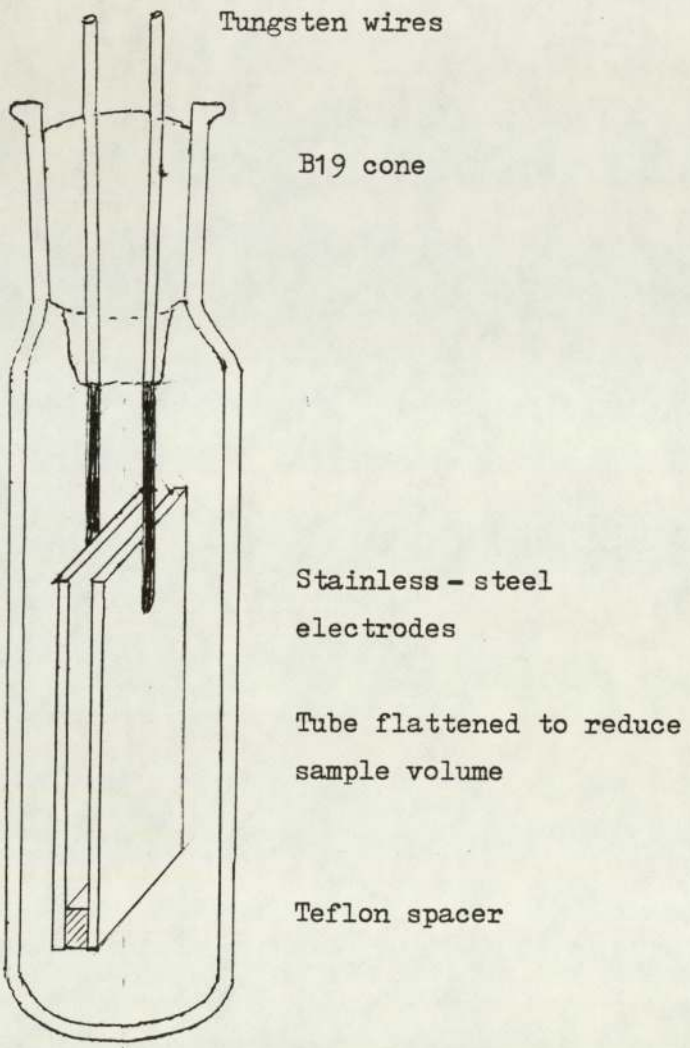

Figure 3.2 The Dielectric cell

leads etc and non-uniform electric fields at the periphery of the electrodes .

An alternative approach , that has proved to be very reliable and accurate is based upon the measurement of the capacitance of a cell when filled with a material possessing an accurately known dielectric permittivity .

Denoting the capacitance of the empty cell , that of the cell filled with sample and that of the fixed stray capacitance by C_a , C_x and C_s , respectively, the dielectric permittivity of the dielectric may be calculated using the following simple expression

$$\varepsilon' = \frac{C_x - C_s}{C_a - C_s} \qquad (3.3)$$

For a fixed cell configuration the quantities C_s and C_a may be regarded as constants and easily determined by the capacitance of the cell when empty and when filled with two liquids of known dielectric permittivity (or dielectric constant) .

The dielectric loss factor , $\tan\delta$, may be calculated by the following expression .

$$\tan\delta = \frac{G}{\omega C} = \frac{G}{2\pi f C} \qquad (3.4)$$

Where ω is the angular frequency of the measuring electric field and f is the normal periodic frequency expressed in Hz . The absorbtion of energy from the applied electric field is denoted by ε'' , the 'loss' , and is the product of the corresponding dielectric permittivity and the loss factor

$$\varepsilon'' = \varepsilon' \tan\delta \qquad (3.5)$$

Plots of ε' against logf (or $\log\omega$) and ε''against log f are called dispersion curves and absorption curves , respectively .

3.1.4 Temperature Control

Great importance is placed upon the accurate control of temperature during the measurement of capacitance and loss of polymeric materials . For such materials it is well known that the position , with respect to frequency , of the maximum dielectric loss (the loss maximum) is quite sensitive to changes in temperature due to relative large activation energy associated with the rotational motion of sections of polymer chains .

Also, at very low temperatures the contribution of d.c. electrical conductivity to energy losses is normally quite small compared to that arising from mechanisms responsible for dielectric loss.

For the work reported in this thesis the accurate control of sample temperature was achieved by means of a Townson and Mercer Cryostat . This apparatus consists of two large capacity reservoirs of acetone . One reservoir, the cold reservoir , is maintained at a temperature of approximately 193K using solid carbon-dioxide . A second reservoir , the regulated reservoir, into which the dielectric cell is placed , is maintained at the required temperature in the range 198K to 263K and is fitted with a stirrer-pump assembly . There is no direct connection between the contents of the two reservoirs . The temperature of the regulated reservoir is controlled by means of a solenoid operated control value which , when open ,permits the coolant of the regulated reservoir to circulate through a heat transfer unit immersed in the cold reservoir . The temperature of the regulated reservoir is continuously monitored by thermistor temperature sensor that is part of the input network of a bridge amplifier .

Any departure of temperature from the set temperature results in either the opening or closing of the control valve . The temperature of the regulated reservoir can be maintained to an accuracy of $\pm$ 0.5 °C , but this can be significantly improved by the manual adjustment of a shutter in the pump assembly . The shutter determines the proportions of coolant sent to the heat exchange unit to that bypassed to the regulated reservoir .

Nuclear Magnetic Resonance spectra (^{1}H, ^{13}C and ^{199}Hg) and spin-lattice relaxation times, T_1, were measured using a Jeol FX 90 Q Fourier Transform Spectrometer. The majority of the ^{13}C spectra were obtained using broad-band proton decoupling.

3.2.1 Materials

Although a range of poly(propylene glycol) polymers with different molecular weights are available , the present study was primarily concerned with studying the dielectric behaviour of solutions of various salts dissolved in polymer samples possessing molecular weights of 2025 (PPG2025) and 4000(PPG4000) . These polymers were supplied by BDH Ltd (PPG2025) and by Aldrich Chemical Co(PPG4000) . The purity and distribution of molecular weights in these samples was ascertained using gel permeation chromatography (g p c) . The gpc chromatograms for PPG2025 and PPG4000 are shown in (Fig3.3). Both of these materials possess narrow molecular weight distributions, implying that ($\bar{M}_n = \bar{M}_w$). The chromatogram of the higher molecular weight material (PPG4000) indicates the presence of a small amount (estimated to be about 0.5 % by weight) of impurity eluting at a point that would correspond to a molecular weight of approximately 2000 . Both PPG2025 and PPG4000 contained small amounts of a relatively low molecular weight material .

It is generally well known that alkyl oxides are usually hygroscopic. The low molecular weight members of this family of compounds may be readily dried using a variety of methods . However , for compounds possessing medium to high molecular weights, ranging through highly viscous liquids to rubbery solids the removal of water is more difficult . For the polymeric liquids , PPG2025 and PPG4000, the addition of a drying agent would not be expected to be an efficient process for the removal of small amounts of water unless aided by vigorous mechanical dispersion . Also the ultimate separation of a finely dispersed drying agent and a viscous polymer is a tedious process. An alternative method is

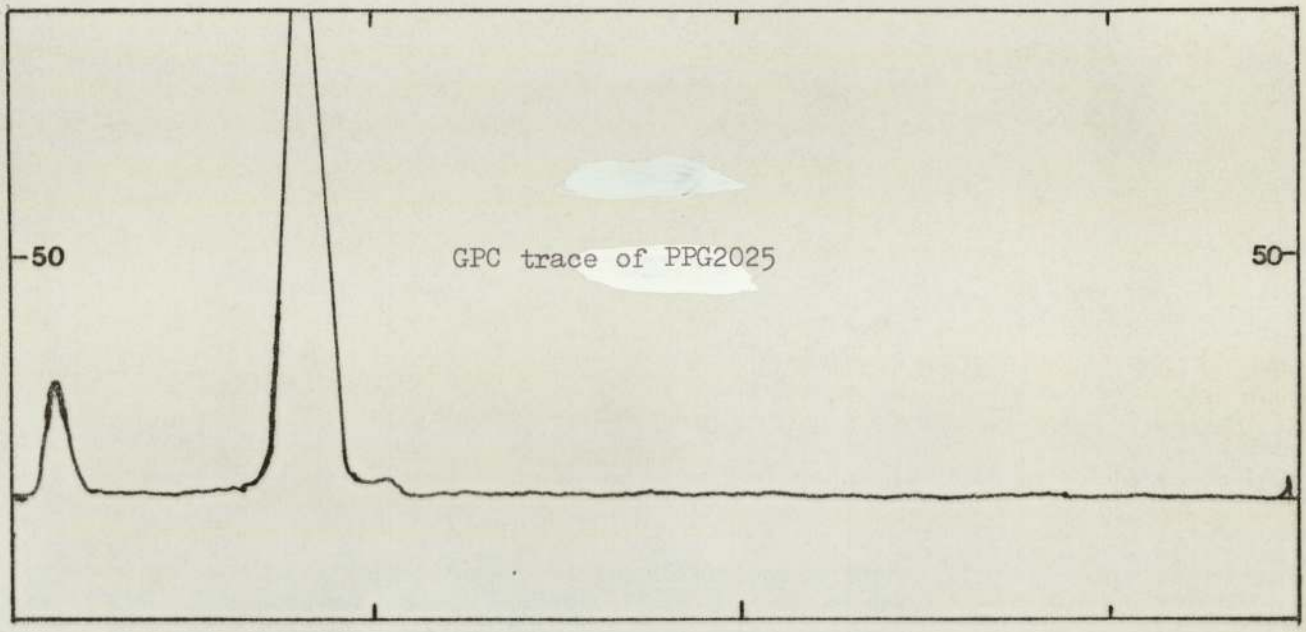

Elution time

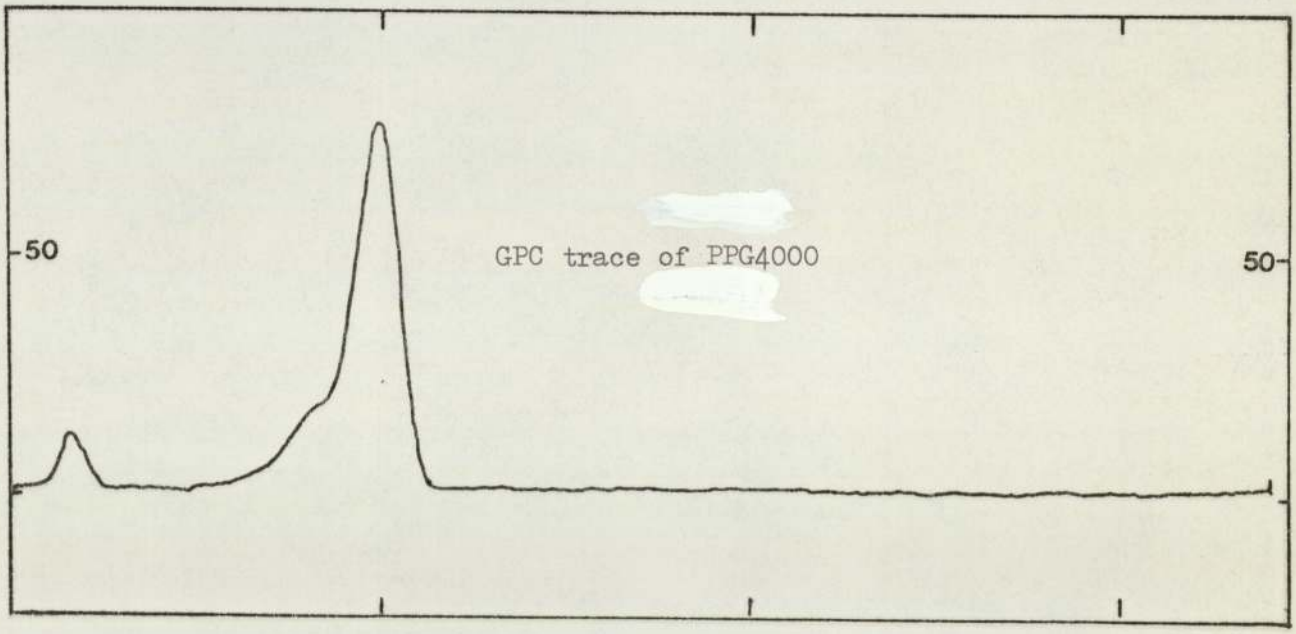

Fig(3.3)

to dry a solution of the polymer in a suitable solvent . This approach, though facilitating the removal of water , is marred by the necessity of having subsequently to remove the solvent . In addition , there is , associated with this method , the distinct possibility of inadvertently replacing the water impurity with solvent impurity . All of the above mentioned methods for removing water were attempted in this study with varying of sucess, but that involving addition of drying agent to PPG4000 was subsequently abandoned . Tests for the presence of water in the parent polymer , using anhydrous $CuSO_4$ and anhydrous $CoCl_2$ proved negative. However, it is recognised that small amounts of tightly-bound water could remain in the polymer samples. The amount of water is believed to be quite small since BDH quote water levels in these polymer that are less then 0.3% i.e. an average of one water molecule for one hundred repeat units .

Details concerning the origin and treatment , where applicable , of the various inorganic salts and organic solutes are presented in the following sections .

3.2.2 Preparation of Solutions

Samples of poly(propylene glycol) containing different amounts of anhydrous mercuric chloride were prepared using a co-solvent technique involving methanol . The methanol was dried by standing over activated zeolite (5A) and then purified by fractional distillation . A 2 mole per cent (based on moles of polymer repeat units) solution of mercuric chloride in PPG4000 was prepared in the following manner . Anhydrous mercuric chloride (BDH purity > 97%) (2.388g) was dissolved in methanol (50 cm^3) placed in a 100 cm^3 tightly stoppered round-bottomed flask. A solution of poly(propylene glycol) (PPG4000) (25g) in methanol (50 cm^3) was also prepared in a 100 cm^3 stoppered flask .

The solution of mercuric chloride was then added to the polymer solution with stirring to give a 2 mole per cent concentration of salt relative to polymer repeat units . The polymer-salt solution was transferred to a 200 cm^3 round-bottomed flask and was fitted with a still-head thermometer and water-cooled condensor . Using this arrangement the major portion of the solvent was removed by distillation under atmospheric pressure. The apparatus was fitted with a $CaCl_2$ trap to prevent ingress of water. The remaining methanol was removed by prolonged vacuum distillation. During this latter stage the temperature of the residue was not allowed to exceed 333K. Higher temperature are believed to lead to a breakdown of the polymer by the inorganic salt.

A 4 mole per cent solution of mercuric chloride in PPG 4000 was also prepared , in the same manner just described , but using 4.87 g of salt . Additional solutions, containing 1.45 mole percent and 2.86 mole percent mercuric chloride , were prepared by dissolving 1.37 g and 2.75 g of salt in 20g of PPG4000 .

The final polymer-salt solutions exhibited viscosities that were obviously substantially greater than the pure polymer . the solutions were colorless and clear . Solutions of mercuric chloride in the lower molecular weight poly(propylene glycol) (PPG2025) were also prepared , using methanol as a co-solvent . The PPG2025 was dried by standing it over activated zeolite for several days . Solutions containing 2 mole percent , 4 mole percent and 7 mole percent of mercuric chloride were prepared by taking 2.38 g , 4.87 g and 8.80 g respectively , and 25 g of polymer .

A 1 mole percent solution of Cobaltous chloride (Hopkin and Williams Ltd, GPR $>$ 97%) in poly(propylene glycol)(PPG4000) was prepared by adding 0.45 g of the salt to 20g of the polymer contained in a 15 mm diameter test tube . The mixture was heated for several minutes over the cool-flame of a bunsen burner to aid

dissolution of the salt . The maximum temperature of the solution was approximately 423K . A 2 mole percent solution of cobaltous chloride in PPG4000 was prepared using the same approach , by dissolving 0.91 g of the salt in 20g of polymer .

Solutions of cadmium iodide (Fisons Analytical Reagent) in PPG4000 were prepared by the direct addition of the salt to the pure polymer . Polymer-salt solutions containing 1 mole percent and 2 mole percent of CdI_2 were made by heating 1.27 g and 2.57 g of salt and 20g of polymer in 15 mm diameter test-tubes .

Attempts were also made to prepare solutions of zinc chloride (May and Baker Ltd $>$ 95%) in PPG4000 . Difficulties were encountered , since $ZnCl_2$ is a deliquescent material . The hydrated salt was placed in a test tube and subjected to gentle heating over the cool-flame of a bunsen burner , in order to drive off the water of crystallization . Whilst still hot the anhydrous zinc chloride was crushed into a powder . The test-tube and contents were then allowed to cool . An estimated quantity of the dry salt was then transferred to a stoppered test tube of known weight . Re-weighing enabled the exact weight of salt to be determined . A quantity of poly(propylene glycol) (PPG4000) (20g) was added and complete dissolution was achieved after heating the mixture to ca. 423K for a period of 5-10 minutes . The same procedure was used to prepare a 0.5 mole percent solution of anhydrous zinc chloride in PPG 4000 .

CHAPTER 4

Results

4.1 Dielectric Data for the poly(propylene glycol) - mercuric chloride system

The temperature and frequency dependence of the static dielectric permittivity, ε', and dielectric loss, ε'', of anhydrous solutions of mercuric chloride in poly(propylene glycol) (PPG 2025 and PPG 4000) have been studied using apparatus described in detail in Chapter 3.

4.2 The Dielectric Permittivity Results

The dependence of the static dielectric permittivity (dielectric constant) on temperature, in the range 218 - 263K, and frequency (0.3 - 20 k Hz) for 2 mole percent. and 4 mole percent solutions of mercuric chloride in PPG 2025 is shown in Figures 1 and 2, respectively. This data corresponds to the principal dielectric relaxation regions exhibited by these two systems. For the PPG 2025 - 2% $HgC\ell_2$ system (Figure 1) the minimum value of ε' is displaced to lower temperatures as the measurement frequency is decreased; behaviour that is typical of a homogeneous, amorphous, dipolar polymer. For PPG 2025 - 2% $HgC\ell_2$ the maximum dielectric constant ($\varepsilon_o \sim 8$) measured at 500 Hz, appears to have been attained at temperatures greater than 248K. The corresponding minimum or high frequency dielectric constant (ε_∞), measured at 218K and 20 k Hz is close to 3. Increasing the concentration of

mercuric chloride to 4 mole % (Figure 2) results in a significant increase in the static dielectric constant of the PPG 2025 system. For the range of temperatures and frequencies considered the maximum value of ε' has not quite been attained, but an estimate of ε'_0 gives a value that is a little greater than 9.

The behaviour of the dielectric permittivity ε' of 2 mole % and 4 mole % solutions of mercuric chloride in PPG 4000 was similar to that observed for the PPG 2025 - $HgCl_2$ solutions (see Figures 3 and 4). The difference in the molecular weight of the polyether was manifested by a displacement of the relaxation region to higher temperatures for any chosen frequency. The value of the high frequency dielectric constant was close to 3. The dispersion curves (ε' vs log f/Hz) for PPG 2025 - $HgCl_2$ (2, 4 and 7 mole %) and PPG 4000 - $HgCl_2$ (2 and 4 mole %) for the temperature range 220 - 252K are presented in Figures 5-9. For the PPG 2025 - $HgCl_2$ solutions the static dielectric permittivity varies from 8 to approximately 11 over the concentration range 2 - 7 mole % $HgCl_2$. The increase in ε' with increasing concentration of mercuric chloride is probably due in part to the highly polarisable molecules of mercuric chloride. However, the high frequency dielectric permittivity ε_∞, only varies slightly (~2.9 to ~3.3) over the entire range of salt concentration. It therefore seems reasonable to conclude that $HgCl_2$ (which is linear and non-polar in the gas-phase) forms dipolar complexes

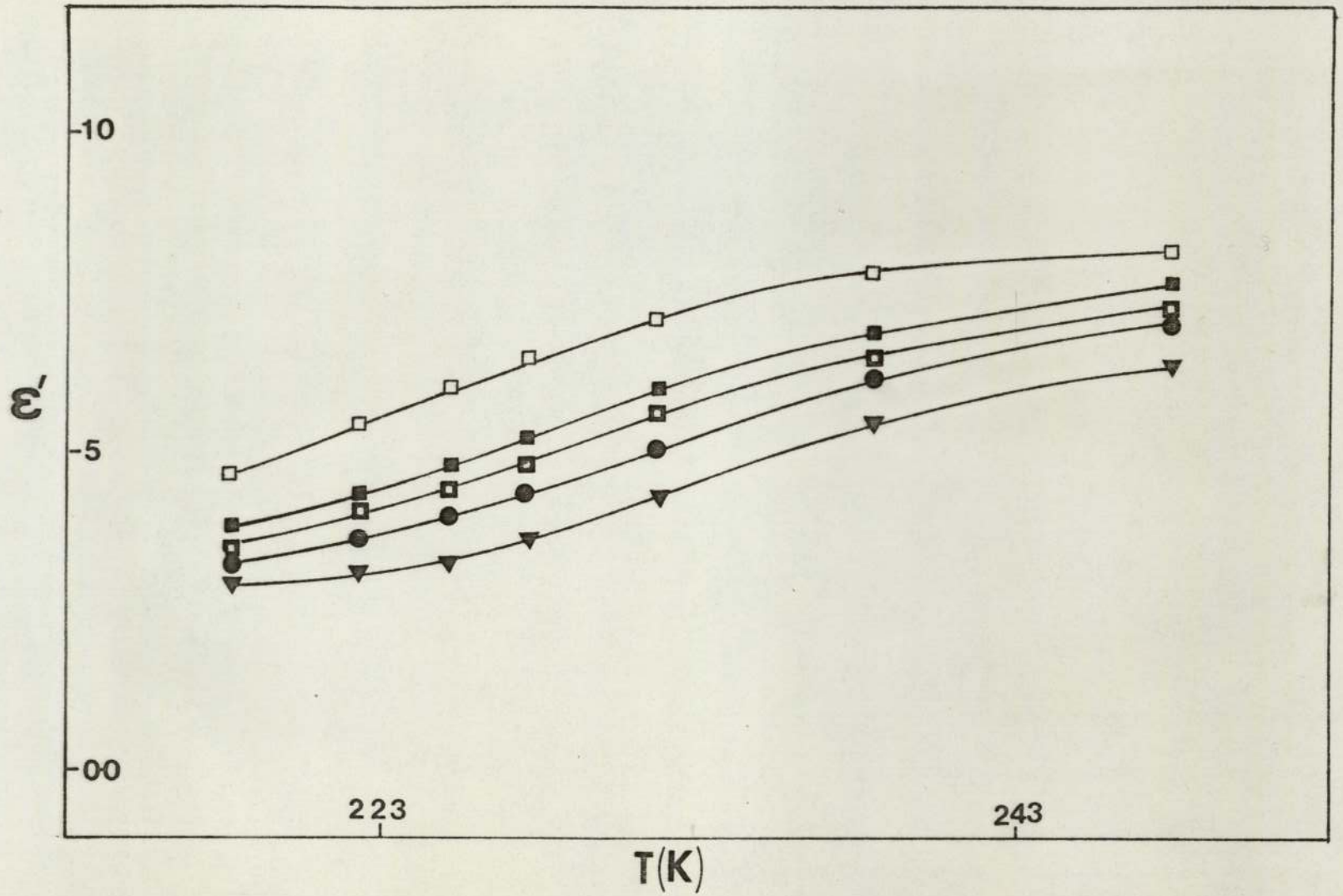

Fig(4.1)

Dielectric constant, ϵ', Vs temperature at □0.5, ■3, ◘5, ●10 and ▼20 KHz for PPG2025+2mole%$HgCl_2$

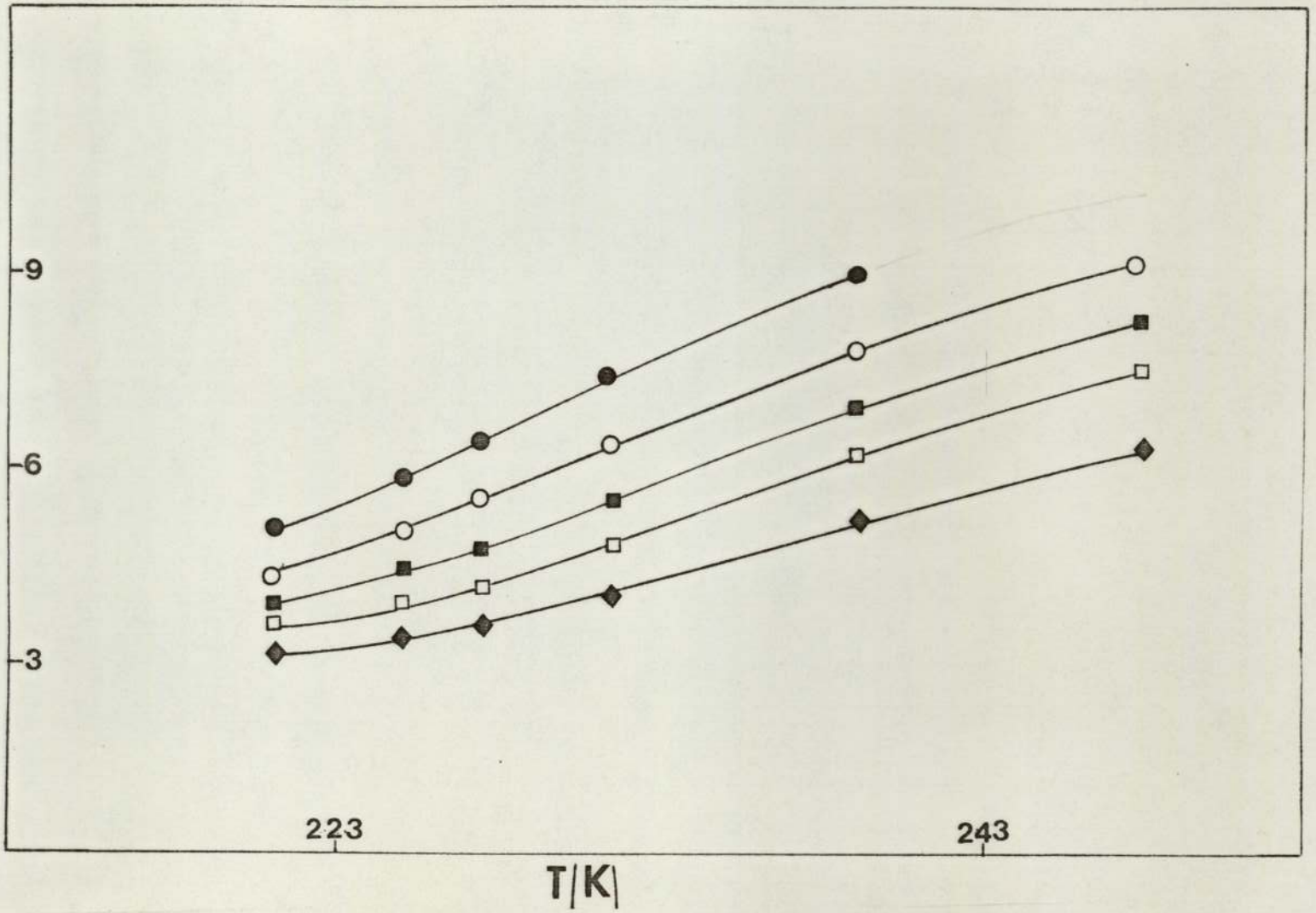

Fig(4.2)

Dielectric constant, ϵ' Vs temperature at ●0.3, ○1, ■3, □7 and ◆20 KHz for PPG2025+4mole%$HgCl_2$

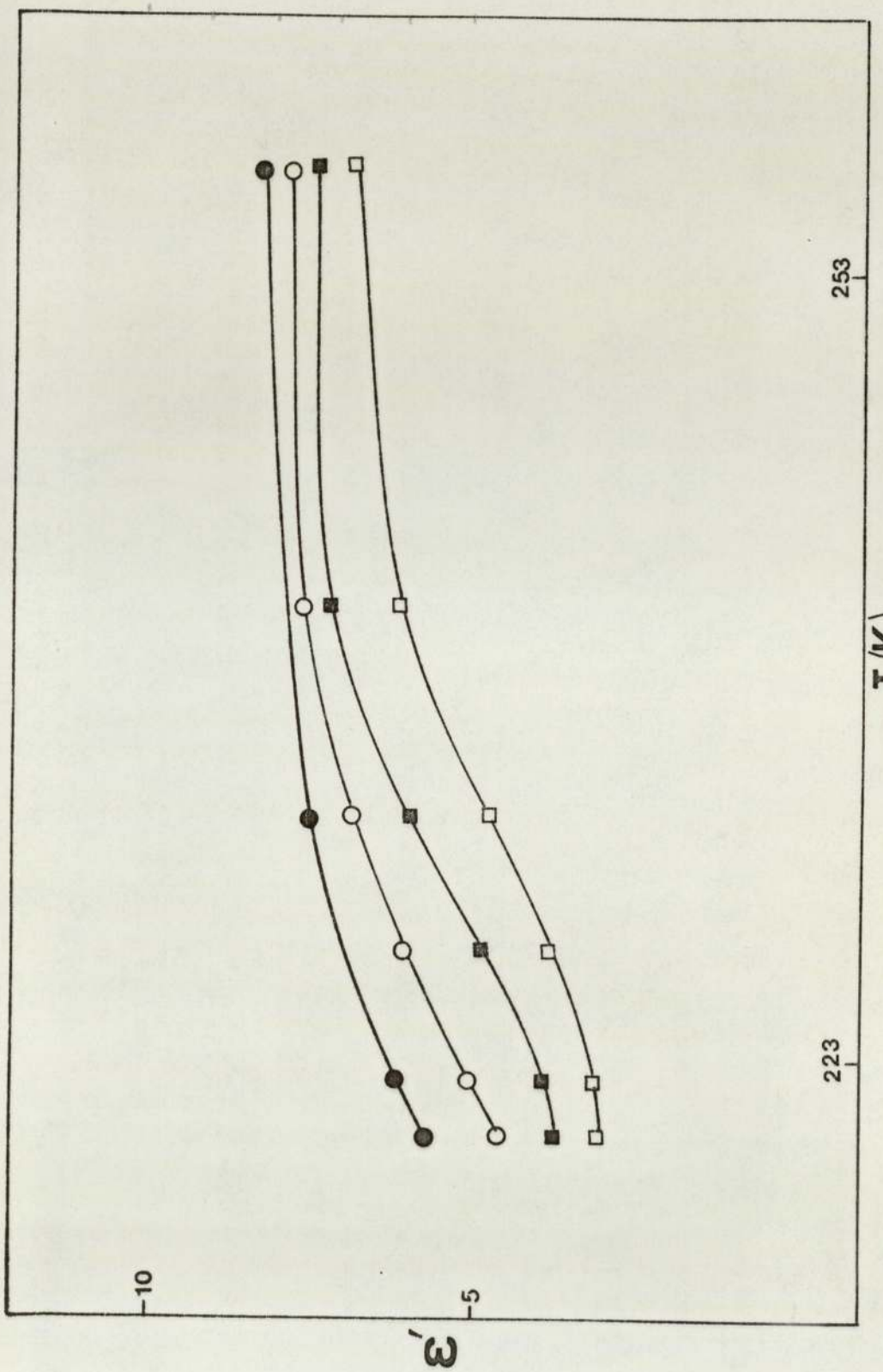

Dielectric constant, ϵ', Vs temperatur at ● 0.2, Ol, ■5, and □20 KHz for PPG4000+2mole%$HgCl_2$

Fig(4.3)

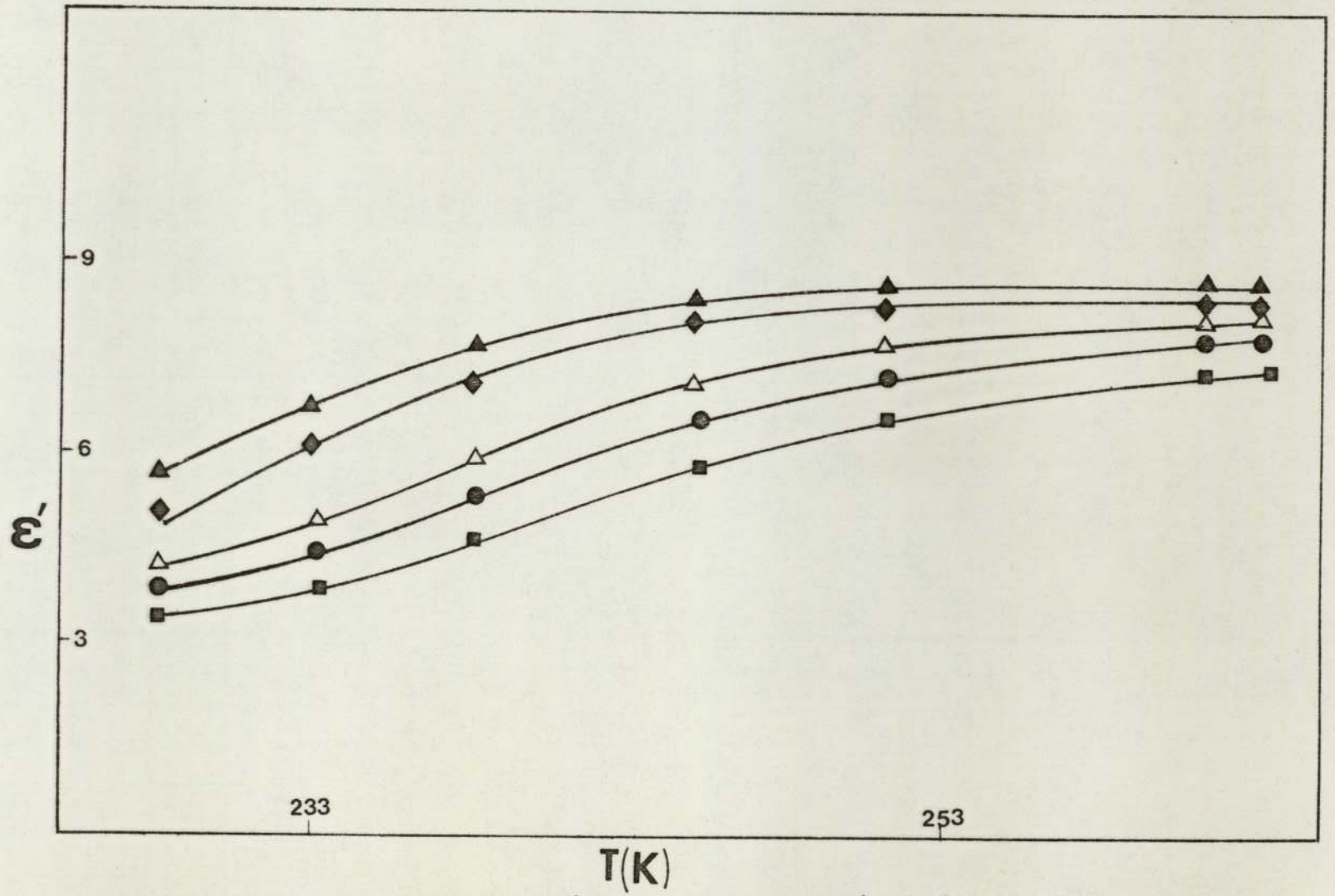

Fig(4.4)

Dielectric constant, ϵ', Vs temperature at ▲0.5, ◆1, △5, ●10 and ■20 KHz for PPG4000+4mole%$HgCl_2$

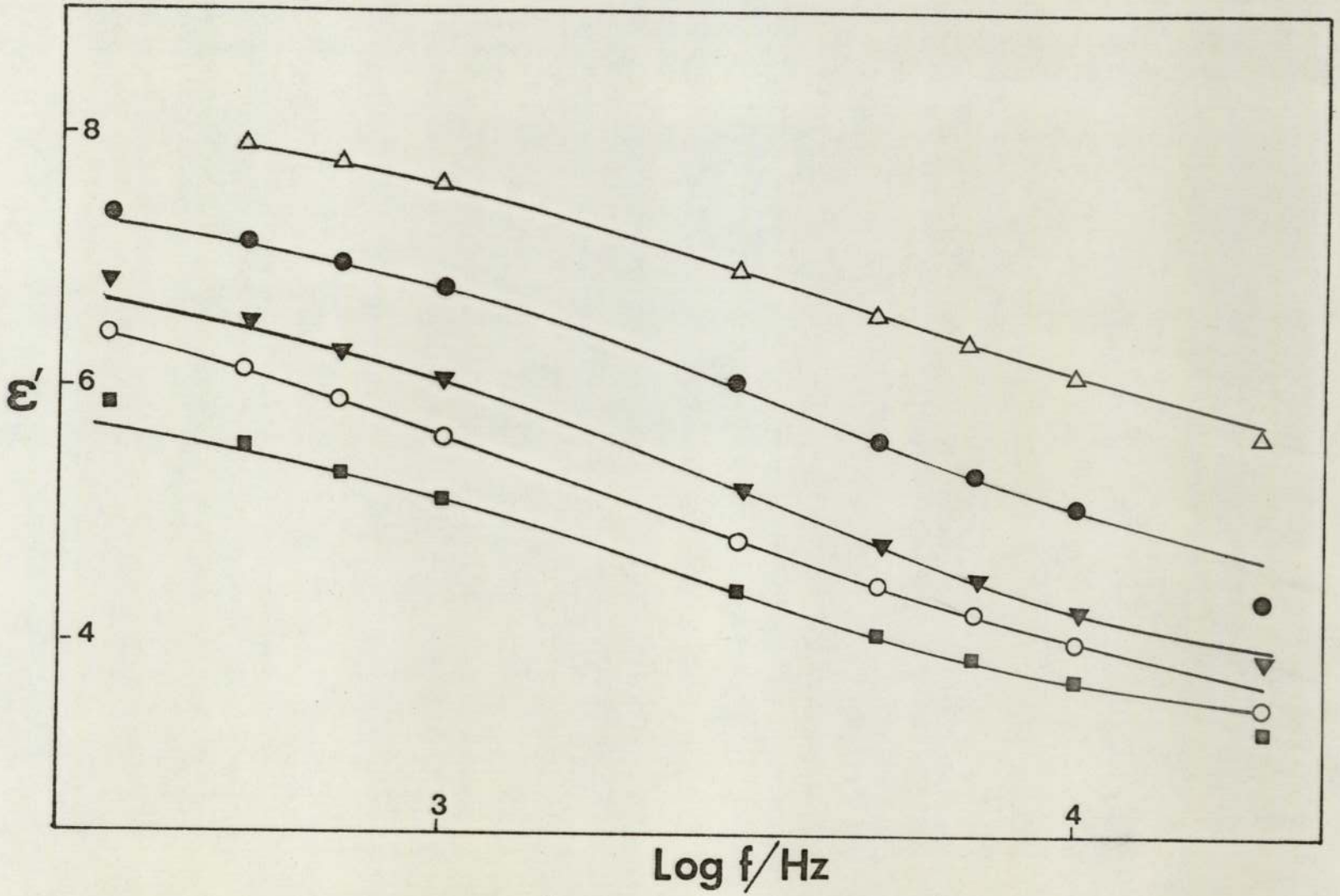

Fig(4.5)

Dielectric constant, ϵ', Vs log f for PPG2025+2mole%HgCl2at various temperature △238.3K, ●231.4, ▼227.4, O225K and■222K

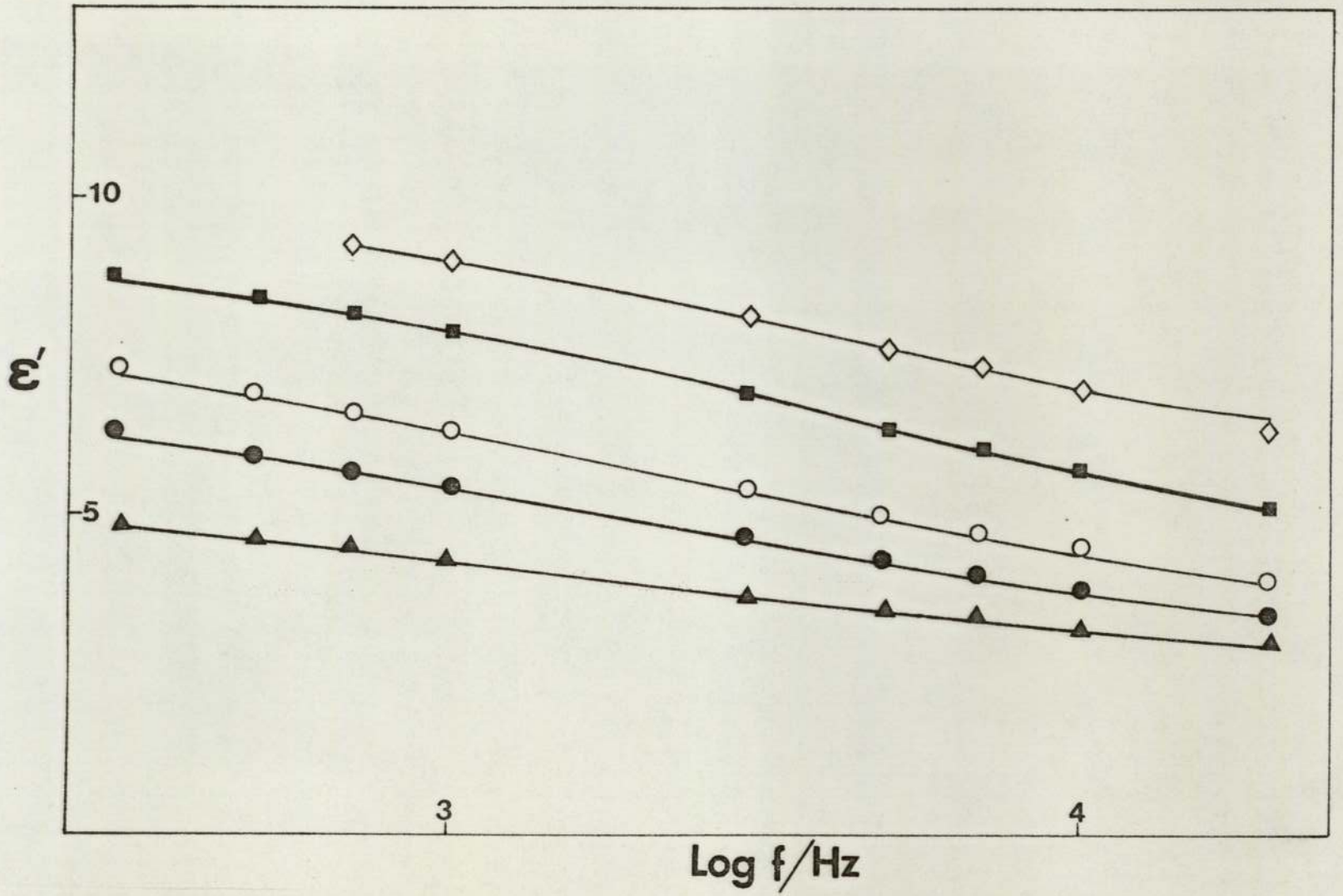

Fig(4.6)

Dielectric constant, ϵ', Vs log f for PPG2025+4mole%$HgCl_2$ at various temperature ◇247.8K, ■239K, ○231.4K, ●227.4K and ▲221K

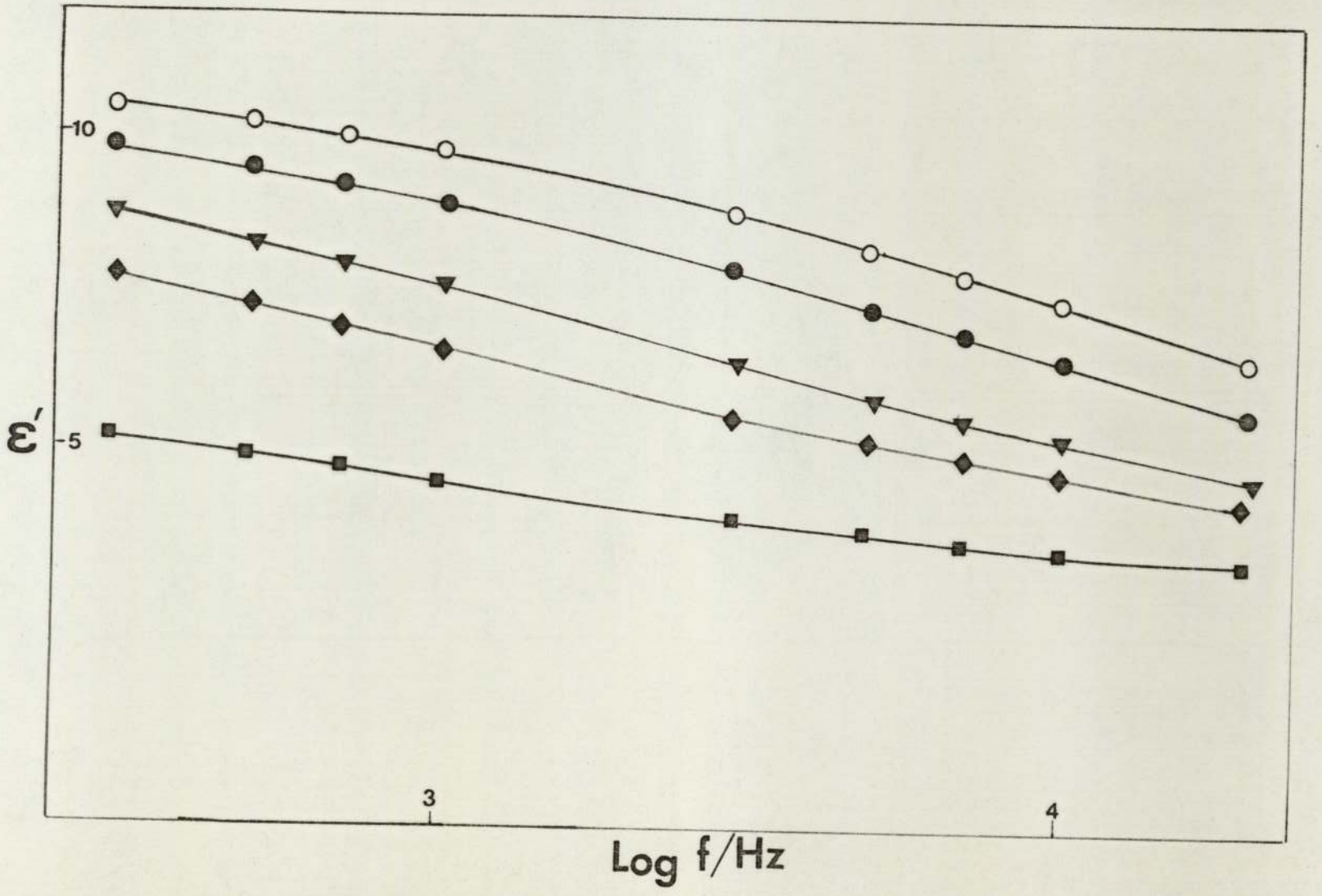

Fig(4.7)

Dielectric constant, ϵ', Vs log f for PPG 1025+7mole%$HgCl_2$ at various temperatures ○252K, ●248K, ▼242K, ◆238K and ■228K

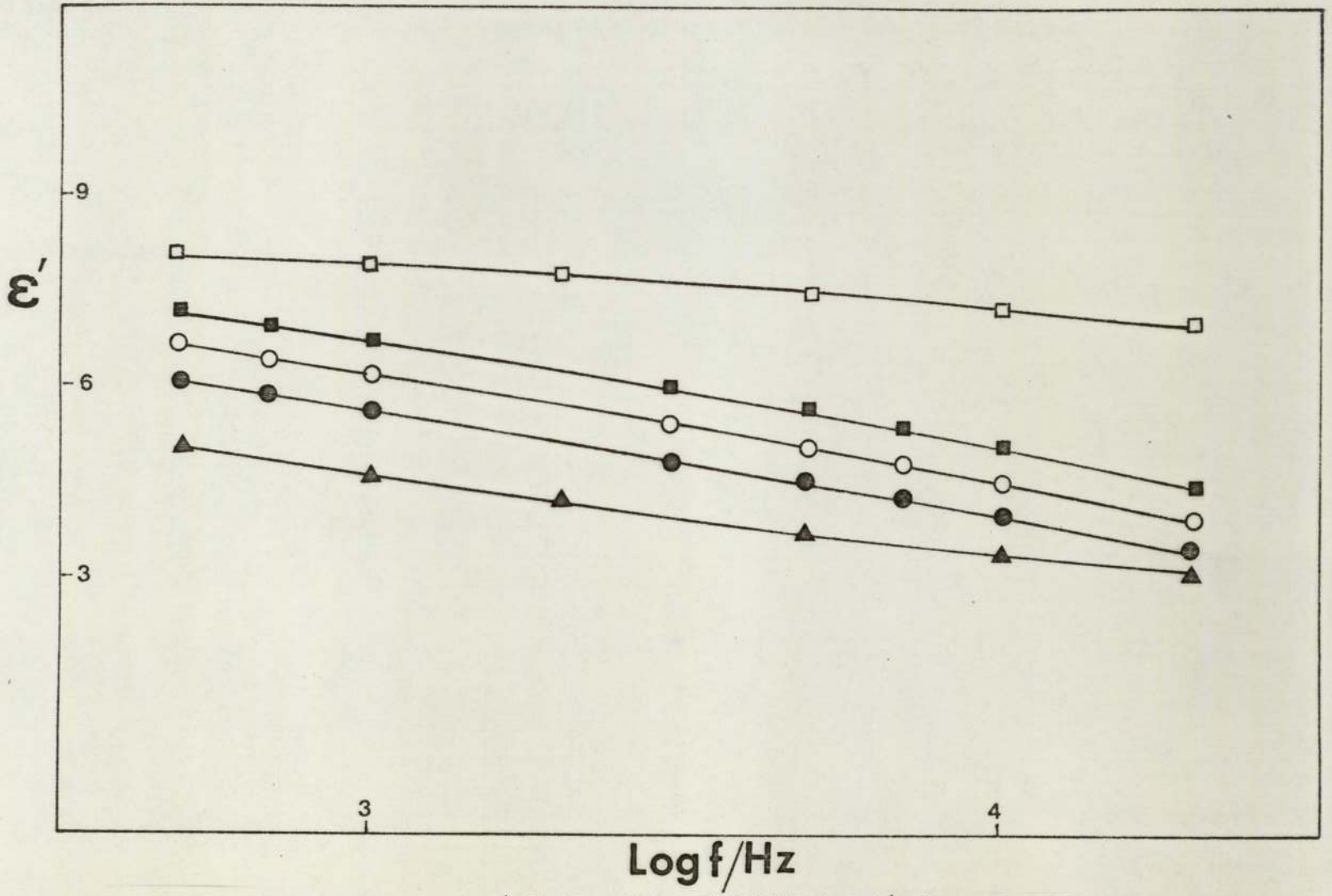

Fig(4.8)

Dielectric constant, ϵ', Vs log f for PPG4000+2mole%$HgCl_2$ at various temperatures □254K, ■230K, ○227K, ●224K and ▲220K

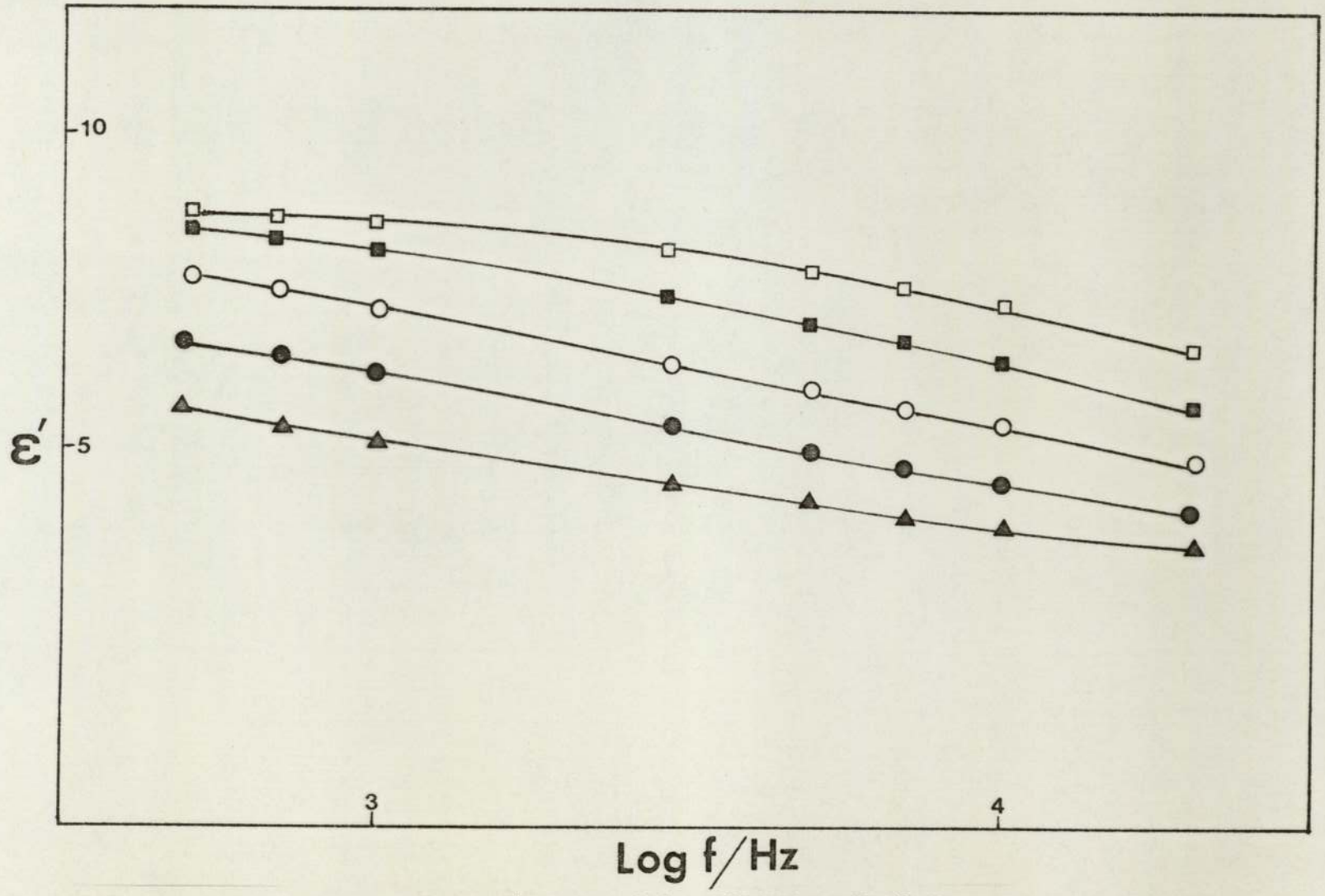

Fig(4.9)

Dielectric constant, ϵ', Vs log f for PPG4000+4mole%$HgCl_2$ at various temperatures □251K, ■245K, ○238K, ●233K and▲228K

with segments of the polyether molecules.

4-3 The Dielectric Loss Results

The variation of the dielectric loss, ε'', with respect to temperature for different spot frequencies in the range 0.3 - 20 kHz is shown in Figures 10 - 13 for PPG 2025 - $HgC\ell_2$ and PPG 4000 - $HgC\ell_2$ solutions containing 2 and 4 mole % concentrations of salt. The presence of a broad α-type relaxation process is readily discernible. For both PPG 2025 and PPG 4000 the magnitude of the loss maximum measured at 20 kHz is increased by approximately 0.1 - 0.3 units when the concentration of mercuric chloride is raised from 2 to 4 mole %. As the temperature is decreased the magnitude of the loss maximum also decreases steadily as its position on the temperature axis moves towards lower temperatures. The maximum loss (~1.3) observed for the PPG 2025 - 4% $HgC\ell_2$ system is slightly greater than that (~1.1) found for PPG 4000 - 4% $HgC\ell_2$. It is difficult to be precise about the origin of this small difference in ε''_{max}. Experimental error could, possibly, account for some if not all of the difference. The presence of a higher concentration (~ x 2) of terminal hydroxyl groups in PPG 2025 could also be a contributing factor.

The variation of dielectric loss, ε'', as a function of frequency, f, can be most clearly seen in plots of ε'' vs f, presented at different temperatures

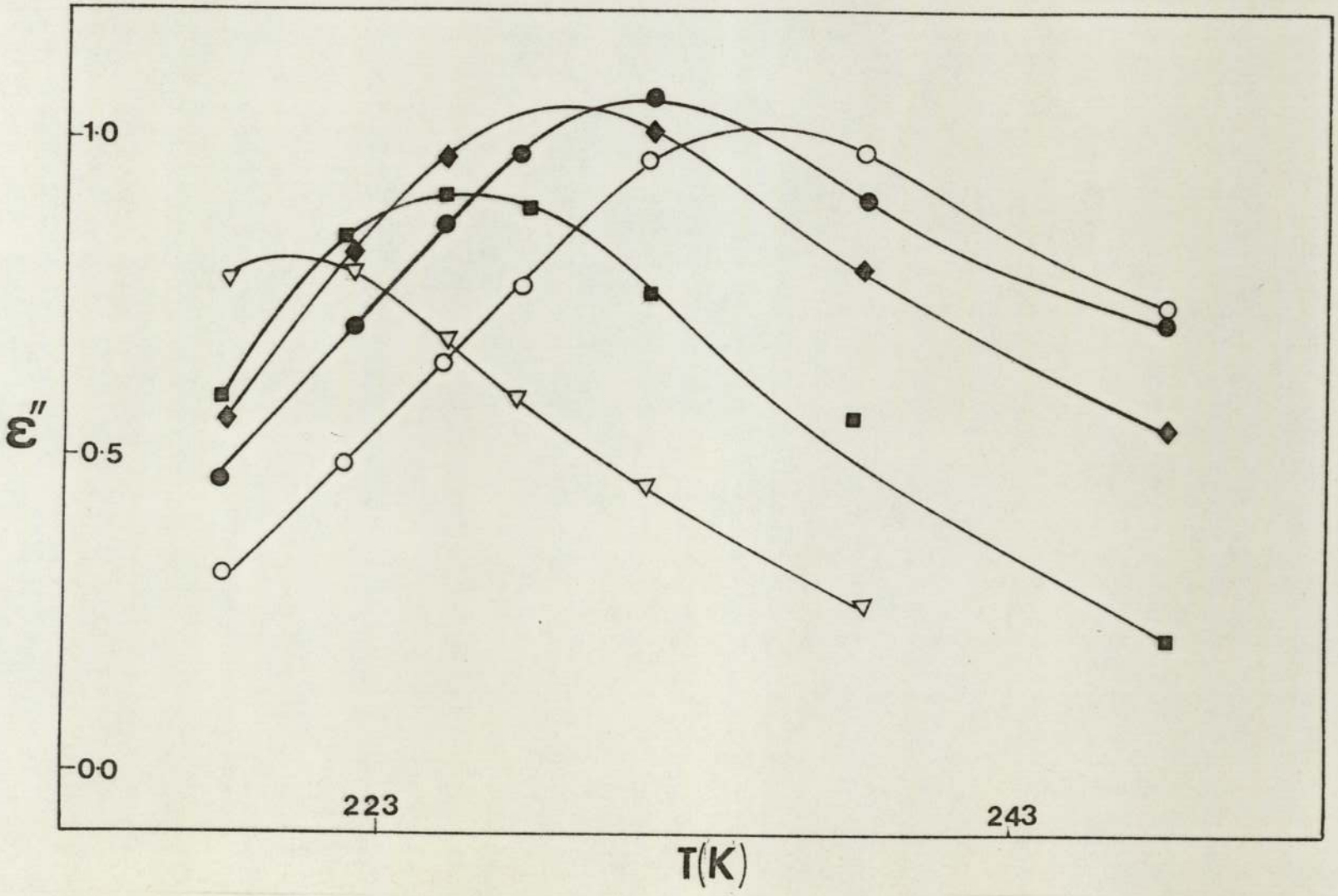

Fig(4.10)

Dielectric loss, ϵ'', Vs temperature at ▽0.5, ■1, ◆3, ●7 and ○20 KHz for PPG2025+1mole%$HgCl_2$

Fig(4.11)

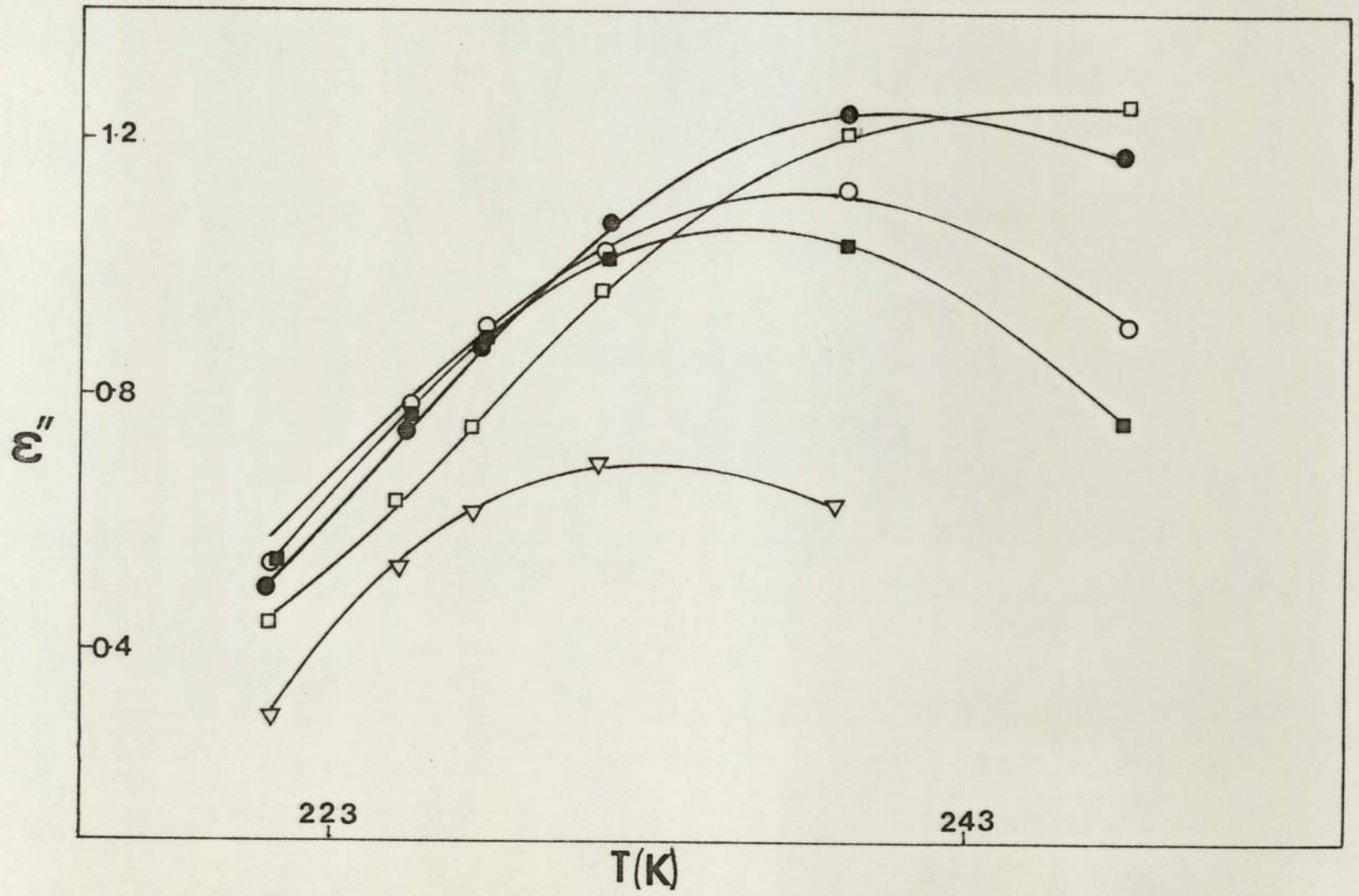

Dielectric loss, ϵ'', Vs temperature at ▽0.3, ■0.7, ○1, ●3 and □7KHz for PPG2025+4mole%$HgCl_2$

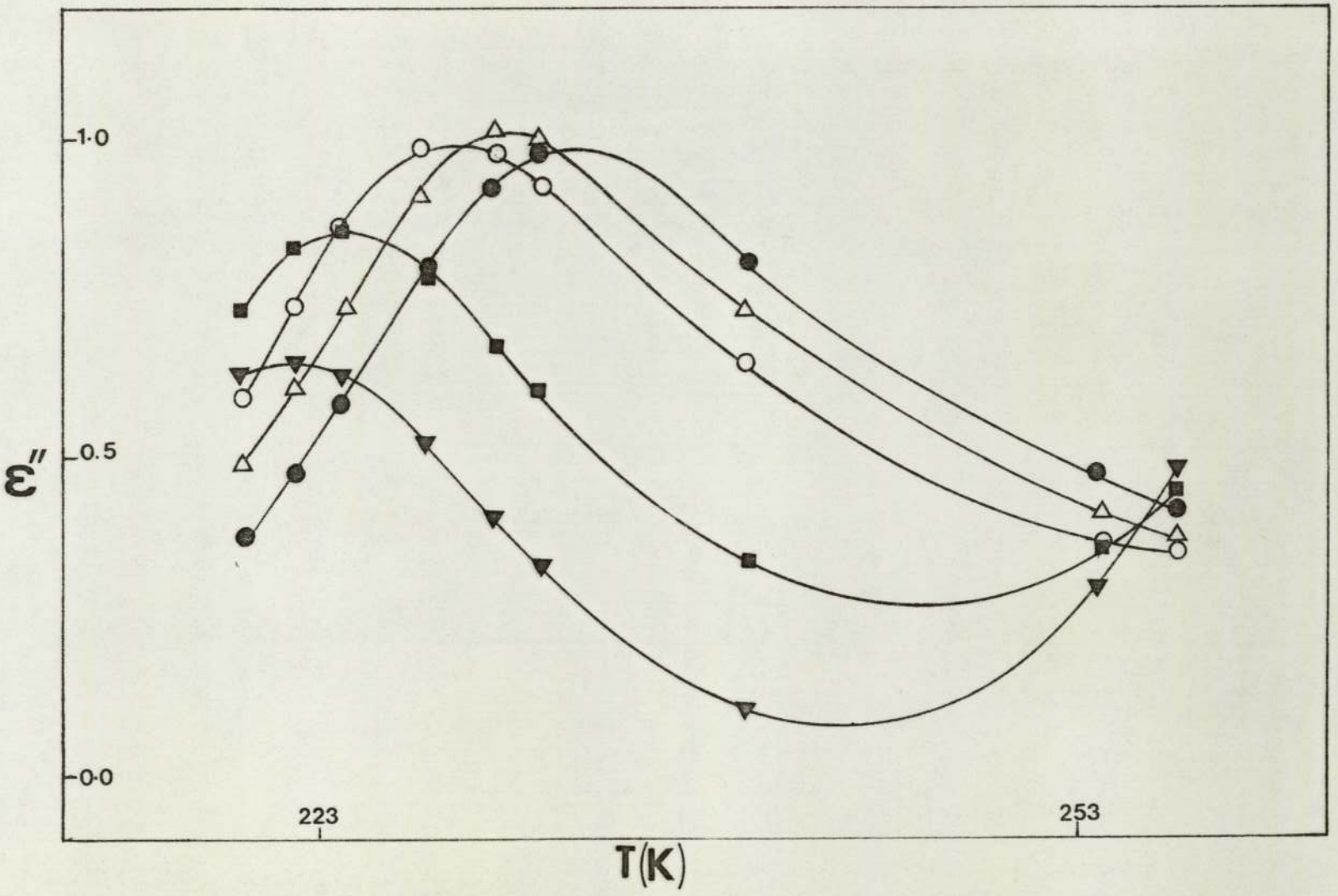

Fig(4.12)

Dielectric loss, ϵ'', Vstemperature at ▼ 0.5, ■ 1, ○ 5, △ 10 and ● 20 KHz for PPG4000+2mole%$HgCl_2$

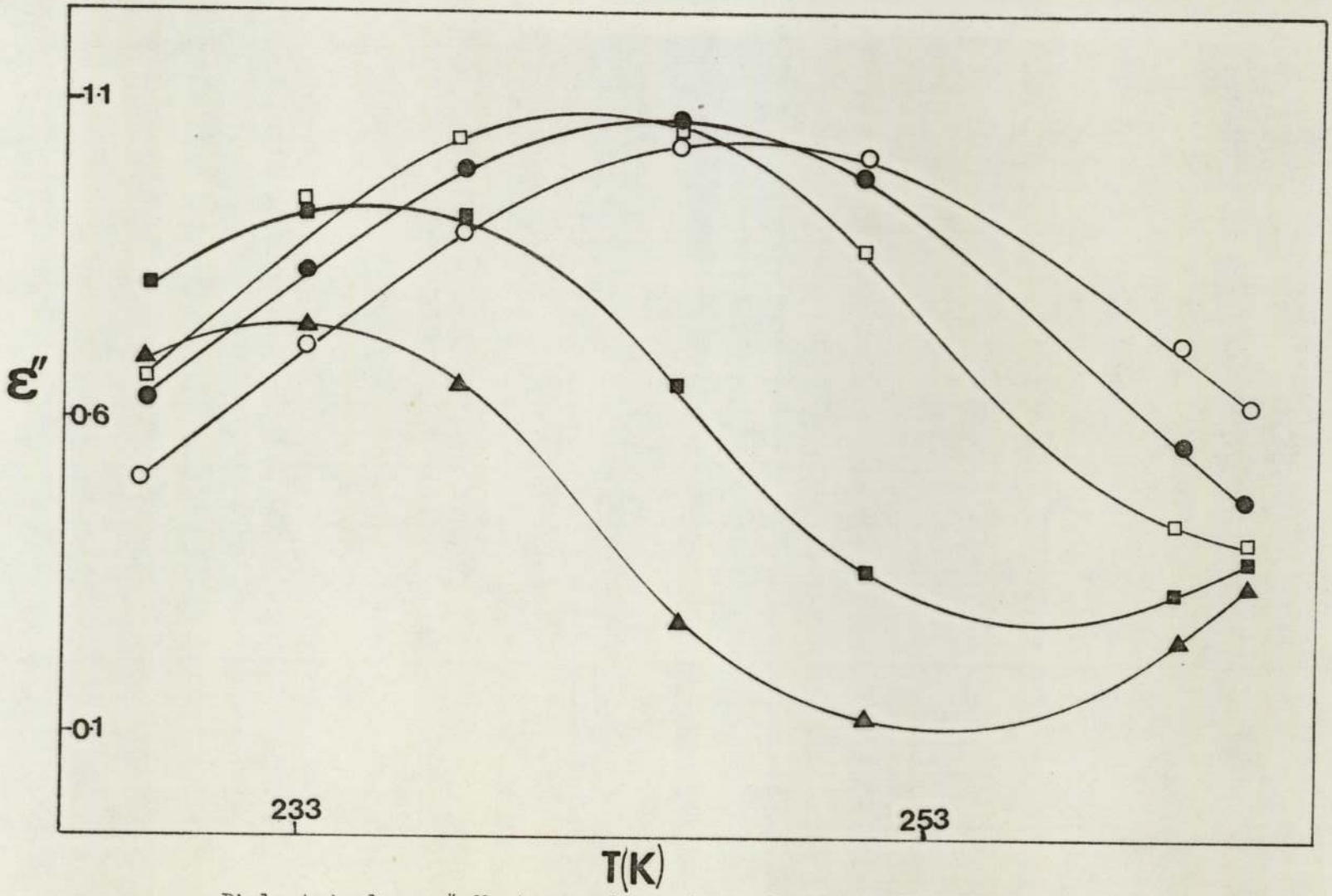

Fig(4.13)

Dielectric loss, ϵ'', Vs temperature at ▲0.5, ■1, □5, ●10 and ○20 KHz for PPG4000+4mole%$HgCl_2$

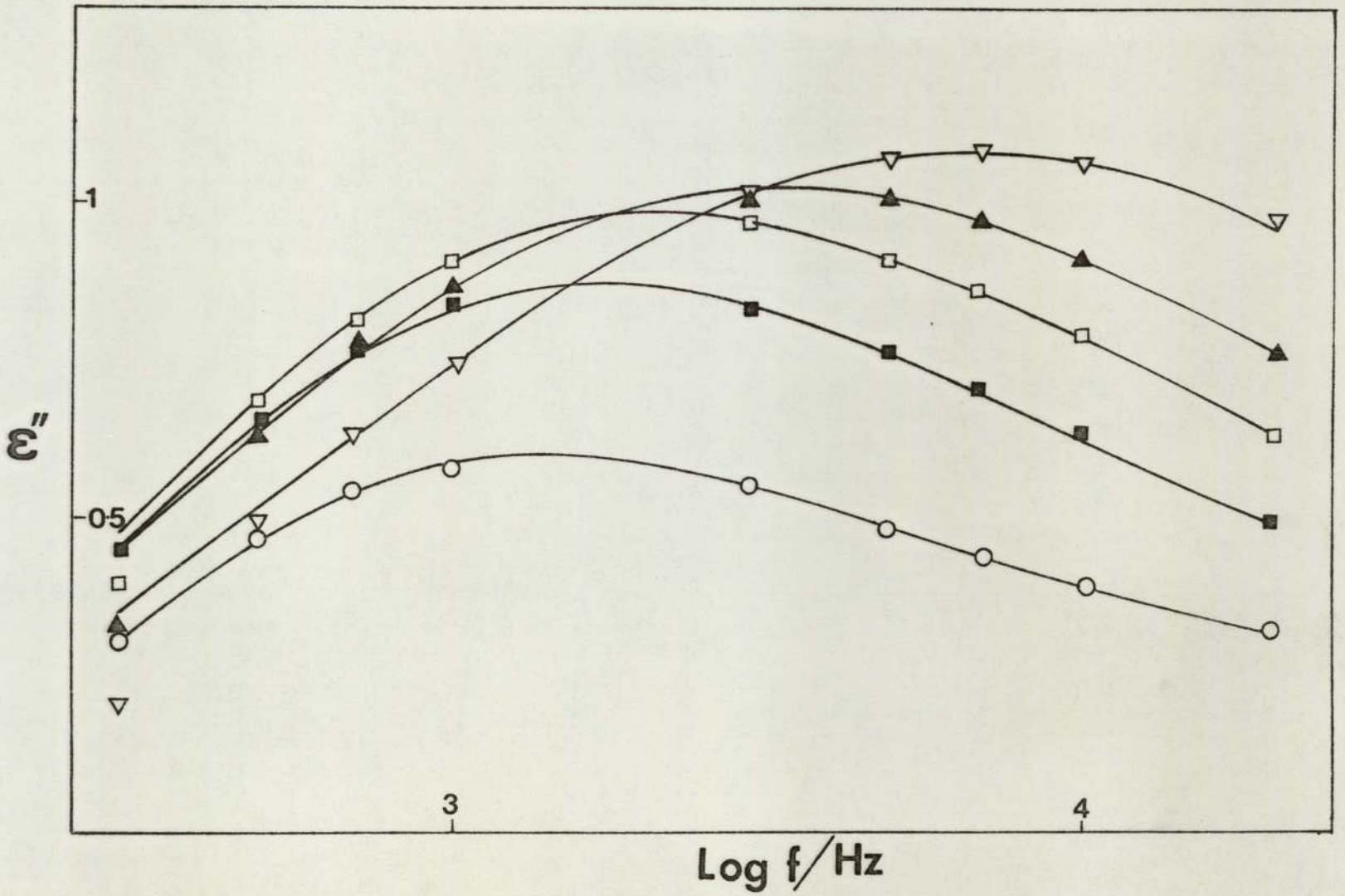

Fig(4.14)

Dielectric loss, ϵ'', Vs log f for PPG2025+2mole%$HgCl_2$ at various temperatures ▽231.4K, △227.4K, □225K, ■222K and ○218K

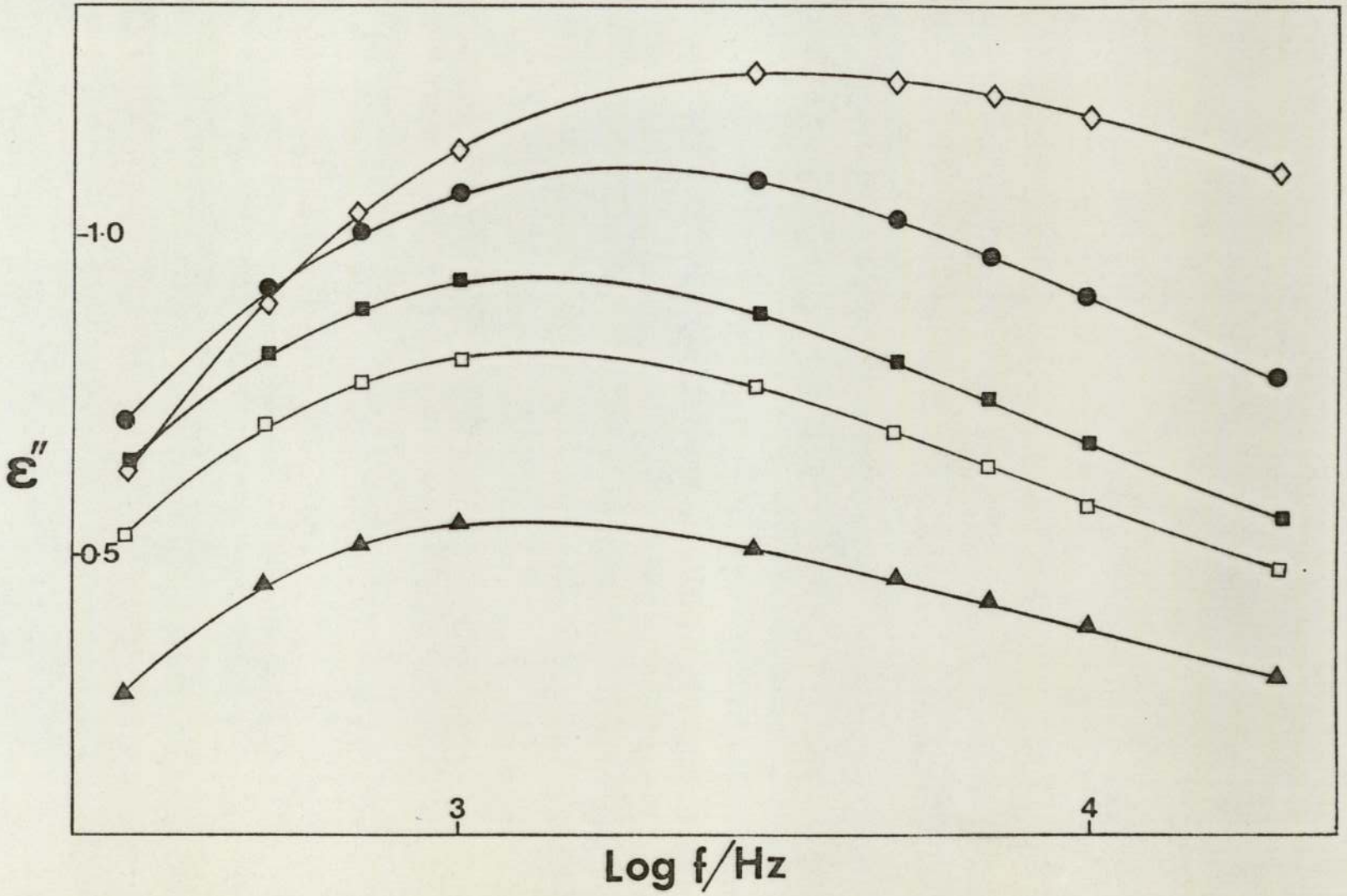

Fig(4.15)

Dielectric loss, ϵ'', Vs log f for PPG2025+4mole%HgCl at various temperatures ◇239K, ◘231.4K, ◙227.4K, □225K and △221K

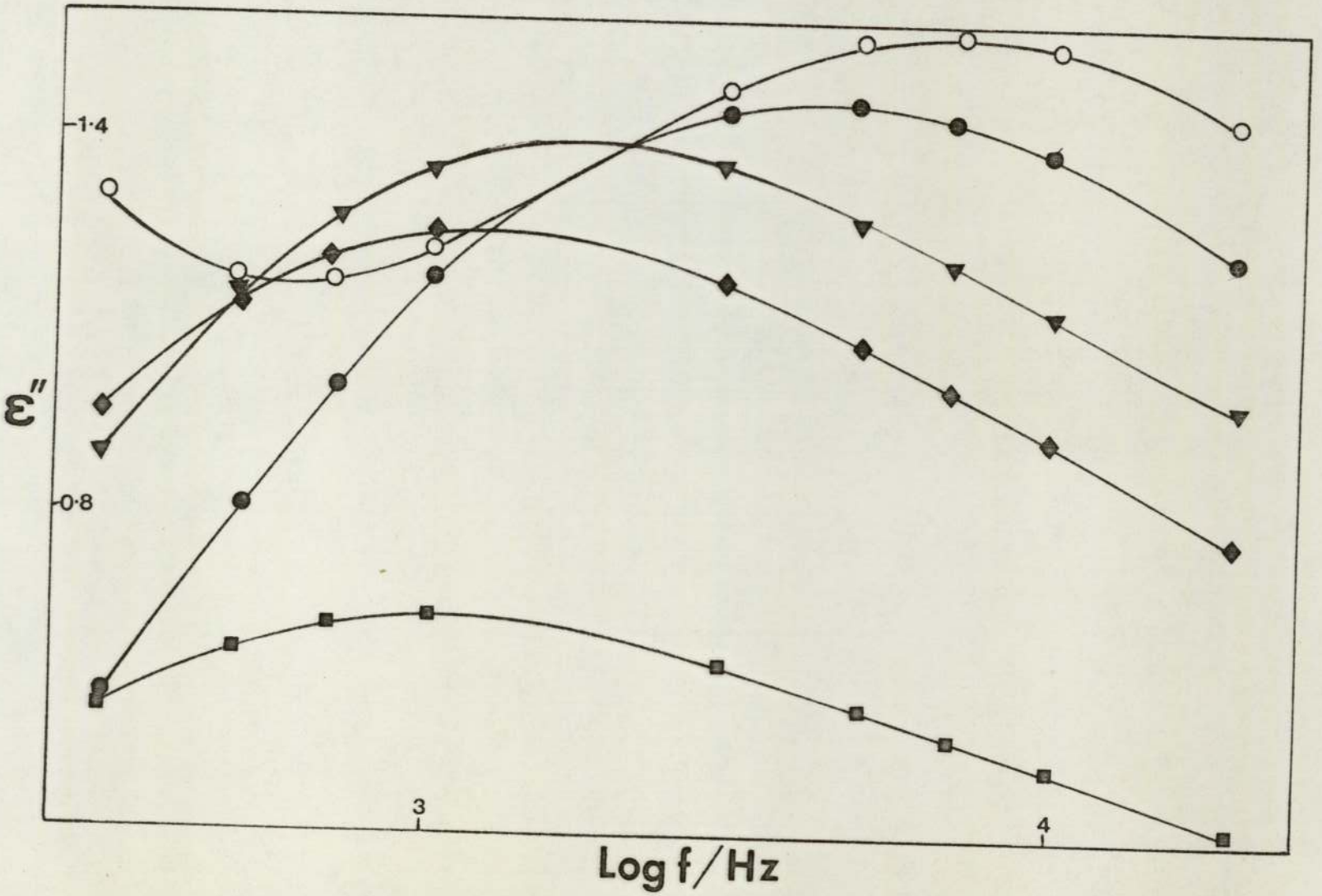

Dielectric loss, ϵ', Vs log f for PPG2025+7mole%$HgCl_2$ at various temperatures ○252K, ●248K, ▽242K, ◇238K and □228K

Fig(4.16)

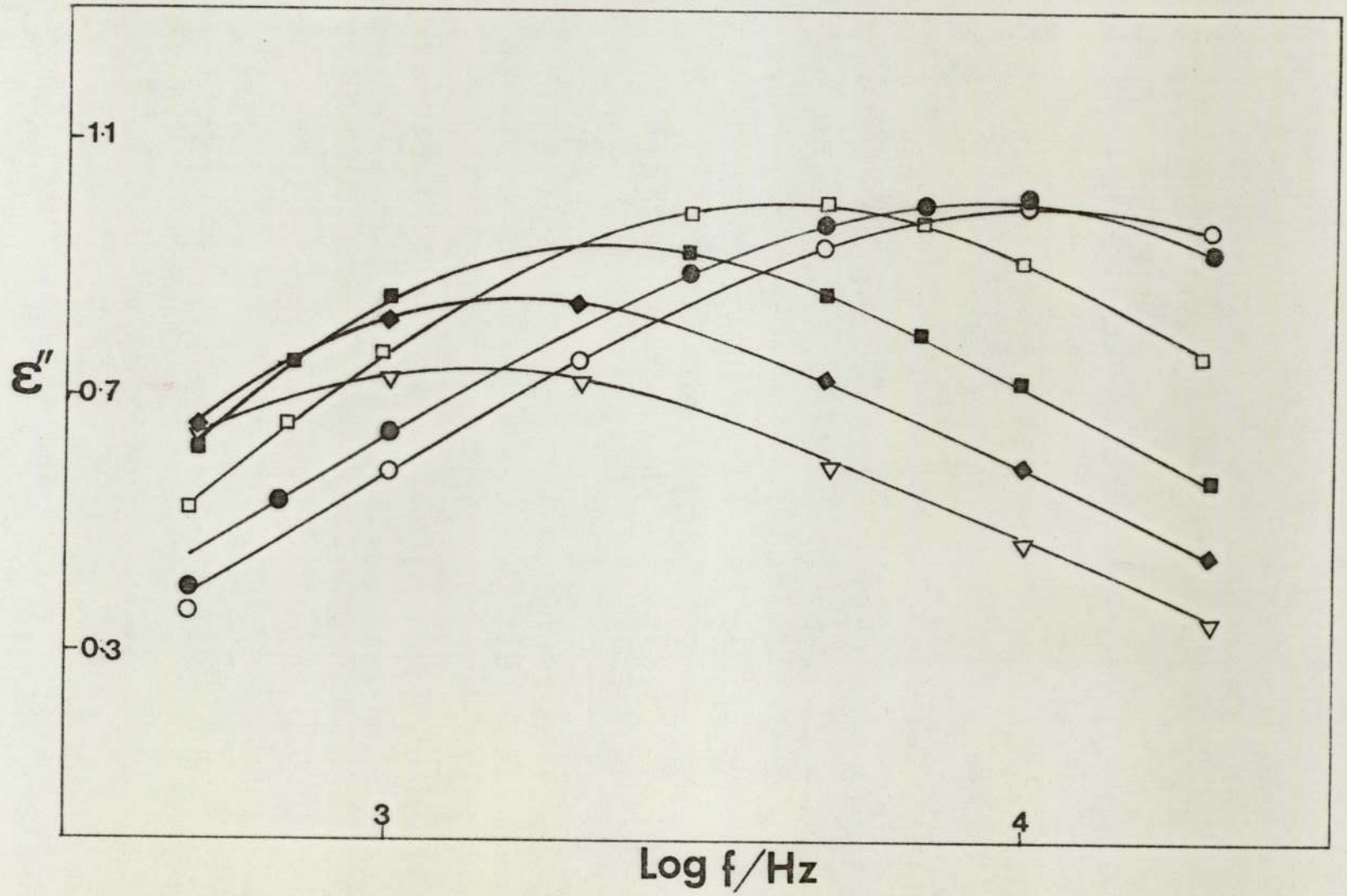

Fig(4.17)

Dielectric loss, ϵ'', Vs log f for PPG4000+2mole%$HgCl_2$ at various temperatures ○232K, ●230K, □227K, ■224K, ◆222K and ▽220K

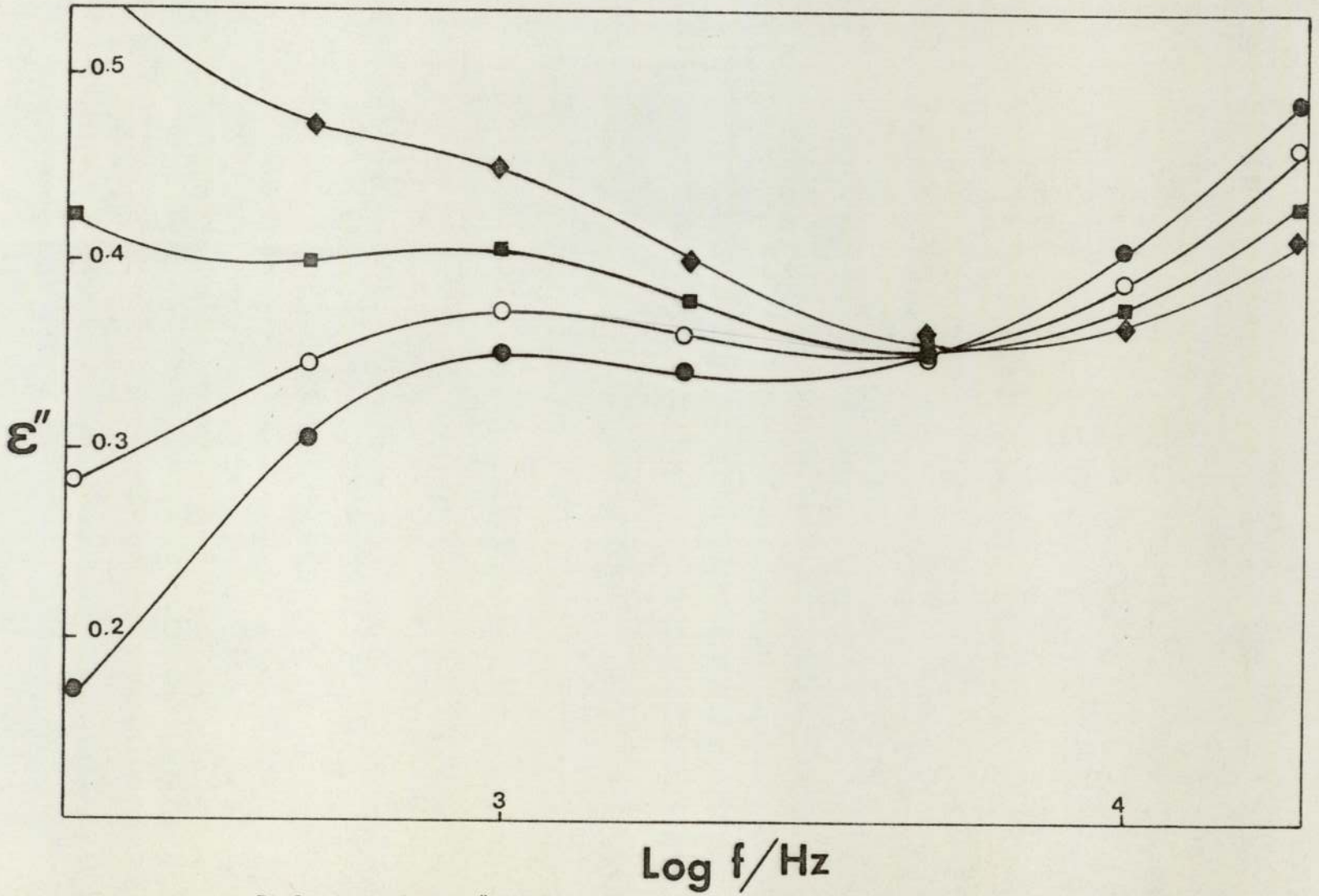

Fig(4.18)

Dielectric loss, ϵ'', Vs log f for PPG4000+2mole%$HgCl_2$ at various temperatures ◆257K, ■256K, ○255K and ●254K

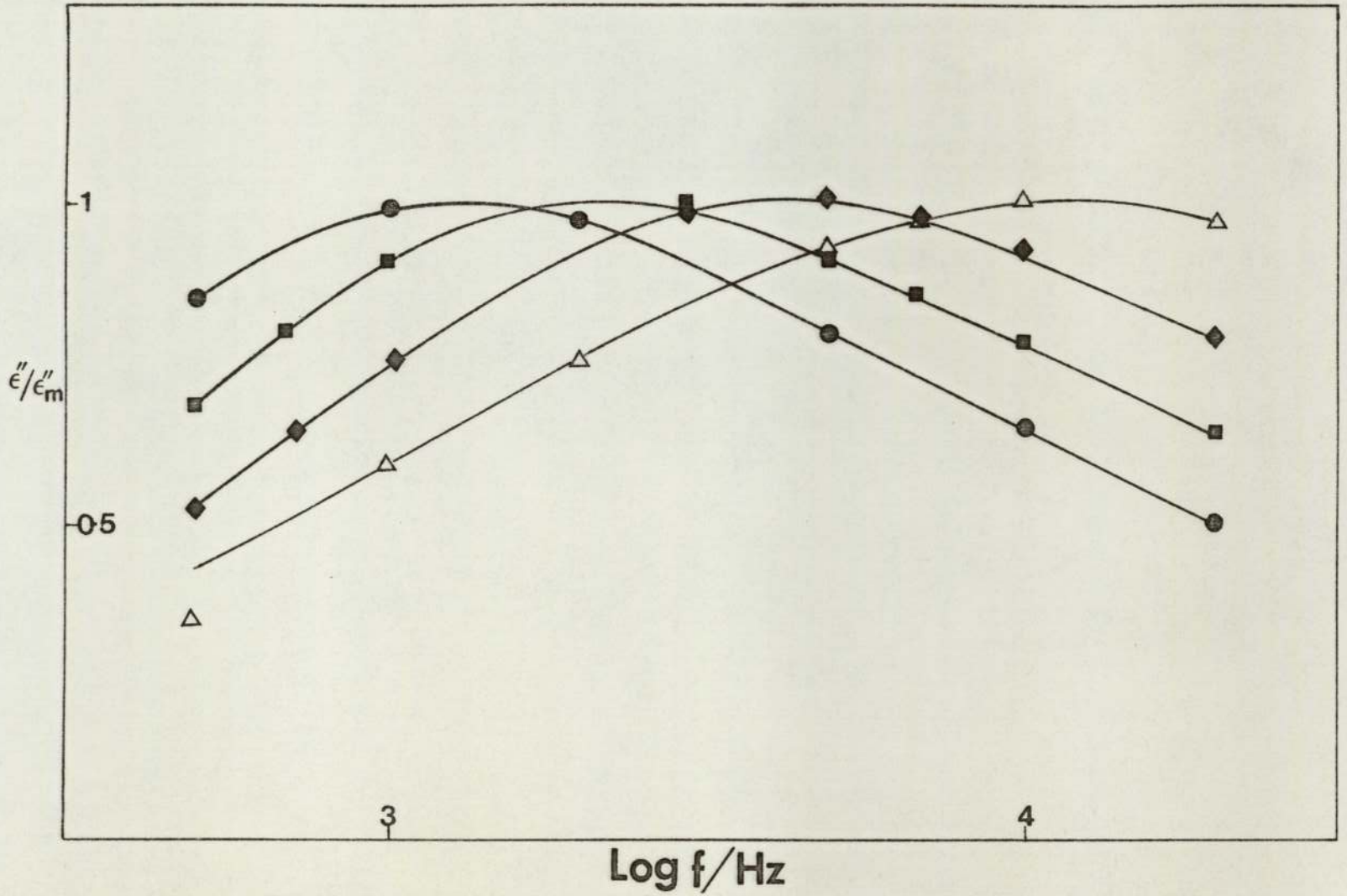

Normalized dielectric loss, ϵ''/ϵ''_m Vs log f for PPG4000+2mole%$HgCl_2$
at various temperatures △232K, ◇227K, □224K and △220K

Fig(4.19)

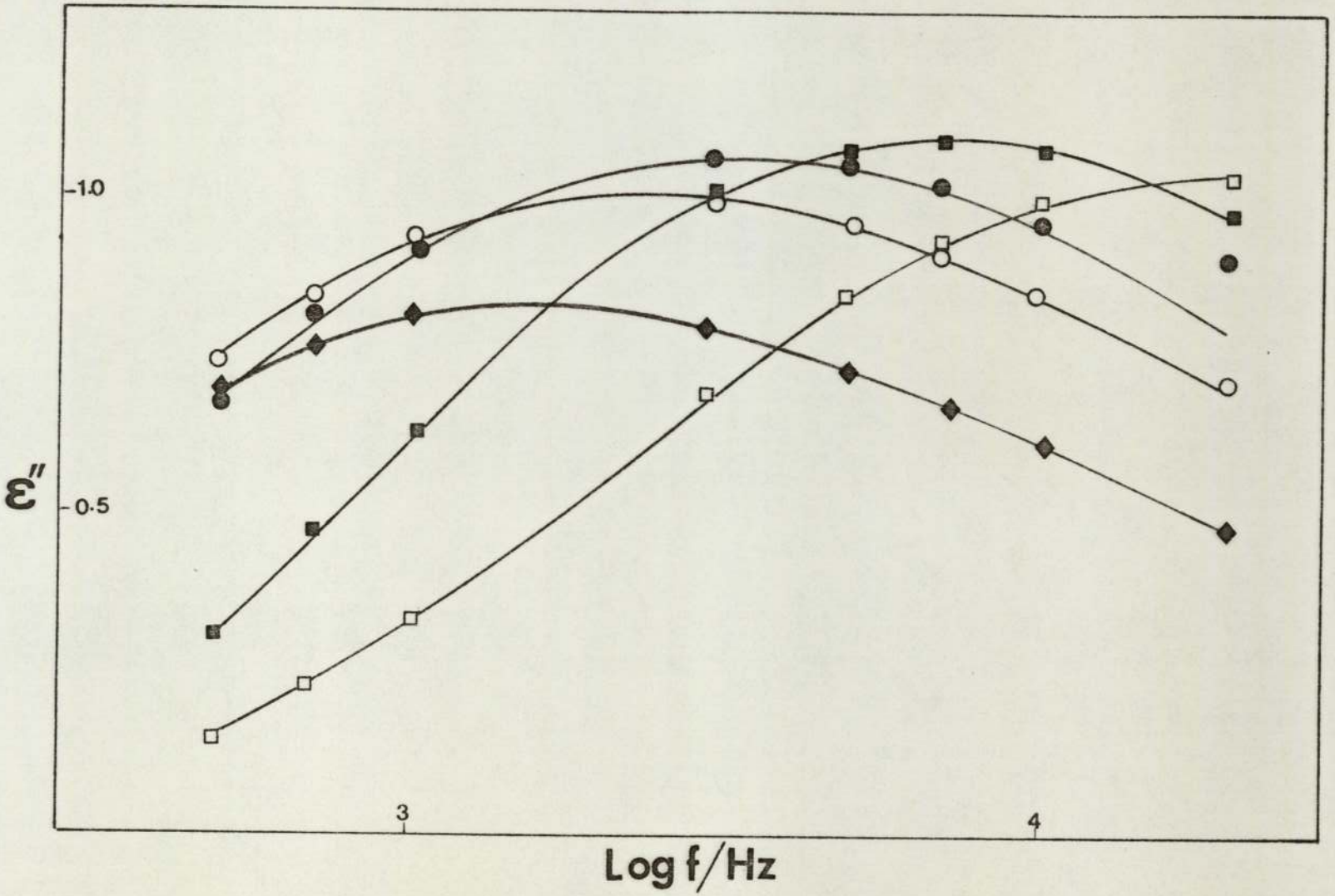

Fig(4.20)

Dielectric loss, ϵ'', Vs log f for PPG4000+4mole%$HgCl_2$ at various temperatures □251K, ■245K, ●238K, ○233K and ◆228K

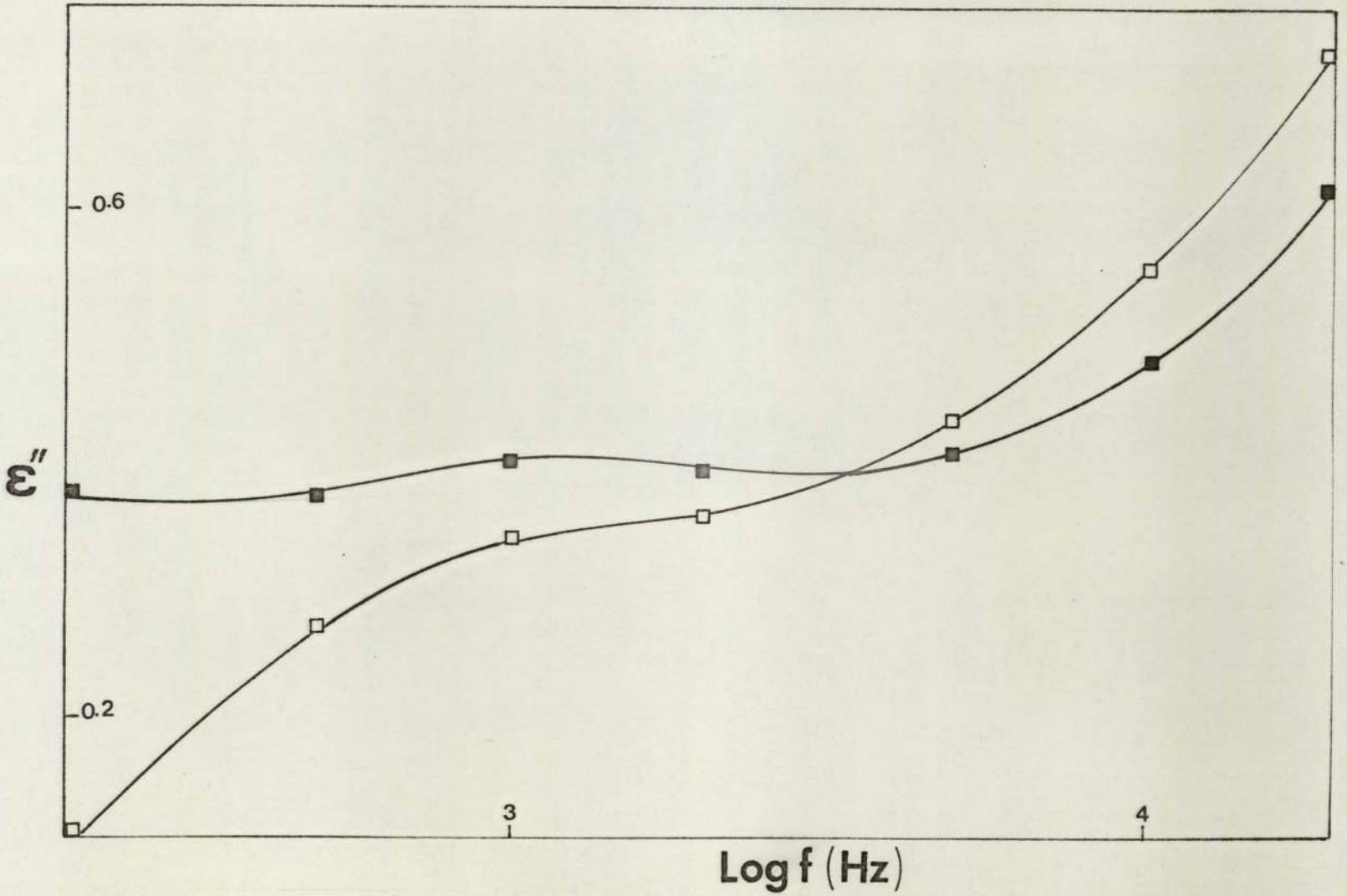

Fig(4.21)

Dielectric loss, ϵ'', Vs log f for PPG4000+4mole%$HgCl_2$ at various temperatures ■263K, □261K

as shown in Figures 14 - 21. For samples of PPG 2025 containing 2, 4 and 7 mole percent of $HgC\ell_2$ the dielectric absorption curve consisted of a single, broad peak, that was slightly skewed to lower frequencies on a logarithmic scale. The lower frequency, secondary relaxation process observed in higher molecular weight samples of PPG - $HgC\ell_2$ was not detected in any of the solutions of $HgC\ell_2$ in PPG 2025. The magnitude of the loss maximum, in the range of temperature studied, is sensitively dependent on temperature and on the concentration of mercuric chloride. Similar loss curves were obtained for PPG 4000 - $HgC\ell_2$ with 2 and 4 mole % concentration of mercuric chloride. However, for this system a small, lower frequency, secondary relaxation process was evident (Figures 18 and 21). This absorption peak was reasonably well resolved from the principal 'α-relaxation' peak, being displaced to lower frequencies by approximately two orders of magnitude. The magnitude of the absorption attributable to the secondary relaxation process does not appear to change significantly as a result of adding mercuric chloride behaviour in direct contrast to that observed for the main absorption process.

4.4 Cole - Cole plots of dielectric relaxation data obtained for poly(propylene glycol) - mercuric chloride complexes

Cole - Cole plots (ε'' vs ε') for pure samples of poly(propylene glycol) possessing molecular weights of

2025 and 4000 are shown in Figure 22, at different temperatures.

Figures 23 - 29 show Cole - Cole plots of PPG 2025 - $HgC\ell_2$ for 2, 4 and 7 mole percent concentrations of mercuric chloride. The effect of decreasing temperatures on the low frequency dielectric constant, as derived from the high value intercept on the ε' axis, can be clearly seen. For PPG 2025 - 2% $HgC\ell_2$ at $T = -25.2^{\circ}C$ ($24^{\circ}C$ above the glass transition temperature) the static dielectric permittivity is estimated to be 8.3. The corresponding values of ε'_o for PPG 2025 - 4% $HgC\ell_2$ at $-25.2^{\circ}C$ and PPG 2025 - 7% $HgC\ell_2$ at $-21^{\circ}C$ were approximately 11 and 11.5, respectively. The mean high frequency dielectric permittivity, ε'_∞, derived from the intercept of the Cole - Cole curves on the ε' axis at $-48^{\circ}C$ for PPG 2025 - 2% $HgC\ell_2$ was 2.8. Values of ε'_∞ for PPG 2025 - 4% $HgC\ell_2$ and PPG 2025 - 7% $HgC\ell_2$ were found to be 2.9 and 3.1 at $-52^{\circ}C$ and $-45^{\circ}C$, respectively. The modest increase in ε'_∞ with increasing concentration of mercuric chloride simply reflects the increase in the high frequency electric polarization of the polymer-salt solutions. The much greater change in the static dielectic permittivity, ε'_o, brought about by increased concentration of $HgC\ell_2$ must be due to the presence of permanent dipole moments and may be taken as evidence for the formation of complexes between molecules of mercuric chloride and polyether segments, a similar conclusion to that deduced

by other workers employing different experimental techniques.

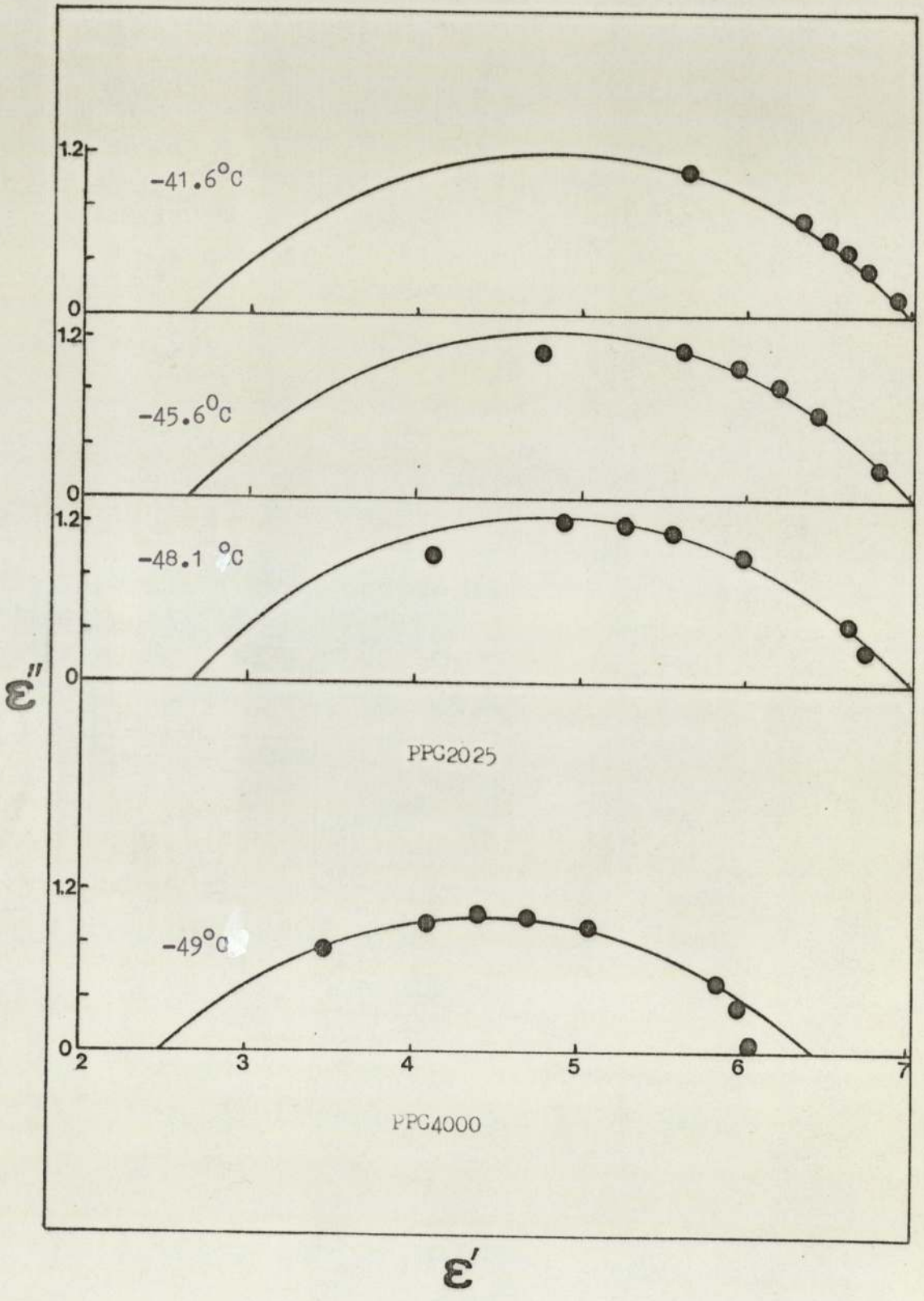

Cole-Cole plots of PPG4000 and PPG2025 at different temperatures

Fig(4.22)

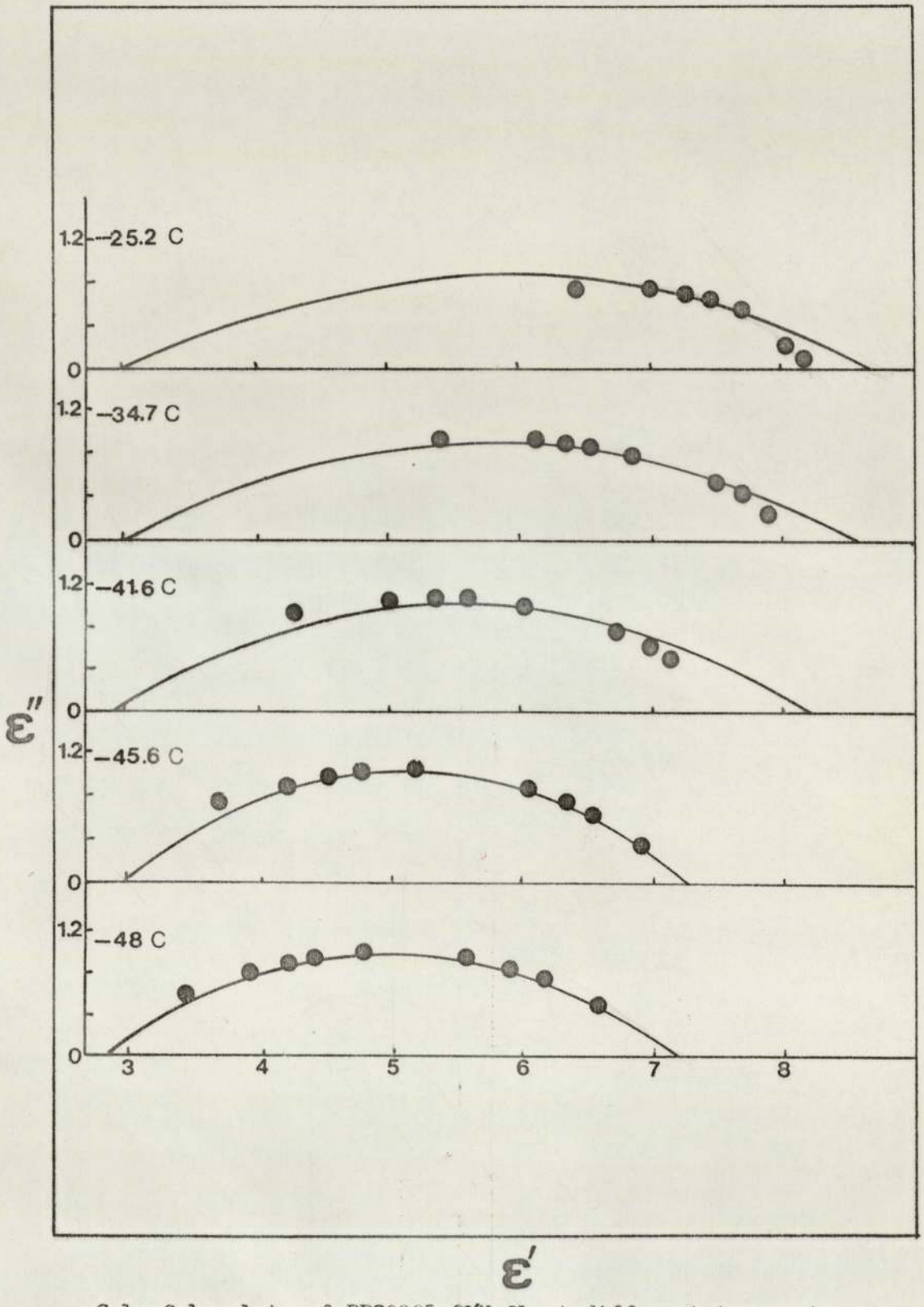

Cole-Cole plots of PPG2025+2% $HgCl_2$ at different temperatures

Fig(4.23)

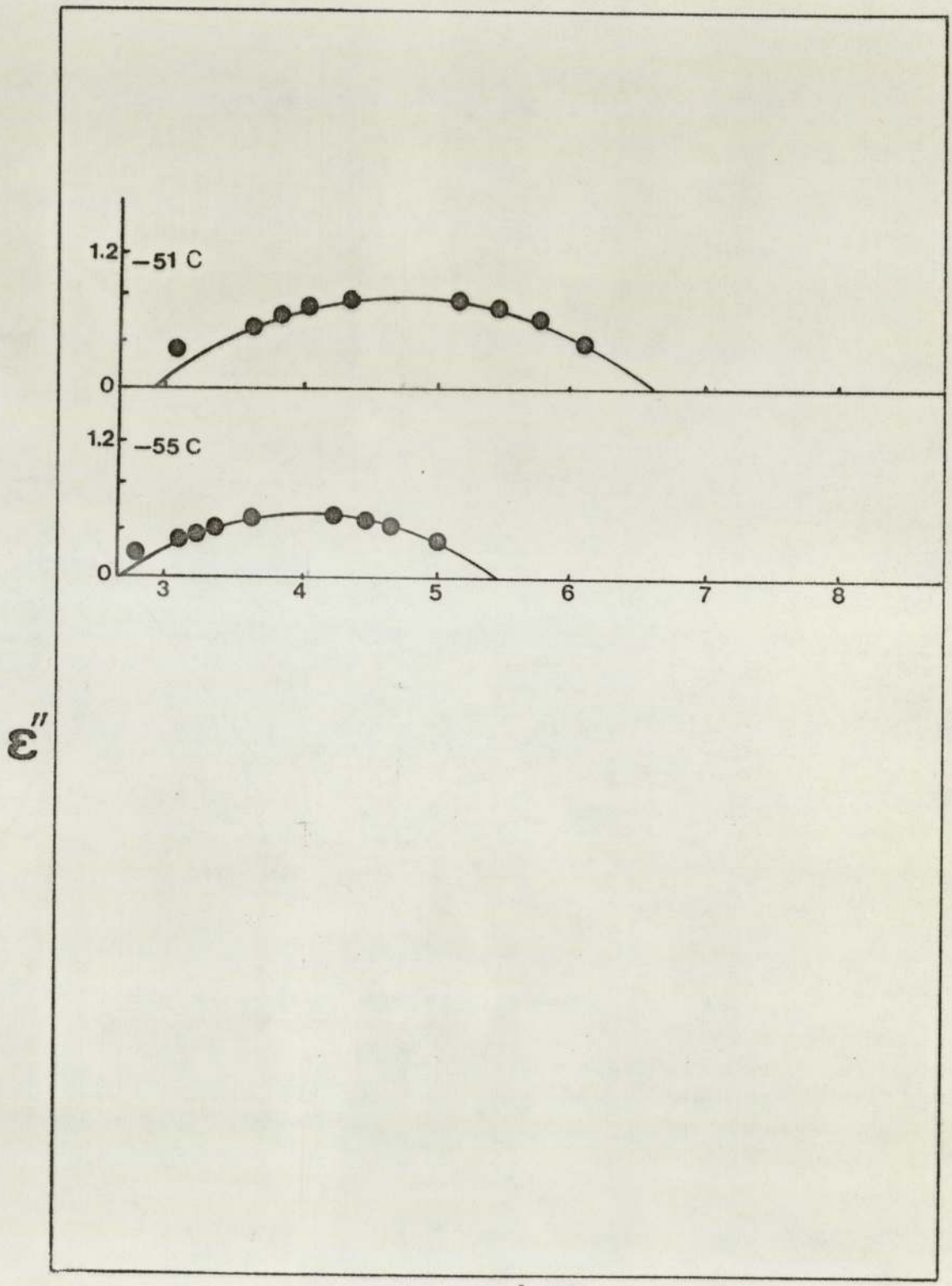

Cole-Cole plots of PPG2025+2%$HgCl_2$ at different temperatures

Fig(4.24)

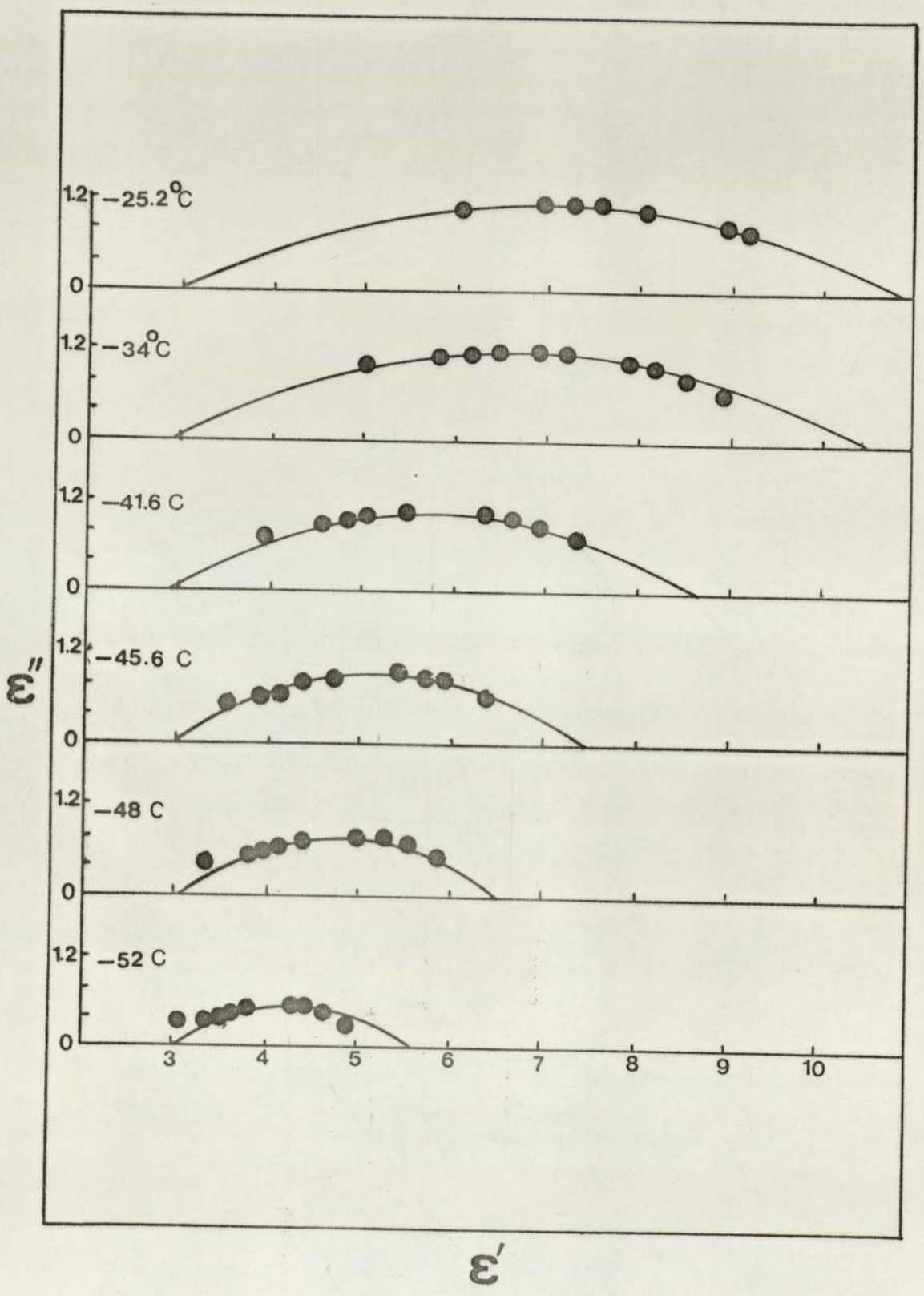

Cole–Cole plots of PPG2025+4%$HgCl_2$ at different temperatures

Fig(4.25)

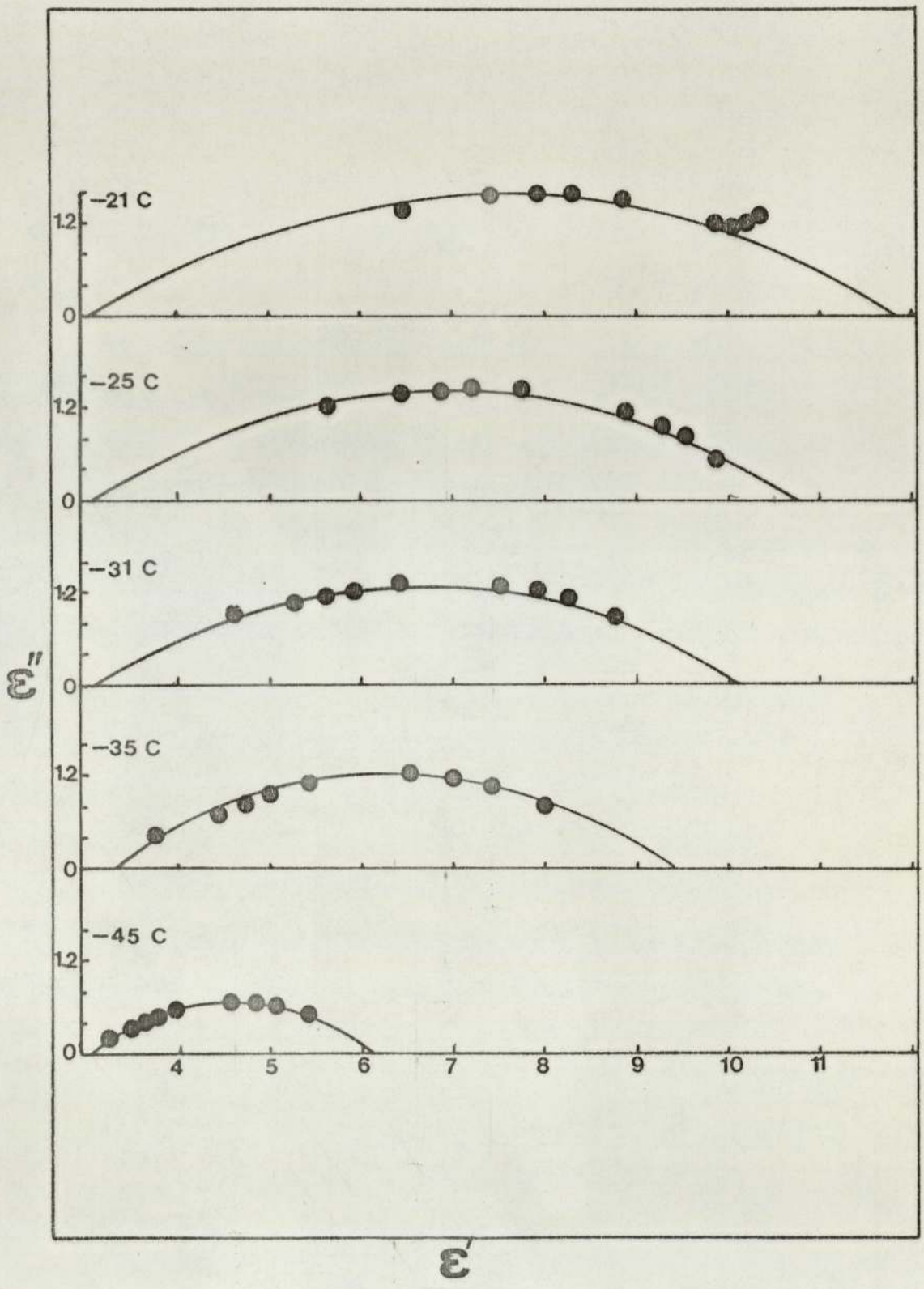

Cole-Cole plots of PPG2025+7%HgCl at different temperatures

Fig(4.26)

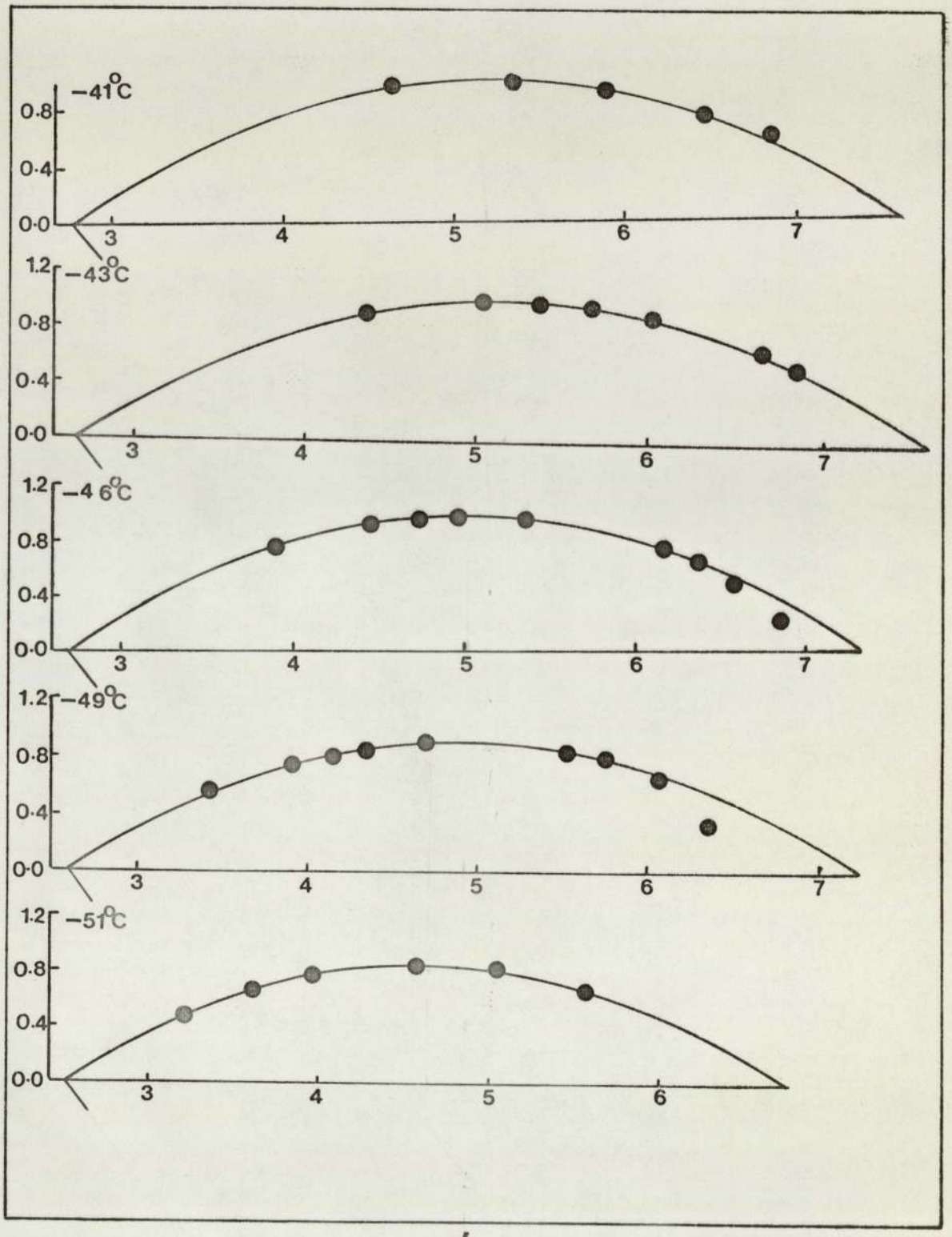

Cole–Cole plots of PPG4000+2%$HgCl_2$at different temperatures

Fig(4.27)

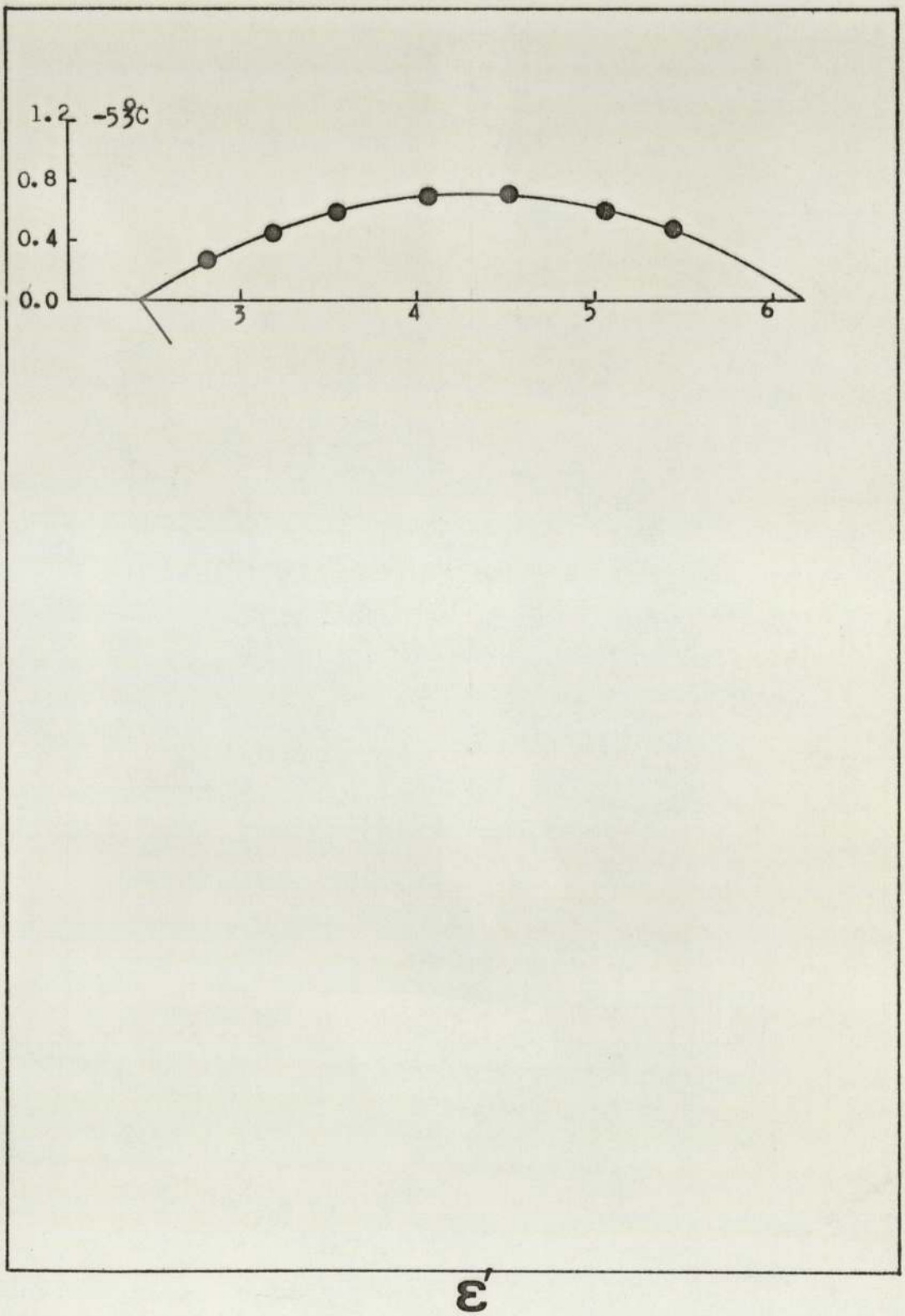

Cole-Cole plots of PPG4000+2%$HgCl_2$at different temperatures

Fig(4.28)

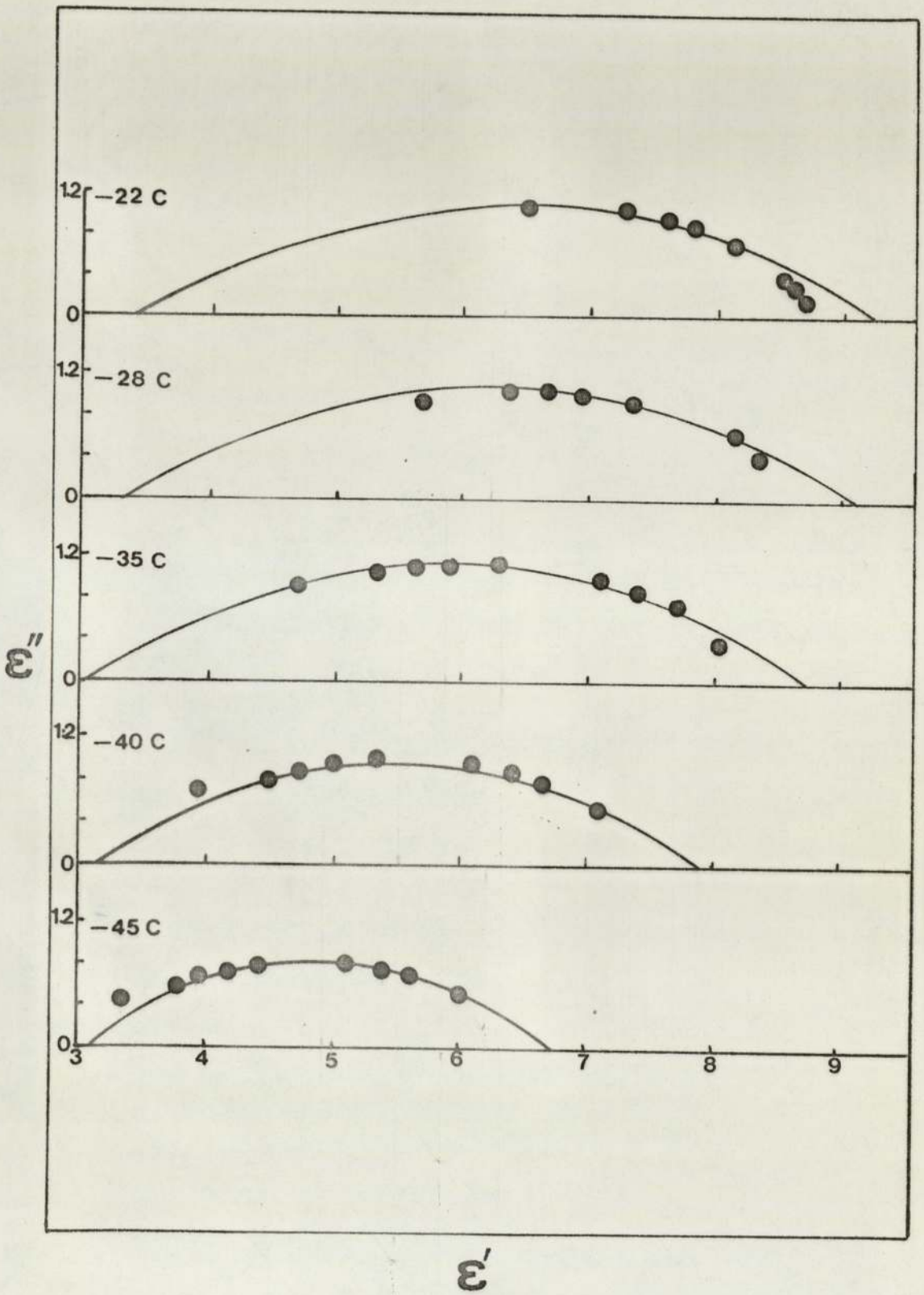

Cole-Cole plots of PPG4000+4%$HgCl_2$ at different temperetures

Fig(4.29)

4.5 Dielectric Relaxation Data for Solutions of Cadmium Iodide, Cobalt Chloride and Zinc Chloride in Poly(propylene glycol)

The previous sections in this chapter have been concerned with the presentation and preliminary discussion of the dielectric results obtained for solutions of mercuric chloride in poly(propylene glycol). This section describes the more limited dielectric relaxation data obtained for solutions of cadmium iodide, cobalt chloride and zinc chloride in poly(propylene glycol) PPG4000.

Figure 4.30 shows a plot of dielectric loss, ε'', versus frequency (log f/Hz) for a 1 mole % solution of cadmium iodide in PPG4000 at temperatures of 221K, 224K, 227K and 230K. The loss curves have a width at half height that is at least two decades of frequency. The high frequency portions of the loss curves possess a ε'' vs. frequency profile that is fairly typical of amorphous polymers. However the low frequency side of the loss curves appear to have an enhanced dielectric loss. For the dielectric data obtained at 230K the loss exhibits a distinct upwards trend as the frequency is decreased; behaviour that is the characteristic of conductive loss.

No sign of conductive loss was observed for a 1 mole % solution of cobalt chloride in PPG4000 in the temperature range 214 - 230K. The curves of ε'' vs. log f for this system are almost symmetrical with respect to the frequency position of the maximum loss (see figure 4.31).

The dielectric relaxation data obtained for a 0.5 mole % solution of zinc chloride in PPG4000 (Fig 4.32) was similar to that

measured for the 1 mole % solution of cadmium iodide in PPG4000. The positions of the loss curves on the frequency axis were also very similar for these two chemical systems. The contribution of conductive loss to the total loss was also present for the PPG4000 - $ZnCl_2$ system at the lower frequencies and highest temperature.

Figure 4.33 shows Arrhenius plots of the logarithm of the frequency corresponding to maximum dielectric loss versus the reciprocal of the absolute temperature for solutions containing 1 mole % of cadmium iodide, 1 mole % cobalt chloride and 0.5 mole % zinc chloride in PPG4000. Similar functional behaviour was observed for the three systems. The dielectric loss data for the solutions of cadmium iodide and zinc chloride were almost the same, with the latter being slightly shifted to higher frequencies. The dielectric relaxation behaviour of the solutions of cobalt chloride differed markedly from the other two types of salt solutions, with the loss curves being shifted by approximately half a decade to the higher frequencies.

For the sake of comparison the dielectric data for an 18 mole % solution of zinc chloride in poly(propylene glycol) has been included in figure 4.33. A linear extrapolation of the Arrhenius curve, obtained for the 18 mole % solution, to lower temperatures indicates that at 220 K the loss maximum of 0.5 mole % and 18 mole % solutions of zinc chloride in PPG are separated by approximately three orders of frequency.

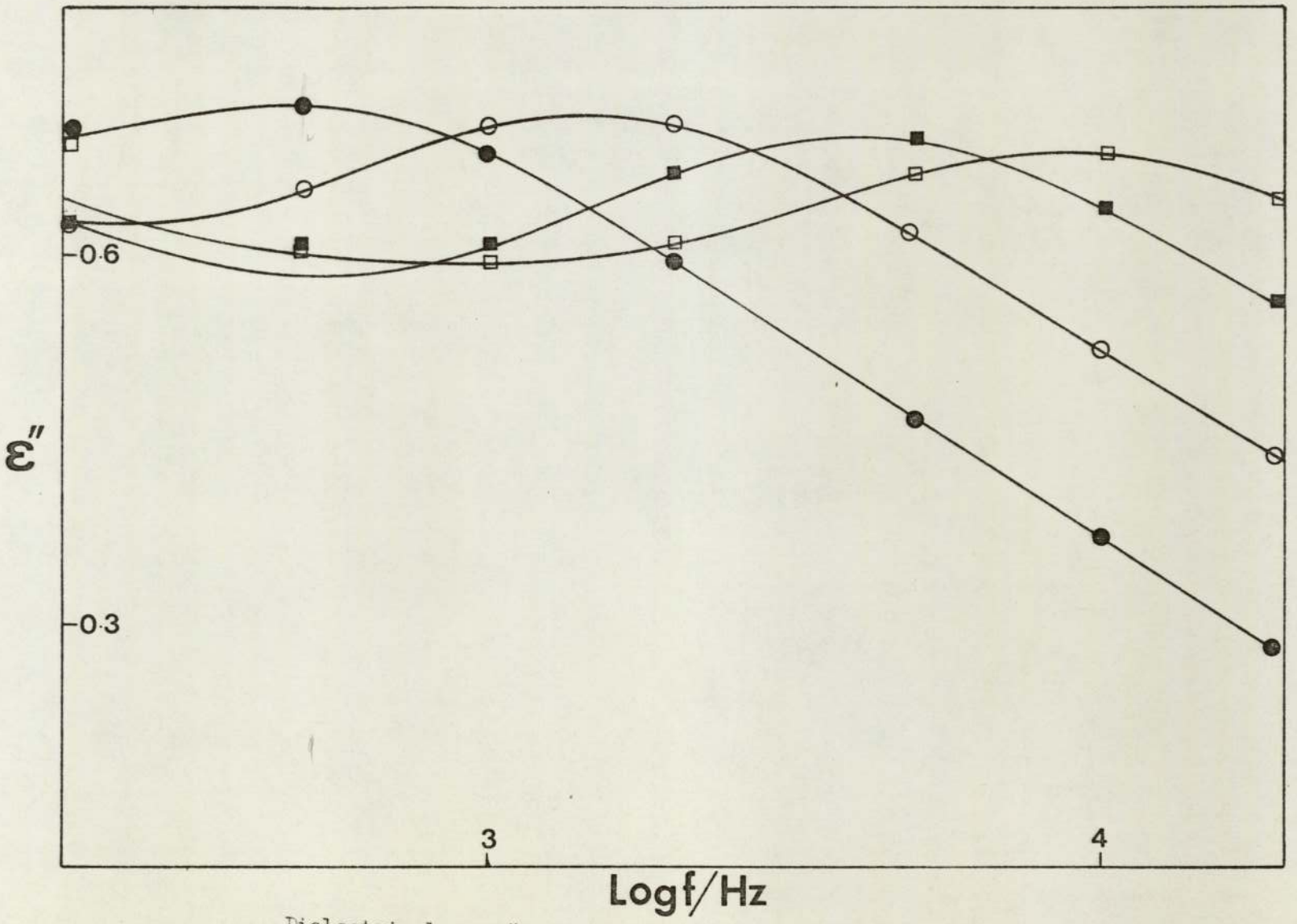

Fig(4.30)

Dielectric loss, ϵ'', Vs log f for PPG4000+1mole%CdI2 at various temperatures □230K, ■227K, ○224K, ●221K

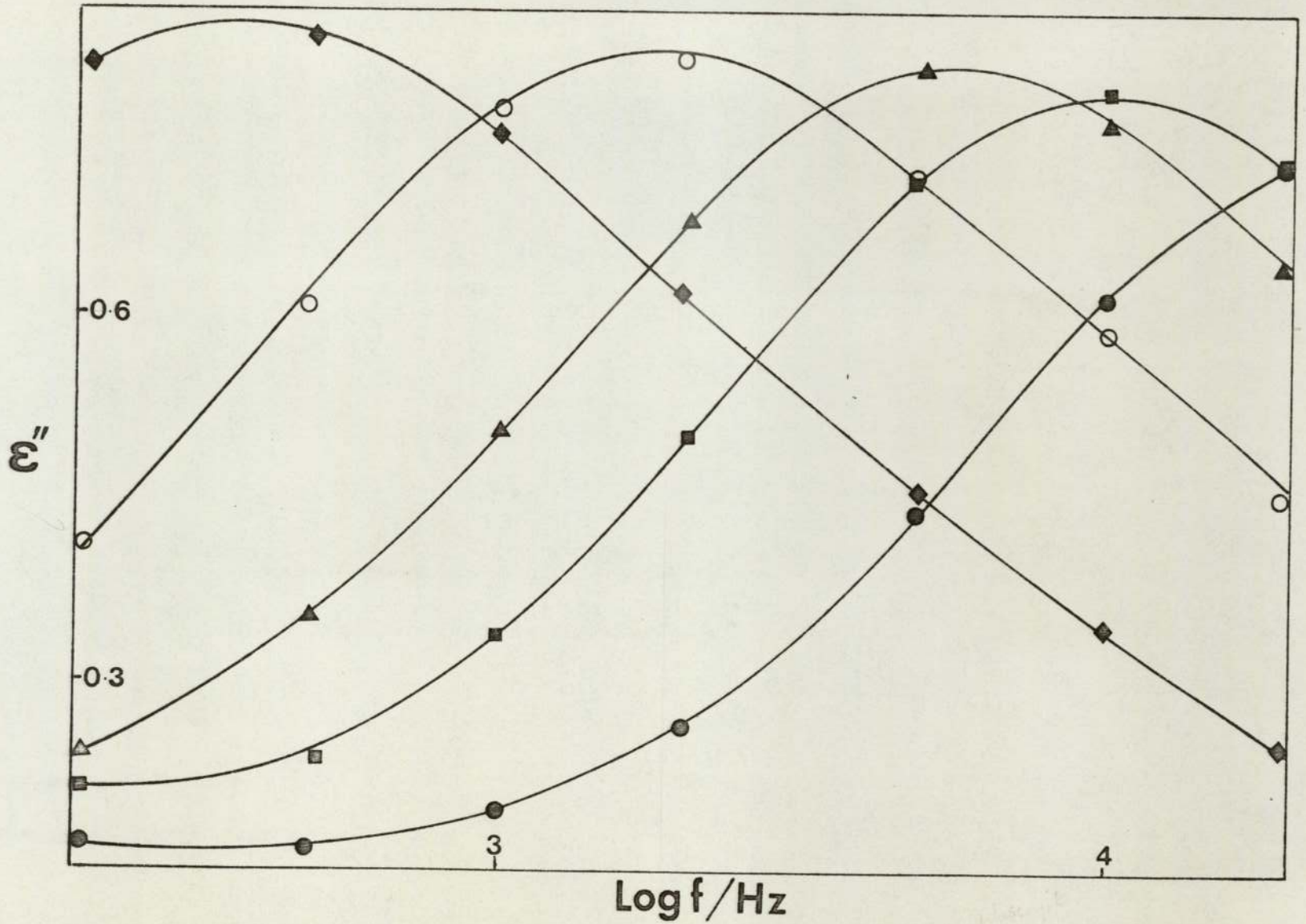

Fig(4.31)

Dielectric loss, ϵ'', Vs log f for PPG4000+1mole%$CoCl_2$ at various temperatures ●230K, ■226K, ▲224K, ○221K and ◆217K

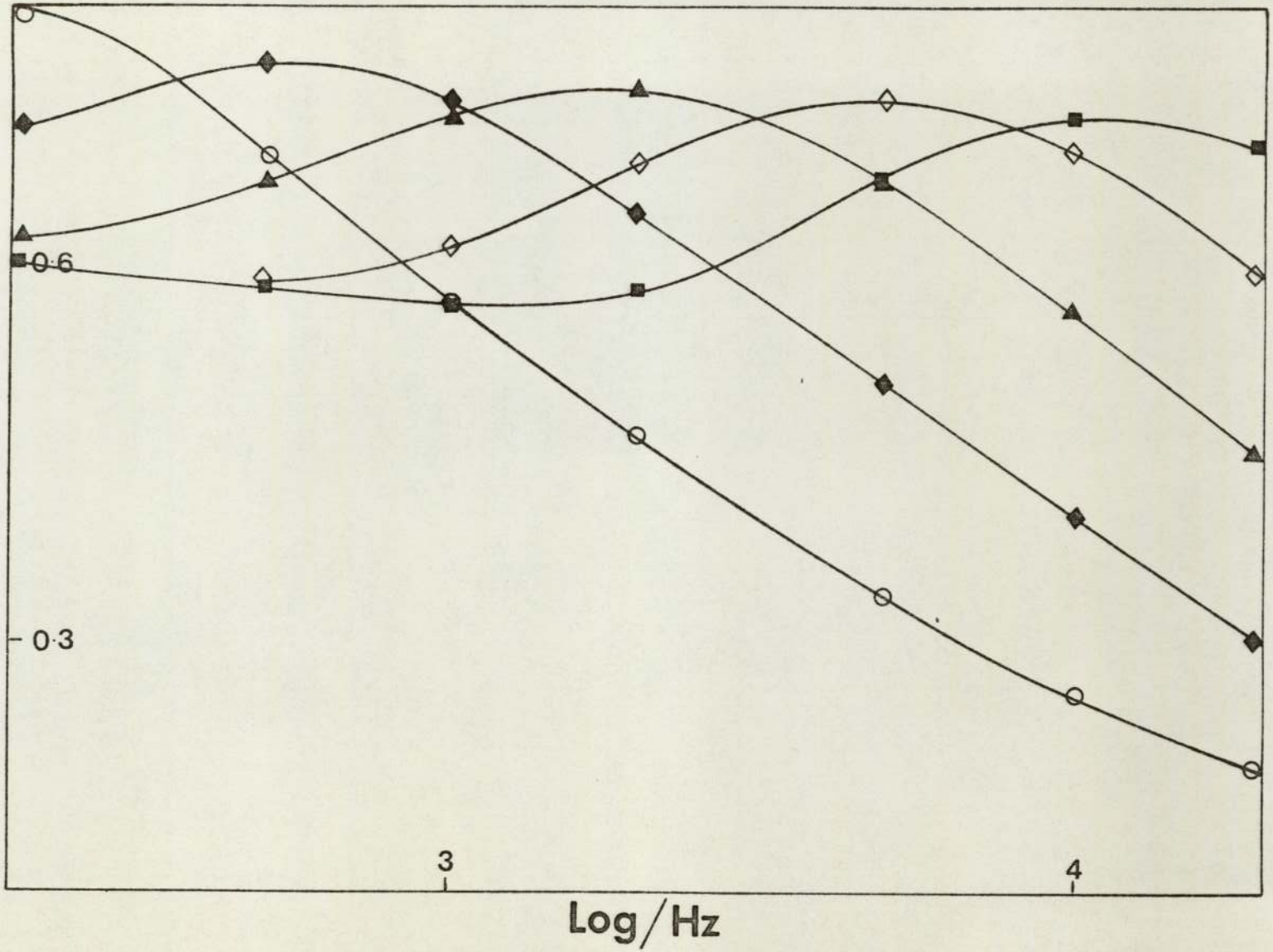

Fig(4.32)

Dielectric loss, ϵ'', Vs log f for PPG4000+0.5mole%ZnCl2 at various temperatures ■230K, □227K, ▲224K, ◆221K and ○218K

R.E.Wetton data(PPG+18%ZnCl2) ■
PPG4000+1mole%CdI2 ●
PPG4000+1moleCoCl2 ▲
PPG4000+0.5moleZnCl2 □
Log fm /Hz
-4
-3
-2
2.8
3.0
4.4
4.6
10^3×(1/T°K)

Fig (4·33)

CHAPTER 5

DISCUSSION OF DIELECTRIC RESULTS

5.1 The Structure of Polyether-Salt Complexes

For approximately two decades the structure and properties of polyether-salt complexes has been the subject of investigations carried out by a number of research groups. In these investigations a variety of techniques have been employed. These included infra-red spectroscopy[2,3,6], nuclear magnetic resonance[22,25], X-ray crystallography[2,6,8], the measurement of various calorimetric data, the determination of electrical conductivity[17,26] and the study of dynamic mechanical relaxation[14,15]. Using X-ray crystallography, Tadokora [7] and Pollock[3] determined, between them, the bond lengths and bond angles in poly(ethylene glycol) - mercuric chloride complexes; (C-C) = 1.54 Å, (C-O) = 1.43 Å, COC = CCO = 109° 28', Hg - O = 2.8 Å and Hg O Hg = 85°. These workers also showed that each mercury atom is coordinated with two ether oxygen atoms of adjacent repeat units of the polyether chain.

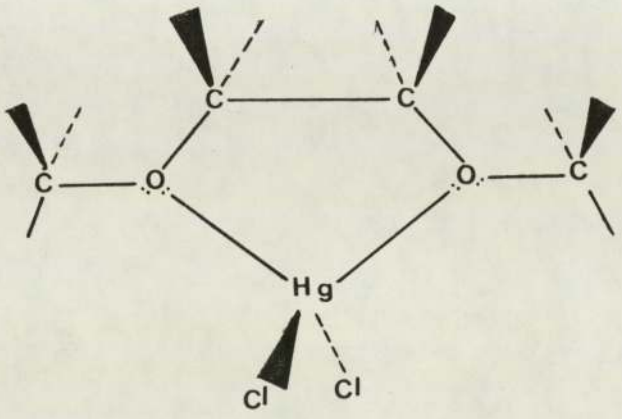

The implications of this proposed structure on the interpretation of dielectric data will be discussed subsequently.

5.2 Preliminary comments concerning the calculation of Dipole moments for the poly(propylene glycol) - mercuric chloride system

The magnitude of the dielectric dispersion, which is proportional to the experimentally determined quantity $(\varepsilon_o - \varepsilon_\infty)$, may be used to derive a mean-square dipole moment for the total number, N, of dipolar units present in unit volume (1 cm^3) of the dielectric. From a knowledge of the magnitude of $(\varepsilon_o - \varepsilon_\infty)$ for the pure polymer and of that for the polymer-salt solutions it is then possible, subject to certain constraints embodied in models adopted to describe the constitution of the system,

to calculate dipole moments associated with the solute or the complexes. For a condensed medium comprised of polar molecules the relationship between dipole moments and dielectric permittivity is normally suitably expressed by means of the Onsager[29] or Fröhlich[30] equations. To a first approximation the orientational correlations between dipolar units may be neglected. The possible effects of this assumption will be discussed in a later section. The Onsager equation, suitable for a polymer, is given as

$$\frac{\langle \mu^2 \rangle}{n} = \frac{9K\, M_m}{4\pi\, N_L} \left[\frac{(\varepsilon_o - \varepsilon_\infty)}{(\varepsilon_\infty + 2)^2} \frac{T}{\rho} \frac{(2\,\varepsilon_o + \varepsilon_\infty)}{\varepsilon_o} \right] \quad 5\text{-}1$$

where $\langle \mu^2 \rangle / n$ is the mean-square dipole moment of the polymer molecule divided by, n, the number of repeat units in the chain. The monomer molecular weight is denoted by M_m and ε_o and ε_∞ are the limiting low frequency and high frequency values of the dielectric permittivity. The quantities K, N_L, ρ and T are the Boltzmann constant, Avogadro's number, density of the medium and the absolute temperature, respectively.

It is sometimes more convenient to express the Onsager equation in terms of, N, the number of dipolar units per unit volume of material. In fact, this form is closer to the original formulation published by Onsager.

Thus

$$< \mu^2 > = \frac{9K}{4 \pi N} \left[\frac{(\varepsilon_o - \varepsilon_\infty)}{(\varepsilon_\infty + 2)^2} \frac{T}{\rho} \frac{(2 \varepsilon_o + \varepsilon_\infty)}{\varepsilon_o} \right] \quad 5\text{-}2$$

For a two-component, miscible mixture comprised of component 1 and component 2 the total number of dipolar units may be calculated using one of the following relationships.[53]

$$N = \frac{(W_1 M_1 + W_2 M_2) \rho N_L}{M_1 M_2 (W_1 + W_2)}$$

$$N = \frac{(n_1 + n_2)}{(n_1 M_1 + n_2 M_2)} \rho N_L \quad 5\text{-}3$$

$$N = \frac{\rho N_L}{(f_1 M_1 + f_2 M_2)}$$

where $W_{1,2}$, $n_{1,2}$, $M_{1,2}$, and $f_{1,2}$ are the weight, number of moles, molecular weight and mole fraction of components 1 and 2, respectively. The derivation of values for the density is considered in the following section.

5.3 Density of poly(propylene glycol)

For pure poly(propylene glycol) possessing molecular weights of 1025 or greater, the polymer density over the temperature range 243K to 293K, may be calculated using the expression

$$\rho = 1/(1.1368 - 0.0025\ T + 7 \times 10^{-6}\ T^2) \qquad 5\text{-}4$$

where p is the density of the polymer expressed in grams per millilitre and T is the absolute temperature. The corresponding expression with T in degrees centigrade is

$$\rho = 1/(0.970 + 0.0013\ T + 7 \times 10^{-6}\ T^2) \qquad 5\text{-}5$$

A table of densities for pure PPG was constructed using equation (4).

Table 5.1

Temperature/K	Density/g cm^{-3}	Temperature/K	Density/g cm^{-3}
293	1.001	243	1.066
288	1.009	238	1.071
283	1.016	233	1.076
278	1.023	228	1.080
273	1.030	223	1.084
268	1.037	218	1.087
263	1.044	213	1.090
258	1.050	208	1.092
253	1.056	203	1.094
248	1.061	198	1.096

Values extrapolated to temperatures below the range specified by Baur[51]

5.4 Densities of solutions of mercuric chloride in poly(propylene glycol)

A knowledge of the densities of solutions of mercuric chloride in poly(propylene glycol) is required in order to calculate the number of dipolar units per unit volume of solution, prior to the calculation of $< \mu^2 >$ using the Onsager equation.

The densities of 2, 4 and 7 mole per cent solutions of mercuric chloride in PPG 2025 shown in Table 5.2 were calculated for various temperatures using appendix (3), the densities of pure PPG shown in Table 5.1, together with the published density of solid mercuric chloride (5.44 g cm^{-3} at 293K). The density of the solid mercuric chloride was assumed to be essentially constant over the range of temperature considered. A check on typical coefficients of thermal volume expansion of solids indicates that this is a reasonable assumption. The additional assumption that mercuric chloride forms ideal solutions with PPG is likely to be the greater source of error. The mean solution molecular weights M_{12} given in Table 5.2 were calculated using the simple alligation formula

$$M_{12} = f_1 M_1 + f_2 M_2 \qquad 5\text{-}6$$

where M_1 and M_2 are the molecular weights of components 1 and 2, respectively.

The densities of 2 and 4 mole per cent solutions of mercuric chloride in PPG 4000 were assumed to be the same as solutions of the salt made up using PPG 2025.

Table 5.2

Densities of 2, 4 and 7 mole % solutions of mercuric chloride in poly(propylene glycol)

Temperature (K)	density/g cm^{-3} of $HgCl_2$ solutions for mole % of 2(M_{12} = 62.3)*	4(M_{12} = 66.5)*	7(73.0)*
293	1.07	1.15	1.27
288	1.08	1.16	1.28
283	1.09	1.17	1.28
278	1.10	1.17	1.29
273	1.10	1.18	1.30
268	1.11	1.19	1.31
263	1.12	1.20	1.32
258	1.12	1.20	1.32
253	1.13	1.21	1.33
248	1.14	1.22	1.34
243	1.14	1.22	1.34
238	1.15	1.23	1.35
233	1.15	1.23	1.36
228	1.16	1.24	1.36
223	1.16	1.24	1.36
218	1.16	1.25	1.37
213	1.17	1.25	1.37
208	1.17	1.25	1.37
203	1.17	1.26	1.38

* Solution molecular weights calculated using equation (6)

5.5 Comments Relating to the interpretation of Cole-Cole plots

The mean dipole moment of polymer may be calculated from the experimental values of the zero frequency and infinite frequency dielectric permittivities, ε_o and ε_∞, respectively. However, it is generally better, from the point of view of improved accuracy, to obtain ε_o and ε_∞ from Cole-Cole plots in which dielectric loss, ε'', the imaginary component of the complex permittivity $\varepsilon^* = \varepsilon' - i\,\varepsilon''$ ($i = \sqrt{-1}$), is plotted against the dielectric permittivity, ε', the real component of ε^*. For polar molecules that rotate at a single rate of rotation, typified by a rotational relaxation time, τ_o, a Cole-Cole plot of pairs of ε' and ε'', measured at different frequencies, f, over the approximate range

$$\frac{10^{-2}}{2\pi\,\tau_o} < f < \frac{10^{2}}{2\pi\,\tau_o}$$

will give a semi-circle with its centre on the ε' axis and a radius equal to the maximum loss ε''_m. (See points on solid line in Figure 5.1).

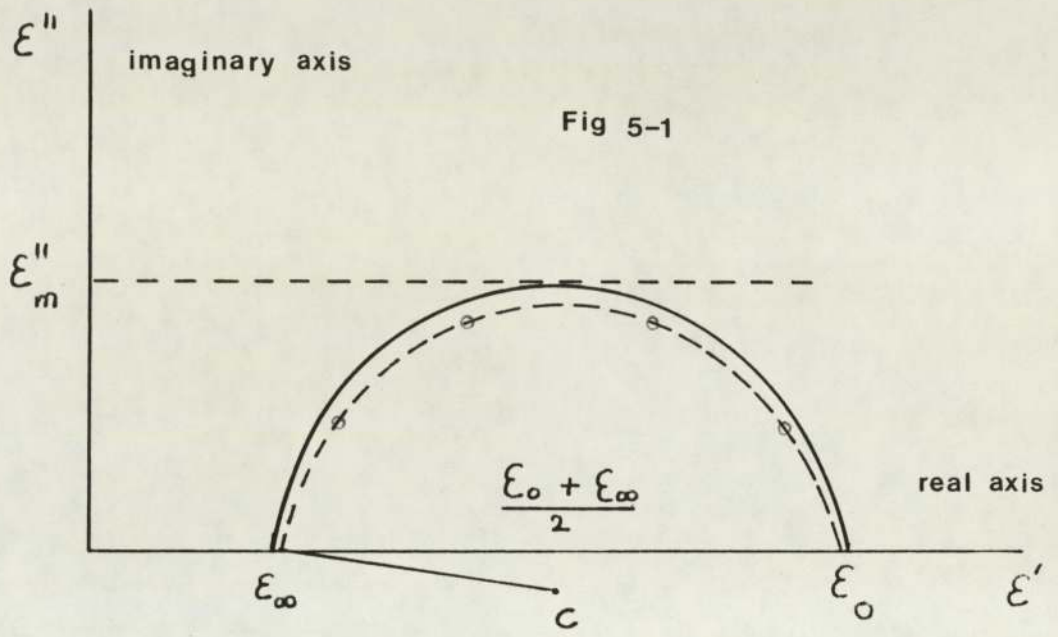

Fig 5-1

A typical set (i.e. a range of τ_o values) of experimental points, shown in Figure 5.1, represent pairs of ε' and ε'' obtained at frequencies decreasing as ε' increase . The relatively simple form of orientational relaxation, characterised by a single relaxation time τ_o, was first described by Debye. It is apparent from even a cursory examination of the curves shown in Figure 5.1 that Cole-Cole plots are a very convenient graphical method for the representation of the entire dielectric properties of a chemical system. Superpositioning of Cole-Cole plots, together with a vertical displacement of curves obtained at different temperatures, permits the

effect of temperature on ε'' and ε' to be easily ascertained. For a complete set of relaxation data, that is to say, a set of ε' and ε'' covering the spectrum of frequency associated with the relaxing system, the limiting values ε_0 and ε_∞ may be obtained form the intersection of the locus of Cole-Cole plots on the ε' axis. Furthermore, departures of Cole-Cole plots from a semicircular shape, usually manifested as a flattening of the locus to give an arc possessing a centre located below the ε' axis, provides information concerning the breadth of the relaxation process or the spectrum (distribution) of relaxation times.

When the data is limited in quantity at either the high frequency or low frequency end of the Cole-Cole locus then it may prove difficult to accurately determine ε_∞ or ε_0. Furthermore, it may be in such instances, difficult to ascertain the breadth of the relaxation process. If the data is not too limited then the gradient of the locus at the point at which it intersects the real axis may be used as an indicator of the breadth of distribution times. For a Debye process the locus of the Cole-Cole plot approaches the ε' axis at 90°. Employing conventional notation for gradients of curves this angle is smaller than 90° at the high frequency limit and greater than 90° at the low frequency limit, for non-Debye relaxation processes. A large body of dielectric data (i.e. pairs of ε'' and ε' measured at the same frequency for a variety

of frequencies covering the relaxation process) can be adequately represented by a circular arc possessing a centre situated below the ε' axis on a line that bisects the distance between ε_0 and ε_∞. The flatter or more shallow the circular arc, then the greater is the span of relaxation frequencies associated with the relaxation process. A quantitative measure of the width of a relaxation process may be obtained from the application of simple geometry to the circular arcs.

The broken curve shown in Figure 5.1 represents a non-Debye relaxation curve that has been fitted to the experimental data (O) by drawing a circular arc with its centre located at point C. The angle between the line connecting C to ε_∞ and the real axis is equal to $\alpha\pi/2$ where α $(0<\alpha<1)$ is an empirical parameter introduced by Cole-Cole into the fundamental complex permittivity equation

$$\varepsilon^* - \varepsilon_\infty = (\varepsilon_0 - \varepsilon_\infty)/(1 + i\omega\tau_0) \qquad 5\text{-}7$$

to yield an equation of the form

$$(\varepsilon^* - \varepsilon_\infty) = (\varepsilon_0 - \varepsilon_\infty)/\left[1 + (i\omega\tau_0)^{1-\alpha}\right] \qquad 5\text{-}8$$

Cole-Cole stressed that the introduction of the empirical quantity merely serves the purpose of relating a large body of, otherwise disparate, dielectric relaxation

data to a common analytical expression; namely a circular arc. The parameter α may then be regarded simply as a convenient means of specifying the broadness of experimental relaxation peaks.

A number of other empirical parameters have been introduced with purposes similar to that placed on α. Davidson and Cole obtained improved fits with experiment using

$$\varepsilon^* - \varepsilon_\infty = (\varepsilon_o - \varepsilon_\infty)/(1 + i\omega\tau_o)^\beta \qquad 5\text{-}9$$

where β lies in the range $0<\beta<1$.

This equation has proved useful in instances where there is a skewed distribution of relaxation times about τ_o. A slightly different approach, used to emulate experimental dielectric relaxation data, has been proposed by Cook, Watts and Williams[54]. Instead of introducing a 'broadness' parameter into the frequency domain equation these authors modified the normally (for Debye processes) exponential time-domain step response to give a decay function of the general form.

$$\psi(t) = e^{-(t/\tau_o)^\gamma} \qquad 5\text{-}10$$

where γ can take possible values $0<\gamma<1$.

5.6 Calculation of ε_∞ values of PPG - Hg $C\ell_2$ solutions at low temperatures

For pure samples of poly(propylene glycol) it has been shown by Williams[55] that because ε_0 is not very large (i.e. $\varepsilon_0 - \varepsilon_\infty$ is relatively small) then the choice of ε_∞ is quite an important decision in the calculation of dipole moments. Some workers have resorted to the approximation $\varepsilon_\infty \approx n^2$ where n is the refractive index determined at visible wavelengths. Williams denotes values of ε_∞ calculated in this manner by ε_{n^2}. Without exception it is found that values of ε_{n^2} are significantly smaller than ε_∞ values obtained from the limiting high frequency intercept of the Cole-Cole[40] plots. The difference between ε_{n^2} and ε_∞ has been attributed, by some workers, to the effects of atomic polarisation. For PPG the ratio $\varepsilon_\infty/\varepsilon_{n^2}$ is approximately 1.2.

For liquid homogeneous, amorphous polymers the 'infinite' frequency permittivity is expected to change only quite slowly with changes in temperature. Provided that the chemical composition is unchanged by changes in temperature, then an approximation of ε_∞ at any temperature T can be calculated from a knowledge of the refractive index, n, and density, ρ, at room temperature by employing the Lorentz-Lorenz[27] relationship for molar refraction

$$R_m = \frac{(n^2 - 1)}{(n^2 + 2)} \frac{M}{\rho} = \frac{(\varepsilon_{n^2} - 1)}{(\varepsilon_{n^2} + 2)} \frac{M}{\rho} \simeq \frac{(\varepsilon_\infty - 1)}{(\varepsilon_\infty + 2)} \frac{M}{\rho} \qquad 5\text{-}11$$

where M is the molecular weight of the repeating unit. Once R_m has been calculated at one temperature it may then be regarded as an unchanging quantity with respect to temperature. The 'infinite' frequency permittivity, $\varepsilon_\infty \simeq \varepsilon_{n^2}$ may then be calculated at any other temperature provided that the corresponding density is known.

For poly(propylene glycol) possessing a molecular weight of ~2000 or greater, the refractive index measured using the sodium -D line at 293°K is 1.456.[37] The required molecular weight and density are 58 and 1.001 g cm^{-3}, respectively. Using equation (11) the molar refraction R_{m^2} is calculated to be 15.75 cm^3. It seems reasonable to regard this value of R as the smallest possible value of molar refraction for poly(propylene glycol). The analysis of dipole relaxation data obtained for a sample of high molecular weight poly(propylene glycol) (M.W $\sim 10^6$) yielded a value close to 3.0 for ε_∞.[55] From an examination of plots of ε' vs frequency for pure PPG 2025 published by Baur and Stockmayer[56] it may be deduced that ε_∞ is probably less than 3.0. Their values of ε_∞ are close to those measured by Alper, Barlow and Gray[57] and Yano et al[58]. Alper and co-workers measured ε_∞ of PPG 4000 at frequencies approaching 200 MHz. They found that ε_∞ increased almost linearly from ~2.5 at

293K to ~2.9 at 209K. The Cole-Cole plots of undiluted poly(propylene glycol) published by Yano et al[58] also indicate a range of values of ε_∞ extending from ~2.4 at 361K to ~2.9 at 215K. Since the determination of ε_∞ at temperatures greater than 273K are often affected by the onset of electrical conduction it seems prudent to calculate molar refractions using values of ε_∞ obtained for PPG at low temperatures. Thus R_∞ was calculated for PPG using a value of $\varepsilon_\infty = 2.9$ determined at 223K (-50^oC) and a density (see Table 5.2) of 1.084 g cm^{-3} and was found to be 20.7 cm^3 (referred to as R_1 in subsequent calculations).

The refractive index, n_D, density and molecular weight of anhydrous, solid mercuric chloride at 293K are 1.859, 5.44 g cm^{-3} and 271.5, respectively. The corresponding molar refraction, R_{n^2}, calculated using equation (11) is found to be 22.5cm^3 (referred to as R_2 in subsequent calculations).

The molar refraction of simple two component solutions can be calculated using the relationship

$$R_{12} = f_1 R_1 + f_2 R_2 \qquad 5\text{-}12$$

where f and R denote the mole fraction and molar refraction respectively. The subscripts 12, 1 and 2 denote quantities associated with the solution, component 1 (often

regarded as the solvent) and component 2 (the solute).

For reasons presented in an earlier section (5.4) the molar refraction, R_2, of mercuric chloride will be assumed to vary little with temperature over the range of temperatures considered in the present study. Using equation (12) together with R_1 = 20.7 cm^3 and R_2 = 22.5 cm^3 the molar refraction of 2, 4 and 7 mole % solutions of mercuric chloride in PPG 2025 were calculated to be 20.74, 20.77 and 20.83, respectively. Taking into account the possible errors associated with the experimental quantities used in this calculation it is concluded that for simple solutions of Hg $C\ell_2$ in PPG polymer the molar refraction is 20.8 cm^3 and approximately constant over the concentration range 2-7 mole percent of salt.

The molar refraction together with the densities and molecular weights listed in Table (5.2) may then be used to calculate ε_∞ values of solutions of mercuric chloride in PPG, at various temperatures, by solving the Lorentz-Lorenz equation (equation (11)). The majority of dielectric data acquired for PPG-Hg $C\ell_2$ in the present study corresponds to the temperature range 223K to 253K. The entries in Table (5.3) indicate that for this particular polymer-salt system, ε_∞ is not expected to change by much more than 3% over the entire ranges of salt concentration and temperature.

Table 5.3

Infinite frequency permittivity, ε_∞, of solutions of mercuric chloride in PPG 2025 calculated using equation (**11**) and solution densities and molecular weights in Table (**5.2**)

Temperature/K	2%	4%	7%
293	2.67	2.69	2.70
283	2.72	2.73	2.72
273	2.74	2.75	2.77
263	2.79	2.80	2.81
253	2.82	2.83	2.83
243	2.84	2.85	2.85
233	2.87	2.88	2.90
223	2.90	2.90	2.90
213	2.92	2.93	2.92
203	2.92	2.95	2.94

5.7 Calculation of Dipole Moments

From the dielectric relaxation data presented in Cole-Cole plots presented in the results chapter (Figures 4.22 - 4.29) together with equations 5.2 and 5.3 the average dipole moment $< \mu_o >$ per dipolar unit may be calculated for the various solutions of mercuric chloride in poly(propylene glycol).

It has been indicated previously that $< \mu_o >$ depends on $(\varepsilon_o - \varepsilon_\infty)$ and on the number of dipolar units per unit volume, N; a quantity that is dependent on the model adopted to describe the nature of the interactions between the salt and PPG. Table 5.4 shows values of N calculated for 2, 4 and 7 mole % solutions of Hg $C\ell_2$ in PPG 2025, at various temperatures, assuming that the salt and the polymer repeat units are independent entities. The values of N given in brackets in Table 5.4 are quantities calculated assuming that all of the mercuric chloride is complexed by the polymer. At 248K the static dielectric permittivity of 2, 4 and 7 mole % solutions of PPG 2025 - Hg $C\ell_2$ is 8.6, 10.9 and 10.8 respectively. The corresponding root-mean-square dipole moments were calculated (using $\varepsilon_\infty = 3$) to be 1.08D, 1.26D and 1.25D respectively. The alternative model, in which every molecule of mercuric chloride is in complexed form, yields dipole moments of 1.10D, 1.31D and 1.35D for the 2, 4 and 7 mole % solutions of PPG 2025 - Hg $C\ell_2$ at 248K. At this temperature, the root-mean-square

Table 5.4 Number of Dipolar Units per Unit Volume of solution for the Poly(propylene glycol) - $HgCl_2$ System

	2 mole %		4 mole %		7 mole %		$[HgCl_2]$
Temp/K	N_1	N_2	N_1	N_2	N_1	N_2	(x 10^{-20})
253	107	2.18	105	4.38	102	7.68	
	(105)		(101)		(94)		
248	108	2.20	106	4.4	103	7.72	
	(106)		(102)		(96)		
243	108	2.20	106	4.41	103	7.74	
	(106)		(102)		(95)		
238	109	2.20	107	4.45	104	7.80	
	(107)		(103)		(96)		
233	109	2.20	107	4.45	104	7.86	
	(107)		(103)		(96)		
228	110	2.24	108	4.49	104	7.86	
	(108)		(104)		(96)		
223	110	2.24	108	4.48	104	7.86	
	(108)		(104)		(96)		

N_1 is the number of 'free' ether repeat units per unit volume. N_2 is the number of 'free' molecules of mercuric chloride per unit volume. The numbers enclosed in brackets are the total number of dipolar units per unit volume of solution for the model in which all the mercuric chloride molecules are fully complexed with the polyether.

dipole moment of pure PPG 2025 was found to be 0.75D.

From a knowledge of the mean dipole moment per repeat unit of pure PPG and the known dipole moment of the Hg-Cℓ bond the mean dipole moments of the various salt solutions may be calculated and compared with the experimental values. Once again the simplest model of the solutions is that in which PPG repeat units and molecules of $Hg\ C\ell_2$ behave as independent dipolar units. Any assumption concerning the dipolar nature of $Hg\ C\ell_2$ implies that the molecule departs from its linear structure observed in the gas phase. For present purposes it will be assumed that in solution in PPG 2025 the molecules of mercuric chloride are tetrahedral. This structural form of $Hg\ C\ell_2$ is best regarded as a limiting case. In reality, the structure of $Hg\ C\ell_2$ in solution in PPG probably lies between the linear and tetrahedral forms. The dipole moment of the tetrahedral form of $Hg\ C\ell_2$ is calculated to be 3.69D ($^{\mu}Hg\ C\ell \equiv 3.2D$ ref*). The root-mean-square dipole moment per dipolar unit for PPG 2025 - $Hg\ C\ell_2$ (molecules independent) may then be calculated using the alligation formula

$$< \mu_o^2 > \ = \ f_1 < \mu^2 >_1 \ + \ f_2 < \mu^2 >_2 \qquad \text{5-13}$$

where $< \mu^2 >_1$ (PPG) $= 0.75^2$ and $< \mu^2 >_2$ ($Hg\ C\ell_2$) $= 3.69^2$. The mean dipole moment per dipolar unit was then found to be 0.91D, 1.22D and 1.22D for 2, 4 and 7 mole % solutions

* J. Am. Chem. Soc. 64 (1942) p830

of PPG 2025 - Hg $C\ell_2$ at 248K.

If the mercuric chloride is assumed to be fully complexed with the polymer then the main changes necessary in the previous calculations relate to the change in the number of dipolar units per unit volume of solution (see Table **5.4**). The theoretical dipole moment per dipolar unit is then calculated to be 0.91D, 1.06D and 1.27D for the 2%, 4 mole % and 7 mole % solutions of PPG 2025 - Hg $C\ell_2$.

Further refinements to the 'complexed' model can be attempted, but their acceptibility must eventually depend on the acquirement of further data from other sources such as, for example, NMR spectroscopy. An obvious refinement concerns the contribution of the polyether segment, involved in the complex, to the dipole moment of the complex. This is difficult to calculate since it requires a detailed knowledge of the structure of the complex (see section 5.1) and of the dipole moments of the Hg - O 'bond' formed between the ether oxygen atoms and the mercury atoms. In addition, there is likely to be a dipole moment contribution from the dipolar C - O bonds of the polyether segments that are directly involved in complex. Assigning a dipole moment of 1.13D (ref **37**) to C - O then the dipole moment of the cis form of the polyether segment -O-C-C-O- is calculated to be 2.23D, based on tetrahedral valence angles. In the liquid polymer-salt solutions it seems

unlikely that the polymer would adopt the fully eclipsed (cis) conformation. A conformation closer to the gauche form ($\phi = \pm 120^{\circ}$) would be energetically more favourable with respect to the conformation of the polymer chain. The dipole moment associated with the gauche form of -O-C-C-O- is calculated to be 1.11D. Thus, the total dipole moment of the polyether - Hg $C\ell_2$ compex is calculated to be 5.92D and 4.80D for the cis and gauche forms of the polyether segment, respectively. The corresponding mean dipole moment per dipolar unit is then calculated to be 1.13D, 1.44D and 1.84D for the 2%, 4% and 7 mole % PPG 2025 - Hg $C\ell_2$ solutions. For the gauche polyether segment, the corresponding theoretical mean dipole moments were formed to be 1.02D, 1.24D and 1.55D.

An alternative approach, but one that is equivalent to that described above involves the calculation of the dipole moment of either the solute (Model 1; Hg $C\ell_2$ molecule moving independently of PPG) or the dipole moment of the complex (Model 2; Hg $C\ell_2$ molecules tightly bound to a segment of the polyether). Thus, for solutions of mercuric chloride in PPG 2025, in which the molecules of Hg $C\ell_2$ are regarded as free solute molecules the experimental mean dipole moments of Hg $C\ell_2$ for 2%, 4% and 7 mole % solutions were determined to be 5.6D, 5.1D and 3.9D, respectivley. For the model in which the Hg $C\ell_2$ is assumed to be fully complexed, the experimentally derived mean dipole moment of the complex was found to be 5.6D, 5.2D and 4.0D for the 2%, 4% and 7% solutions.

The gradual decrease in the experimental dipole moments of the solute (or complex) with increasing concentration of salt may be associated with the raising of the glass transition temperature and/or to the increase in salt-salt interactions. The first effect causes the gradual 'freezing out' of contributions to ε_o while for the second effect it is envisaged that at increasingly higher concentrations of salt the intersection between salt molecules leads to non-polar aggregates.

It is not possible to distinguish between models 1 and 2 using arguments based solely on a comparison of dipole moments. However, for both of these models an important assumption employed in the interpretation of the dielectric data has been that the Hg $C\ell_2$ is regarded as non-linear with an angle $\angle C\ell$ Hg $C\ell$ equal to 109^o. However, this assumption must be regarded with some caution for two main reasons. Firstly, the structure of Hg $C\ell_2$ in the gas-phase is linear and hence non-polar. Secondly, the molecules of Hg $C\ell_2$ in crystalline complexes of poly(ethylene oxide) are only slightly non-linear ($\angle C\ell$ Hg $C\ell = 176^o$)[6] and possess an estimated dipole moment of 0.2D. ($\mu_{Hg - C\ell} = 3.2D$).

Thus, if the molecules of Hg $C\ell_2$ in PPG 2025 - Hg $C\ell_2$ complexes are nearly linear then there remains the problem of explaining the relatively large dipole moments arising from the addition of Hg $C\ell_2$ to PPG.

The maximum contribution to the dipole moment of the complex from the polyether segment -O-C-C-O- is approximately 2.2D (cis conformation). The experimental dipole moment of the complex is calculated to be approximately 5.4D. Thus, for complexes in which the molecules of Hg $C\ell_2$ are linear the moiety

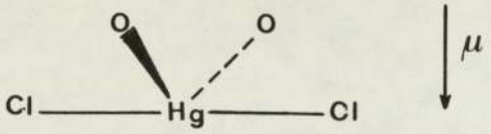

must possess a dipole moment of 3.2D in the direction indicated in order to give a total dipole moment of 5.4D for the complex.

In crystals of poly(ethylene oxide) - mercuric chloride complexes the molecules of mercuric chloride are flanked by two chains of poly(ethylene oxide) . This structural arrangement for the closely packed crystals of PEO - Hg $C\ell_2$ provides an almost symmetrical environment for the molecules of mercuric chloride. For dilute solutions of Hg $C\ell_2$ in liquid, atactic poly (propylene glycol) the requirements necessary for regular packing of molecules are relaxed or completely absent. Thus the environment of mercuric chloride in solution

in poly(propylene glycol) may be significantly different from that of molecules of mercuric chloride in solution in poly(ethylene glycol); different in the sense that for the former solutions the mercuric chloride molecules may be able to adopt shapes departing significantly from the linear form. It is interesting to pursue this tentative hypothesis.

A comparison of the experimental and theoretical dipole moments of the complex PPG - Hg $C\ell_2$ indicates that, for tetrahedrally-shaped molecules of mercuric chloride, the segment of polyether chain (O-C-C-O) participating in the complex adopts a conformation that is closer to the gauche form. An examination of scale molecular models of the structure shown in section 5.1 lends support to this conclusion. For the cis type of structure the distance between the oxygen atoms of adjacent ether groups is calculated, employing simple geometry, to be 3.54 $\mathring{A}$. X-ray studies[2,6] of PEO - Hg $C\ell_2$ complexes give a value of 2.8 $\mathring{A}$ for the length of the Hg - O distance. For a symmetrically positioned Hg $C\ell_2$, relative to the two oxygen atoms involved in the complex, the angle $\angle$O Hg O was found to be 79° in the present study. If the complexed segment of the polyether is allowed to adopt a gauche conformation then the distance between oxygen atoms is increased to 4.18 $\mathring{A}$ and (for Hg - O distance equal to 2.8 $\mathring{A}$) the angle $\angle$O Hg O is increased to 87°. It is interesting that this angle is close to the value

of 85° deduced for ∠O Hg O from the X-ray data of crystalline complexes of poly(ethylene glycol) and mercuric chloride[6] .

The cis and gauche forms of the PPG - Hg Cl_2 complex are represented in Figure 5.2 . The structures shown in this figure depict the approximate relative positions of the atoms involved in the complex. It is interesting to note that for the gauche type of structure the pendent methyl group tends to produce a 'locking' action since it lies on a plane that bisects the two methylene hydrogen atoms of the adjacent backbone carbon atom and is, therefore, much less sterically hindered than the methyl group in the cis type of complex, in which the methyl group is eclipsed by a hydrogen atom. For poly(ethylene glycol) which does not possess a pendant methyl group such a 'locking' action is much less probable and the polyether segment associated with the mercuric chloride complex is able to adopt a cis conformation that is virtually sterically unhindered.

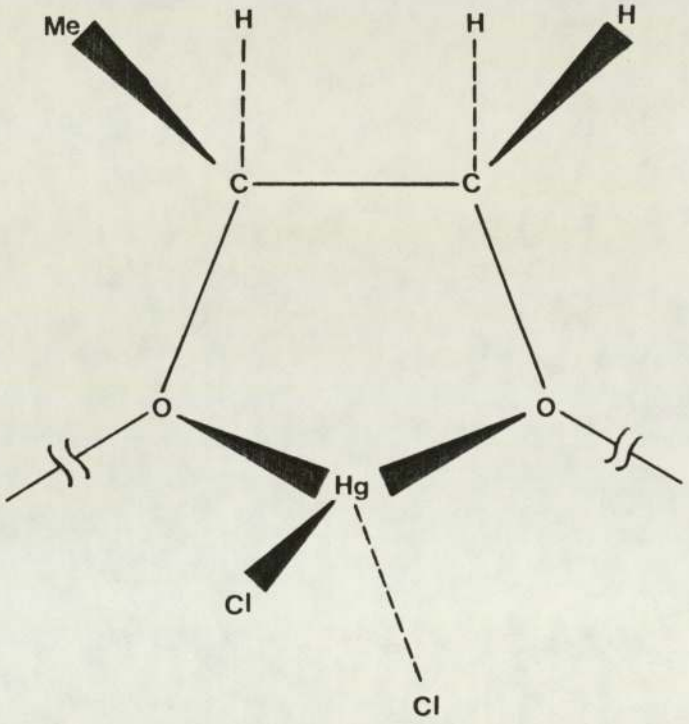

cis form of PPG–$HgCl_2$ Complex

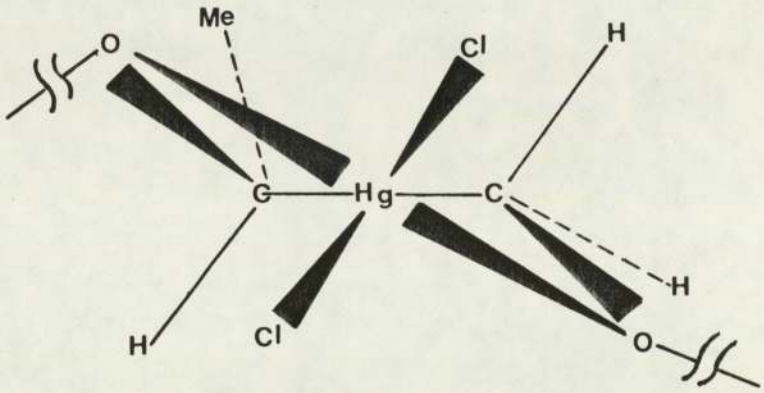

gauche form of PPG–$HgCl_2$ Complex

Fig 5–2

5.8 Effect of Mercuric Chloride on the Average Conformations of Poly(propylene glycol) Chains.

In a paper concerned with the dielectric relaxation behaviour of pure poly(propylene glycol) Williams[37] calculated the average cosine of the bond rotational angle, φ, namely $\langle \cos \varphi \rangle$ (often denoted by η), using the Marchal-Benoit relation.[36]

$$\frac{\langle \mu^2 \rangle}{n} = \frac{2 \mu_o^2 (1 - \eta^2)(1 - v^2)}{(1 + v + v^2)[(1 + \eta^2) + \eta f(v)]} \qquad 5\text{-}14$$

where

$$f(v) = \frac{1 - 2v - 2v^2}{1 + v + v^2} \qquad 5\text{-}15$$

Since v is the cosine of the valence angle supplement, θ, it follows that for tetrahedral angles ($v = 1/3$) and $f(v) = 1/13$. The other important parameters are μ_o (1.13 D) , the C-O bond dipole moment and $\langle \mu^2 \rangle / n$, the mean-square dipole moment of the polymer chain divided by the degree of polymerisation, n.

For a polymer chain in which the rotational states occupied by a skeletal bond are independent of the rotational states of adjacent skeletal bonds the average cosine of the rotational bond angle is readily expressed in terms of a three-state rotational isomeric state model. A commonly applied rotational isomeric state model for polymer chains is one in which the backbone bonds can adopt trans ($\varphi = 0^\circ$), gauche + ($\varphi = 120^\circ$) and gauche - ($\varphi = -120^\circ$) conformations. For a symmetrical energy barrier the energy difference between the trans and gauche states is equal to ΔE. Denoting the Boltzmann factor $\exp(\Delta E/RT)$ by σ then

obtained. The question then arises as to which ΔE is acceptable. Certain values of η may be readily eliminated because they give rise to negative values of the statistical weight, σ. Such solutions are unacceptable since σ must always be a positive quantity ($\sigma = \exp(\Delta E/RT)$). The dependence of σ on η is shown in figure 5.3. The shaded area shown in this figure represents the physically acceptable range of values of σ (and hence those of η). Acceptable values of η (i.e. $\langle \cos\varphi \rangle$) lie in the range $-0.5 \leqslant \eta \leqslant 1$.

The Marchal-Benoit approach, described above, may be used to examine the conformational behaviour of poly(propylene glycol). Since poly(ethylene glycol) is a crystalline solid at normal temperatures, the comparative analysis implicit in equation 19 must be undertaken at temperatures above the melting point of this material. At 340 K the static dielectric permittivity ε_o (=7.7) and the infinite frequency dielectric permittivity ε_∞ (=2.06) for PEG[55]. The corresponding values for PPG are 4.15 and 2.10 ($\varepsilon_n^2 = 1.456^2$). Substitution of these values into equation 19 yields $Z = 0.52$; a value close to 0.53 obtained by Williams[37]. Solution of the quadratic relation implicit in equation 19 yields $\eta = 0.55$ or $\eta = -.58$. For reasons discussed previously the negative value of η may be discarded in the subsequent calculation of σ. Substitution of $\eta = 0.55$ into equation 16 gives a value of $\sigma = 4.67$ from which $\Delta E = 1041$ cal mole^{-1}. This is significantly larger than the value of 500 cal mole^{-1} obtained by Williams[55]. The reason for the difference is not clear. However, a close examination of the results published by Williams[55] reveals that this author considered negative values of σ to be acceptable solutions

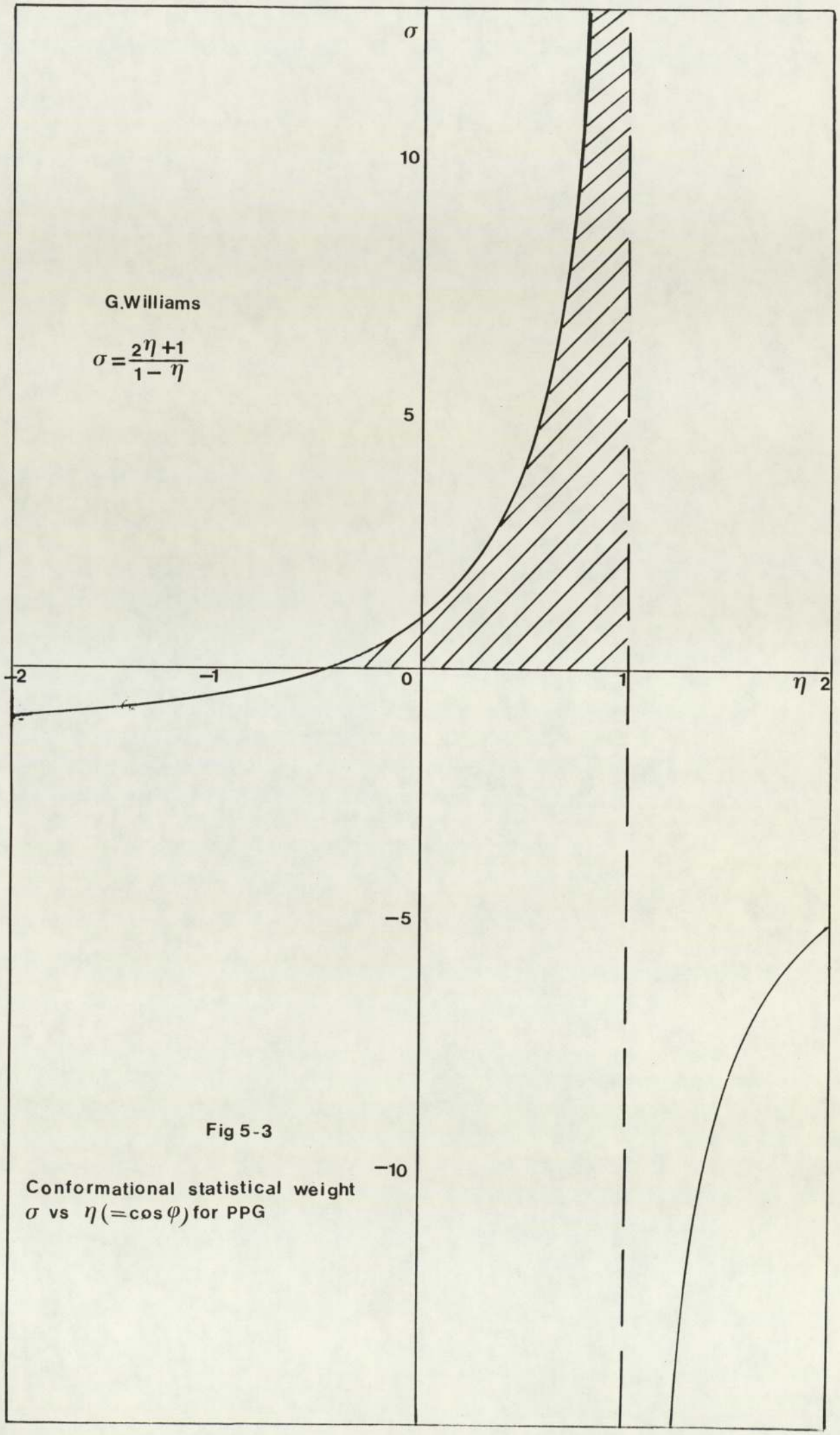

Fig 5-3

Conformational statistical weight
σ vs $\eta(=\cos\varphi)$ for PPG

of the Marchal-Benoit equation; a conclusion that must be refuted on physical grounds since statistical weights are always positive, i.e. the quantity $\exp(\Delta E/RT)$ is always positive. The larger positive value of ΔE obtained in the present calculations indicates, that for pure poly(propylene glycol), a significantly larger fraction of bonds occupying trans conformations.

For pure PPG at 248 K, $\varepsilon_o = 4.5$, $\varepsilon_\infty = 3.0$, $\rho = 1.06$ g cm^{-3} and $\eta = 0.787$ ($\sigma = 12.1$, $\Delta E = 1230$ cal mole^{-1}) or $\eta = -.80$ ($\sigma = -.334$, ΔE = indeterminate). At 248 K, $\varepsilon_o = 8.6$, $\varepsilon_\infty = 3.0$ and $\rho = 1.14$ g cm^{-3} (see table **3**) for a solution of 2 mole % $HgCl_2$ in PPG2025. Substitution of these quantities into the Onsager relation and the Marchal-Benoit equation, followed by the elimination of $\langle \mu^2 \rangle / n$ eventually yields $\eta = 0.41$ ($\sigma = 3.09$, $\Delta E = 555$ cal mole^{-1}) or $\eta = -0.44$ ($\sigma = 0.08$, $\Delta E = -1240$ cal mole^{-1}). Similar calculations performed for 4 mole % $HgCl_2$ in PPG2025 at 248 K using $\varepsilon_o = 10.9$, $\varepsilon_\infty = 3.0$ and $\rho = 1.22$ g cm^{-3} gave $\eta = 0.229$ ($\sigma = 1.89$, $\Delta E = 314$ cal mole^{-1}) or $\eta = -.265$ ($\sigma = 0.371$, $\Delta E = -489$ cal mole^{-1}). Calculation for solutions containing 7 mole % $HgCl_2$ in PPG2025 at 248 K with $\varepsilon_o = 10.8$, $\varepsilon_\infty = 3.0$ and $\rho = 1.34$ g cm^{-3} gave $\eta = 0.319$ ($\sigma = 2.41$, $\Delta E = 434$ cal mole^{-1}) or $\eta = -.354$ ($\sigma = 0.216$, $\Delta E = -755$ cal mole^{-1}).

For pure PPG, 2%, 4% and 7 mole % solutions of $HgCl_2$ in PPG2025 the positive ΔE values are 1230, 558, 314 and 434 cal mole^{-1}. Thus, with the exception of the 7 mole % solution an increasing concentration of mercuric chloride causes a decrease in ΔE; a trend indicative of an increasing proportion of gauche conformations (see figure 4). This conclusion seems reasonable when the previous comments of

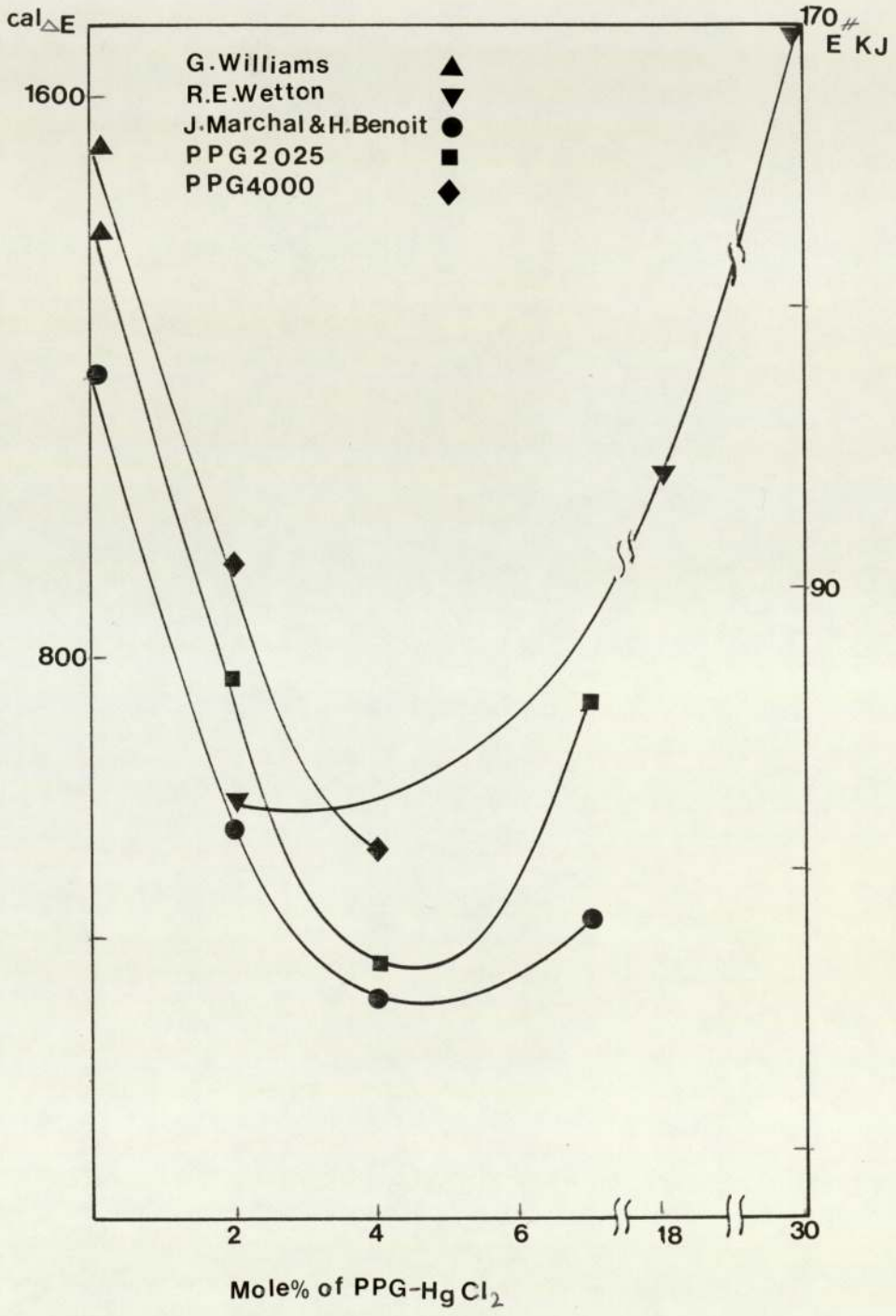
cal △E
1600
800
170 #
E KJ
90
G.Williams
R.E.Wetton
J.Marchal & H.Benoit
PPG2025
PPG4000
2
4
6
18
30
Mole% of PPG-Hg Cl2

Fig 5-4

earlier sections, relating to the possible cis and trans forms of the PPG - $HgCl_2$ complex, are recalled. The alternative solutions of the Marchal - Benoit equation, namely those leading to negative values of ΔE, exhibit exactly the opposite trend with respect to an increasing concentration of mercuric chloride, i.e. an increase in trans conformations with increase in salt content. This behaviour seems unacceptable when considered in terms of the probable cis/gauche structure of the PPG - $HgCl_2$ complex.

Also included in figure 4 are the dielectric relaxation activation energies for solutions of mercuric chloride in PPG2025 and PPG4000 calculated from gradients of log f_{max} against 1/T (see figures 5.5 , 5.6 and table 3). For the PPG2025 system the graph shows a distinct minimum in the activation energy corresponding to approximately 5 mole % concentration of $HgCl_2$. The data presented for the solutions of $HgCl_2$ in PPG4000, though lacking the data for a 7 mole % solution, appear to behave in a similar manner, but the activation energies are larger by approximately 50% relative to the corresponding solutions of $HgCl_2$ in PPG2025. It is noteworthy that the position of the minima of the dielectric activation energy, $E^{\#}$, with respect to the concentration of mercuric chloride is the same, within experimental error as that found for ΔE, the difference in energy between trans and gauche rotational states calculated from experimental values of ε_o and ε_∞ using the Marchal - Benoit treatment. Activation energies for solutions of zinc chloride in poly(propylene glycol), taken from the dielectric studies of Wetton et al **10** , also appear to exhibit minimal behaviour, but the available values of $E^{\#}$ do not permit a precise location of the

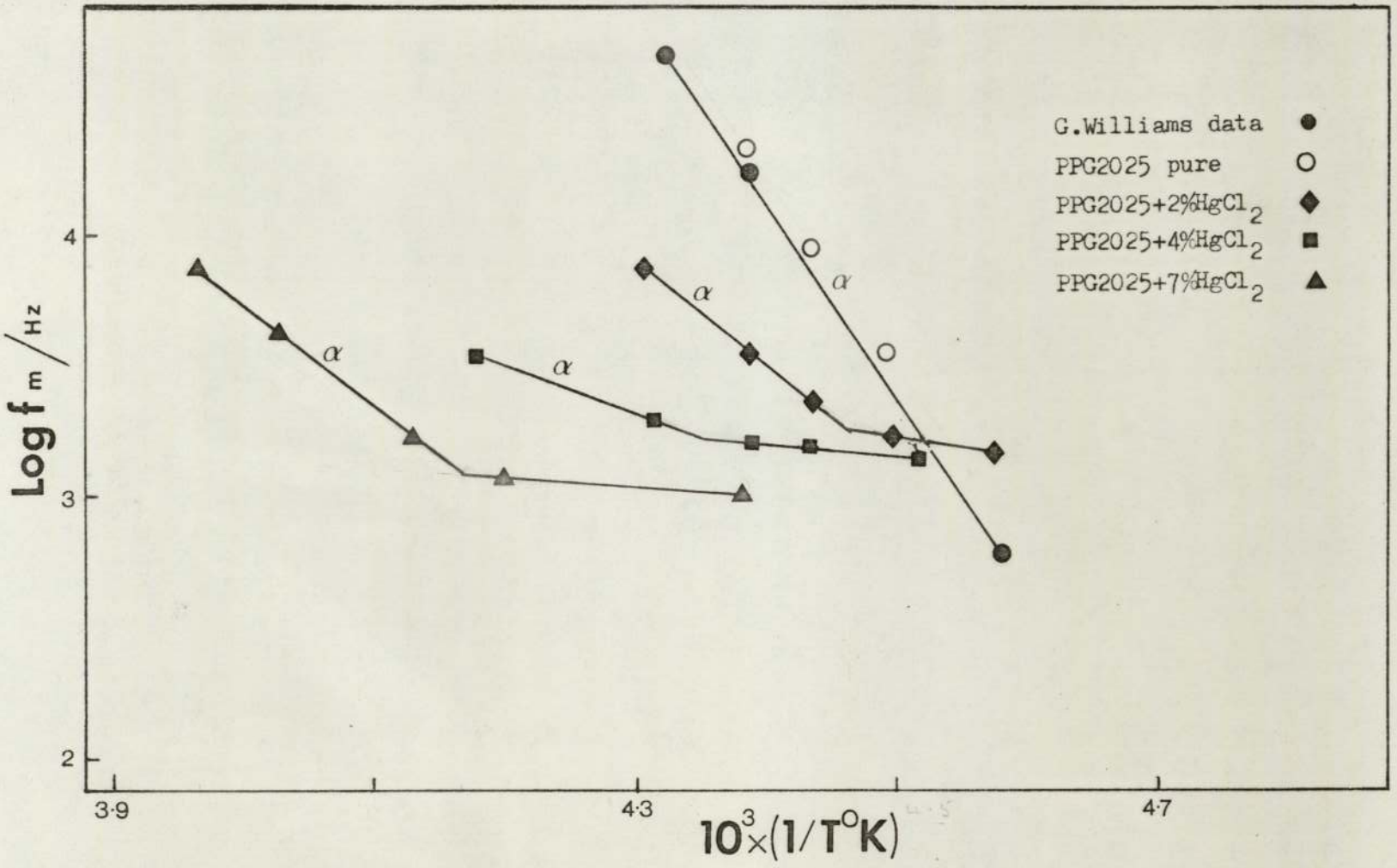
G.Williams data
PPG2025 pure
PPG2025+2%HgCl2
PPG2025+4%HgCl2
PPG2025+7%HgCl2
α
α
α
α
Log fm /Hz
4
3
2
3·9
4·3
4·7
10³×(1/T°K)

Fig(5.5)

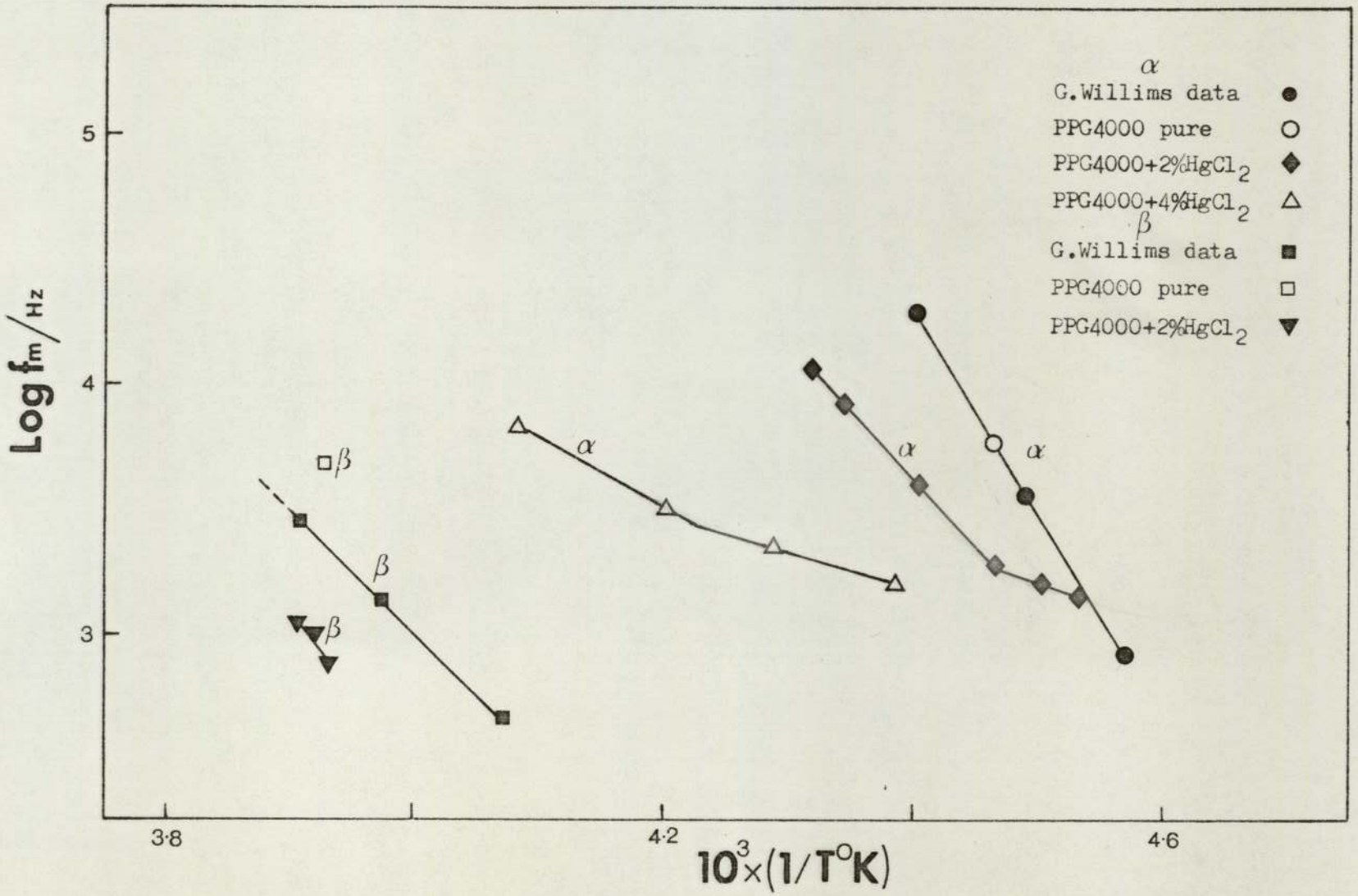
α
G.Willims data
PPG4000 pure
PPG4000+2%HgCl2
PPG4000+4%HgCl2
β
G.Willims data
PPG4000 pure
PPG4000+2%HgCl2
Log fm/Hz
5
4
3
3·8
4·2
4·6
10³×(1/T°K)
α
α
α
β
β
β

Fig(5.6)

minimum on the concentration axis.

The minimal behaviour of the activation energy as a function of the concentration of mercuric chloride is interpreted in terms of two competing effects. For low concentrations of mercuric chloride (< 5 mole %) the addition of mercuric chloride results in a lowering of the activation energy due to an increase in the rotational freedom of ether units that flank the pair of ether units directly involved in the polymer - salt complex. For any particular rotatable section of the polyether chain the adjacent repeat units, in the absence of mercuric chloride, are able to contribute via steric hindrance to the rotational energy barrier. However, for ether units that are adjacent to a complexed ether unit the steric interaction between the adjacent ether units is modified. The cyclic nature of the complex effectively inhibits or reduces the steric hindrance between ether units that flank either side of a complexed pair of ether units. The activation energy associated with the rotational motion of the complex (i.e. pair of ether units plus a molecule of mercuric chloride) is regarded as sufficiently high to exclude its contribution to the total dielectric loss. Further addition of mercuric chloride eventually reduces the number of free ether units and the activation energy begins to rise steadily to a value corresponding to the fully complexed material. This explanation of the dependence of the activation energy with respect to the concentration of mercuric chloride must be regarded as tentative. Further work, perhaps involving different salts, together with additional experimental techniques (e.g. measurement of N.M.R spin-lattice relaxation times) is required before more

reliable conclusions can be made concerning the relationship between the molecular structure of the polymer-salt complex and activation energy.

Referring to figures 5 and 6 it can be seen that plots of log f_{max} vs. 1/T for the various solutions of mercuric chloride in poly(propylene glycol) exhibit a marked change in gradient. This change, which corresponds to a change in the activation energy, is regarded as indicative of a rubber-to-glass transition. The difference in activation energy is most marked for the solutions of $HgCl_2$ in PPG2025. For example, for a 4 mole % solution of $HgCl_2$ in PPG2025 the activation energies at temperatures above and below the glass-transition temperature, T_g, were determined to be 35.4 kJ mol^{-1} and 7.7 kJ mol^{-1}. The corresponding values observed for 4 mole % solutions of $HgCl_2$ in PPG4000 were 53.8 kJ mol^{-1} and 26.9 kJ mol^{-1}, respectively. The processes contributing to the dielectric loss at temperatures below the glass transition temperature may arise from two possible sources. Conduction, due to the presence of free ions is one possible contribution to the total loss [59]. Another explanation for the existance of a relaxation process operating at temperatures below T_g is based on the presence of a rotator phase. However, the latter mechanism appears less likely in view of the most probable structure proposed for the complex (refer to earlier sections).

Glass-transition temperatures deduced from the curves shown in figures 5 and 6 are shown in figure 7 as a function of the mole fraction of co-ordinated monomer. Two additional data points are also included in this figure; one for a 17.5 mole % solution of

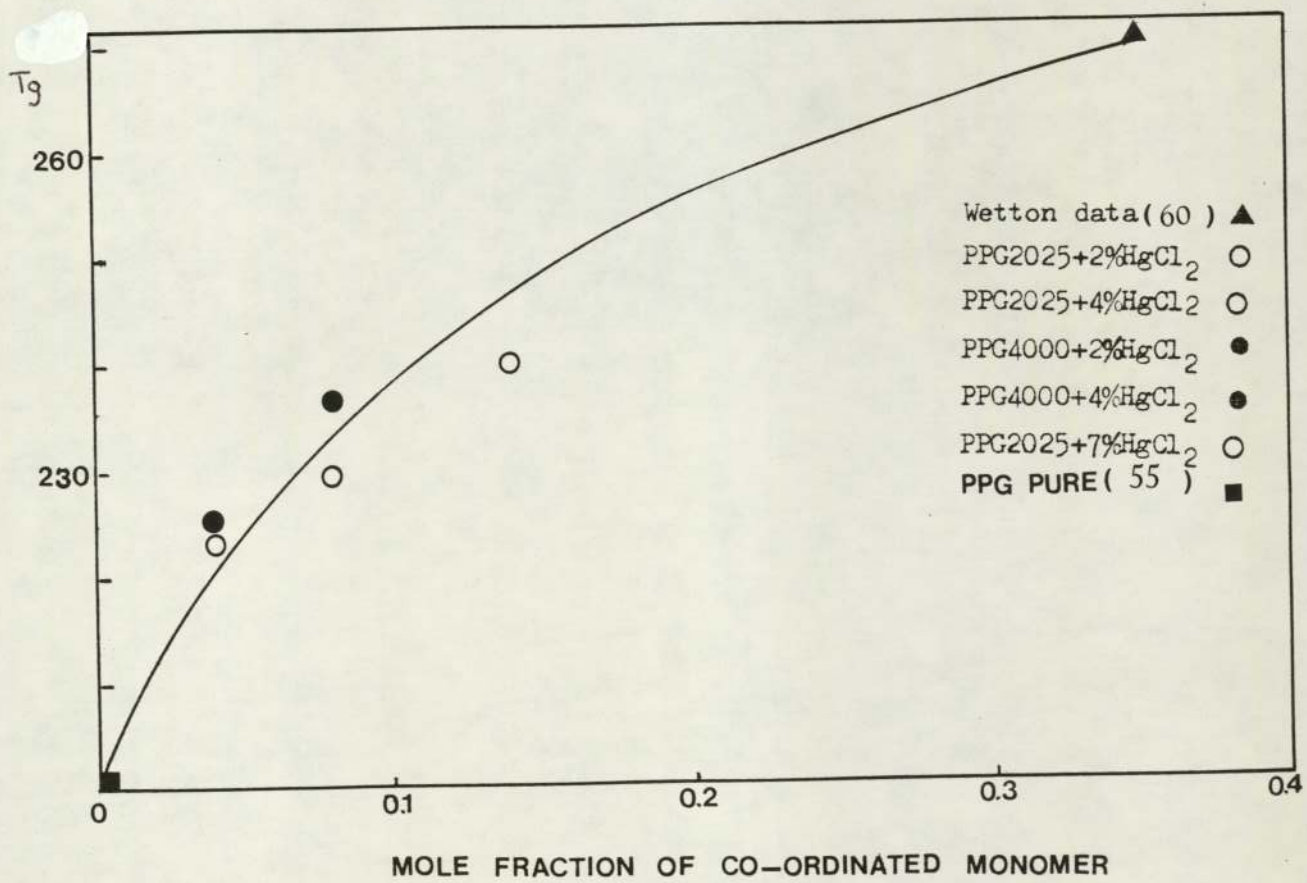
Tg
260
230
0
0.1
0.2
0.3
0.4
Wetton data(60)
PPG2025+2%HgCl2
PPG2025+4%HgCl2
PPG4000+2%HgCl2
PPG4000+4%HgCl2
PPG2025+7%HgCl2
PPG PURE(55)
MOLE FRACTION OF CO-ORDINATED MONOMER

Fig(5.7)

mercuric chloride in poly(propylene glycol) obtained from a patent application filed by Wetton and James[60], and another point for pure poly(propylene glycol)[55]. The dependence of the glass-transition temperature of solutions of mercuric chloride in poly(propylene glycol) on the concentration of added salt appears to be best described by a curved line.

5.9 Distribution of Dielectric Relaxation Times for the Poly(propylene glycol) - Mercuric Chloride System

Referring to figures 4.22 - 4.29, which show Cole-Cole diagrams for the dielectric relaxation behaviour of the PPG - $HgCl_2$ system, it can be seen that the majority of the experimental data can be reasonably well represented by circular arcs. The Cole-Cole distribution parameters, α, listed in Table 5-5 were determined for each Cole-Cole diagram using the approach described in section 5.5. For pure samples of poly(propylene glycol) the Cole-Cole parameter α was determined to be 0.46 and 0.51 for samples of pure PPG2025 and PPG4000, respectively, at temperatures in the range 224 - 232 K. These values of α compare favourably with those deduced from Cole - Cole plots of pure poly(propylene glycol) published by Yano et al[58]. An examination of their Cole - Cole plots for PPG at 222 K gave a value of α close to 0.5. The addition of mercuric chloride to poly(propylene glycol) causes a significant broadening of the distribution of relaxation times. Thus, for 2 mole %, 4 mole % and 7 mole % solutions of mercuric chloride in PPG, the value of α is 0.69, 0.71 and 0.61, respectively. Figure 5-8 shows the Cole - Cole parameter,

Table 5.5 Cole - Cole Distribution parameter α for Solutions of Mercuric Chloride in Poly(propylene glycol)

PPG2025 - $HgCl_2$ system

	$[HgCl_2] = 0\%$		$[HgCl_2] = 2\%$		$[HgCl_2] = 4\%$		$[HgCl_2] = 7\%$	
T =	231.4	0.46	247.8	0.69	247.8	0.71	252.0	0.63
	227.4	0.46	238.3	0.67	238.3	0.69	248.0	0.61
	224.9	0.45	231.4	0.62	231.4	0.65	242.0	0.63
			227.4	0.53	227.4	0.59	238.0	0.60
			225.0	0.57	225.0	0.57	228.0	0.58
			222.0	0.56	221.0	0.61		
			218.0	0.60				

PPG4000 - $HgCl_2$ system

	$[HgCl_2] = 0\%$		$[HgCl_2] = 2\%$		$[HgCl_2] = 4\%$	
T =	224.0	0.51	232.0	0.58	251.0	0.62
			230.0	0.59	245.0	0.62
			227.0	0.59	238.0	0.60
			224.0	0.59	233.0	0.59
			222.0	0.59	228.0	0.57
			220.0	0.60		

Fig 5_8

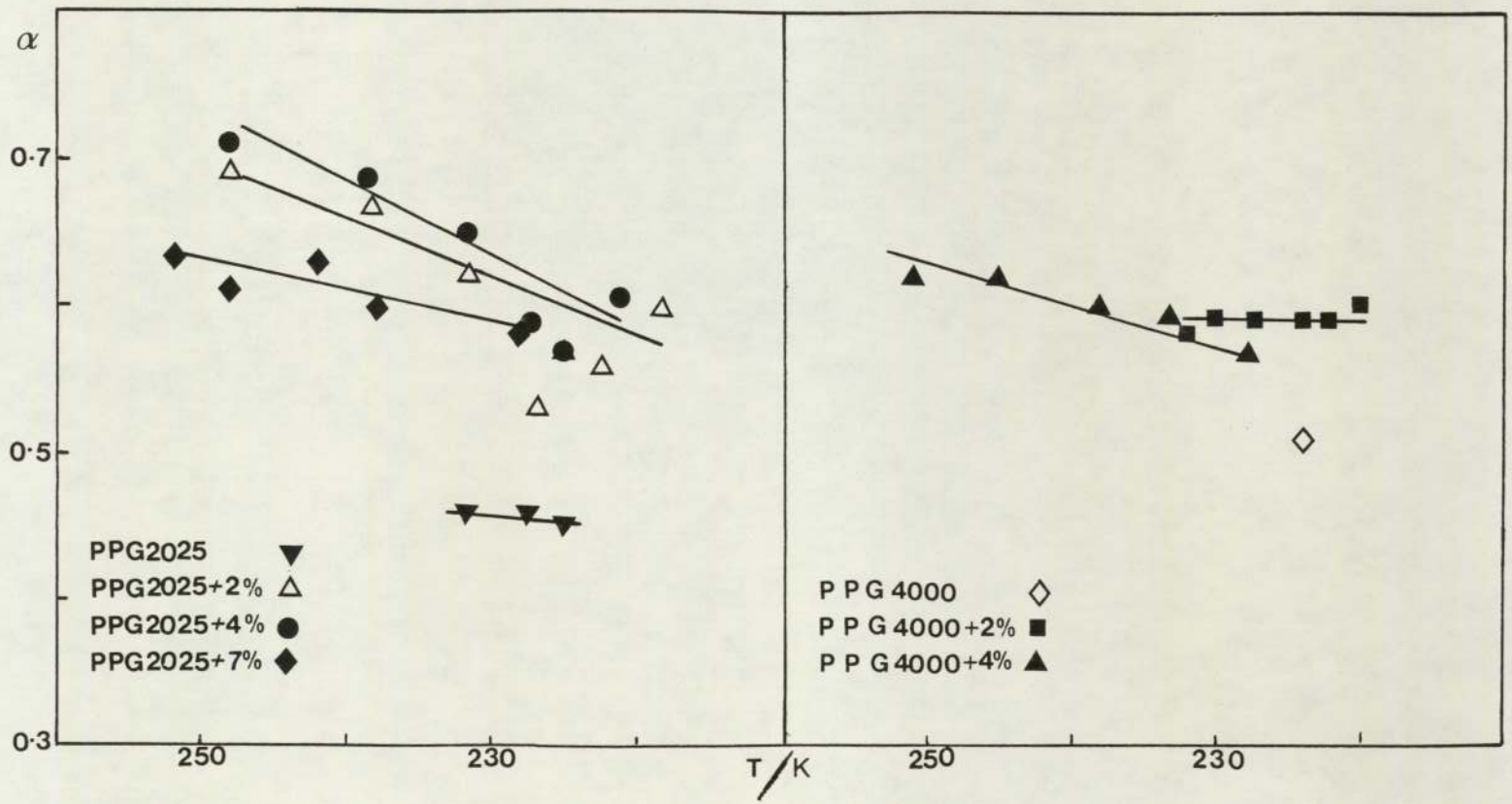

Cole–Cole α parameter of PPG+$HgCl_2$ complexes

α, plotted as a function of temperature for the various solutions of mercuric chloride in poly(propylene glycol). For each of the solutions of $HgCl_2$ in PPG2025 it is observed that α decreases steadily with decreasing temperature. This behaviour is opposite to that normally observed for dipolar amorphous polymers. However, these observations must be regarded with some degree of caution since the plots of ε'' vs. ε' for the 2 mole % solutions of mercuric chloride in PPG2025 may be better described by the Cole-Davidson analysis; in which the denominator $(1 + \omega^2 \tau_o^2)^{1-\alpha}$ is used in place of $(1 + (\omega^2 \tau_o^2)^{1-\alpha})$. Plots of the Cole-Cole distribution parameter α as a function of the concentration of mercuric chloride in PPG2025 at 223 K and 248 K are presented in figure 9. The fitted curves show a distinct maximum positioned at a concentration of approximately 4 mole % of $HgCl_2$; behaviour that complements that exhibited by the activation energy $E^{\#}$ and the energy difference between trans and gauche states for solutions of $HgCl_2$ in PPG (see figure 2). The maximum is better defined at the higher temperature.

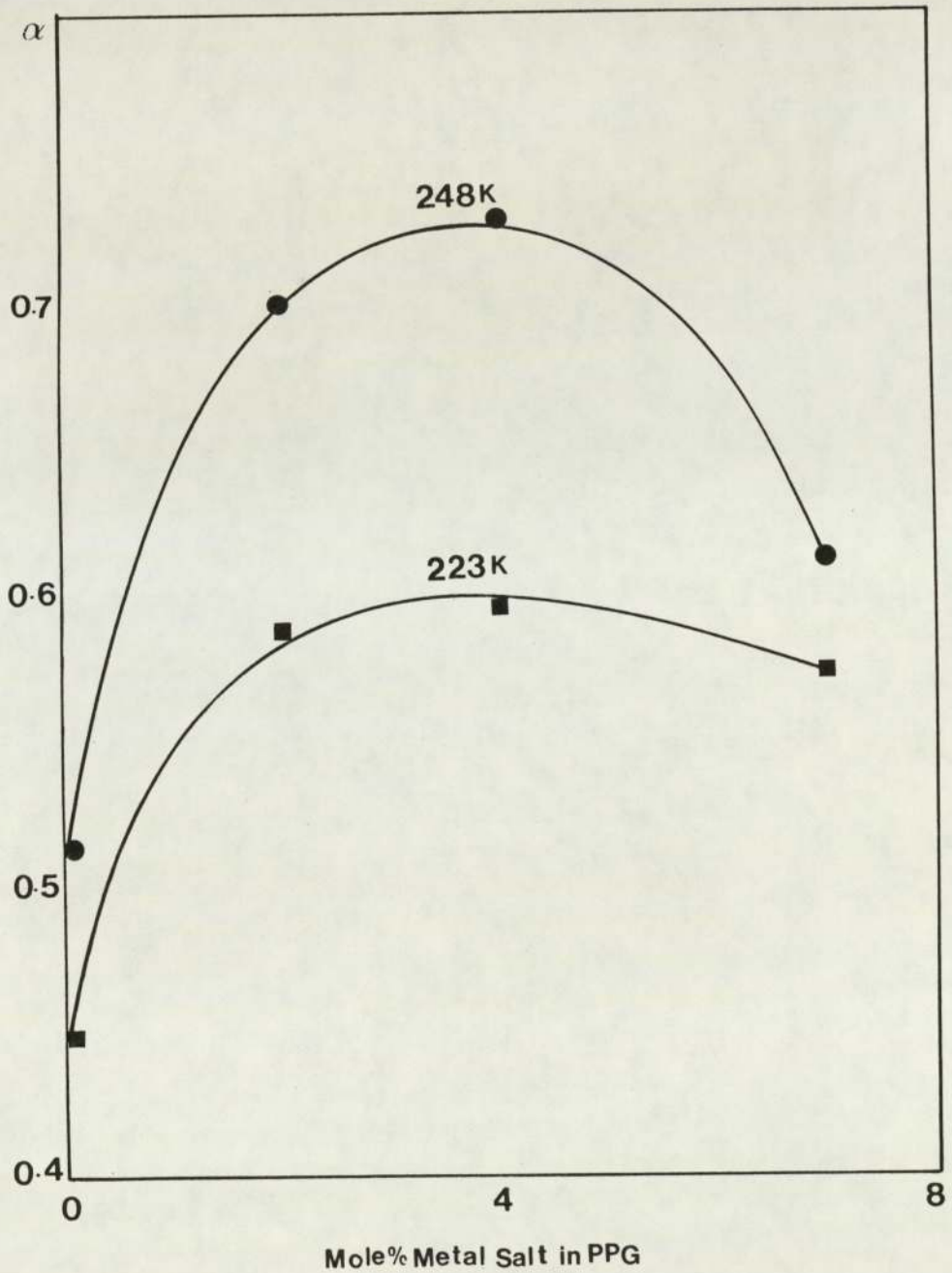

Fig 5–9

CHAPTER 6

Nuclear Magnetic Resonance Studies of Polyether-Metal Salt Complexes

6.1 Poly(ethylene glycol) - Metal Salt Complexes

Proton and carbon-13 nuclear magnetic resonance data may provide important information about the structure of polyether -metal salt complexes. The close proximity of the metal ion to selected segments of the polyether chain, due to the formation of a five-membered chelate ring for example, may induce different chemical shifts in the atoms involved, especially if the metal ion is paramagnetic. The measurement of the spin-lattice relaxation time, T_1, of the various absorptions of the samples may also provide extra information concerning the interaction between the metal ion and the polyether. Since the spin-lattice relaxation time depends on the average time (the rotational correlation time t_c) it takes for a molecule, or part of a molecule, to rotate through an angle of one radian it is anticipated that T_1 will be influenced by the type of complex formed between the metal ions and the polyether chain. The presence of water may also be reasonably expected to affect T_1 via its participation in the coordination shell of the metal ion.

Figures 1 and 2 show proton NMR spectra obtained for solutions of ferric chloride (anhydrous) in poly(ethylene glycol) of molecular weight 400 (PEG400) at 303 K. Two absorption peaks are observed (the two small peaks positioned symmetrically about the large peak are spinning side-bands and may be ignored). The larger peak is assigned to the protons of the central methylene groups (i.e. methylene groups of non-terminal ether units), their

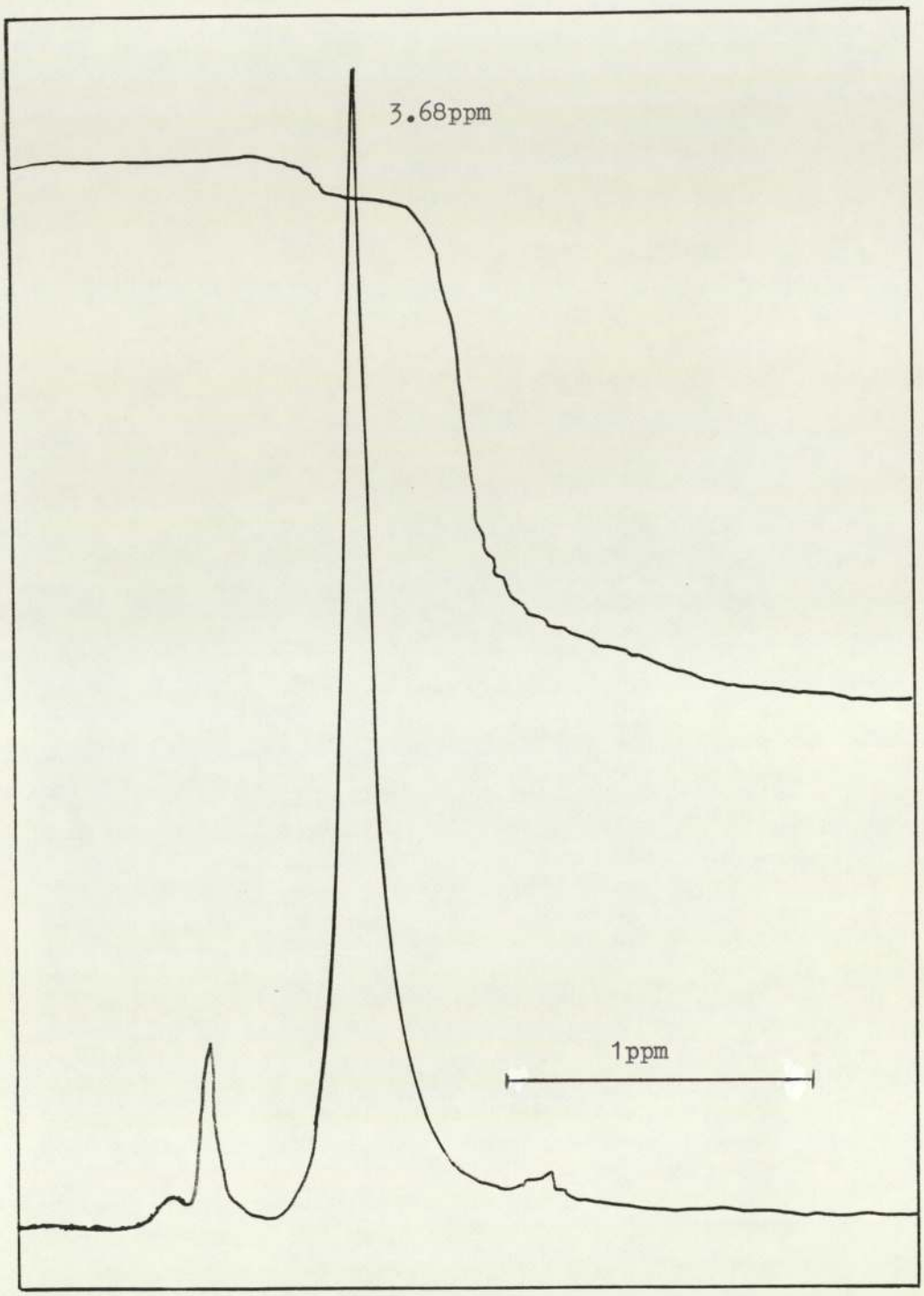

Proton NMR spectrum of .01% w/w solution of $FeCl_3$ in PEG400 at 298 K.

Fig 6-1

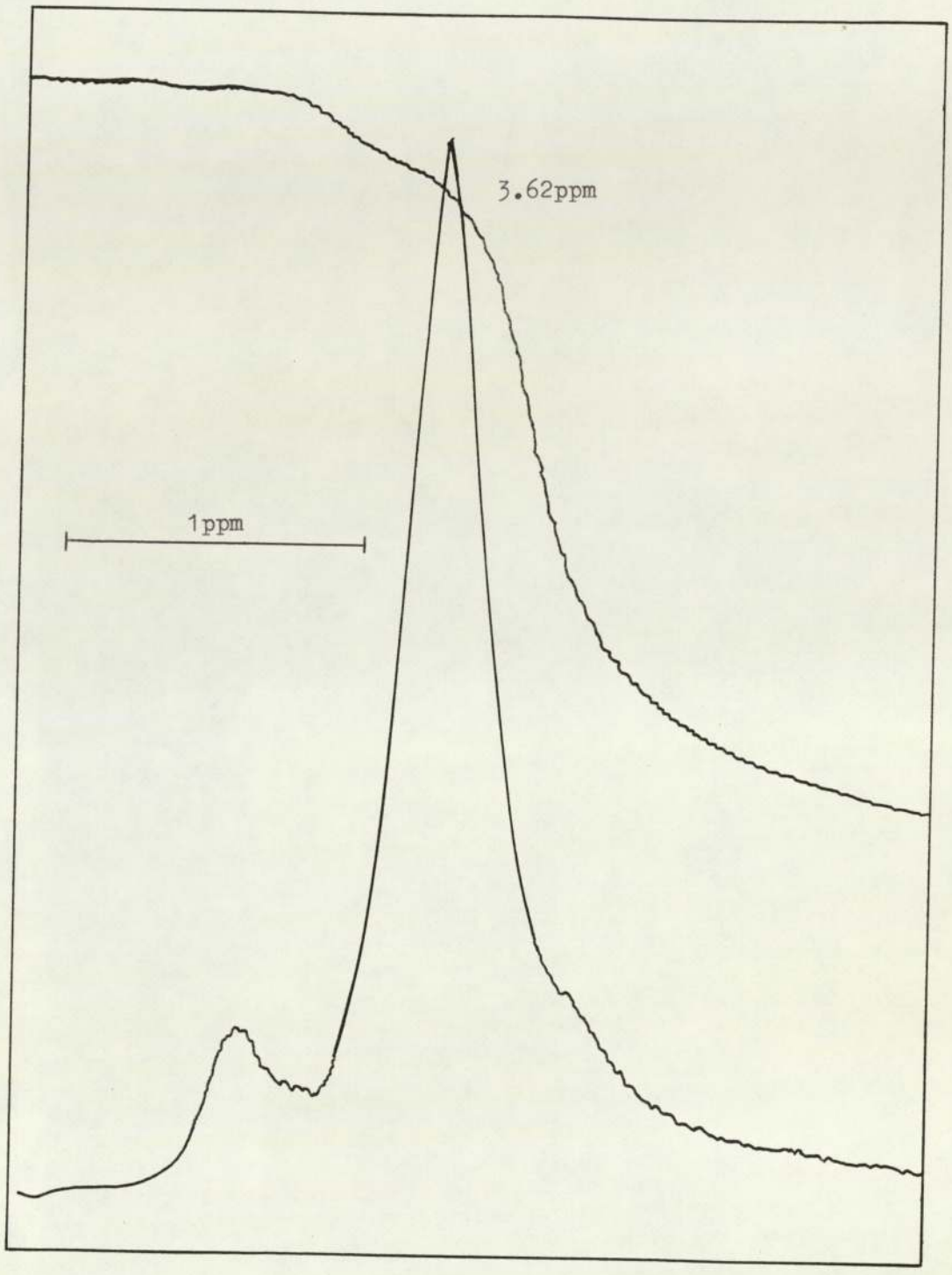

Proton NMR spectrum of 0.1% w/w solution of $FeCl_3$ in PEG400 at 298 K.

Fig 6-2

chemical shift being typical of methylene groups adjacent to an ether oxygen atom. The smaller peak is assigned to the protons of the terminal methylene groups which are shifted slightly downfield because of the adjacent hydroxyl group. The integral of this spectrum supports this interpretation. Assuming that the sample of poly(ethylene glycol) is monodisperse and has a molecular weight of 400 then the ratio of the peak areas of the central and terminal methylene absorptions is predicted to be 8:1 which compares favourably with 10:1 obtained experimentally.

Increasing the concentration of the ferric chloride has a marked effect on the width of the peaks and this is attributed to the paramagnetic properties of the ferric ion.

Carbon-13 NMR spectra of PEG300, PEG400 and PEG600 are reproduced in figures 3, 4 and 5. In all three samples three different types of carbon absorptions are observed. The most intense peak is readily assigned to the carbon atoms of the non-terminal methylene groups. The two smaller peaks are believed to be associated with carbon atoms in the terminal units of the polyether chain. For convenience the peaks are numbered 1,2 and 3 in order of increasing chemical shift. If the smaller peaks (1 and 3) are associated with the terminal units then their intensity, relative to the absorptions of the non-terminal units, should decrease as the molecular weight of the polyether is increased. This is supported by an inspection of the ratio of peak heights (areas should be used for better accuracy) for peaks 2 and 1 for polyethylene glycols of different molecular weights. Ratios of 2.7, 3.8 and 8.0 were found for PEG300, PEG400 and PEG600, respectively. A more detailed assignment of the two

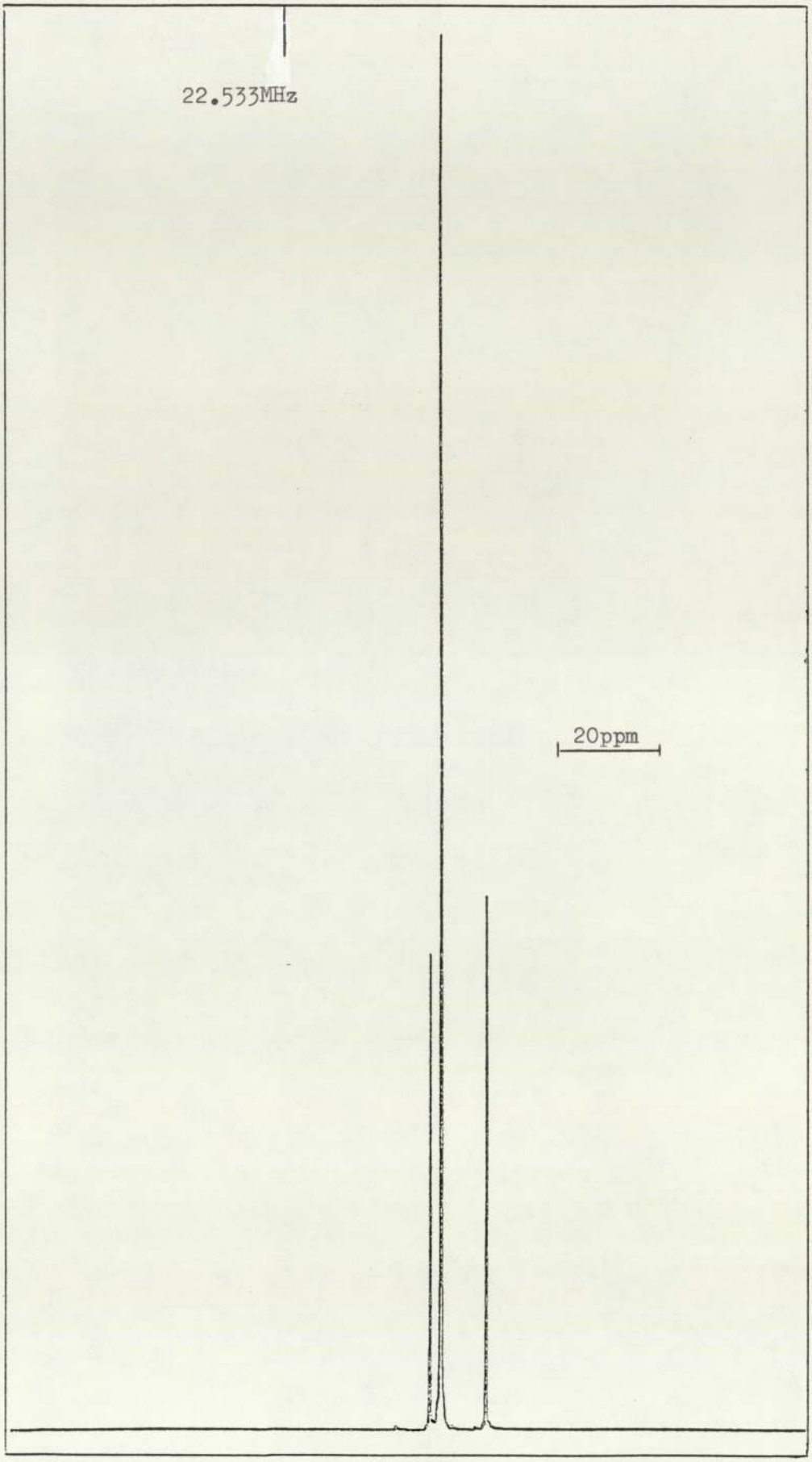

Carbon-13 NMR spectrum of PEG300 at 298 K.

Fig 6-3

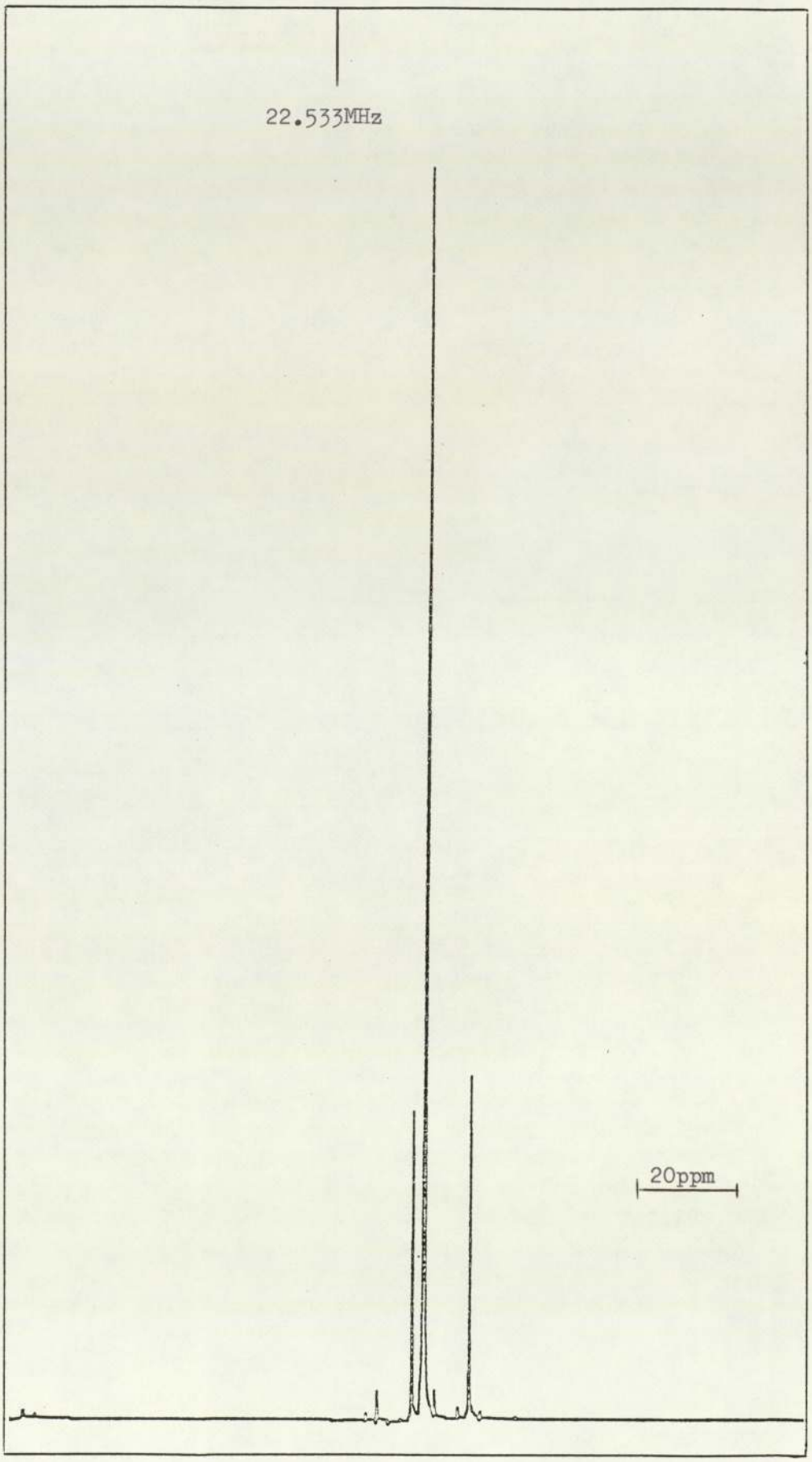

Carbon-13 NMR spectrum of PEG400

Fig 6 - 4

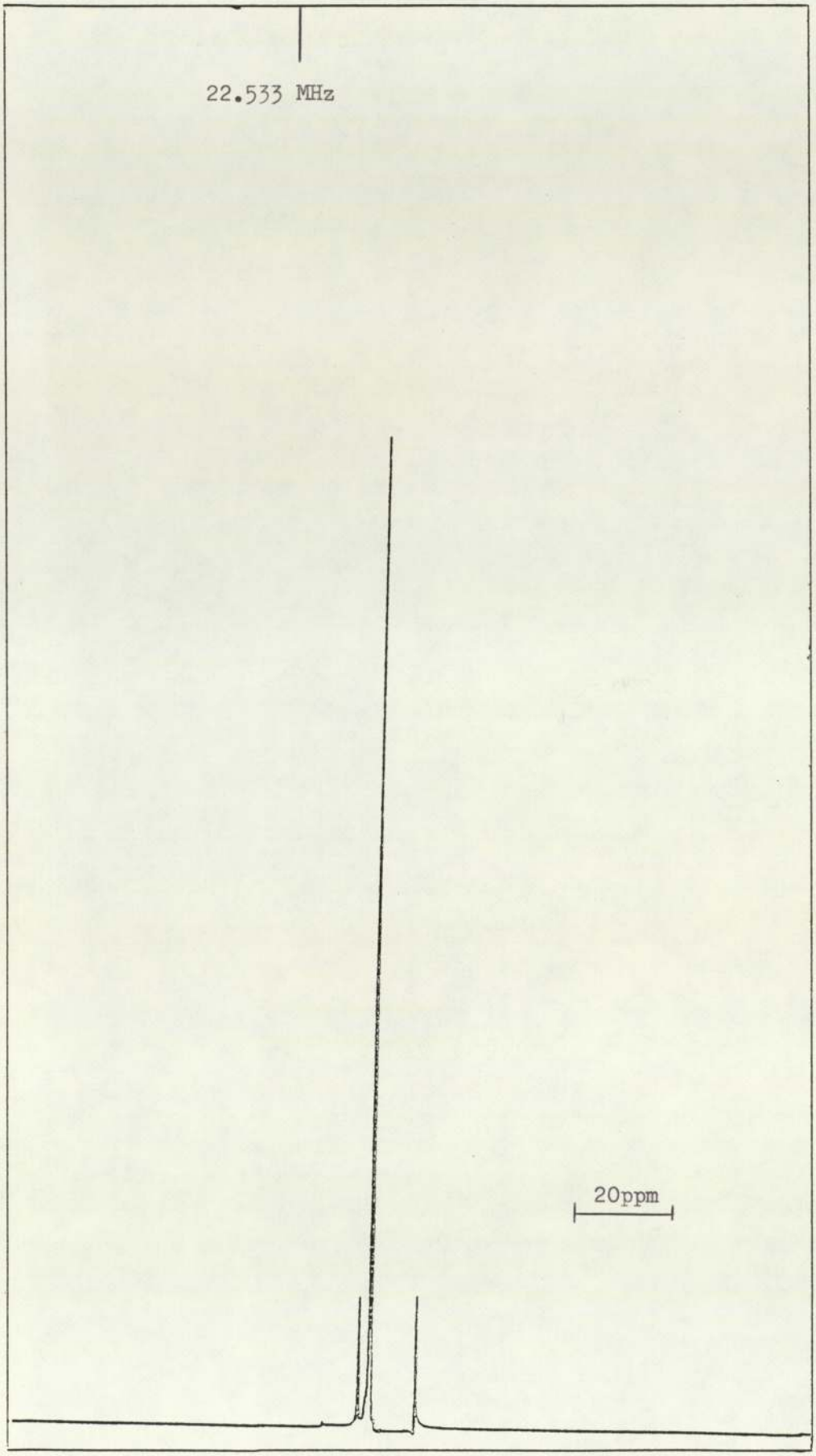

Carbon-13 NMR spectrum of PEG600 at 298 K.

Fig 6-5

smaller peaks is more difficult. A peculiar feature of the carbon-13 spectrum is the presence of a small peak positioned upfield from the main peak associated with the non-terminal carbon atoms. A consideration of the most likely structure of the terminal region of the poly(ethylene glycol) chain leads to the conclusion that the positions of the NMR peaks for the terminal carbon atoms should be downfield with respect to the carbon atoms of the non-terminal repeat units of the polyether chain.

$$-(\underbrace{CH_2CH_2O}_{\text{peak 2}})-\underbrace{CH_2CH_2OH}_{\text{peaks 1,3}}$$

A carbon-13 spectrum obtained without broad-band decoupling of the protons confirms that all three carbon atoms are methylene carbon atoms since all three absorption peaks are split into triplets in the ratios of 1:2:1 (see figure 6).

Figure 7 shows a series of carbon-13 NMR spectra obtained for a pure sample of PEG400 at 298 K using a pulse sequence of

$$90^\circ, \text{ (homospoil)}, \tau, 90^\circ$$

for different values of τ. From a plot of the logarithm of magnetic intensity of a particluar absorption as a function of time τ the spin-lattice relaxation time, T_1, may be calculated (see Appendix 3 for further details). Thus, for pure PEG400 the spin-lattice relaxation times found for the carbon atoms 1, 2, and 3 are 0.22s, 0.13s and 0.18s, respectively. It is interesting to compare these relaxation times with the corresponding values of 0.10s, 0.062s and 0.09s obtained for PEG400 containing

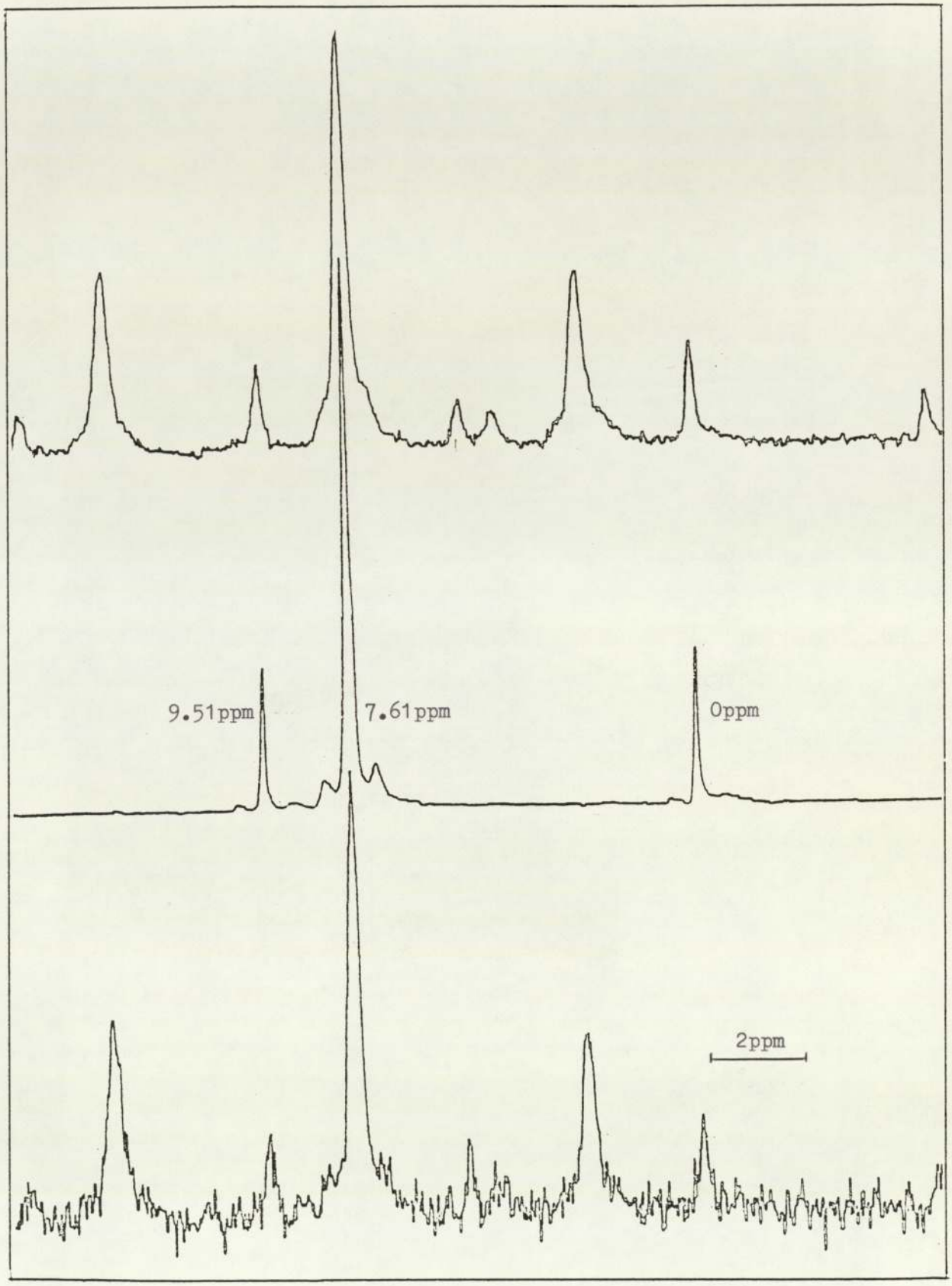

Proton-coupled carbon-13 NMR spectrum of PEG400.

Fig 6-6

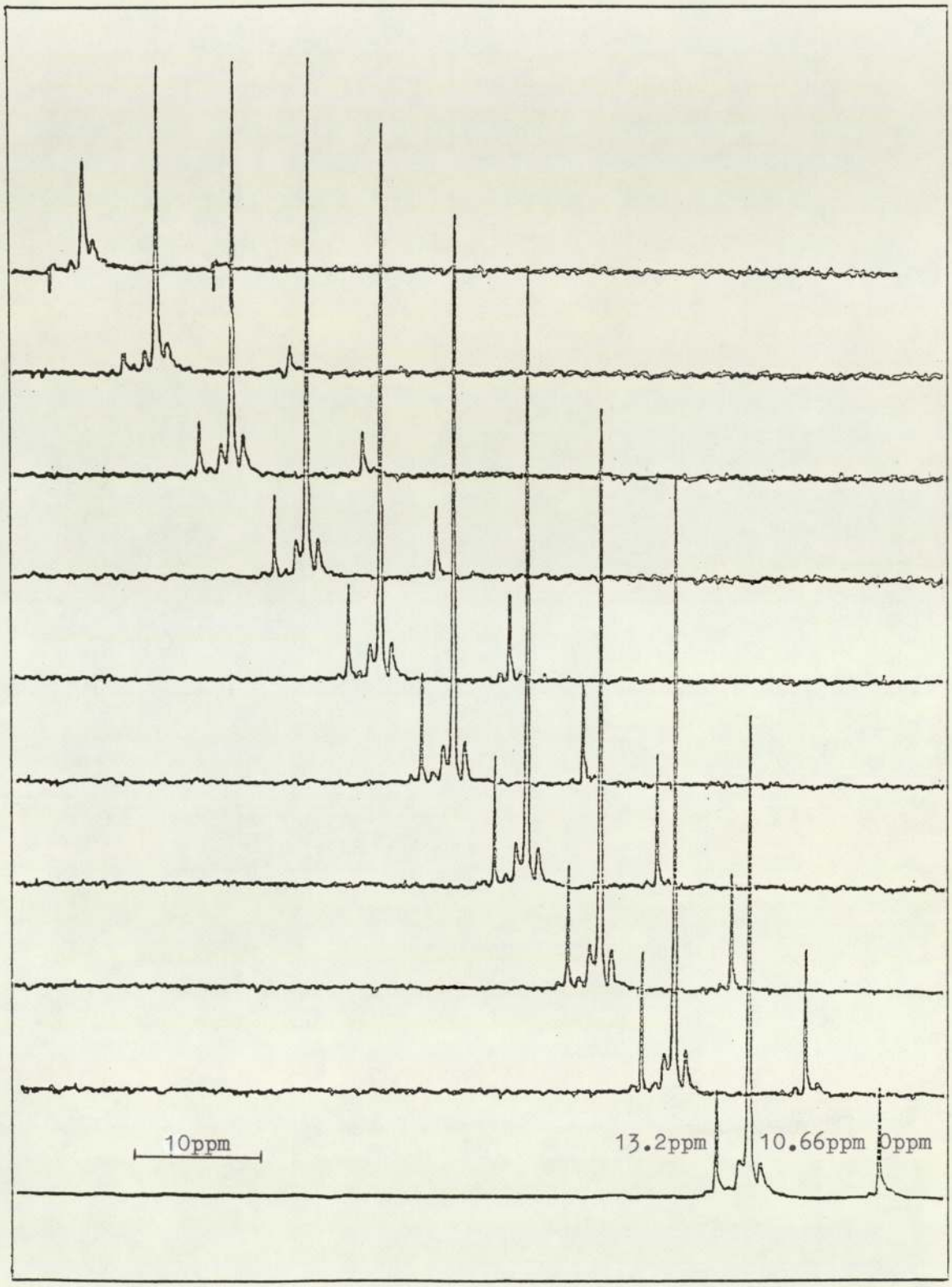

Fig 6-7

Carbon-13 NMR relaxation of PEG400 at 298 K obtained using the pulse sequence 90^{o}, (homospoil), τ, 90^{o}.

1% by weight of anhydrous $FeCl_3$ (see figure 8). The carbon atoms associated with peaks 2 and 3 appear to be equally affected by the presnce of ferric chloride in that their relaxation times have both been reduced by a factor close to 2. This value may be compared with a value of 2.3 found for the carbon atom associated with peak 1, which may indicate that the ferric ion is slightly closer to this terminal atom.

6.2 Model Compounds of Poly(ethylene glycol)

In an attempt to simplify the problems associated with the interpretation of NMR data obtained for solutions of metal salts in poly(ethylene glycols) a series of solutions of ferric chloride in various well-defined small molecular weight ethers were prepared for examination by NMR. Possible model compounds included 1,2-dimethoxyethane

$$CH_3OCH_2CH_2OCH_3$$

ethyl digol

$$CH_3CH_2OCH_2CH_2OCH_2CH_2OH$$

and 1,2-dimethyl ethanol

$$CH_3CH_2CH(CH_3)OH$$

The solubility of various metal salts in these ether compounds was also investigated. These included $FeCl_3 6H_2O$, $FeCl_3$, $FeCl_2 4H_2O$, $ZnCl_2$, CuI, $HgCl_2$, $SnCl_2$, $NiBr_2 2H_2O$ and $NiBr_2$ which all dissolved in the above mentioned solvents to give solutions containing up to several percent by weight of metal salt.

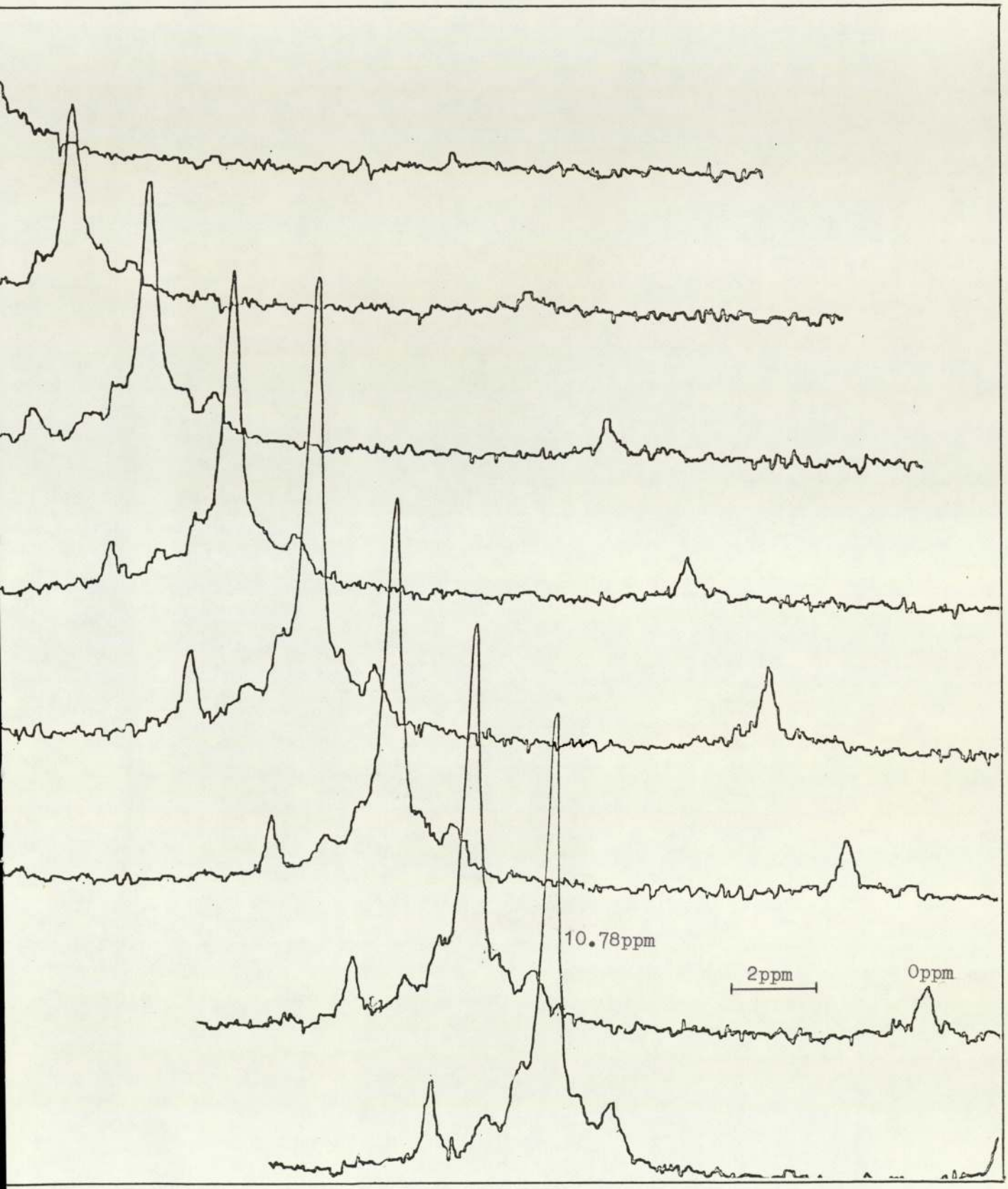

Fig 6-8

Carbon-13 NMR relaxation of PEG400 containing 1% w/w $FeCl_3$ at 298 K.

Carbon-13 spectra of pure 1,2-dimethoxyethane obtained with and without broadband decoupling of protons are shown in figures 9 and 10. Assignments were made by examining the carbon-13 spectrum obtained in the absence of broadband decoupling (see figure 9). The methyl carbon is split into a quartet (1:3:3:1) and the methylene carbon is split into a triplet (1:2:1). Carbon-13 relaxation data for pure 1,2-dimethoxyethane are shown in figures 11,12. The spin-lattice relaxation times for CH_2 and CH_3 carbon atoms were found to be 16s and 24s, respectively. These relaxation times may be compared with the corresponding values of 0.4s and 0.47s obtained for a 1% by weight solution of ferric chloride in 1,2-dimethoxyethane at 298 K. Carbon-13 spin-lattice times were also measured for a 2% by weight solution of stannous chloride in 1,2-dimethoxyethane. From the ralaxation data obtained for this system (see figure 13) the T_1 relaxation times for the methylene and methyl carbon atoms were found to be 11s and 10s, respectively. Since spin-lattice relaxation times are probably affected by the proximity of the metal ion to the carbon atoms in 1,2-dimethoxy ethane and also by paramagnetic effects further analysis is not possible without additional NMR data.

Previous sections have been concerned with the NMR data obtained for either the polyether molecules or the low molecular weight model compounds. A complementary approach involves measuring the NMR absorption spectrum of the metal atoms of the added inorganic salt. The NMR spectrum shown in figure 14 is for the ^{199}Hg absorption of a solution of mercuric chloride in 1,2-dimethoxyethane at 298 K. The chemical shift of the mercury peak, relative to the mid-point frequency of the spectrum was calculated to be 104.7 ppm. Separate measurements of the

Figure 6.9 Proton-coupled carbon-13 NMR spectrum of 1,2-dimethoxyethane at 298 K

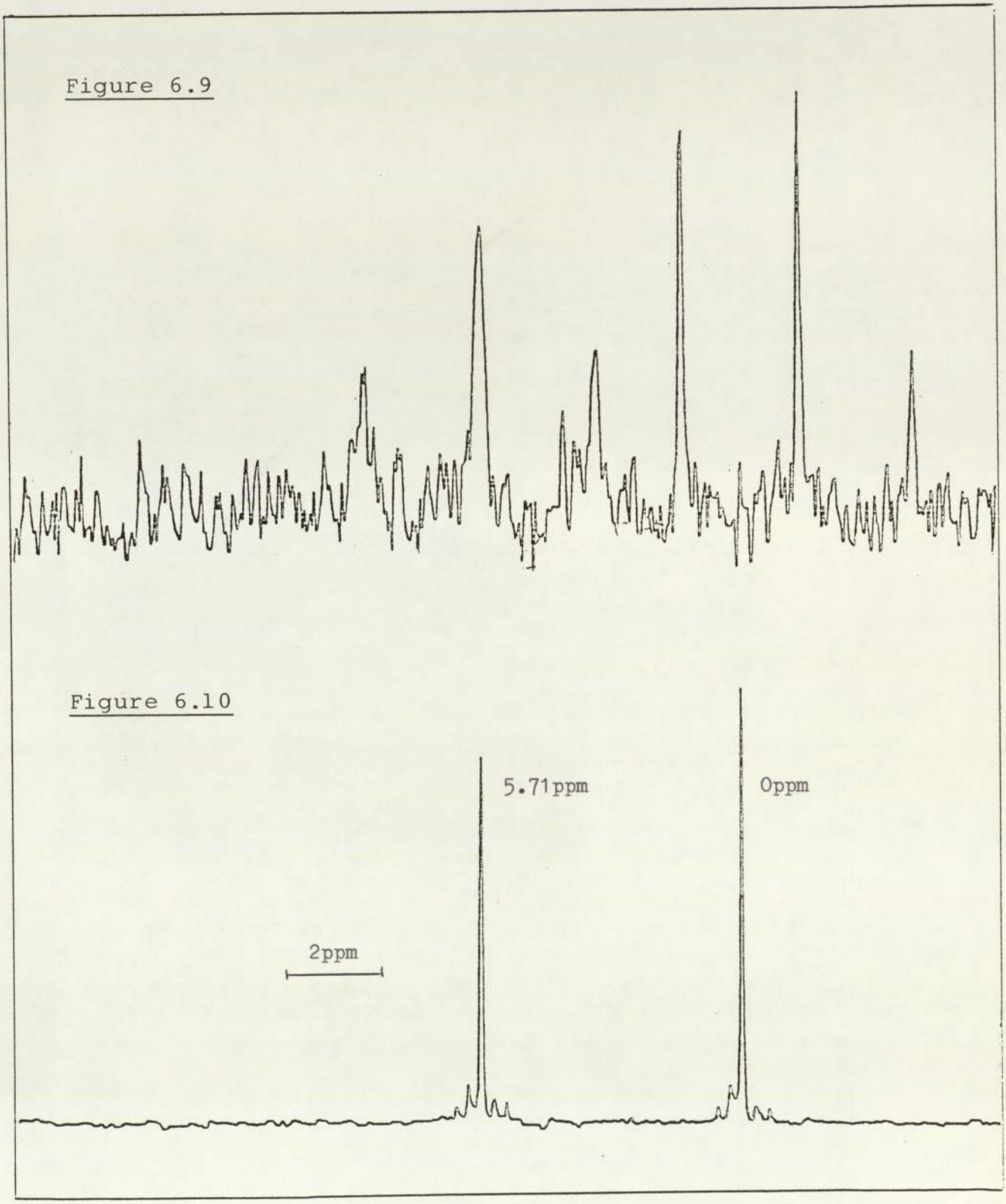

Figure 6.10 Carbon-13 NMR spectrum of 1,2-dimethoxyethane obtained under conditions of broadband proton decoupling at 298 K

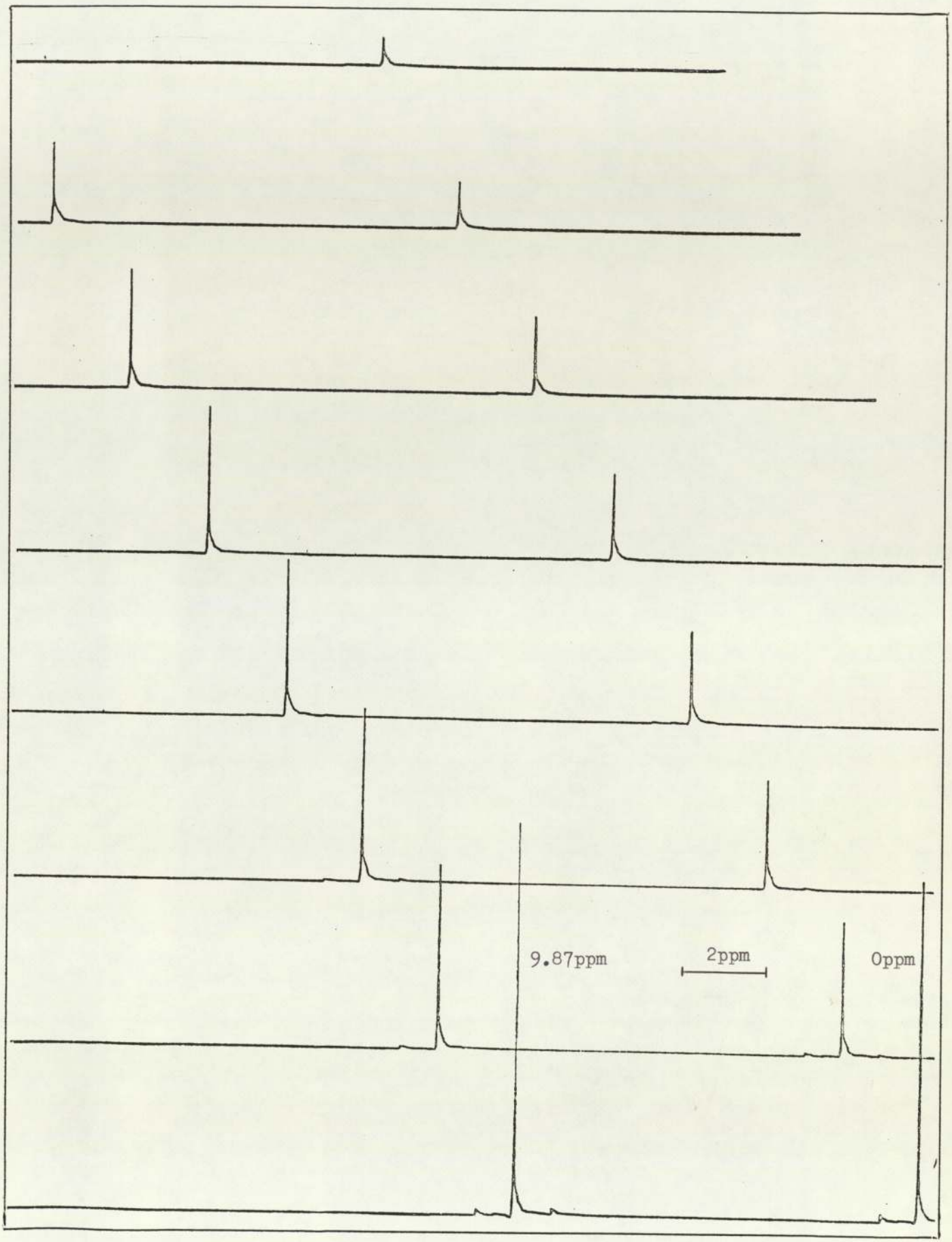

Figure 6.11 Carbon-13 spin-lattice relaxation of 1,2-dimethoxyethane

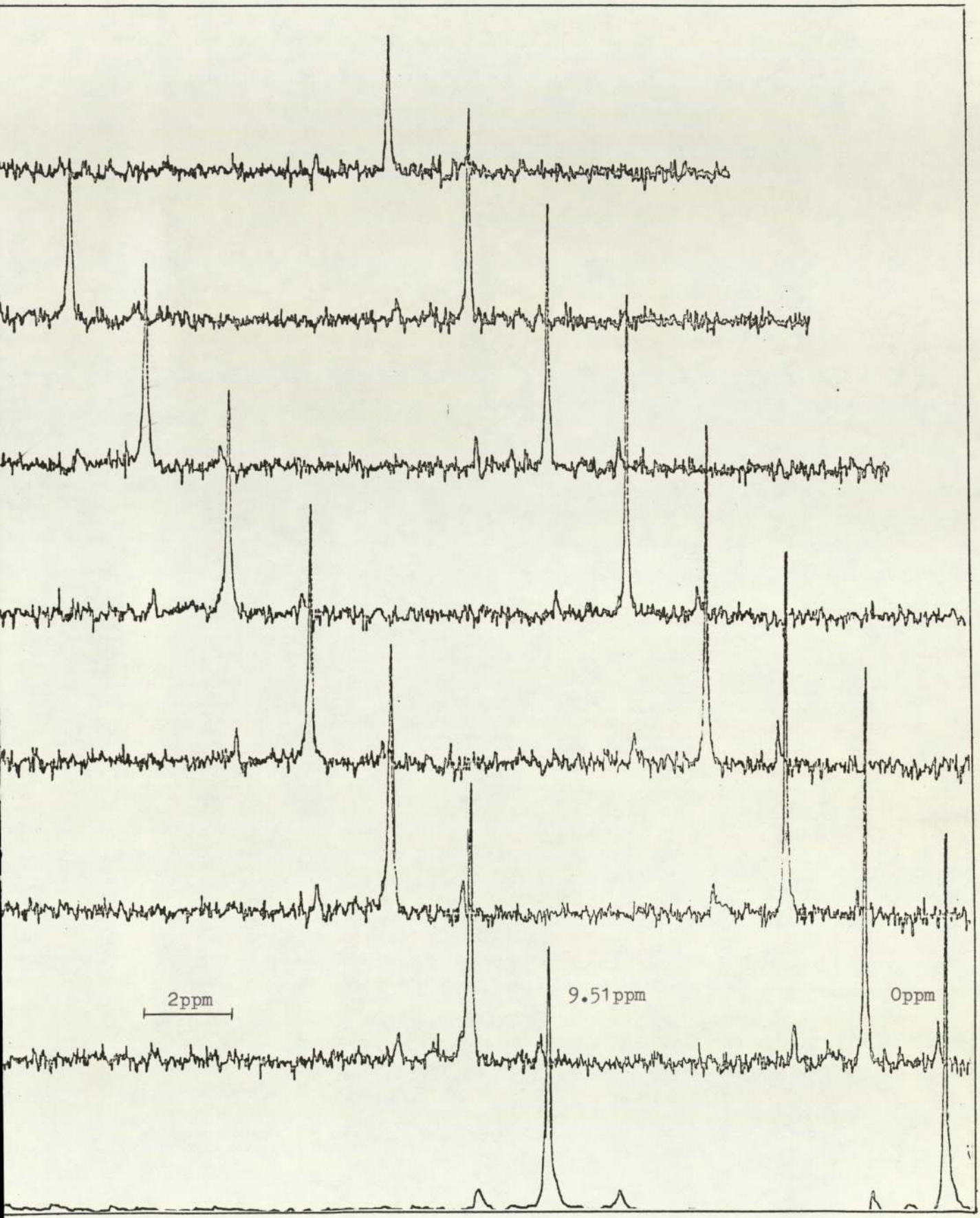

igure 6.12 Carbon-13 spin-lattice relaxation of a 1% w/w solution of $FeCl_3$ in 1,2-dimethoxyethane at 298 K

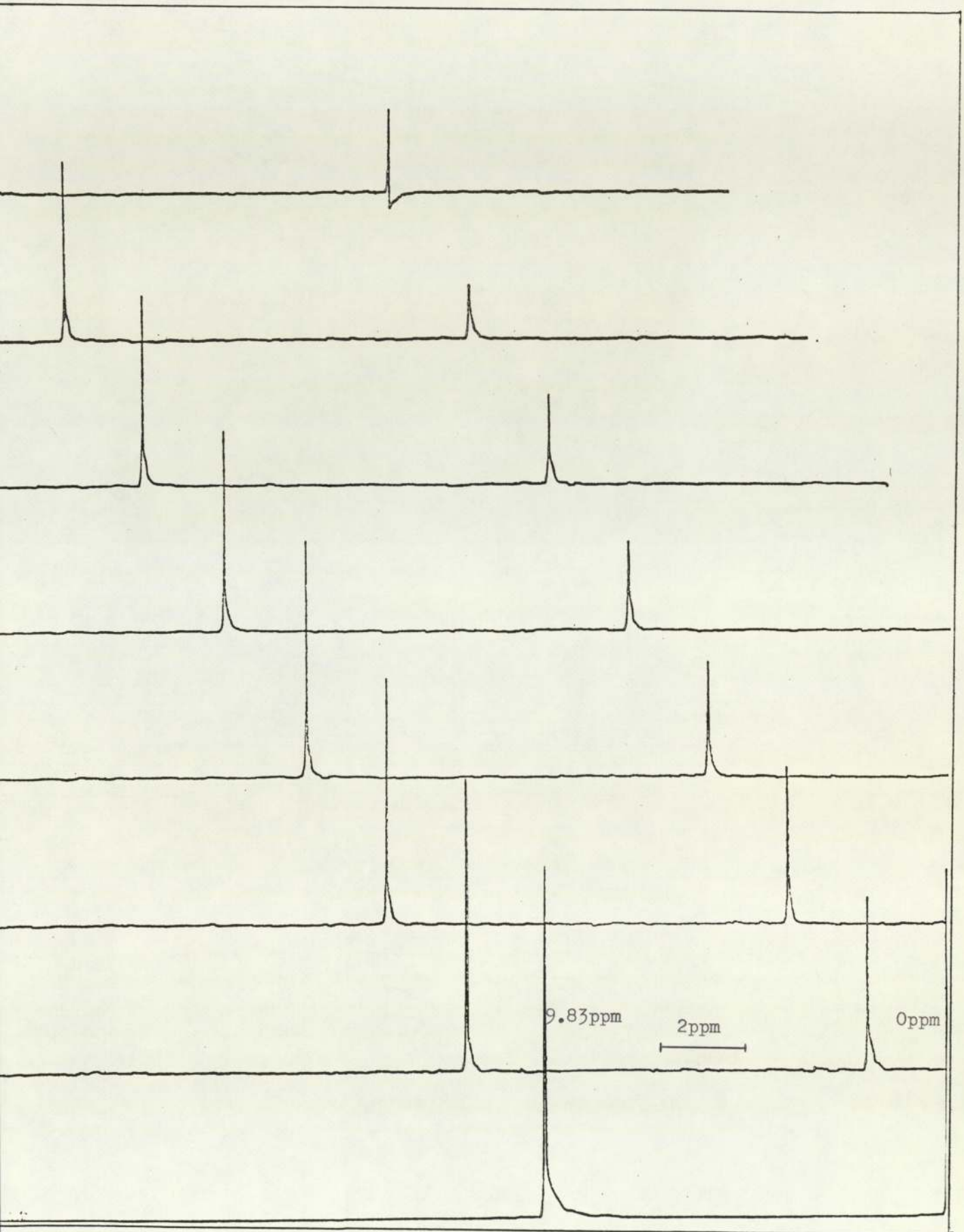

Figure 6.13 Carbon-13 spin-lattice relaxation of a 2% w/w solution of $SnCl_2$ in 1,2-dimethoxyethane at 298 K

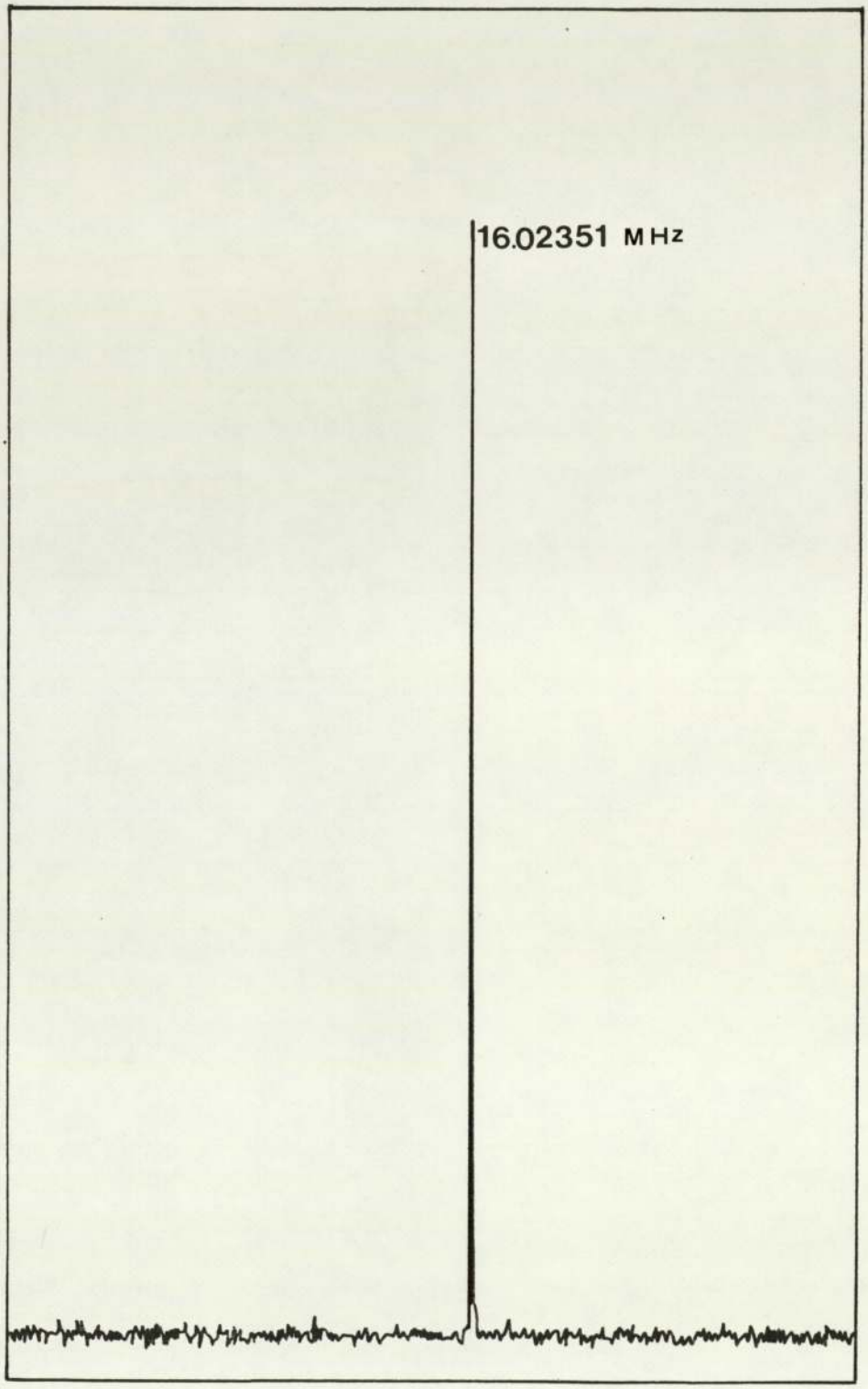

Hg-199 N.M.R. spectrum of $HgCl_2$ in 1,2-dimethoxyethane

Fig 6-14

chemical shift of ^{199}Hg in solution in 1,2-dimethyl ethanol (see figure 15) gave a peak position of 147.6 ppm. It is tempting to interpret this difference in the observed peak positions as a consequence of a variation in the degree of complexation of the mercury atom. The hydroxyl group of 1,2-dimethyl ethanol, because it is more basic than the ether oxygen atom, would be expected to form the stronger complex with the mercury atom, thus producing the greater shift downfield. However, this interpretation must be viewed with caution since a change in solvent susceptibility would also be expected to cause a relative displacement of the absorption peak of mercuric chloride.

6.3 Carbon-13 and Mercury-199 N.M.R. of Solutions of Mercuric Chloride in Poly(propylene glycol)

The carbon-13 and mercury-199 nuclear magnetic resonance absorption spectra and the corresponding spin-lattice relaxation times were determined for solutions of mercuric chloride in solution in poly(propylene glycol) at 303 K using a Jeol FX90Q Fourier Transform spectrometer. The method used to obtain spectra and spin-lattice relaxation times, T_1, was based on a pulse driven equilibrium technique (DESPOT - see reference **61**). This method has been developed recently within the Department of Molecular Sciences at the University of Aston. It enables NMR spectra and spin-lattice relaxation times to be obtained more rapidly than methods based on conventional pulse sequences. For example, DESPOT is approximately one hundred times faster than techniques based on the well known pulse sequence $180^{\circ} - \tau - 90^{\circ}$. The computer program necessary for the evaluation of NMR data collected under DESPOT

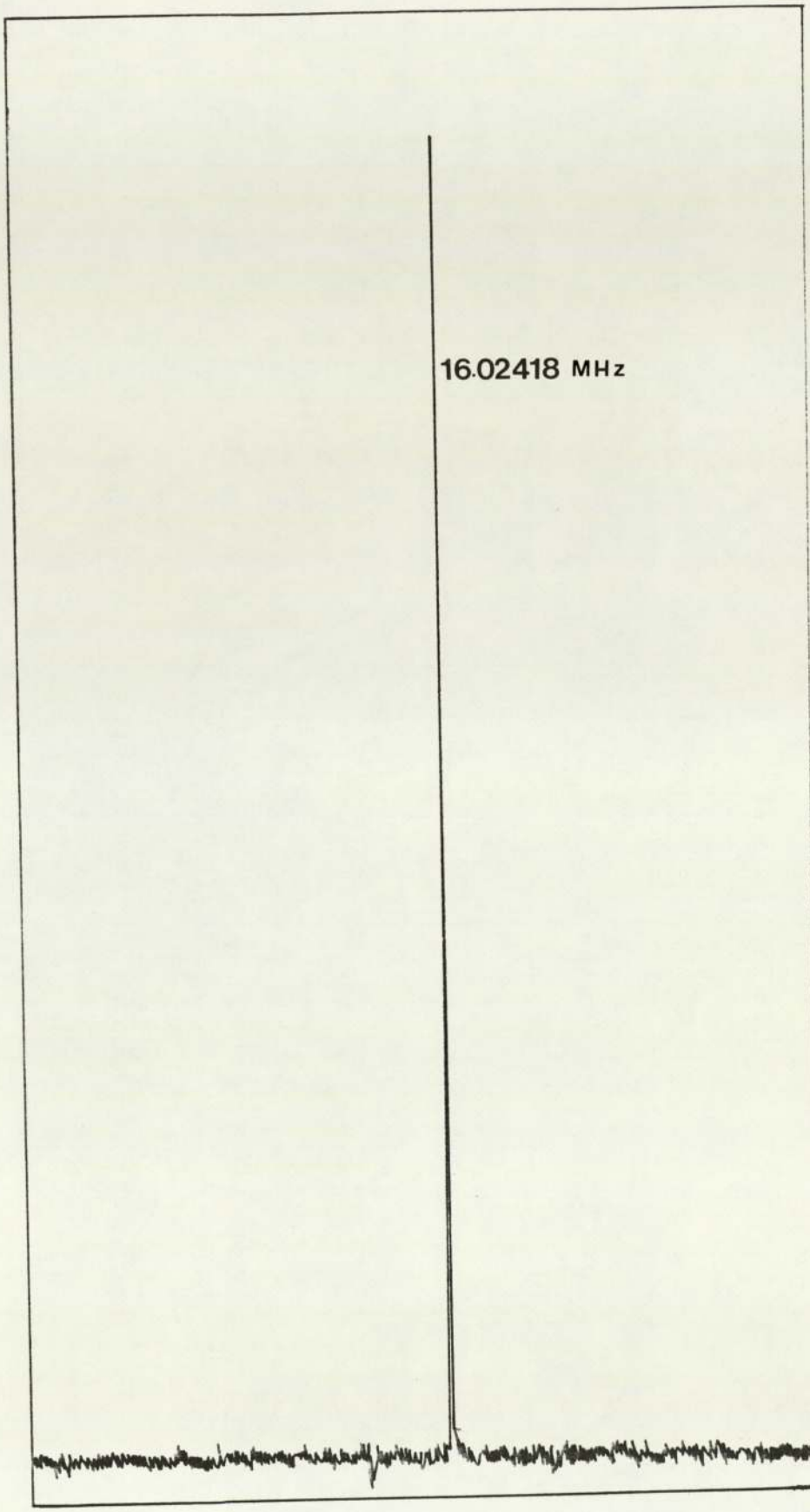

Hg-199 N.M.R. spectrum of $HgCl_2$ in 1,2-dimethylethanol at 303K

Fig 6-15

conditions is included in Appendix 2.

Figure 16 shows a proton-decoupled spectrum obtained for a sample of poly(propylene glycol) of molecular weight 425. This spectrum shows six major absorption peaks. The absolute frequency of the absorption peak at highest field (the right of the spectrum) was found to be 22.54 MHz. For convenience the peak at highest field was arbitrarily assigned a chemical shift of zero parts per million (ppm). Proton coupled ^{13}C spectra indicated that the absorptions at 0 ppm and 2.08 ppm were due to methyl carbons and that the peaks at 55.8 ppm and 57.9 ppm were attributable to CH and CH_2 types of carbons, respectively, of the non-terminal ether units $-(CH_3)CHCH_2O-$. The smaller absorption peaks at 2.08 ppm, 48.4 ppm and 49.1 ppm are almost absent from spectra of the higher molecular weight samples of poly(propylene glycol). The high field peak at 2.08 ppm was assigned to the methyl group attached to a terminal unit of the polyether chain. This absorption peak is shifted downfield relative to the absorption peaks of the non-terminal repeat units, which suggests that it is associated with a carbon atom that is close to a terminal hydroxyl group, viz. $HO(CH_3)CH-CH_2O-$. It was not possible to assign the absorption peaks at 48.4 ppm and 49.1 ppm, but these two absorptions are believed to be associated with methine and methylene carbon atoms in the terminal ether units. The ^{13}C spectra obtained for samples of higher molecular weight poly(propylene glycol) (Mol. Wt. = 2025), reproduced in figure 17 show a much reduced contribution from carbon atoms of the terminal units. The proton-decoupled ^{13}C spectra in figure 17 were obtained for 2 mole%,

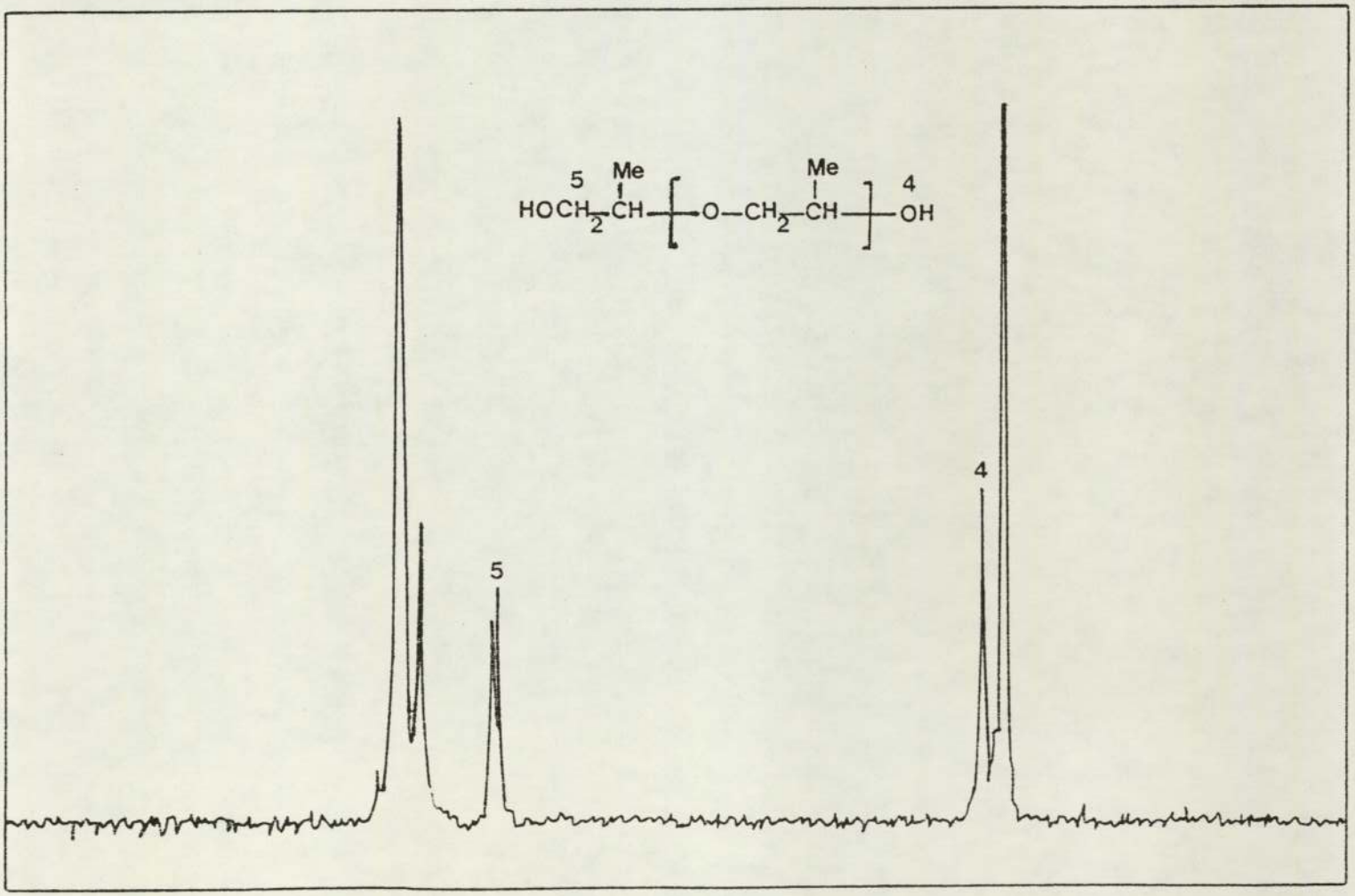

Fig 6-16

C-13 , proton-decoupled spectrum of PPG425 at 303K

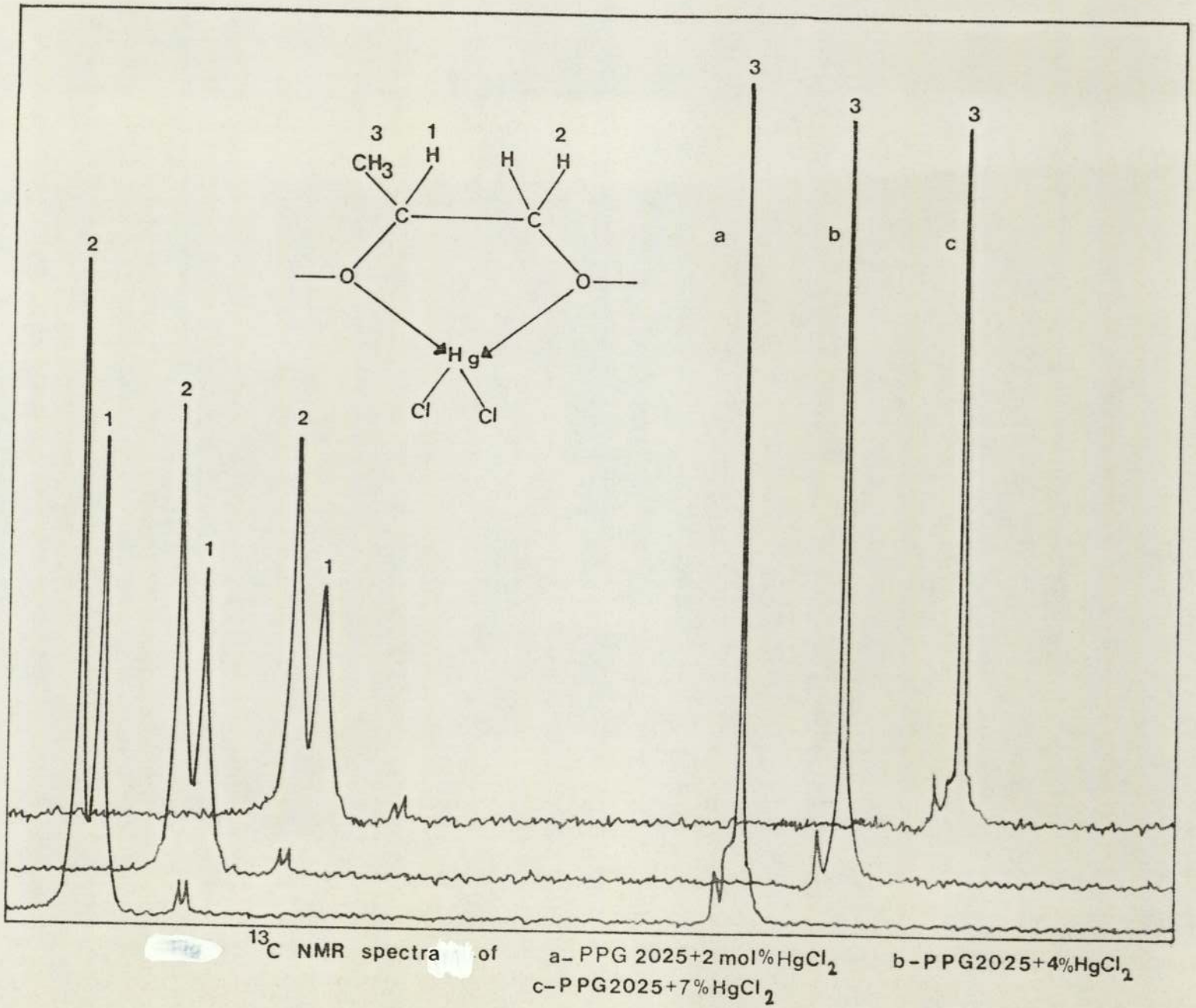

Fig 6-17

^{13}C NMR spectra of a- PPG 2025+2 mol% $HgCl_2$ b- PPG2025+4% $HgCl_2$ c- PPG2025+7% $HgCl_2$

4 mole % and 7 mole % solutions of mercuric chloride in PPG2025 at 303 K. A superficial inspection of the absorption peaks, based on peak heights, indicates that increasing mercury content produces a reduction of the intensities of the methine and methylene carbon absorptions. However, a more detailed analysis of the spectra, based on the measurement of peak areas, A, leads one to conclude that the peak areas associated with the three principal carbon absorptions for CH, CH_2, and CH_3 groups are equal to one another within experimental error. Thus, the mean proportions of peak areas $A(CH) : A(CH_2) : A(CH_3)$ were found to be 1.0 : 1.1 : 1.0. It is concluded, therefore, that the ^{13}C methine and methylene absorptions are broadened relative to the methyl absorption upon the addition of mercuric chloride. The peak width at half height for the methyl absorption is also increased as a consequence of increasing mercuric chloride content, but the degree of broadening is significantly less than that observed for the methine and methylene absorptions.

These observations lend some support to the proposals made earlier concerning the attachment of the mercuric chloride to the polyether chain through the formation of a 5-membered ring. A dynamic equilibrium involving mercuric chloride-polyether complexes and free mercuric chloride would be expected to give rise to a variety of magnetic environments in the vicinity of a complexed polyether unit, thus leading to a broadening of the NMR lines. The ^{13}C absorption of the methyl group is least affected because, firstly, it is furthest away from the mercuric chloride and secondly, it is efficiently relaxed by virtue of relatively easy rotation about the methyl-carbon bond. The latter point is not expected to be greatly

modified by complexation of the associated ether unit to a molecule of mercuric chloride.

Spin-lattice relaxation times, T_1, for the methine (peak 1), methylene (peak 2) and methyl (peak 3) carbon atoms of poly(propylene glycol) (PPG2025) are shown in figure 18 as a function of the concentration of mercuric chloride. The relaxation data were all measured at 303 K using the DESPOT technique (see Appendix 2 and reference 61). The dependence of T_1 on the concentration of $HgCl_2$ was observed to be very similar for the methine and methyl carbon atoms, with T_1 decreasing by approximately a factor of two as the concentration of $HgCl_2$ increases from 2 mole % to 4 mole %. Increasing the concentration of $HgCl_2$ to 7 mole % produced only a slight decrease in T_1 for the methine and methyl carbons. The similarity in the behaviour of T_1 for the methine and methyl carbons probably reflects the rigid structural connectivity of this pair of atoms. For the methylene carbon atom the dependence of T_1 on the concentration of mercuric chloride is quite different from that observed for the methine and methyl carbons, in that the curve for the methylene carbon T_1 exhibits a maximum positioned at approximately 5 mole %. At the present time no explanation is put forward to account for the overall difference in the relaxation behaviour of methylene carbons compared to that of methine/methyl carbons. Further experiments are believed to be necessary to confirm (or deny) these results; perhaps using a polymer possessing a different molecular weight.

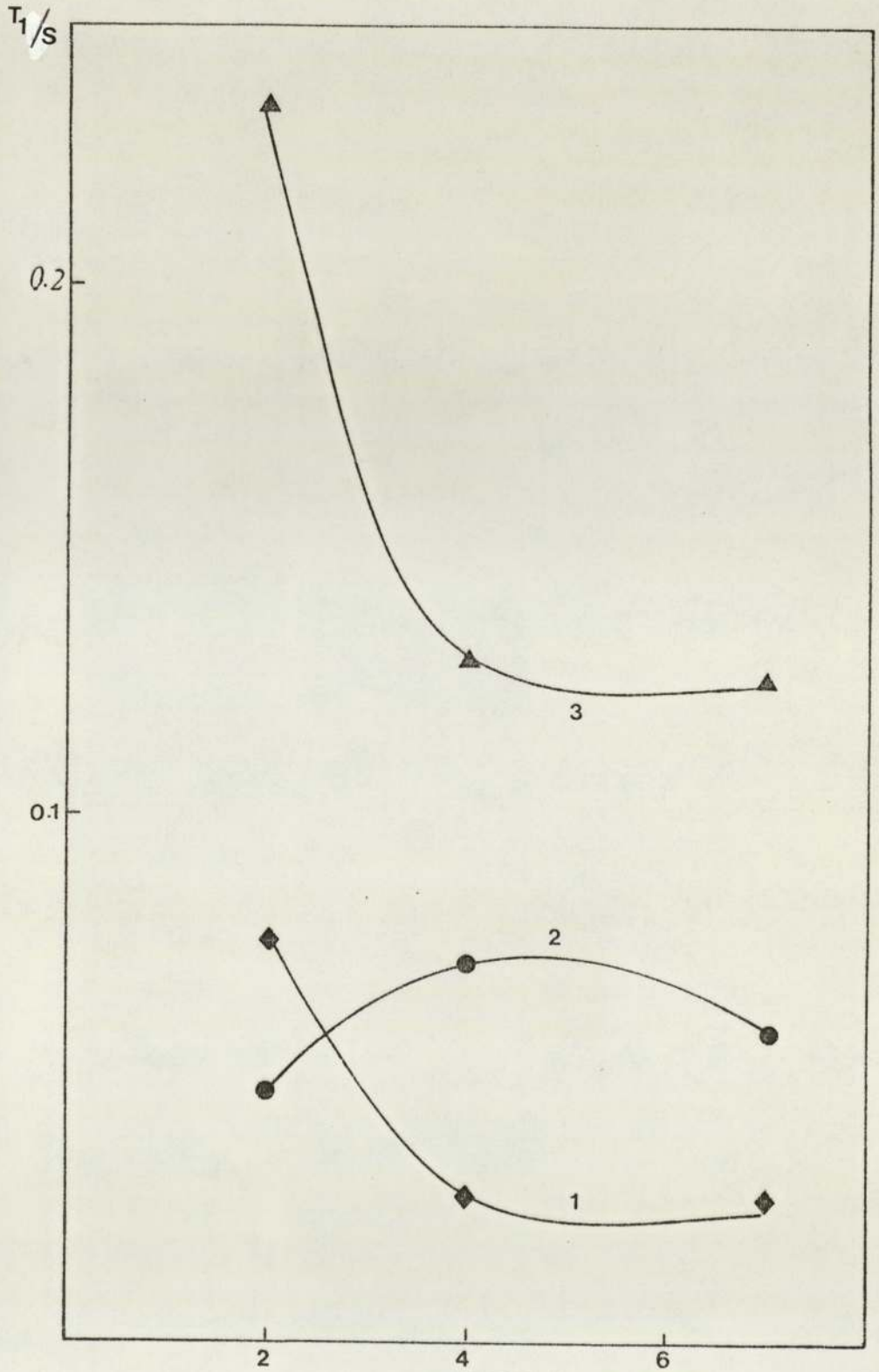

C-13 T_1 relaxation time

Fig 6-18

CHAPTER 7

Conclusions and Suggestions for Further Work

The major proportion of this thesis has been concerned with a study of the dielectric relaxation behaviour of solutions of inorganic salts in polyethers. Particular emphasis has been given to the study of dielectric properties of solutions of mercuric chloride in poly(propylene glycol) over a wide range of temperature and frequency. Some multinuclear N.M.R. investigations of this system have also been undertaken. Two distinct models, describing the nature of the PPG - $HgCl_2$ solutions have been considered. One model considers the mixture of mercuric chloride and poly(propylene glycol) to be essentially an ideal solution in which the molecules of mercuric chloride are completely free (i.e. not complexed). However, this model does not facilitate an acceptable explanation of the significant observed increases in the static permittivity relative to the infinite frequency dielectric permittivity. If the assumption concerning the 'free', uncomplexed form of $HgCl_2$ is to be upheld then it must be concluded that the 'free' mercuric chloride molecules are non-linear. Since this model precludes strong interactions between $HgCl_2$ and PPG this conclusion appears to be unlikely. A more reasonable approach regarding the interpretation of the permittivity data is that in which each molecule of $HgCl_2$ is closely associated with a segment or a number of segments of the polyether chain. This model of the PPG - $HgCl_2$ system also enjoys some support from multinuclear N.M.R. and X-ray studies of solutions of inorganic salts in polyethers. Such studies have indicated

that the metal atom interacts with the ether oxygen atoms. In some solid complexes the nature of the complex and the disposition of the metal and ether atoms is quite well understood. However, for solutions the structure of the complexes is much more difficult to study. The dielectric data obtained for the PPG - $HgCl_2$ system supports the view that the mercuric chloride forms a 5 - membered cyclic complex with poly(propylene glycol) in which each molecule of mercuric chloride is associated with two oxygen atoms of a pair of adjacent ether units. Although the enhancement of the mean dipole moment gives support to this conclusion the shape of the complexed molecule of mercuric chloride is not proven. An interesting observation concerns the dependence of the dielectric relaxation activation energy on the concentration of mercuric chloride, which exhibited a distinct minimum when the concentration of mercuric chloride was approximately equal to 5 mole %. This behaviour was paralleled by the difference in energy, ΔE, between the gauche and trans states of PPG, calculated using the Marchal - Benoit analysis of chain conformations. It was noted that the quantity ΔE also exhibited a minimum value when the concentration of mercuric chloride was close to 5 mole %. A re - examination of the dielectric data obtained for solutions of $ZnCl_2$ in PPG, published by Wetton[10], also indicated a minimal behaviour of the dielectric relaxation activation energy, but the sparsity of the data did not permit the exact location of the minimum with respect to the concentration of $ZnCl_2$. In order to account for these observations it has been proposed that the ether units flanking a complexed ether unit are partly relieved of steric hindrance from their immediate neighbours, relative to units that are adjacent to uncomplexed

ether segments.

The analysis of dielectric permittivity data obtained over a range of frequencies, using the Marchal - Benoit treatment, leads to the conclusion that the gauche conformations of the C - C skeletal bond in PPG are increasingly favoured relative to the trans state as the concentration of mercuric chloride is increased over the range 0 - 5 mole %. The 'locking - action' of the pendent methyl group is also believed to be an important factor in the stabilisation of the 5 - membered cyclic complex.

The Cole - Cole distribution parameter, α, for solutions of mercuric chloride in poly(propylene glycol) also reflects the minimal behaviour exhibited by the gauche - trans energy difference ΔE and the dielectric relaxation activation energy $E^{\neq}$, except that curves of α vs. concentration of $HgCl_2$ in PPG show a distinct maximum for concentrations in the region of 4 mole %. Thus, for concentrations below 4 mole % the addition of $HgCl_2$ produces a broadening of the distribution of dielectric relaxation times. When the concentration of $HgCl_2$ exceeds 4 mole % the distribution of relaxation frequencies narrows upon the addition of $HgCl_2$, indicating that the dipolar ether units are beginning to experience very similar steric environments; perhaps indicative of an increase in structural order. It is noted that the minimal/maximal behaviour observed for the solutions of mercuric chloride and zinc chloride in PPG was not found for CdI_2, $CoCl_2$. However the dielectric data obtained for the solutions of these salts in PPG was less extensive than that available for the PPG - $HgCl_2$ system.

Proton, carbon-13 and mercury-199 nuclear magnetic resonance spectroscopy of solutions of various metal salts in polyether compounds and polyether-like model compounds has demonstrated that multinuclear N.M.R. can play an important role in the investigation of interactions between metal salts dissolved in polyethers.

In the present study the principal ^{13}C absorption peaks in poly(ethylene glycol) and poly(propylene glycol) have been assigned and attributed to carbon atoms in terminal and non-terminal ether units. The effect of dissolved inorganic salts on the ^{13}C N.M.R. spectra has also been considered. Particular attention has been focussed on the PPG-$HgCl_2$ system. For the concentration range 0 - 5 mole %, only small chemical shifts were observed for this particular polymer-salt combination. However, the spin-lattice relaxation times, T_1, which may be shown to be related to viscosity of the medium surrounding the observed nucleus, were significantly affected by the addition of mercuric chloride to PPG. It was found that the addition of $HgCl_2$ caused a broadening of the methine and methylene absorption peaks relative to the largely unaffected methyl peak. This broadening effect has been tentatively attributed to the complex formation between molecules of $HgCl_2$ and the polyether segments via the formation of dynamic 5-membered cyclic complex.

Appendix 1 Dielectric Data for Solutions of Inorganic Salts in Poly(propylene glycol)

This appendix contains tabulations of dielectric permittivity and dielectric loss measured over a range of frequency at various temperatures, for a number of selected inorganic salts in solution in poly(propylene glycol).

Table 1	PPG2025	+ 2	mole %	$HgCl_2$
" 2	"	+ 4	"	"
" 3	"	+ 7	"	"
" 4	PPG4000	+ 2	"	"
" 5	"	+ 4	"	"
" 6	"	+ 1	"	$CoCl_2$
" 7	"	+ 0.5	"	$ZnCl_2$
" 8	"	+ 1	"	CdI_2

Table 1 PPG2025+2mole%$HgCl_2$

f/KHz	ϵ'	ϵ''	ϵ''/ϵ''_m
	T = 247.8 K		
0.5	8.14	-	
0.7	8.12	0.085	
1	8.05	0.214	
3	7.69	0.544	
5	7.42	0.646	
7	7.24	0.701	
10	7.01	0.734	
20	6.42	0.767	
	T = 238.3 K		
0.5	7.88	0.271	
0.7	7.73	0.446	
1	7.54	0.577	
3	6.91	0.801	
5	6.57	0.859	
7	6.36	0.892	
10	6.12	0.935	
20	5.44	0.987	
	T = 231.4 K		
0.3	7.42	0.189	0.176
0.5	7.15	0.486	0.453
0.7	6.96	0.627	0.589
1	6.74	0.745	0.694
3	6.02	1.006	0.938
5	5.59	1.063	0.991

Table 1 PPG2025+2mole%$HgCl_2$

f/KHz	ϵ'	ϵ''	ϵ''/ϵ''_m
7	5.33	1.072	1.000
10	5.00	1.064	0.992
20	4.29	0.964	0.899
	T = 227 K		
0.3	6.88	0.315	0.302
0.5	6.54	0.619	0.594
0.7	6.32	0.767	0.736
1	6.06	0.884	0.848
3	5.22	1.042	1.000
5	4.77	1.016	0.975
7	4.53	0.971	0.931
10	4.24	0.915	0.878
20	3.70	0.764	0.733
	T = 225 K		
0.3	6.53	0.389	0.396
0.5	6.16	0.675	0.688
0.7	5.91	0.816	0.832
1	5.61	0.909	0.927
3	4.80	0.965	0.984
5	4.41	0.910	0.928
7	4.32	0.857	0.874
10	3.96	0.789	0.805
20	3.45	0.626	0.638
	T = 222 K		
0.3	5.92	0.442	0.508
0.5	5.59	0.682	0.783

Table 1 PPG2025+2mole%$HgCl_2$

f/KHz	ϵ'	ϵ''	ϵ''/ϵ''_m
0.7	5.34	0.776	0.891
1	5.11	0.830	0.954
3	4.40	0.821	0.943
5	4.10	0.758	0.871
7	3.93	0.703	0.808
10	3.72	0.643	0.739
20	3.25	0.484	0.556
	T = 218 K		
0.3	4.93	0.305	0.512
0.5	4.63	0.467	0.784
0.7	4.46	0.554	0.931
1	4.24	0.581	0.976
3	3.74	0.552	0.927
5	3.50	0.478	0.803
7	3.36	0.438	0.736
10	3.24	0.391	0.657
20	2.94	0.311	0.522

Table 2 PPG2025+4mole%$HgCl_2$

f/KHz	ϵ'	ϵ''	ϵ''/ϵ''_m
3	5.43	1.085	0.977
5	5.04	1.023	0.921
7	4.78	0.971	0.874
10	4.55	0.915	0.825
20	3.96	0.773	0.697
	T = 227.4 K		
0.11	7.13	--	
0.3	6.39	0.631	0.611
0.5	5.98	0.821	0.873
0.7	5.74	0.893	0.950
1	5.48	0.931	0.991
3	4.72	0.873	0.929
5	4.36	0.803	0.854
7	4.16	0.744	0.792
10	3.96	0.687	0.731
20	3.51	0.557	0.593
	T = 225 K		
0.11	6.40	-	
0.3	5.89	0.526	0.645
0.5	5.52	0.707	0.867
0.7	5.27	0.771	0.946
1	5.03	0.802	0.984
3	4.37	0.758	0.930
5	4.10	0.688	0.844
7	3.94	0.639	0.785

Table 2 PPG2025+4mole%$HgCl_2$

f/KHz	ϵ'	ϵ''	ϵ''/ϵ''_m
	T = 247.8 K		
0.7	9.27	0.776	
1	9.08	0.900	
3	8.20	1.193	
5	7.72	1.246	
7	7.42	1.257	
10	7.05	1.253	
20	6.21	1.195	
	T = 239 K		
0.11	9.37	—	
0.3	8.89	0.631	0.505
0.5	8.48	0.897	0.717
0.7	8.14	1.046	0.836
1	7.88	1.127	0.901
3	6.90	1.242	0.993
5	6.43	1.237	0.989
7	6.14	1.221	0.976
10	5.79	1.197	0.957
20	5.06	1.103	0.882
	T = 231.4 K		
0.11	8.09	—	
0.3	7.35	0.705	0.635
0.5	6.93	0.928	0.836
0.7	6.63	1.019	0.918
1	6.34	1.073	0.966

Table 2 PPG2025+4mole%$HgCl_2$

f/KHz	ϵ'	ϵ''	ϵ''/ϵ''_m
10	3.75	0.585	0.718
20	3.35	0.473	0.518
	T = 221 K		
0.3	4.93	0.273	0.497
0.5	4.64	0.461	0.838
0.7	4.47	0.509	0.926
1	4.28	0.543	0.987
3	3.79	0.507	0.922
5	3.61	0.466	0.848
7	3.50	0.430	0.783
10	3.38	0.393	0.716
20	3.02	0.315	0.574

Table 3 PPG2025+7mole% $HgCl_2$

f/KHz	ϵ'	ϵ''	ϵ''/ϵ''_m
	T = 252 K		
0.11	10.75	2.182	-
0.3	10.41	1.305	0.834
0.5	10.19	1.181	0.755
0.7	10.01	1.168	0.746
1	9.80	1.216	0.777
3	8.85	1.481	0.946
5	8.27	1.558	0.996
7	7.87	1.564	1
10	7.42	1.546	0.988
20	6.44	1.421	0.908
	T = 248 K		
0.3	9.79	0.494	0.338
0.5	9.49	0.808	0.553
0.7	9.22	1.010	0.691
1	8.91	1.181	0.808
3	7.77	1.458	0.998
5	7.21	1.456	0.997
7	6.85	1.421	0.973
10	6.45	1.368	0.936
20	5.62	1.213	0.830
	T = 242 K		
0.3	8.77	0.894	0.643
0.5	8.29	1.155	0.830
0.7	7.91	1.281	0.921

Table 3 PPG2025+7mole%$HgCl_2$

f/KHz	ϵ'	ϵ''	ϵ''/ϵ''_m
1	7.52	1.348	0.969
3	6.41	1.344	0.966
5	5.94	1.252	0.900
7	5.63	1.189	0.855
10	5.32	1.120	0.805
20	4.61	0.951	0.684
	T = 238 K		
0.3	7.79	0.968	0.768
0.5	7.28	1.148	0.911
0.7	6.93	1.218	0.966
1	6.55	1.244	0.987
3	5.58	1.157	0.918
5	5.19	1.066	0.846
7	4.95	1.000	0.793
10	4.69	0.932	0.739
20	4.10	0.772	0.612
	T = 228 K		
0.3	5.27	0.484	0.755
0.5	4.94	0.593	0.925
0.7	4.73	0.631	0.984
1	4.53	0.641	1
3	4.00	0.553	0.862
5	3.80	0.486	0.758
7	3.70	0.440	0.686
10	3.55	0.393	0.613
20	3.22	0.303	0.472

Table 4 PPG4000+2mole%$HgCl_2$

f/KHz	ϵ'	ϵ''	ϵ''/ϵ''_m
	T = 224 K		
0.3	6.35	0.315	0.335
0.5	6.06	0.619	0.658
0.7	5.77	0.762	0.810
1	5.55	0.855	0.909
3	4.74	0.926	0.985
5	4.37	0.860	0.914
7	4.16	0.803	0.854
10	3.91	0.729	0.775
20	3.44	0.577	0.613
	T = 222 K		
0.2	6.20	0.015	0.017
0.5	5.56	0.650	0.760
1	5.03	0.836	0.977
2	4.55	0.844	0.987
5	3.97	0.730	0.850
10	3.61	0.606	0.708
20	3.22	0.473	0.553
	T = 220 K		
0.2	5.73	0.078	0.105
0.5	5.02	0.631	0.852
1	4.56	0.739	0.998
2	4.16	0.712	0.962
5	3.71	0.590	0.790
10	3.40	0.480	0.648
20	3.05	0.365	0.493

Table 4 PPG4000+2mole%$HgCl_2$

f/KHz	ϵ'	ϵ''	ϵ''/ϵ'_m
	T = 257 K		
0.11	8.32	0.918	
0.2	8.28	0.631	
0.5	8.05	0.473	
1	7.88	0.442	
2	7.68	0.399	
5	7.43	0.356	
10	7.26	0.363	
20	6.90	0.409	
	T = 256 K		
0.11	8.40	0.488	
0.2	8.27	0.426	
0.5	8.06	0.397	
1	7.83	0.401	
2	7.69	0.375	
5	7.46	0.347	
10	7.26	0.370	
20	6.87	0.428	
	T = 255 K		
0.2	8.27	0.284	
0.5	8.03	0.347	
1.	7.82	0.372	
2	7.66	0.360	
5	7.42	0.347	
10	7.24	0.383	
20	6.87	0.454	

Table 4 PPG4000+2mole%$HgCl_2$

f/KHz	ϵ'	ϵ''	ϵ''/ϵ''_m
	T = 230 K		
0.3	7.32	0.105	0.094
0.5	7.09	0.397	0.357
0.7	6.89	0.541	0.487
1	6.68	0.666	0.600
3	6.01	0.911	0.821
5	5.65	0.980	0.882
7	5.37	1.001	0.902
10	5.04	1.002	0.902
20	4.35	0.923	0.831
	T = 227 K		
0.3	6.86	0.210	0.210
0.5	6.58	0.505	0.505
0.7	6.38	0.654	0.654
1	6.16	0.776	0.776
3	5.37	0.986	0.986
5	4.96	0.987	0.987
7	4.72	0.957	0.957
10	4.45	0.912	0.912
20	3.88	0.778	0.778

Table 4 PPG4000+2mole%$HgCl_2$

f/KHz	ϵ'	ϵ''	ϵ''/ϵ''_m
	T = 254 K		
0.2	8.24	0.173	
0.5	8.01	0.303	
1	7.80	0.347	
2	7.64	0.341	
5	7.43	0.351	
10	7.23	0.405	
20	6.79	0.474	
	T = 240 K		
0.5	7.97	0.094	
1	7.79	0.322	
2	7.56	0.484	
5	7.30	0.647	
10	6.75	0.730	
20	6.15	0.785	
	T = 232 K		
0.2	7.50	-	-
0.5	7.19	0.328	0.328
1	6.83	0.606	0.606
2	6.47	0.765	0.765
5	5.90	0.917	0.917
10	5.36	0.985	0.985
20	4.66	0.968	0.968

Table 5 PPG4000+4mole%$HgCl_2$

f/KHz	ϵ'	ϵ''	ϵ''/ϵ''_m
	T = 263 K		
0.11	8.96	0.401	
0.2	8.86	0.379	
0.5	8.69	0.372	
1	8.54	0.382	
2	8.34	0.380	
5	8.14	0.403	
10	7.93	0.486	
20	7.48	0.624	
	T = 261 K		
0.2	8.87	0.094	
0.5	8.69	0.271	
1	8.51	0.334	
2	8.34	0.358	
5	8.13	0.437	
10	7.89	0.564	
20	7.32	0.728	
	T = 251 K		
0.3	8.85	-	-
0.5	8.73	0.126	0.124
0.7	8.66	0.239	0.235
1	8.56	0.350	0.344
3	8.31	0.706	0.695
5	7.85	0.862	0.849
7	7.60	0.86	0.99

Table 5 PPG4000+4mole%$HgCl_2$

f/KHz	ϵ'	ϵ''	ϵ''/ϵ''_m
0.7	6.42	0.857	0.836
1	6.15	0.925	0.915
3	5.35	0.987	0.977
5	4.97	0.952	0.942
7	4.76	0.915	0.905
10	4.51	0.870	0.861
20	3.94	0.740	0.732
	T = 228 K		
0.3	6.00	0.473	0.566
0.5	5.64	0.699	0.837
0.7	5.39	0.767	0.918
1	5.16	0.818	0.979
3	4.44	0.793	0.949
5	4.17	0.728	0.871
7	3.97	0.676	0.809
10	3.80	0.619	0.741
20	3.38	0.493	0.590

Table 5 PPG4000+4mole%$HgCl_2$

f/KHz	ϵ'	ϵ''	ϵ''/ϵ''_m
10	7.29	1.005	0.990
20	6.52	1.015	1
	T = 245 T		
0.3	8.71	-	-
0.5	8.53	0.277	0.257
0.7	8.38	0.482	0.448
1	8.21	0.656	0.610
3	7.42	1.023	0.952
5	7.01	1.069	0.995
7	6.74	1.074	1
10	6.41	1.067	0.993
20	5.71	1.005	0.935
	T = 238 K		
0.3	8.103	0.326	0.307
0.5	7.74	0.663	0.625
0.7	7.48	0.821	0.774
1	7.19	0.934	0.881
3	6.33	1.052	0.992
5	5.94	1.042	0.983
7	5.68	1.026	0.967
10	5.39	1.005	0.948
20	4.74	0.933	0.880
	T = 233 K		
0.3	7.08	0.505	0.500
0.5	6.69	0.745	0.737

Table 6 PPG4000+1mole% $CoCl_2$

f/KHz	ϵ'	ϵ''	ϵ''/ϵ''_m
	T = 230 K		
0.11	5.00	0.186	
0.20	4.92	0.171	
0.50	4.88	0.159	
1.0	4.82	0.191	
2.0	4.76	0.263	
5.0	4.56	0.441	
10	4.28	0.412	
20	3.75	0.722	
	T = 226 K		
0.20	4.90	0.216	
0.50	4.85	0.232	
1.0	4.76	0.335	
2.0	4.67	0.507	
5.0	4.14	0.725	
10	3.67	0.781	
20	3.16	0.719	
	T = 224 K		
0.11	4.96	0.186	
0.20	4.92	0.239	
0.50	4.82	0.351	
1.0	4.65	0.508	
2.0	4.37	0.681	
5.0	3.77	0.797	
10	3.32	0.751	
20	2.87	0.629	

f/KHz	ϵ'	ϵ''	ϵ''/ϵ''_m
	T = 221 K		
0.11	4.90	0.269	
0.20	4.85	0.422	
0.50	4.56	0.625	
1.0	4.27	0.766	
2.0	3.80	0.805	
5.0	3.18	0.712	
10	2.86	0.586	
20	2.52	0.452	
	T = 217 K		
0.11	4.60	0.684	
0.20	4.31	0.798	
0.50	3.75	0.821	
1.0	3.34	0.746	
2.0	3.01	0.619	
5.0	2.65	0.456	
10	2.46	0.349	
20	2.22	0.253	
PPG4000 + 0.5 mole % $ZnCl_2$			
	T = 230 K		
0.11	5.59	0.622	
0.20	5.35	0.604	
0.50	5.01	0.584	
1.0	4.74	0.570	
2.0	4.55	0.584	
5.0	4.11	0.668	
10	3.72	0.718	
20	3.24	0.691	

Table 7

f/KHz	ϵ'	ϵ''	ϵ''/ϵ''_m
		T = 227 K	
0.11	5.33	0.705	
0.20	5.05	0.604	
0.50	4.75	0.588	
1.0	4.49	0.616	
2.0	4.22	0.678	
5.0	3.69	0.733	
10	3.29	0.693	
20	2.84	0.586	
		T = 224 K	
0.11	4.97	0.643	
0.20	4.76	0.627	
0.50	4.42	0.661	
1.0	4.10	0.721	
2.0	3.75	0.742	
5.0	3.20	0.673	
10	2.87	0.561	
20	2.53	0.441	
		T = 221 K	
0.11	4.61	0.684	
0.20	4.36	0.707	
0.50	3.90	0.752	
1.0	3.53	0.727	
2.0	3.18	0.637	
5.0	2.75	0.505	
10	2.54	0.396	
20	2.30	0.300	

f/KHz	ϵ'	ϵ''	ϵ''/ϵ''_m
	T = 218 K		
0.11	4.14	0.746	
0.20	3.75	0.798	
0.50	3.29	0.675	
1.0	2.98	0.570	
2.0	2.75	0.465	
5.0	2.47	0.336	
10	2.30	0.257	
20	2.15	0.199	

PPG4000 + 1 mole % CdI_2 **Table 8**

	T = 230 K		
0.11	5.66	0.684	
0.20	5.43	0.695	
0.50	5.06	0.625	
1.0	4.76	0.600	
2.0	4.52	0.604	
5.0	4.08	0.664	
10	3.73	0.684	
20	3.25	0.641	
	T = 227 K		
0.11	5.33	0.684	
0.20	5.04	0.627	
0.50	4.74	0.606	
1.0	4.47	0.625	
2.0	4.18	0.668	
5.0	3.71	0.690	
10	3.32	0.647	
20	2.89	0.549	

f/KHz	ϵ'	ϵ''	ϵ''/ϵ''_m
	T = 224 K		
0.11	4.89	0.622	
0.20	4.65	0.627	
0.50	4.33	0.652	
1.0	4.00	0.700	
2.0	3.65	0.706	
5.0	3.15	0.627	
10	2.85	0.524	
20	2.53	0.414	
	T = 221 K		
0.11	4.47	0.684	
0.20	4.26	0.718	
0.50	3.81	0.721	
1.0	3.47	0.684	
2.0	3.14	0.604	
5.0	2.75	0.466	
10	2.56	0.371	
20	2.32	0.279	

APPENDIX 2

The main computer programs employed in the analysis of experimental dielectric data are presented in this appendix. Each program is accompanied by an outline of its function, together with a list of parameters required as input by the program. All of the programs were written in Basic and were run on an Apple II computer in the Department of Molecular Sciences.

Program 1 Calculation of the Mean-square Dipole Moment per Unit Volume

Mean-square dipole moments per unit volume, $\langle \mu_o^2 \rangle$ were calculated using the Onsager expression (see Equation 5.2) The computer program requests the following input:

1. Static dielectric permittivity, ε_o.
2. Infinite frequency dielectric permittivity, ε_∞ . (These values normally being derived from Cole-Cole plots)
3. Absolute temperature, T.
4. Number of dipolar units per unit volume, N (molecules per cm^3).

The quantity N may be input from the keyboard directly, or calculated by the program. The latter action results in the display of a short menu in which three options are provided for the evaluation of N. These options concern the units which the user of the program wishes to employ for the concentration of components; these being weights, moles or mole fractions. Once a choice has been made, the user is then requested to input the appropriate quantities for the chemical system. The density, $\rho(g/cm^3)$, of the medium and the molecular weight of each component are also requested by the program.

The program then prints (to screen) the mean-square dipole moment and the root-mean square dipole moment.

Program Notes:- The assignment of the principal parameters in the program are as follows:

Static dielectric permittivity, E0

Infinite frequency dielectric permittivity, EI

Dipolar units per unit volume:

Total No., NT

Component 1, N1

Component 2, N2

Mean square dipole moment, MS

PROGRAM 1 EVALUATION OF ONSAGER EQUATION

```
10  REM  EVALUATION OF ONSAGER EQUATION
20  REM  TO CALCULATE THE MEAN-SQUARE
30  REM  ELECTRIC DIPOLE MOMENT
40  HOME
50  PRINT  SPC( 5)"EVALUATION OF ONSAGER'S EQUATION"
60  PRINT
70  PRINT "STATIC PERMITTIVITY ";
80  INPUT EO
90  PRINT : PRINT "INF. FREG. '' ";
100  INPUT EI
140  PRINT
150  PRINT "ABSOLUTRE TEMPERATURE/K ";
160  INPUT T
170  PRINT
180  PRINT : PRINT "   CALCULATE DIPOLES PER CM^3 ? (Y/N)"
185  GET K$: IF K$ = "" THEN 185
186  IF K$ = "Y" THEN  GOSUB 1000: GOTO 190
187  IF K$ <  > "N" THEN 185
188  GOTO 200
190  HOME : PRINT : PRINT "  DIPOLAR UNITS PER CM^3 (*10^-20)": PRIN
191  PRINT "    TOTAL           = "; INT (NT * 100) / 100
192  PRINT "    COMPONENT 'A'   = "; INT (N1 * 100) / 100
193  PRINT "    COMPONENT 'B'   = "; INT (N2 * 100) / 100
200  PRINT : INPUT "       INPUT VALUE.....";ND
205 NU = (EO - EI) * (2 * EO + EI) * 9 * 1.3805 * T
210 DE = EO * (EI + 2) * (EI + 2) * 4 * 3.14153 * ND
220 MS = NU / DE
230 M =  SQR (MS)
240  PRINT
250  PRINT "MEAN-SQUARE MOMENT PER DIPOLAR UNIT"
260  PRINT "IS (DEBYES)^2.....  "; INT (MS * 100) / 100
270  PRINT
280  PRINT "ROOT-MEAN-SQUARE DIPOLE MOMENT PER"
290  PRINT "DIPOLAR UNIT (DEBYES).....   "; INT (M * 100) / 100
300  PRINT : PRINT : PRINT  SPC( 10)"ANOTHER GO ? (Y/N) "
310  GET K$: IF K$ = "" THEN 310
320  IF K$ = "Y" THEN 40
330  IF K$ <  > "N" THEN 310
340  HOME
350  END
```

```
1000  HOME : PRINT "  CALCULATION OF DIPOOLAR UNITS PER CM^3"
1010  PRINT
1020  PRINT  SPC( 5)"1. WORK IN WEIGHTS (GRAMS)"
1030  PRINT
1040  PRINT  SPC( 5)"2. WORK IM MOLES"
1050  PRINT
1060  PRINT  SPC( 5)"3. WORK IN MOLE FRACTIONS"
1070  PRINT
1080  PRINT  SPC( 6)"   CHOOSE NUMBER REQUIRED"
1090  GET K$: IF K$ = "" THEN 1090
1100 K =  VAL (K$): IF K < 1 OR K > 3 THEN 1090
1110  ON K GOTO 1200,1500,1800
1200  HOME : PRINT
1210  INPUT "WEIGHT OF COMPONENT 'A'    ";WA
1220  INPUT "MOLECULAR WEIGHT OF 'A'    ";MA
1230  PRINT
1240  INPUT "WEIGHT OF COMPONENT 'B'    ";WB
1250  INPUT "MOLECULAR WEIGHT OF 'B'    ";MB
1260  PRINT
1270  INPUT "DENSITY OF SOLUTION G/CM^3 ";DS
1280 NT = ((WA / MA) + (WB / MB)) * DS * 6022 / (WA + WB)
1285 N1 = (WA / MA) * DS * 6022 / (WA + WB)
1287 N2 = (WB / MB) * DS * 6022 / (WA + WB)
1290  GOTO 1910
1500  HOME : INPUT "MOLES OF COMPONENT  'A' ";NA
1510  PRINT
1520  INPUT "MOLECULAR WEIGHT OF 'A' ";MA
1530  PRINT
1540  INPUT "MOLES OF COMPONENT  'B' ";NB
1550  PRINT
1560  INPUT "MOLECULAR WEIGHT OF 'B' ";MB
1570  PRINT
1580  INPUT "DENSITY OF SOLUTION G/CM^3 ";DS
1590 NT = (NA + NB) * DS * 6022 / (NA * MA + NB * MB)
1595 N1 = NA * DS * 6022 / (NA * MA + NB * MB)
1597 N2 = NB * DS * 6022 / (NA * MA + NB * MB)
1600  GOTO 1910
1800  HOME
1810  INPUT "MOLE FRACTION OF 'A' ";FA
1820  PRINT
1830  INPUT "MOLECULAR WEIGHT OF 'A' ";MA
1840  PRINT
1850  INPUT "MOLE FRACTION OF 'B' ";FB
```

```
1860  PRINT
1870  INPUT "MOLECULAR WEIGHHT OF 'B' ";MB
1880  PRINT
1890  INPUT "DENSITY  OF SOLUTION  G/CM^3 ";DS
1900 NT = DS * 6022 / (FA * MA + FB * MB)
1905 N1 = FA * DS * 6022 / (FA * MA + FB * MB)
1907 N2 = FB * DS * 6022 / (FA * MA + FB * MB)
1910  RETURN
```

Program 2 Evaluation of the Marchal and Benoit Equation for the Calculation of $\langle\cos\varphi\rangle$

This computer program calculates the average cosine of the rotational bond, φ, of a polymer molecule comprised of identical repeat units. The evaluation employs an equation (the Marchal-Benoit equation) that may be regarded as a combination of the Onsager equation and equations derived from the application of rotational isomeric state models. The latter relate the mean-square dipole moment of a polymer chain to $\eta=\langle\cos\varphi\rangle$. For further details, see Chapters 2 and 5.

The program requires the following inputs:

For Polymer 1 and Polymer 2:-

1. Absolute temperature, T.
2. Static dielectric permittivity, ε_o.
3. Infinite frequency dielectric permittivity, ε_∞
4. Density of the polymer, ρ (g/cm^3).
5. Molecular weight.

The program then displays on the screen two possible values of $\eta=\langle\cos\varphi\rangle$ and the corresponding statistical weights, σ, calculated using the expression

$$\sigma = (2\eta + 1)/(1 - \eta)$$

Negative values of σ are rejected (since $\sigma = \exp(\Delta E/RT)$ values are always positive) and energy differences, ΔE, are also calculated.

Program Notes:- Static dielectric permittivity, E0

Infinite frequency dielectric permittivity, EI

Density, D

Molecular weight, M1, M2

η values, X1 and X2

σ values, S1 and S2

ΔE values, D1 and D2

PROGRAM 2 EVALUATION OF LORENTZ-LORENZ EQUATION

```
10  REM  LORENTZ-LORENZ
20  HOME : PRINT
30  PRINT "DATA FOR COMPONENT 'A' ": PRINT
40  INPUT "    MOLECULAR WEIGHT = ";MA
50  INPUT "    DENSITY......... = ";DA
60  INPUT "    REFRACTIVE INDEX = ";NA
70  PRINT
80  PRINT "DATA FOR COMPONENT 'B' ": PRINT
90  INPUT "  MOLECULAR WEIGHT = ";MB
100  INPUT "  DENSITY......... = ";DB
110  INPUT "  REFRACTIVE INDEX = ";NB
120  PRINT
130  PRINT "DATA FOR SOLUTION": PRINT
140  INPUT "    WEIGHT OF 'A'    = ";WA
150  INPUT "    WEIGHT OF 'B'    = ";WB
160  PRINT : PRINT
170  PRINT "PRESS SPACE-BAR TO CONTINUE"
180  GET K$: IF K$ = "" THEN 180
190  REM  CALCULATE MOLE FRACTIONS
200 FA = (WA / MA) / ((WA / MA) + (WB / MB))
210 FB = 1 - FA
220  REM  MOLAR REFRACTION OF 'A'
230 RA = ((NA * NA - 1) * MA) / ((NA * NA + 2) * DA)
240  REM  MOLAR REFRACTION OF 'B'
250 RB = ((NB * NB - 1) * MB) / ((NB * NB + 2) * DB)
260  REM  CALCULATE MOLAR REFRACTION OF SOLUTION
270 RS = FA * RA + FB * RB
280  REM  CALC MOLECULAR WEIGHT OF SOLUTION
290 MS = FA * MA + FB * MB
300  REM  CALC MOLAR VOLUME OF 'A'
310 VA = MA / DA
320  REM  CLAC MOLAR VOLUME OF 'B'
330 VB = MB / DB
340  REM  CALC MOLAR VOLUME OF SOLUTION
350 VS = FA * VA + FB * VB
360  REM  CALC DENSITY OF THE SOLUTION
370 DS = MS / VS
380  REM  CALC REFRACTIVE INDEX OF SOLUTION
390 NS =  SQR ((MS + 2 * RS * DS) / (MS - DS * RS))
400  REM  NOW PRINT RESULTS TO SCREEN
410  HOME
420  PRINT " COMPONENT 'A'": PRINT
430  PRINT "    MOLAR VOLUME       = ";VA
440  PRINT "    MOLAR REFRACTION   = ";RA
450  PRINT
460  PRINT " COMPONENT 'B'": PRINT
470  PRINT "    MOLAR VOLUME       = ";VB
480  PRINT "    MOLAR REFRACTION   = ";RB
490  PRINT
```

```
500  PRINT " SOLUTION": PRINT
510  PRINT "    MOLAR VOLUME       = ";VS
520  PRINT "    MOLAR REFRACTION   = ";RS
530  PRINT "    REFRACTIVE INDEX   = ";NS
535  PRINT "    R.INDEX SQUARED    = ";NS ^ 2
540  PRINT
550  PRINT "<SPACE-BAR> TO CONTINUE"
560  GET K$: IF K$ = "" THEN 560
570  HOME
580  PRINT "    <M> FOR ANOTHER CALCULATION"
590  PRINT "    <F> TO FINISH "
600  GET K$: IF K$ = "" THEN 600
610  IF K$ = "M" THEN 20
620  IF K$ <  > "F" THEN 600
630  HOME : VTAB (10)
640  PRINT  TAB( 16)"E N D"
650  FOR TD = 1 TO 1000: NEXT TD
660  HOME
670  END
```

Program 3 Calculation of Solution Refractive Indices

This program uses the Lorenz-Lorentz equation to calculate the refractive index of solutions of salts in poly(propylene glycol). It is assumed that the molar refraction of the solutions, R_{12}, is given by

$$R_{12} = f_1 R_1 + f_2 R_2$$

where the subscripts 1,2 and 12 define quantities associated with the solvent (PPG), solute (inorganic salt) and solution, respectively. The mole fractions of the components are denoted by f.

The program requires the following inputs:

1. Molecular weight of each component.
2. Density (g/cm^3) of each component.
3. Refractive index of each component (same λ).
4. Weight of each component (g).

The program then calculates and displays the molar volume and molar refraction of the individual components and those of the solution. The refractive index of the solution is calculated using the Lorenz-Lorentz relationship and is printed to the screen.

Program notes:

Molecular weight, density and refractive index of component A are denoted by variables, MA, DA and NA respectively.

The corresponding quantities for component B are MB, DB and NB respectively.

Further details may be found in the PRINT and REMARK statements of the program.

PROGRAM 3 EVALUATION OF MARCHAL-BENOIT EQUATION

```
10  REM  MARCHAL AND BENOIT EQUATION
20  HOME : PRINT "MARCHAL AND BENOIT EQUATION"
30  PRINT "FOR CALCULATION OF <COS PHI>"
40  PRINT : INPUT "TEMPERATURE ";T
50  PRINT : PRINT "POLYMER 1 (PPG)"
60  INPUT "STATIC PERMITTIVITY ";E0
70  INPUT "INF.FREQ.    ''       ";EI
80  INPUT "DENSITY G/CM^3        ";D
85  INPUT "MOL.WT.               ";M1
90 G1 = (E0 - EI) * T * (2 * E0 + EI)
100 G1 = G1 / ((EI + 2) * (EI + 2) * D * E0)
200  PRINT
210  PRINT "POLYMER 2 (PEG)": PRINT
220  INPUT "STATIC PERMITTIVITY ";E0
230  INPUT "INF.FREQ.             ";EI
240  INPUT "DENSITY G/CM^3        ";D
245  INPUT "MOL.WT.               ";M2
250 G2 = (E0 - EI) * T * (2 * E0 + EI)
260 G2 = G2 / ((EI + 2) * (EI + 2) * D * E0)
270 Z = (M1 * G1) / (M2 * G2)
280 T1 =  - Z / 13:T2 = Z * Z / 169
290 T3 = 4 * (Z + 1) * (Z - 1):T5 = 2 * (Z + 1)
300  IF T2 < T3 THEN  PRINT "ROOTS IMAGINARY": GOTO 410
310 T4 =  SQR (T2 - T3)
320 X1 = (T1 + T4) / T5
330 X2 = (T1 - T4) / T5
340  PRINT : PRINT "ETA= ";X1;" , ";X2
350 S1 = (1 + 2 * X1) / (1 - X1)
360 S2 = (1 + 2 * X2) / (1 - X2)
370  PRINT : PRINT "SIGMA= ";S1;" , ";S2
375  IF S1 <  = 0 THEN 385
380 D1 = 1.987 * T *  LOG (S1)
385  IF S2 <  = 0 THEN 400
390 D2 = 1.987 * T *  LOG (S2)
400  PRINT : PRINT "DELTA E= ";D1;" , ";D2
410  PRINT : PRINT "ANOTHER CALCULATION ? (Y/N)"
420  GET K$: IF K$ = "" THEN 420
430  IF K$ = "Y" THEN 20
440  IF K$ <  > "N" THEN 420
450  HOME
460  END
```

Program 4 Calculation of Densities

The calculation of mean-square dipole moments per dipolar unit per unit volume, using the Onsager equation, requires a knowledge of the number of dipolar units per unit volume, which in turn requires a knowledge of the density of the medium.

This program permits two types of calculation to be accomplished. One section of the program permits the calculation of the density of a solution using the densities and known quantities of the individual components. This calculation assumes ideal behaviour. Another section of the program calculates the density of pure poly(propylene glycol) as a function of temperature. The expression used for this purpose was determined by Baur and, strictly speaking, only applies over the range 243K-293K.

Program Notes:

The first part of the program requires the densities and amounts of components A and B of the binary mixture. The program allows the user to choose the units in which he wishes the concentration to be expressed (a choice of weight, number of moles and mole fractions).

PROGRAM 4 CALCULATION OF DENSITIES

```
5  GOTO 1000: REM  GOTO MENU
10  REM  DENSITY CALCULATIONS
20 :
30  HOME : PRINT  SPC( 3)"DENSITY CALCULATIONS OF SOLUTIONS"
40  PRINT
50  PRINT " DENSITY (G/CM^3) OF COMPONENT A ";
60  INPUT DA
70  PRINT
80  PRINT " DENSITY (G/CM^3) OF COMPONENT B ";
90  INPUT DB
100  PRINT
110  PRINT "WORK IN MOLES OR WEIGHT ? (M/W)"
120  GET K$: IF K$ = "" THEN 120
130  IF K$ = "M" THEN  GOSUB 500: GOTO 200
140  IF K$ <  > "W" THEN 120
150  PRINT : PRINT "WEIGHT OF COMPONENT A";
160  INPUT WA
170  PRINT
180  PRINT "WEIGHT OF COMPONENT B";
190  INPUT WB
200 WT = WA + WB
210 VA = WA / DA:VB = WB / DB:VT = VA + VB
220 DS = WT / VT
230  PRINT : PRINT
240  PRINT "DENSITY OF SOLUTION ="; INT (DS * 100) / 100;" (G/CM^3)"
242  PRINT "WEIGHT A=";WA;" WEIGHT B=";WB
250  PRINT
260  PRINT "ANOTHER GO? (Y/N)"
270  GET K$: IF K$ = "" THEN 270
280  IF K$ = "Y" THEN 30
290  IF K$ <  > "N" THEN 270
300  GOTO 1000
500  REM  WORKING IN MOLES OR MOLE FRACTIONS
510  PRINT : PRINT "MOLESOF,ORMOLE FRACTION OF A ";
520  INPUT FA
530  PRINT : PRINT " MOLECULAR WEIGHT OF A ";
540  INPUT MA
550  PRINT : PRINT "MOLES OF,OR MOLE FRACTION OF B ";
560  INPUT FB
570  PRINT : PRINT "MOLECULAR WEIGHT OF B ";
580  INPUT MB
590 WA = FA * MA:WB = FB * MB
600  RETURN
1000  HOME
```

```
1010  PRINT "1. CALC SOLUTION DENSITIES"
1020  PRINT
1030  PRINT "2. CALC PPG DENSITY AT DIFFERENT TEMPS"
1035  PRINT : PRINT "3. QUIT PROGRAM"
1040  PRINT
1050  GET K$: IF K$ = "" THEN 1050
1060 K =  VAL (K$)
1070  IF K < 0 OR K > 3 THEN 1050
1080  ON K GOTO 30,2000,3000
2000  REM  CALC DENSITY OF PPG AT DIFFERENT TEMPERATURES
2010  HOME : PRINT "DENSITY OF POLY(PROPYLENE GLYCOL)"
2020  PRINT
2030  PRINT "TEMPERATURE IN CENTIGRADE (-30 TO 20)";
2040  INPUT " ";T
2050 D = 1 / (0.970 + 0.0013 * T + 7 * (10 ^ ( - 6)) * T * T)
2060  PRINT
2070  PRINT "DENSITY AT ";T;" C IS ....";
2075  PRINT  INT (D * 1000) / 1000;" G/CM^3)"
2080  PRINT : PRINT "ANOTHER GO ? (Y/N)"
2090  GET K$: IF K$ = "" THEN 2090
2100  IF K$ = "N" THEN 1000
2110  IF K$ <  > "Y" THEN 2090
2120  GOTO 2010
3000  REM  QUIT
3010  HOME : END
```

Program 5 Calculation of ε_∞ from the Molar Refraction, Molecular Weight and Density

This is a short, but useful, utility program that enables the infinite frequency dielectric premittivity, ε_∞, to be calculated using the Lorenz-Lorentz relationship (see Section

The program requires the molar refraction, density and molecular weight.

PROGRAM 5 CALCULATION OF MOLAR REFRACTION

```
10  HOME : PRINT "CALCULATES EPSILON INFINITY FROM THE"
15  PRINT "MOLAR REFRACTION,  MOL.WT.,AND DENSITY": PRINT
20  INPUT " MOLAR REFRACTION ";MR
30  PRINT
40  INPUT " DENSITY..... ";D
50  PRINT
60  INPUT " MOLECULAR WEIGHT ";MW
70  PRINT
80 EP = ((MW / D) + 2 * MR) / ((MW / D) - MR)
90  PRINT
100  PRINT "EPSILON INFINITY = ";EP
105  PRINT "SQUARE ROOT OF EPS.INF. =";EP ^ .5: PRINT
110  PRINT
120  PRINT "ANOTHER GO ? (Y/N)"
130  GET K$: IF K$ = "" THEN 130
140  IF K$ = "Y" THEN 10
150  IF K$ <  > "N" THEN 130
160  HOME : END
```

Program 6 Calculation of Spin-Lattice Relaxation Times, T_1, using DESPOT: Driven-Equilibrium Single-Pulse Observation of T_1 Relaxation

This computer program was used to calculate spin-lattice relaxation times, T_1, from the sets of pulse width-magnetic intensity data (t_p - I_z). The program requires a knowledge of the 90° pulse width for the nucleus being studied and an approximate idea of the range in which T_1 lies. The latter quantity enables a 'good' value to be chosen for the pulse repetition time t_i. Further comments and help pages are available when the program is RUNning. More detailed background information concerning the more theoretical aspects of DESPOT can be found in reference 61 .

A typical set of pulsewidth vs. intensity data, obtained for a 2 mole % solution of mercuric chloride in poly(propylene glycol) is included below for the ^{13}C nucleus, together with a plot of signal intensity against pulse width t_p. The plot shows the experimental points and solid curve fitted using a least-mean-squares analysis. The maximum of this curve θ_{max} is used to calculate T_1 (provided that t_i is known) using the simple relationship

$$\cos \theta_{max} = \exp(-t_i/T_1)$$

which may be rearranged to give

$$T_1 = \frac{-t_i}{\log_e(\cos \theta_{max})}$$

PROGRAM 6 CALCULATION OF SPIN-LATTICE RELAXATION TIMES

```
1  REM  'DESPOT' - T1 FROM PEAK MAXIMUM
10 LOC = 16385: IF  PEEK (103) +  PEEK (104) * 256 <  > LOCT THEN
 POKE LOC - 1,0: POKE 103,LOC -  INT (LOC / 256) * 256: POKE 1
04, INT (LOC) / 256: PRINT  CHR$ (4);"RUN MAXIMUM DESPOT"
20 SZ = 50: REM  MAX NO. OF DATA PAIRS
30  DIM PW(SZ),IN(SZ),XD(SZ),YZ(Z),XC(60),YC(60),FG$(SZ),YD(SZ
)
40 MX = 0:MY = 0:ND = 0
50  FOR I = 1 TO 50:FG$(I) = "+": NEXT I
70  GOSUB 500
90  HOME : PRINT  SPC( 4);: INVERSE : PRINT "'DESPOT'";: NORMAL
: PRINT " - FROM PEAK MAXIMUM": PRINT
100  PRINT " 0- TITLE SCREEN & SOURCE REFERENCE"
110  PRINT " 1- BRIEF INFORMATION": PRINT
120  PRINT " 2- EDIT/VIEW COMMENTS/RESULTS SUMMMARY"
130  PRINT " 3- EDIT/VIEW OR KEY IN DATA"
140  PRINT " 4- EDIT/VIEW 90 DEG & DELAY TIMES": PRINT
150  PRINT " 5- DERIVE EQUATION & CALCULATE T1": PRINT
160  PRINT " 6- DRAW NEW GRAPH ON SCREEN"
170  PRINT " 7- VIEW A PREVIOUSLY PLOTTED GRAPH": PRINT
180  PRINT " 8- SEND DATA & RESULTS TO PRINTER"
190  PRINT " 9- OPEN FILE TO LOAD OR SAVE DATA": PRINT
200  PRINT " Q- QUIT PROGRAM"
210  PRINT : PRINT  SPC( 5);: INVERSE : PRINT " CHOOSE OPTION
";: NORMAL : PRINT " 0-9 OR Q"
230  GET K$
240  IF K$ = "Q" THEN  GOSUB 1500: GOTO 90
250 K =  ASC (K$)
260  IF K < 48 OR K > 57 THEN 230
270  ON (K - 47) GOSUB 500,1000,2000,2500,3500,4000,6000,6000,
8000,9000
280  GOTO 90
300 :
499  REM  ******************** TITLE SCREEN
500  HOME
510  PRINT  SPC( 8)" **********************"
520  PRINT  SPC( 8)"**** D E S P O T ****"
530  PRINT  SPC( 8)" **********************"
540  PRINT : PRINT  SPC( 4)"DRIVEN EQUILIBRIUM SINGLE PULSE"
550  PRINT " OBSERVATION OF SPIN-LATTICE RELAXATION"
560  PRINT : PRINT : PRINT  SPC( 6)"JOHN HOMER & MARTIN BEEVER
S": PRINT
570  PRINT : PRINT : PRINT  SPC( 5)"MOLECULAR SCIENCES - CHEMI
STRY"
580  PRINT  SPC( 11)"UNIVERSITY OF ASTON"
590  PRINT  SPC( 12)"BIRMINGHAM - U.K."
600  PRINT : PRINT : PRINT "    J.MAG.RES.1985,VOL.63.PP287-29
7"
610  PRINT
```

```
620  PRINT  SPC( 6);: INVERSE : PRINT " PRESS ANY KEY TO CONTI
NUE ": NORMAL
630  GET K$
640  RETURN
999 :
1000  REM  ****************INST/INFO
1010  HOME
1020  INVERSE : PRINT "'DESPOT'";: NORMAL : PRINT "CALCULATION
 OF SPIN LATTICE"
1030  PRINT "RELAXATION TIME, T1, FROM THE PEAK"
1040  PRINT " MAXIMUM OF A PLOT OF PULSE WIDTH VS."
1050  PRINT " SIGNAL INTENSITY. THE EXPERIMENTAL"
1060  PRINT " DATA IS FITTED TO A CUBIC EQUATION."
1070  PRINT
1120  INVERSE : PRINT "BEFORE PROCEEDING YOU REQUIRE:-"
1130  PRINT
1140  PRINT " THE 90 DEGREE PULSE WIDTH/MICROSECS."
1150  PRINT
1160  PRINT " THE PULSE REPETITION TIME/SECS."
1170  PRINT
1180  PRINT " N PAIRS OF PULSE WIDTH/US & INTENSITY."
1190  PRINT : PRINT "(ORDINAL ORDER  OF PULSES NOT ESSENTIAL)"

1200  PRINT
1210  PRINT  SPC( 5);: INVERSE : PRINT " PRESS ANY KEY TO CONT
INUE": NORMAL
1220  GET K$
1230  RETURN
1499 :
1500  REM  **************** QUIT PROGRAM
1510  HOME
1520  PRINT : PRINT "  DO YOU WANT TO QUIT PROGRAM ? (Y/N)"
1530  GET K$
1540  IF K$ = "N" THEN 1580
1550  IF K$ <  > "Y" THEN 1530
1560  HOME : END
1580  RETURN
1999 :
2000  REM  **************** USER HEADINGS/RESULTS
2010  FOR I = 1 TO 5
2020  IF CT$(I) = "" THEN CT$(I) = "NO ENTRY"
2030  NEXT I
2040  HOME
2050  PRINT " 1.TITLE: ";CT$(1):CM$(1) = "TITLE"
2060  PRINT : PRINT " 2.NAME: ";CT$(2):CM$(2) = "NAME"
2070  PRINT : PRINT " 3.DATE: ";CT$(3):CM$(3) = "DATE"
2080  PRINT : PRINT " 4.COMMENTS: ";CT$(4):CM$(4) = "COMMENTS"

2090  PRINT : PRINT " RESULTS: ";CT$(5)
2095  PRINT : PRINT "  CUBIC COEFFICIENTS ARE:-": PRINT
2096  PRINT " A(CUBE)=`"; INT (X(0) * 1000) / 1000;" B(SQUARE=
 "; INT (X(1) * 1000) / 1000
2097  PRINT
```

```
2098  PRINT " C(LIN)= "; INT (X(2) * 1000) / 1000;" D(CONST)=
"; INT (X(3) * 1000) / 1000
2100  PRINT : PRINT  SPC( 5);: INVERSE : PRINT "PRESS 1-4 TO U
PPDATE, ELSE N": NORMAL
2110  GET K$
2120  IF K$ = "N" THEN 2190
2130 K =  VAL (K$)
2140  IF K < 1 OR K > 4 THEN 2110
2150  PRINT : PRINT " PLEASE ENTER "; CHR$ (34);CM$(K); CHR$ (
34);" (USE QUOTES)"
2160  INPUT ">";CT$(K)
2170  GOTO 2040
2190  RETURN
2499 :
2500  REM  ******* EDIT/VIEW INTENSITIES
2510  HOME
2520  IF ND = 0 THEN 2760
2530  FOR I = 1 TO ND
2540  IF I = 16 THEN  VTAB (1)
2550  IF I > 15 THEN  PRINT  SPC( 20);I" ";PW(I);" ";IN(I);FG$
(I): GOTO 2570
2560  PRINT I;") ";PW(I);" ";IN(I);" ";FG$(I)
2570  NEXT I
2580  VTAB (19): PRINT "EDIT PRESENT DATA ? (Y/N)
2590  GET K$
2600  IF K$ = "N" THEN 2760
2610  IF K$ <  > "Y" THEN 2590
2620  VTAB (19): PRINT "    WHICH PAIR OF VALUES ";
2630  INPUT EI: IF EI > ND + 1 THEN 2620
2635  IF EI = ND + 1 THEN ND = EI
2640  IF EI < 0 AND FG$( ABS (EI)) = "+" THEN FG$( ABS (EI)) =
"-": GOTO 2510
2645  IF EI < 0 AND FG$( ABS (EI)) = "-" THEN FG$( ABS (EI)) =
"+": GOTO 2510
2650  INPUT "   PULSE WIDTH/MICROSECS ";PW(EI):PW(EI) =  ABS (
PW(EI))
2660  INPUT "                INTENSITY ";IN(EI):IN(EI) =  ABS (
IN(EI))
2670  GOTO 2510
2760  HOME
2770  PRINT "NEW DATA SET TO BE ENTERED ? (Y/N)"
2780  GET K$
2790  IF K$ = "N" THEN  RETURN
2800  IF K$ <  > "Y" THEN 2780
2840  FOR I = 1 TO 50:FG$(I) = "+": NEXT I:MX = 0:MY = 0:ND =
0:F1 = 0
2850  HOME
2860  INPUT "NUMBER OF DATA PAIRS ";ND:ND =  ABS (ND)
2870  IF ND > SZ THEN  PRINT : PRINT " MAX=50 SEE LINE 20": FOR
T = 1 TO 2000: NEXT : GOTO 2850
2880  HOME
2890  PRINT "ARE PULSE WIDTHS EQUALLY SPACED ? (Y/N)"
2900  GET K$
```

```
2910  IF K$ = "Y" THEN 3040
2920  IF K$ <  > "N" THEN 2900
2930  FOR I = 1 TO ND
2940  HOME : PRINT "ENTER PULSE WIDTH ";I;" IN MICROSECS";
2950  INPUT PW(I):PW(I) =  ABS (PW(I))
2960  PRINT "& THE CORRESPONDING INTENSITY ";
2970  INPUT IN(I):IN(I) =  ABS (IN(I))
2980  PRINT : PRINT "THESE VALUES O.K ? (Y/N)"
2985  GET K$
2990  IF K$ = "N" THEN I = I - 1
3000  HOME
3020  NEXT I
3030  GOTO 2510
3040  HOME
3050  PRINT "FIRST PULSE WIDTH/MICROSECS"
3060  PRINT : INPUT FP:FP =  ABS (FP)
3070  PRINT : PRINT "PULSE WIDTH INCREMENT/MICROSECS"
3080  PRINT : INPUT IW:IW =  ABS (IW)
3090  PRINT : PRINT "THESE VALUES O.K ? (Y/N)"
3100  GET K$
3110  IF K$ = "N" THEN 3040
3120  IF K$ <  > "Y" THEN 3100
3130  HOME
3140  FOR I = 1 TO ND
3150 PW(I) = (I - 1) * IW + FP
3160  PRINT "INTENSITY FOR PULSE WIDTH OF ": PRINT PW(I);" MIC
ROSECS ";
3170  INPUT IN(I):IN(I) =  ABS (IN(I))
3180  PRINT : PRINT "THIS VALUE O.K ? (Y/N)"
3190  GET K$
3200  IF K$ = "N" THEN I = I - 1
3220  HOME
3230  NEXT I
3240  GOTO 2510: REM  UPDATE SCREEN
3499 :
3500  REM  ***** 90 DEG &  PULSE REP TIME
3510  HOME
3520  PRINT "1- 90 DEG PULSE WIDTH/MICROSECS = ";T90
3530  PRINT "2- TIME DELAY/SECONDS            = ";TD
3540  PRINT
3550  PRINT " PRESS 1 OR 2, ELSE N"
3560  GET K$
3570  IF K$ = "N" THEN 3670
3600 K =  VAL (K$)
3610  IF K < 1 OR K > 2 THEN 3560
3620  IF K$ = "2" THEN 3650
3630  PRINT : PRINT "PLEASE TYPE 90 DEG PULSE/MICROSECS ";
3640  INPUT T90:T90 =  ABS (T90): GOTO 3510
3650  PRINT : PRINT "ENTER NEW DELAY TIME/SECS ";
```

```
3660  INPUT TD:TD =  ABS (TD): GOTO 3510
3670  RETURN
3999 :
4000  REM  ************ CURVE TERMS
4005  IF T90 = 0 THEN  RETURN
4010  IF ND > 0 THEN 4020
4014  HOME : PRINT : PRINT  SPC( 5)"SORRY - NO DATA": FOR T =
1 TO 1500: NEXT : GOTO 4300
4020  HOME : VTAB (13): PRINT  SPC( 9)"WORKING - PLEASE WAIT"
4030 :
4100  FOR J = 0 TO 3: FOR K = 0 TO 3:CT(J,K) = 0: NEXT K,J: FOR
J = 0 TO 3:CT(J,4) = 0: NEXT J
4110 :
4120  FOR J = 0 TO 3
4130  FOR K = 0 TO 3
4140  FOR I = 1 TO ND
4150  IF FG$(I) = "-" THEN 4180: REM  IF - EXCLUDE.IF + INCLUD
E
4160 :
4170 CT(J,K) = CT(J,K) + PW(I) ^ (6 - J - K)
4180  NEXT I
4190  NEXT K,J
4200  FOR I = 1 TO ND
4220  IF FG$(I) = "-" THEN 4270
4230 CT(3,4) = CT(3,4) + IN(I)
4240 CT(2,4) = CT(2,4) + IN(I) * PW(I)
4250 CT(1,4) = CT(1,4) + IN(I) * PW(I) * PW(I)
4260 CT(0,4) = CT(0,4) + IN(I) * PW(I) * PW(I) * PW(I)
4270  NEXT I
4280 N = 4: GOSUB 4500
4290  GOSUB 5000
4300  RETURN
4499 :
4500  REM  ********** CURVE COEFFICIENTS
4510  FOR L = 1 TO N
4520 CT(0,L) = CT(0,L) / CT(0,0)
4530  NEXT L
4540 M = 0
4550  FOR LL = 1 TO (N - 1)
4560 M = M + 1
4570  FOR L = LL TO (N - 1)
4580 SU = 0
4590  FOR K = 0 TO (M - 1)
4600 SU = SU - CT(L,K) * CT(K,M)
4610  NEXT K
4620 CT(L,M) = CT(L,M) + SU
4630  NEXT L
4640  FOR MM = (M + 1) TO N
```

```
4650 SU = 0
4670  FOR K = 0 TO (LL - 1)
4680 SU = SU - CT(LL,K) * CT(K,MM)
4690  NEXT K
4700 CT(LL,MM) = (CT(LL,MM) + SU) / CT(LL,LL)
4710  NEXT MM
4720  NEXT LL
4740 X(N - 1) = CT(N - 1,N)
4750  FOR K = N - 2 TO 0 STEP  - 1
4760 SU = 0
4770  FOR L = (K + 1) TO N - 1
4780 SU = SU - CT(K,L) * X(L)
4790  NEXT L
4800 X(K) = CT(K,N) + SU
4810  NEXT K
4820  RETURN
4999 :
5000  REM  ******PRINT EQN & T1 TO SCREEN
5010  HOME
5020  PRINT "THE DATA HAS BEEN FITTED TO A CUBIC EQN"
5030  PRINT
5040  PRINT "    3        2"
5050  PRINT " A*X  +  B*X  + C*X + D = Y (INTENSITY"
5060  PRINT : PRINT  SPC( 5)"WHERE A = "; INT (X(0) * 1000) /
1000
5070  PRINT : PRINT  SPC( 11)"B = "; INT (X(1) * 1000) / 1000
5080  PRINT : PRINT  SPC( 11)"C = "; INT (X(2) * 1000) / 1000
5090  PRINT : PRINT  SPC( 7)"AND D = "; INT (X(3) * 1000) / 10
00
5100  REM  FIND MAXIMUM OF FITTED CURVE
5105  VTAB (15): PRINT  SPC( 9)"WORKING - PLEASE WAIT"
5110 XM(1) = X(1) * X(1) - 3 * X(0) * X(2): IF XM(1) < 0 THEN
5130
5120 XM(1) = ( - X(1) +  SQR (XM(1))) / (3 * X(0))
5130 XM(2) = X(1) * X(1) - 3 * X(0) * X(2): IF XM(2) < 0 THEN
5140
5135 XM(2) = ( - X(1) -  SQR (XM(2))) / (3 * X(0))
5140  IF XM(1) < 0 AND XM(2) < 0 THEN 5190
5150 F1 = 6 * X(0) * XM(1) + 2 * X(1)
5160 FB = 6 * X(0) * XM(2) + 2 * X(1)
5170  IF FA < 0 THEN MX = XM(1): GOTO 5200
5180  IF FB < 0 THEN MX = XM(2): GOTO 5200
5190  PRINT : PRINT "   CANNOT FIND A REAL MAXIMUM !": FOR T =
1 TO 1500: NEXT : RETURN
5200  REM  CAL PULSE WIDTH OFFSET
5210 OS = 0:IN = MX:CN = 0
5220 Y = X(0) * (OS ^ 3) + X(1) * (OS ^ 2) + X(2) * OS + X(3):
CN = CN + 1
5225  IF CN < 100 THEN 5230
5226  PRINT "WARNING! PULSE WIDTH OFFSET SET TO ZERO":OS = 0
5227  FOR T = 1 TO 2000: NEXT : GOTO 5280
5230  IF  ABS (Y) < 0.01 THEN 5270: REM  TOLERANCE CAN BE ALTE
RED IF DESIRED
5240  IF Y > 0 THEN 5260
```

```
5250 OS = OS + IN:IN = IN / 2: GOTO 5220
5260 OS = OS - IN: GOTO 5220
5270  REM  CALCULATE T1 USING CORRECTED PULSE WIDTHS, I.E. PW(
I)-OS
5280 AN = (((MX - OS) * 90) / (T90 - OS)) * 0.0174533: REM  AN
GLE IN RADS
5285  IF AN =  > 1.5708 THEN AN = 180 * .0174533 - AN
5290 T1 =  - TD / ( LOG ( COS (AN))): REM  NAT LOG
5295 MY = X(0) * (MX ^ 3) + X(1) * (MX ^ 2) + X(2) * MX + X(3)

5300  VTAB (15)
5310  PRINT " SPIN-LATTICE RELXN TIME = "; INT (T1 * 10) / 10;
" SECS"
5320  PRINT
5330  PRINT " PULSE WIDTH OFFSET = "; INT (OS * 10) / 10;" MIC
ROSECS"
5340  PRINT
5350  PRINT  SPC( 8);: INVERSE : PRINT " ANY KEY FOR MENU ": NORMAL

5360  GET K$
5370 CT$(5) = "T1 = " +  STR$ ( INT (T1 * 1000) / 1000) + " S
 OS= " +  STR$ ( INT (OS * 100) / 100) + " US"
5375 CT$(5) = CT$(5) +  STR$ ( INT (MO))
5380  RETURN
5999 :
6000  REM  ************ PLOT ROUTINE
6010  IF MX > 0 AND MY > 0 THEN 6020
6015  HOME : PRINT  SPC( 5)"NO PLOT AND/OR DATA": FOR T = 1 TO
1500: NEXT : GOTO 6790
6020  IF K$ = "7" THEN 6200
6025  HOME : VTAB (6): PRINT  SPC( 8);: INVERSE : PRINT "WORKI
NG - PLEASE WAIT": NORMAL
6040 YS = 150 / MY
6050 XU = PW(ND)
6060 XS = 200 / XU
6070  FOR I = 1 TO ND
6080 YD(I) = IN(I) * YS
6090 XD(I) = PW(I) * XS
6100  NEXT I
6110  REM  PRODUCE SCALED POINTS FOR CURVE
6130  FOR I = 1 TO 50:II = (I * 5) / XS
6140 YC(I) = (X(0) * (II ^ 3) + X(1) * (II ^ 2) + X(2) * II +
X(3)) * YS:XC(I) = I * 5
6150  NEXT I
6200  REM  NOW PLOT EXPL DATA
6210  HOME : HGR
6220 :
6230  HCOLOR= 3
6240  FOR I = 1 TO ND
6250 X% = XD(I) - 2:Y% = 170 - YD(I)
6260  HPLOT X%,Y% TO X% + 4,Y%
6270  IF FG$(I) = "+" THEN Y% = 172 - YD(I):X% = XD(I): HPLOT
X%,Y% TO X%,Y% - 4
6290  NEXT I
```

```
6300  REM  PLOT FITTED CURVE
6310  FOR I = 1 TO 60
6320 X% = XC(I):Y% = 170 - YC(I): IF X% < 0 OR Y% < 0 THEN 634
0
6330  HPLOT X%,Y%
6340  NEXT I:F1 = 1: REM  SET PLOT FLAG
6350  REM  DRAW AXES
6360 X% = 0:Y% = 150
6370  HPLOT X%,Y% TO 250,Y%
6380 NI% = (PW(ND) / 5) + .1:XI = 250 / PW(ND)
6390  FOR I = 1 TO NI%:XI% = I * XI * 5
6400  HPLOT X%,150 TO X%,155: NEXT
6410  FOR I = 1 TO PW(ND):X% = I * XI: HPLOT X%,150 TO X%,147:
 NEXT I
6420  HPLOT 0,1 TO 0,150
6430 NI% = (MY / 1000) + .1:YI = 150 / MY
6440  FOR I = 1 TO NI%:Y% = 170 - I * YI * 1000
6450  HPLOT 1,Y% TO 5,Y%: NEXT I
6520  HCOLOR= 1:X% = XD(IP):Y% = 165 - YD(IP): HPLOT X%,Y%
6530 Y% = Y% - 1: HPLOT X%,Y%:Y% = Y% - 1: HPLOT X%,Y%
6540  GET K$
6550  IF K$ =  CHR$ (13) THEN 6780
6560  IF K$ <  > "R" THEN 6610
6570  IF FG$(IP) = "-" THEN 6540
6580  HCOLOR= 0:X% = XD(IP):Y% = 168 - YD(IP): HPLOT X%,Y%:Y% =
Y% + 1: HPLOT X%,Y%
6590 Y% = Y% + 2: HPLOT X%,Y%:Y% = Y% + 1: HPLOT X%,Y%
6600 FG$(IP) = "-": GOTO 6540
6610  IF K$ <  > "A" THEN 6660
6620  IF FG$(IP) = "+" THEN 6540
6630  HCOLOR= 1:X% = XD(IP):Y% = 150 - YD(IP): HPLOT X%,Y%:Y% =
Y% + 1: HPLOT X%,Y%
6640 Y% = Y% + 2: HPLOT X%,Y%:Y% = Y% + 1: HPLOT X%,Y%
6650 FG$(IP) = "+": GOTO 6540
6660  IF K$ <  >  CHR$ (8) THEN 6720: REM  CURSOR LEFT
6670  HCOLOR= 0:Y% = 165 - YD(IP): HPLOT X%,Y%:Y% = Y% - 1: HPLOT
X%,Y%:Y% = Y% - 1: HPLOT X%,Y%
6680 IP = IP - 1: IF IP < 1 THEN IP = ND
6690 X% = XD(IP):Y% = 165 - YD(IP): HPLOT X%,Y%:Y% = Y% - 1: HPLOT
X%,Y%:Y% = Y% - 1: HPLOT X%,Y%
6700  GOTO 6540
6710 :
6720  IF K$ <  >  CHR$ (21) THEN 6540: REM  CURSOR RIGHT
6730  HCOLOR= 0:Y% = 165 - YD(IP): HPLOT X%,Y%:Y% = Y% - 1: HPLOT
X%,Y%:Y% = Y% - 1: HPLOT X%,Y%
6740 IP = IP + 1: IF IP > ND THEN IP = 1
```

```
6750  HCOLOR= 1:X% = XD(IP):Y% = 165 - YD(IP): HPLOT X%,Y%:Y% =
Y% - 1: HPLOT X%,Y%:Y% = Y% - 1: HPLOT X%,Y%
6760  GOTO 6540
6770 :
6780  TEXT
6790  RETURN
7999 :
8000  REM  ******PRINT DATA & RESULTS
8010  IF ND > 0 THEN 8030
8020  HOME : PRINT : PRINT  SPC( 5)"SORRY - NO DATA": FOR T =
1 TO 1500: NEXT : GOTO 8290
8030  HOME : PRINT "DO YOU WANT TO PRINT ? (Y/N)": GET K$
8035  IF K$ = "N" THEN  RETURN
8037  IF K$ <  > "Y" THEN 8030
8040  PRINT "PRESS Y IF PRINTER IS READY"
8050  GET K$
8060  IF K$ <  > "Y" THEN 8050
8070  PR£ 1
8080  PRINT " D E S P O T  - T1 FROM PEAK MAXIMUM"
8090  PRINT
8100  FOR I = 1 TO 4
8110  IF CT$(I) = "" THEN 8120
8115  PRINT  SPC( 5)CT$(I)
8120  NEXT I: PRINT
8125  PRINT " A= "; INT (X(0) * 1000) / 1000;" B= "; INT (X(1)
 * 1000) / 1000
8126  PRINT " C= "; INT (X(2) * 1000) / 1000;" D= "; INT (X(3)
 * 1000) / 1000: PRINT
8130  PRINT "90 DEG PULSE: ";T90;" USECS,"; SPC( 3);"DELAY TIM
E: ";TD;" SECS": PRINT
8140  PRINT "PULSE WIDTH/USECS  EPXL.INT       CALC.INT."
8150  PRINT "    (MICROSECS)": PRINT
8160  FOR I = 1 TO ND:TX = PW(I): PRINT  SPC( 4);PW(I), INT (I
N(I) * 10) / 10
8170  PRINT  INT ((X(0) * (TX ^ 3) + X(1) * (TX ^ 2) + X(2) *
TX + X(3)) * 10) / 10
8180  NEXT I
8190  PRINT
8200  PRINT "SPIN-LATTICE RELAXATION TIME: "; INT (T1 * 10) /
10;" MICROSECS"
8210  PRINT
8220  PRINT "PULSE WIDTH OFFSET: "; INT (OS * 10) / 10;" USECS
"
8230  PRINT
8240  PR£ 0
8250  HOME : PRINT : PRINT  SPC( 5)"ANOTHER COPY ? (Y/N)"
8260  GET K$
8270  IF K$ = "Y" THEN 8030
8280  IF K$ <  > "N" THEN 8260
8290  RETURN
```

D E S P O T - T1 FROM PEAK MAXIMUM

PEAK 1 MAR 84 DATA
F. HAKIEMPOOR
8 OCT 1985
ETHYL BENZENE TEST DATA

A= 6.117 B= -145.965
C= 1045.56 D= -593.127

90 DEG PULSE: 22 USECS, DELAY TIME: 5 SECS

PULSE WIDTH/USECS (MICROSECS)	EXPL.INT.	CALC.INT.
1	330	312.5
2	927	963
3	1392	1395
4	1679	1645.1
5	1754	1750.1
6	1741	1746.7
7	1643	1671.6
8	1583	1561.5
9	1450	1453
10	1322	1382.9
11	1222	1388
12	1135	1504.8
13	1029	1770.1
14	939	2220.6
15	889	2893
16	818	3824
17	761	5050.3
18	697	6608.6
19	668	8535.6
20	617	10868.1
21	563	13642.6
22	535	16895.9

SPIN-LATTICE RELAXATION TIME: 96.5 MICROSECS

PULSE WIDTH OFFSET: .6 SECS

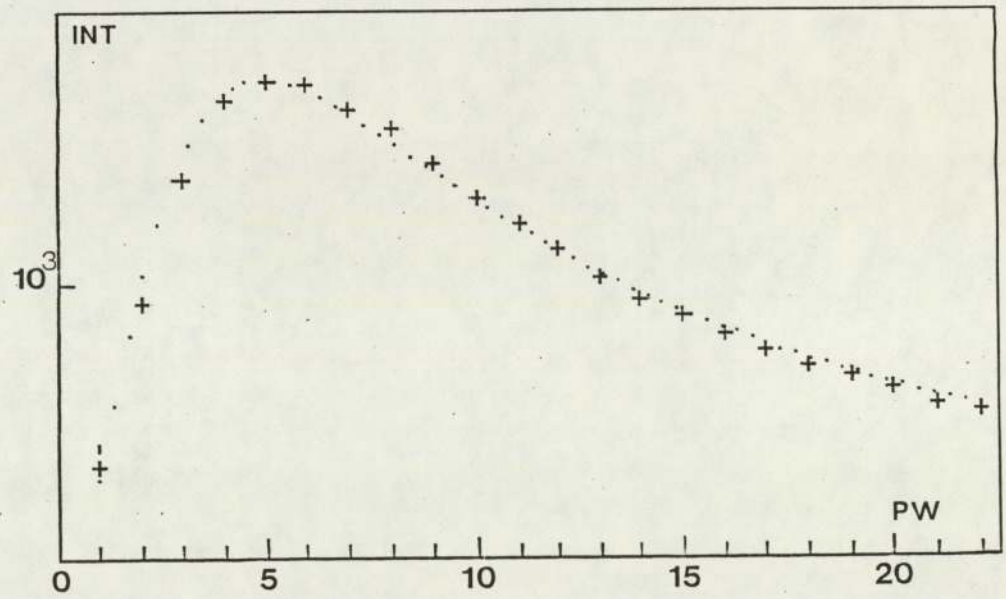

APPENDIX 3

Theory and Measurement of the N.M.R. Spin-Lattice Relaxation Time. T_1

When a sample is placed in the main magnetic field, B_o, of the NMR spectrometer the nuclear spins align with and against the direction of B_o. At equilibrium there is a net magnetic moment, M_o, induced in the sample that is aligned parallel and in the same direction as B_o. Theory predicts that individual spins will precess about B_o at a rate of radians per second and that only their component along the direction of B_o (taken to be the z-axis) will remain constant with time. This situation may be visualised as follows

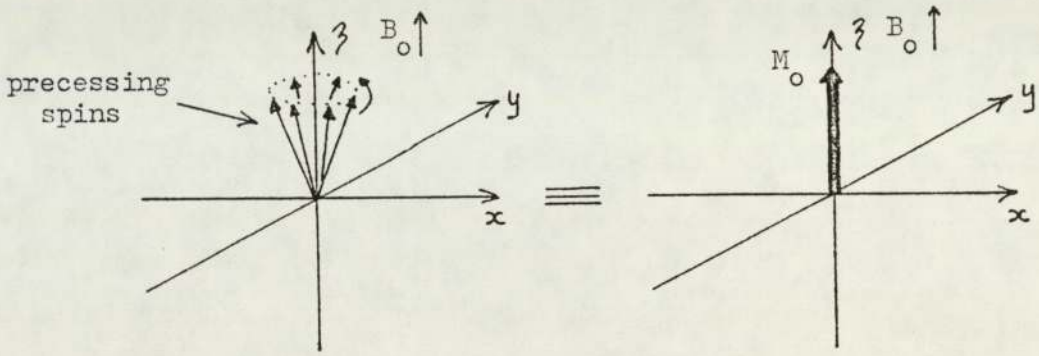

If the direction of B_o was suddenly reversed then the magnetic moment M_o would not suddenly invert and become $-M_o$ but would, instead, gradually decrease to zero and then increase along the negative direction of the z-axis to give a final value of $-M_o$. This effect arises as a result of relaxation processes (molecular motion in the rotational sense) which are always oresent in the sample being examined. The tumbling motion of the molecules produces fluctuating magnetic fields which can interact with nuclear spins and cause them to flip from a direction parallel to to a direction which is antiparallel or vice versa. Merely

After this preliminary discussion of the origin of spin-lattice relaxation a method for measureing T_1 will now be described.

When B_o and a strong magnetic field B_1 (supplied by an rf generator) are present at the same time the magnetic moment M_z can be tipped through an angle θ . The value of θ depends on the strength of B_1, the duration of the time, t_p, for which B_1 is applied and the gyromagnetic ratio, δ, of the nuclei involved, viz.

$$\theta = \delta B_1 t_p$$

The pulse duration t_p may be chosen such that $\theta = 90^o$ and this may be depicted as

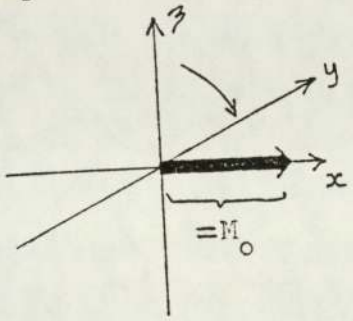

If the homogeneity of the magnetic field B_o is deliberately spoiled for a brief period of time (homospoiling) then the magnetic moment in the xy plane can be rapidly reduced to zero. This may be illustrated as follows

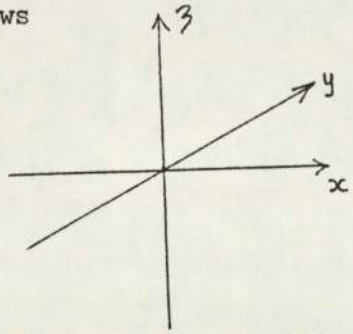

This is identical to the point at which the sample has just been placed in the magnetic field and M_z will start to increase from zero to its final value of M_o at a rate described by T_1 (see eqn.1). After a time τ ($\tau \lesssim T_1$) the magnetic moment will have grown to some

value $M(\tau)$

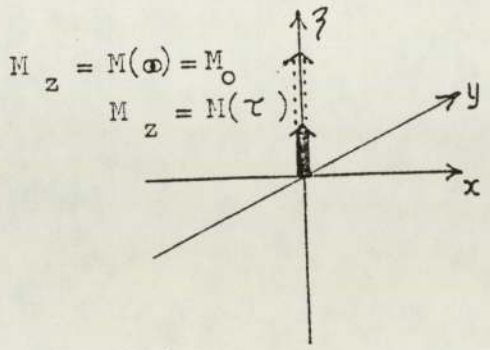

The magnitude of $M(\tau)$ can be measured by applying B_1 again so that $M(\tau)$ now rotates into the xy plane. The xy plane contains the axes of the detector coils and permits the measurement of any magnetic moment lying in the xy plane. The above sequence of events (ie. 90°, homospoil, 90°) can be repeated for different values of τ. From equation it can be seen that

$$M(\tau) = M_o[1 - \exp(\tau/T_1)] \qquad 3$$

Rearranging and taking logs yields

$$-\log_e(1 - M(\tau)/M_o) = \tau/T_1 \qquad 4$$

Hence, a plot of τ against $-\log_e(1 - M(\tau)/M_o)$ should give a straight line with a gradient equal to T_1. Bloembergen showed that under certain conditions the rate of spin-lattice relaxation for a given nuclei i in a molecule comprised of j identical nuclei of spin 1/2 will be given by

$$T_{1i}^{-1} = \frac{96}{5}\left(\frac{\pi}{h}\right)^2 \mu^4 \sum_{j \neq i} r_{ij}^{-6} \left[\frac{t}{4\pi^2 v_o^2 t^2 + 1} + \frac{4t}{1 + 16\pi^2 v_o^2 t^2}\right]$$

where μ is the magnetic moment, r_{ij} is the distance between the nuclei i and j, t is the rotational correlation time (the time for rotational diffusion of the molecule) and v_o is the precessional rate of the nuclear spins expressed in Hz ($v_o = 2\pi\omega_o$). In

practice it is often the case that only pairs on interacting nuclei need to be considered. The Bloembergen equation may then be simplified to give

$$T_1^{-1} = 96 \left(\frac{\pi}{h}\right)^2 \mu^4 \frac{t}{r^6} \qquad 6$$

If the distance between the interacting nuclei is of interest then t may be estimated using the Debye expression for the rotational diffusion

$$t = 4\pi \eta a^3 / 3 k T \qquad 7$$

in which 'a' is the effective hydrodynamic radius of the molecule and η is the reduced viscosity of the sample. The radius may be estimated with reasonable accuracy and the viscosity can be measured.

REFERENCES

1. Morrison and Boyd, Organic Chemistry,3rd Edn.,New York,(1980).
2. T.M.Doscher,G.E.Myers and D.C.Atkins,Jr.,J.Colloid Sci.,6,223,(1951).
3. A.A.Blumberg and S.S.Pollack,J.Polym.Sci.,A2,2499,(1964).
4. A.A.Blumberg and J.Wyatt,J.Polym.Lett.,4,653,(1966).
5. P.A.Laurent and E.Arsenio,Bull.Soc.Chim.France,618,(1958).
6. P.J.Hendra and D.B.Powell,J.Chem.Soc.,5105,(1960).
7. M.Yokoyama,H.Ishihara,R.Iwamoto and H.Tadokoro,Macromol.,2,184,(1969).
8. R.D.Lundberg,F.E.Bailey and R.W.Callard,J.Polym.Sci., Al,4,1563,(1966).
9. D.E.Fenton,J.M.Parker and P.V.Wright,Polym.,14,589, (1973).
10. R.E.Wetton,D.B.James and W.Whiting,Polym.Lett.Edn.,14, 577,(1976).
11. D.B.James,R.E.Wetton and D.S.Brown,Polym.,20,187,(1979).
12. M.J.Hannon and K.F.Wissbrun,J.Polym.Sci.Polym.Phys.Ed., 13,113,(1975).
13. D.Acierno,E.Bianchi,A.Ciferri,B.DeCindio,C.Migliaresi and L.Nicolais,J.Polym.Sci.,54,259,(1976).
14. A.Kills,J.F.LeNest,A.Gandini and H.Cheradame,J.Polym. Sci.,Polym.Phys.Edn.,19,1073,(1981).
15. A.Kills,J.F.LeNest.A.Gandini and H.Cheradame,Makromol. Chem.,183,1037,(1982).

16. M.L.Williams,R.F.Landel and J.D.Ferry,J.Am.Chem.Soc., 77,3701,(1955).

17. A.Kills.J.F.LeNest,A.Gandini and H.Cheradame,Macromol., 17,63,(1984).

18. K.J.Liu,Macromol.,1,308,(1968).

19. K.J.Liu and J.E.Anderson,Macromol.,2,235,(1969).

20. A.Ricard,Eur.Polym.J.,15,1,(1979).

21. J.A.Ibemesi and J.B.Kinsinger,18,1123,(1980).

22. E.Florin,Macromol.,18,360,(1985).

23. C.C.Lee and P.V.Wright,Polym.,19,234,(1978).

24. C.C.Lee and P.V.Wright,Polym.,23,681,(1982).

25. I.Ando,M.Morita,A.Nishioka and K.Sato,Polym.,23,598, (1982).

26. D.R.Payne and P.V.Wright,Polym.,23,690,(1982).

27. A.R.Blythe,'Electrical Properties of Polymers',1st. Edn.,(1980).

28. P.Debye,'Polar Molecules',Chem.Catalog,New York,(1929).

29. L.Onsager,J.Am.Chem.Soc.,58,1486,(1936).

30. H.Frohlich,'Theory of Dielectrics',Oxford University Press,(1949).

31. P.J.Flory,'Statistical Mechanics of Chain Molecules', (1969).

32. J.G.Kirkwood and R.M.Fuoss,J.Chem.Phys.,9,329,(1941).

33. P.Debye and F.Bueche,J.Chem.Phys.,19,589,(1951).

34. M.V.Volkenstein,'Configurational Statistics of Polymeric Chains',New York,(1963).

35. B.E.Read,Trans.Faraday Soc.,61,2140,(1965).

36. J.Marchal and H.Benoit,J.Chim.Phys.,52,518,(1955).

37. G.Williams and R.Wetton,Trans.Faraday Soc.,61,2132, (1965).

38. K.Bak,G.Elefante and J.E.Mark.,J.Phys.Chem.,71,4007, (1967).

39. A.Abe,T.Hirano and T.Tsuruta,Macromol.,12,1092,(1979).

40. R.H.Cole and K.S.Cole,J.Chem.Phys.,9,341,(1941).

41. D.W.Davidson and R.H.Cole,J.Chem.Phys.,18,1417,(1950).

42. L.Boltzman,Pogg.Ann.Physik,7,108,(1876).

43. O.Nakada,J.Phys.Soc.(Japan),10,804,(1955).

44. O.Nakada,J.Polym.Sci.,43,149,(1960).

45. R.Cerf,Compt.Rend.Acad.Sci.,241,496,(1955).

46. R.Cerf,Advan.Polym.Sci.,1,382,(1959).

47. B.H.Zimm,J.Chem.Phys.,24,269,(1956).

48. P.E.Rouse,J.Chem.Phys.,21,1272,(1953).

49. L.K.Van Beek and J.J.Hermans,Polym.Sci.,23,211,(1957).

50. F.Bueche,J.Polym.Sci.,54,597,(1961).

51. W.H.Stockmayer and M.Baur,J.Am.Chem.Soc.,86,3485,(1964).

52. K.Yamafuji and Y.Ishida,Kolloid Z.,183,15,(1962).

53. R.E.Wetton,W.J.MacKnight,J.R.Fried and F.F.Karasz, Macromol.,11,158,(1978).

54. M.Cook,D.C.Watts and G.Williams,Trans.Faraday Soc.,66, 2503,(1970).

55. G.Williams,Trans.Faraday Soc.,61,1564,(1965).

56. M.E.Baur and W.H.Stockmayer,J.Chem.Phys.,43,4319,(1965).

57. T.Alper,A.J.Barlow and R.W.Gray,Polym.,17,665,(1976).

58. S.Yano,R.R.Rahalkar,S.P.Hunter,C.H.Wang and R.H.Boyd, 14,1877,(1976).

59. H.Sasabe and S.Saito,J.Poly.Sci.Part A-2,6,1401,(1968).

60. U.K.Patent specification 1590472/81.

61. J.Homer and M.Beevers,J.Mag.,63,287,(1985)